Microalgal Biofilms for Wastewater Treatment

N.C. Boelee

Microalgal Biofilms for Wastewater Treatment

Nadina Catharina Boelee

Thesis committee

Promotor
Prof. Dr R.H. Wijffels
Professor of Bioprocess Engineering
Wageningen University

Co-promotors
Dr B.G. Temmink
Assistant professor, Sub-department of Environmental technology
Wageningen University
Dr M.G.J. Janssen
Assistant professor, Bioprocess Engineering
Wageningen University

Other members
Prof. Dr L.E.M. Vet, *Wageningen University*
Prof. Dr Dr H.C.O. Pulz, *University of Applied Sciences Lausitz (HSL), Nuthetal, Germany*
Prof. Dr P.N.L. Lens, *UNESCO-IHE, Delft*
Dr M.H. Zandvoort, *Waternet, Almere*

Microalgal Biofilms for Wastewater Treatment

Nadina Catharina Boelee

Deel je eten en het zal beter smaken.
Deel je blijdschap en ze zal groter worden.
Deel je zorgen en ze zullen minder zwaar zijn.
Deel je enthousiasme en je zult elkaar aansteken.
Deel je kennis en ze zal aangevuld worden.
Deel je liefde en je zult liefde krijgen.
Deel je leven en je zult mens worden.

— Greet Brokerhof-Van der Waa

Table of Contents

Chapter 1

Microalgal Biofilms for Wastewater Treatment: Introduction

1

MICROALGAE

Microalgae are a large and diverse group of microorganisms that are able to use light energy as the only energy source to fuel their metabolism. These unicellular organisms incorporate inorganic carbon as dissolved carbon dioxide (CO_2) or bicarbonate (HCO_3^-) into their biomass. Hence, this type of metabolism is referred to as photoautotrophic growth. It is unknown how many algae species exist, but it is certain there are many more than the approximate 40 000 species that are currently described. Estimations of the number of microalgae vary from three times to 250 times the currently recognized number of species (Norton et al. 1996). These microalgae live in most soils and in many different aquatic habitats ranging from freshwater to saline, from acidic to alkaline, and from the arctic to hot springs. Most freshwater microalgae are either green algae (Chlorophyta), diatoms (Bacillariophyta), red algae (Rhodophyta) or blue-green algae (Cyanophyta). While all microalgae are eukaryotes, the blue-green algae are prokaryotic as they are actually phototrophic bacteria. Blue-green algae are also known as cyanobacteria. In this thesis the word 'microalgae' will be used to describe all these phototrophic microorganisms, including microalgae and cyanobacteria.

Microalgae are known for their green color due to the presence of chlorophyll *a*. Microalgae can also contain chlorophyll *b*, *c*, or *d* and accessory pigments such as phycobilins and carotenoids, whose presence is characteristic of a particular algal groups. These photosynthetic pigments can mask the green color of chlorophyll *a* and provide color variation between microalgae, hence names such as 'red' algae and 'blue-green' algae (Brock et al. 2000; Stevenson 1996). The pigments are located in the thylakoid membranes in the chloroplast(s) of microalgae and in stacks of thylakoid membranes arranged in the cytoplasm in cyanobacteria (Brock et al. 2000).

The photosynthetic pigments absorb light in the wavelength range of 400-700 nm which is referred to as photosynthetic active radiation (PAR), and almost corresponds to light visible for humans (Hill 1996). The light energy which is captured by the pigments is transferred to ATP and NADPH in the so called light-reactions, which involves splitting water into oxygen (O_2) and electrons, and reducing $NADP^+$ into NADPH with these electrons. A few hundredths of a second following the light-reactions the dark reactions occur. During the dark reactions the chemical energy is employed and ATP and NADPH are utilized to reduce CO_2 into sugars. These sugars are the building blocks to produce new microalgal biomass (Brock et al. 2000; Hill 1996).

During the day microalgae are usually in the growth phase, and carbon and energy are fixed during photosynthesis. At night, phototrophs utilize the carbohydrates that they have accumulated during the day for protein synthesis, cell division and respiration

(Lacour et al. 2012; Needoba and Harrison 2004; Torzillo et al. 1991). The potential for night growth is probably determined by a complex of environmental factors including light intensity history, nutrient status, and the species composition of the population (Cuhel et al. 1984). The assimilation of nitrogen (N) and phosphorus (P) into the microalgal biomass exhibits oscillations with increased assimilations during the day over those during the night (Lacour et al. 2012; Ahn et al. 2002; Vincent 1992).

Light intensity and temperature are determining factors for microalgal growth. At low light intensities, microalgal growth increases linearly with increasing light until the light becomes saturating, generally around 200-400 μmol/m^2/s (Hill 1996). At light intensities above the saturating intensity, microalgal growth will stabilize at its maximum level. At low temperatures, microalgal growth also increases with increasing temperature up to an optimal growth temperature. Each microalgal species has its own optimal growth temperature but, generally, maximum growth rates of mesophilic microalgae are between 20 and 25°C. Microalgal growth rapidly decreases at temperatures above the optimum growth temperature until lethal temperatures are attained (Ras et al. 2013).

Microalgae can grow in unicellular, colonial, or in filamentous forms. Microalgae growing in suspension in the water column are named phytoplankton. Benthic microalgae are microalgae that live on, or in association with, substrata. The word periphyton refers to microalgae growing on substrata with other microorganisms (Stevenson 1996) and is in general, a synonym for a microalgal biofilm.

MICROALGAL BIOFILMS

On any material that is subjected to a certain amount of moisture, a biofilm can form, usually visible as a slimy layer. Biofilms can, therefore, be discovered in all natural environments; in aquatic and soil environments, on tissues of plants and also on animals. In addition, biofilms can be observed in many technical systems such as filters and other porous materials, reservoirs, plumbing systems, pipelines, ship hulls, heat exchangers, and separation membranes (Flemming and Wingender 2001). If enough light is present, the biofilm will also contain microalgae and will often exhibit a green color. Microalgal biofilms are defined as phototrophic populations which are attached to each other and/or attached to surfaces, and are entrapped in a gel-like matrix of extracellular polymeric substances (EPS) (Di Pippo et al. 2011; Sekar et al. 2002). Biofilms include populations grown on (flat) carrier materials as well as microbial aggregates and flocs. This thesis will focus on biofilms grown on carrier materials. Figure 1.1 depicts scanning electron microscope (SEM) pictures of microalgal biofilms grown on municipal wastewater effluent from the wastewater treatment plant in Leeuwarden, the Netherlands.

Microalgal biofilms can grow on any surface or carrier material that receives sufficient moisture and light. This is emphasized by the great range of materials that have been successfully tested as carrier material for microalgal biofilms. Tested materials include many different plastics: polyvinylchloride (PVC), polyethylene (PE), polyurethane (PUR), polymethyl methacrylate (PMMA), polystyrene, polycarbonate, polyamide (nylon); different natural materials: old reed stems, green reeds, bamboo pipe, granite, andesite; and many other materials such as borosilicate glass, cardboard, loofah sponge, fibrous scrubber, ceramic tiles (Irving and Allen 2011; Johnson and Wen 2009; Ács et al. 2008; Khatoon et al. 2007; Kröpfl et al. 2006). The type of carrier material influences the colonization of different microalgal and cyanobacterial species, and in this way influences biofilm formation (Khatoon et al. 2007 ; Kröpfl et al. 2006). Irving and Allen (2011) determined that the surface roughness influences the initial colonization rate; surfaces with grooves are colonized faster compared to smooth surfaces, but this effect disappears after a few days.

The growth of a microalgal biofilms begins with the colonization of the carrier material often by diatoms and green algae (Johnson et al. 1997; Biggs 1996). The biomass initially grows exponentially and, later, linearly and the community evolves toward filamentous green algae and cyanobacteria (Sekar et al. 2002; Johnson et al. 1997; Biggs 1996). Subsequently, the biofilm growth decreases and at a certain biofilm thickness, the growth is equal to the losses experienced through respiration, cell death, parasitism, disease, grazing, and sloughing and finally these losses exceed the biomass growth (Biggs 1996). Biofilm detachment can occur when external forces, such as shear, are larger than the internal strength of the matrix holding the biofilm together. Biofilm detachment, therefore, takes place when the internal strength of a biofilm has decreased or when external shear forces are increased (Horn et al. 2003).

A biofilm is held together by the matrix of EPS which are excreted by both prokaryotic and eukaryotic microorganisms including microalgae. These EPS consist mainly of polysaccharides, but also contain proteins, nucleic acids and lipids (Flemming and Wingender 2001). Besides their role in the cohesion of the biofilm, EPS also plays an important role in the adhesion of the microorganisms to a substratum. Furthermore, EPS can serve as a water storage and protect organisms within from drying out, can protect the organisms from grazers outside the biofilm and may bind a variety of trace elements. Therefore, the EPS matrix helps create a stable environment with optimal growth conditions (Stal 2003). EPS is also involved in the motility of diatoms, enabling them to glide along a surface in any direction (Lind et al. 1997; Wang et al. 1997; Edgar and Pickett-Heaps 1983). In addition, the growth of benthic diatoms and their release of EPS was discovered to be influenced by the presence of bacteria (Bruckner et al. 2011), and a biofilm consisting of both microalgae and bacteria was determined to be more stable with its mixed assemblage of EPS than only bacterial or microalgal biofilms (Lubarsky et al. 2010).
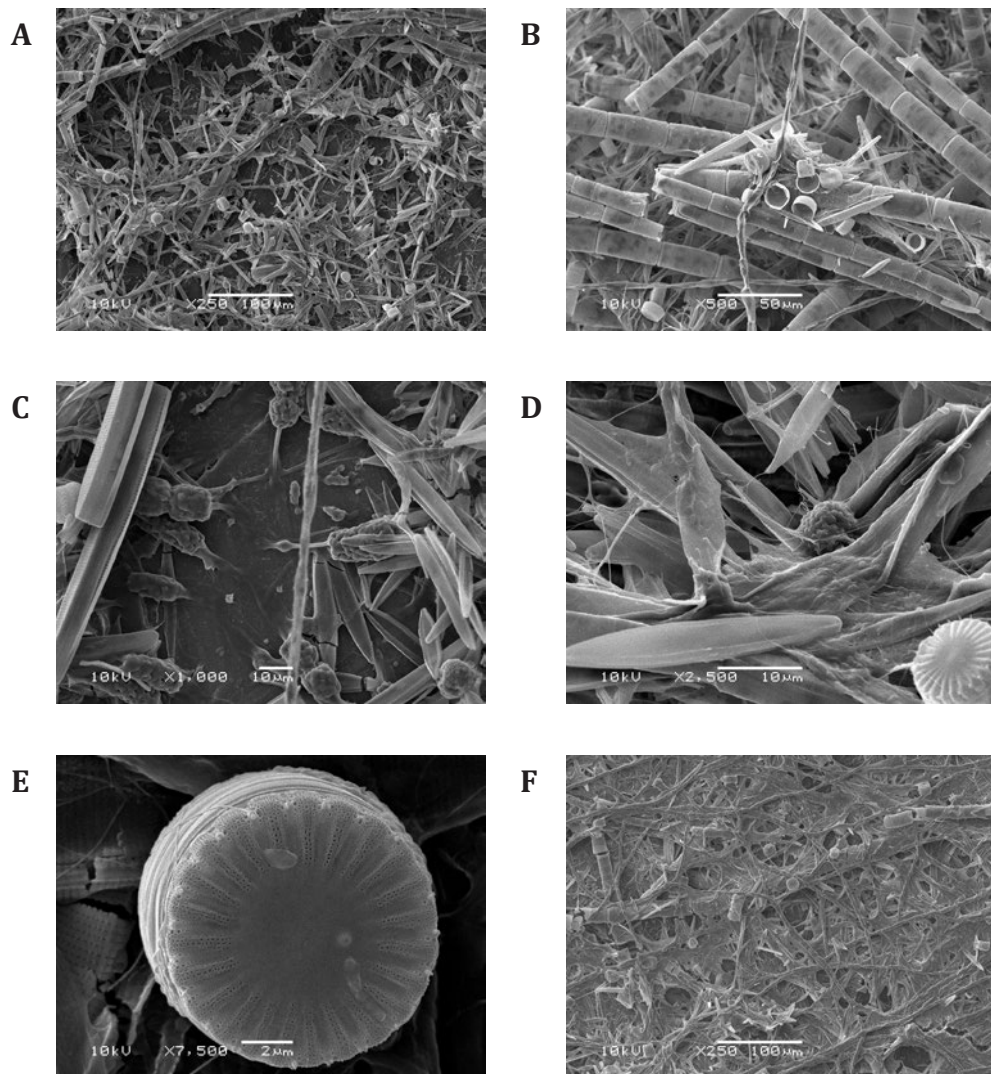
Figure 1.1 — *SEM pictures of microalgal biofilms grown on municipal wastewater effluent; the microalgal biofilm with microalgae entrapped in the network of EPS (A,B, F), adhesion of the biofilm to the PVC carrier material (C), diatoms and a bacteria colony (D) and a* Cyclotella *(E).*

MICROALGAE IN WASTEWATER TREATMENT

Microalgae have been employed for municipal wastewater treatment in algal ponds on a limited scale for many years. Microalgae remove inorganic N and P from wastewater as ammonium (NH_4^+) and phosphate (PO_4^{3-}), and from (nitrified) wastewater effluent as nitrate (NO_3^-) and PO_4^{3-}, by assimilating these nutrients into their biomass. The assimilated N is utilized for the synthesis of proteins and nucleic acids, and for the latter also P is utilized. Phospholipids are also synthesized from P and in addition luxury uptake of P can occur, i.e., the internal storage of PO_4^{3-} as polyphosphates (Powell et al. 2008). Besides by assimilation, PO_4^{3-} can also be removed by precipitation. When microalgae take up NO_3^- and/or more carbon than can be supplied via absorption from the atmosphere, the pH of the water will rise. At elevated pH dissolved PO_4^{3-} can precipitate with cations such as Ca^{2+} and Mg^{2+}, generally present in municipal wastewater (Metcalf & Eddy 2003).

Microalgae frequently investigated for nutrient removal of wastewaters are *Chlorella* and *Scenedesmus* (Johnson and Wen 2009; Shi et al. 2007), but also *Nannochloris*, *Botryococcus braunii* and the cyanobacteria *Phormidium* and *Spirulina* have been investigated (Jiménez-Pérez et al. 2004; An et al. 2003; Olguín et al. 2003; Laliberté et al. 1997). However, most microalgal systems treating wastewater are not based on a mono culture of microalgae and the above mentioned microalgae may be observed together with many other species.

MICROALGAL BIOFILMS FOR THE TREATMENT OF MUNICIPAL WASTEWATER

Besides in suspended systems such as the previously mentioned algal ponds, microalgae can also be grown in biofilm systems to treat municipal wastewater. A biofilm forms a natural separation between the biomass and the treated wastewater and in contrast to suspended systems no separation of algal biomass and water is required. This presumably makes harvesting of the biomass much easier than in suspended systems (Roeselers et al. 2008; Schumacher and Sekoulov 2003). Furthermore, microalgal biofilm systems can operate at short hydraulic retention times of 0.3 to 0.8 days for effluent polishing compared to two to six days in algal ponds (Hoffmann 1998). Finally, while suspended microalgal biomass systems experience an elevated energy input of 9-386 MJ per kg biomass produced, biofilm systems are expected to exhibit a diminished energy demand due to the easier harvesting and the absence of stirring of around 5 MJ/kg biomass produced (Ozkana et al. 2012).

Microalgal biofilm systems can be composed of large biofilm panels over which the wastewater flows. These panels can either be placed horizontally, or vertically in rows. The Algal Turf Scrubber is an example of a near horizontal microalgal biofilm system and cultures microalgal biofilms on a sloping floway which has been indicated to effectively polish wastewater treatment plant effluent (Schumacher and Sekoulov 2003; Craggs et al. 1996). The Twin Layer is a vertical microalgal biofilm system which separates microalgae from the bulk of the wastewater by immobilizing microalgae on a substrate layer exposed to atmosphere, and letting nutrients diffuse through an enclosing second layer (Shi et al. 2007).

Microalgal biofilm systems can be applied for the treatment of (pre-settled) municipal wastewater, for instance in a symbiotic biofilm system. In symbiotic microalgal-bacterial biofilms microalgae remove N and P and produce the O_2 which is required for the heterotrophic degradation of the organic pollutants in wastewater, and the bacteria produce the CO_2 required for microalgal growth. Microalgal biofilms appear especially interesting for the post-treatment of municipal wastewater effluents as microalgae present a more sustainable alternative to existing post-treatment systems. Many municipal wastewater treatment plants in the Netherlands and other EU member states are required to further reduce their N and P emissions due to the EU Water Framework Directive. In concordance with this directive, the N and P concentrations must be reduced from the current European discharge requirements of 10 mg N/L and 1 mg P/L to concentrations appropriate for discharge to 'sensitive' water bodies. Current Dutch guidelines for these sensitive water bodies are 2.2 mg/L total N and 0.15 mg/L total P.

To meet the stricter requirements, multiple wastewater treatment plants in the Netherlands have installed sand filtration systems in the last couple of years (Roeleveld et al. 2010). Sand filters can remove residual N, present as NO_3^- in the effluent, through denitrification by bacteria growing in the filter. However, the addition of an organic carbon source such as methanol is required as the wastewater effluent no longer contains easily biodegradable organic pollutants. P can be removed by precipitation in the filter by adding a precipitation agent such as ferrous sulphate (Hultman et al. 1994). Some wastewater treatment plants in the Netherlands employ a constructed wetland as polishing step (Roeleveld et al. 2010), where nutrient removal can occur through combined uptake by vegetation and microorganisms, and further N removal by denitrification and PO_4^{3-} removal by adsorption and chemical precipitation with for instance iron or calcium present in the soil (Nichols 1983). Other systems for additional NO_3^- removal are ion exchange processes and different membrane technologies such as reverse osmosis. Due to the high costs associated with these technologies they usually are not applied (Roeleveld et al. 2010).

Microalgae exhibit the ability to assimilate N and P down to very low concentrations (Collos et al. 2005; Hwang et al. 1998) and can, therefore, be utilized to further reduce the N and P concentrations in wastewater effluent. Microalgae employ light energy and CO_2 to produce new biomass and in contrast to denitrifying sand filters, do not require an organic carbon source. Moreover, the addition of chemicals is not required for the precipitation of P as the P will be incorporated into the microalgal biomass. The N and P can potentially be recovered from the biomass produced by a microalgal system. Therefore, microalgae present an interesting and more sustainable alternative to existing post-treatment systems such as sand filters, and will be further investigated in this thesis.

THESIS OUTLINE

The objective of this thesis was to explore the possibilities of using microalgal biofilms for the treatment of municipal wastewater, with a focus on the post-treatment of municipal wastewater effluent. The potential of microalgal biofilms for wastewater treatment was first investigated using a scenario analysis in **Chapter 2**. Based on the area requirement, the effluent concentrations achieved, and the biomass production, the most interesting of the three investigated applications were indeed phototrophic biofilms for the post-treatment of municipal wastewater effluent and also symbiotic microalgal-bacterial biofilms for full wastewater treatment. These two applications were further investigated.

In **Chapter 3** biofilms were grown on wastewater treatment plant effluent in horizontal flow cells under different nutrient loads to determine the maximum uptake capacity of the biofilms for NO_3^- and PO_4^{3-}. It was possible to achieve the target effluent concentrations of 2.2 mg N/L and 0.15 mg P/L. Subsequently, microalgal biofilms were grown in a vertical laboratory-scale biofilm reactor, discussed in **Chapter 4**. The effect of harvesting and biofilm thickness on the biomass production and nutrient removal was investigated. Regular and partial harvesting of the biofilm proved to result in consistent low effluent nutrient concentrations at areal nitrogen and phosphorus removal rates of 0.69 g N/m^2/d and 0.073 g P/m^2/d.

The biofilm reactor was taken outdoors and a vertical pilot-scale biofilm reactor was evaluated as post-treatment of municipal wastewater in a pilot-study in **Chapter 5**. The biofilm reactor was placed at the wastewater treatment plant in Leeuwarden (the Netherlands) where it treated the effluent of this wastewater treatment plant from June until the end of October 2012. The areal nitrogen and phosphorus removal rates of 0.13 g N/m^2/d and 0.023 g P/m^2/d of the pilot-scale biofilm reactor were lower than the rates of the laboratory-scale reactor in Chapter 4.

Finally, symbiotic microalgal-bacterial biofilms were investigated for full treatment of (pre-settled) wastewater in **Chapter 6**. In these experiments the symbiotic biofilms grown in flow cells removed acetate without an external O_2 or CO_2 supply.

In **Chapter 7** the application of phototrophic biofilm reactors for the treatment of municipal wastewater is discussed by comparing the results of the laboratory-scale and pilot-scale biofilm reactor to the performance in the scenario analysis of Chapter 2. Furthermore, destinations are considered for the produced biomass and improvements are proposed for the biofilm reactor design.

Chapter 2

Scenario Analysis of Nutrient Removal from Municipal Wastewater by Microalgal Biofilms

Nadine C. Boelee
Hardy Temmink
Marcel Janssen
Cees J.N. Buisman
René H. Wijffels

ABSTRACT

Microalgae can be used for the treatment of municipal wastewater. The application of microalgal biofilms in wastewater treatment systems seems attractive, being able to remove nitrogen, phosphorus and COD from wastewater at a short hydraulic retention time. This study therefore investigated the area requirement, achieved effluent concentrations and biomass production of a hypothetical large-scale microalgal biofilm system treating municipal wastewater. Three scenarios were defined: using microalgal biofilms: (1) as a post-treatment; (2) as a second stage of wastewater treatment, after a first stage in which COD is removed by activated sludge; and (3) in a symbiotic microalgal/heterotrophic system. The analysis showed that in the Netherlands, the area requirements for these three scenarios range from 0.32 to 2.1 m^2 per person equivalent. Moreover, it was found that it was not possible to simultaneously remove all nitrogen and phosphorus from the wastewater, because of the nitrogen:phosphorus ratio in the wastewater. Phosphorus was limiting in the post-treatment scenario, while nitrogen was limiting in the two other scenarios. Furthermore, a substantial amount of microalgal biomass was produced, ranging from 8 to 59 g per person equivalent per day. These findings show that microalgal biofilm systems hold large potential as seasonal wastewater treatment systems and that it is worthwhile to investigate these systems further.

INTRODUCTION

The conventional treatment of municipal wastewater consists of activated sludge processes with a combination of nitrification and denitrification and biological or chemical phosphorus removal. However, other treatment systems are also used, including systems based on microalgae, eukaryotic microorganisms and prokaryotic cyanobacteria that carry out oxygenic photosynthesis (Brock et al. 2000). Microalgae have a high affinity for nitrogen (N) and phosphorus (P), illustrated by the low values reported for half-saturation constants, ranging from 0.56 to 3094 µg N/L, and from 0.001 to 81.9 µg P/L (Collos et al. 2005; Hwang et al. 1998; Halterman and Toetz 1984; Eppley et al. 1969). Microalgae can either grow in suspension (phytoplankton) or on substrata (benthic) in biofilms (Stevenson 1996). Microalgal biofilms are attached microbial consortia of phototrophs and chemotrophs entrapped in an exopolymeric matrix, and are omnipresent in aquatic environments (Di Pippo et al. 2011; Sekar et al. 2002). Although not given a lot of attention, microalgal biofilms systems could form interesting wastewater treatment systems. A microalgal biofilm system can operate at short hydraulic retention times due to the ability of the biofilm to retain the biomass. It is also expected that, in contrast to suspended microalgal systems, little or no separation of microalgae and water is required before discharging the effluent (Roeselers et al. 2008; Schumacher et al. 2003). Furthermore, no mixing is needed in the system, resulting in a lower energy requirement than for suspended systems.

Algal biofilms systems can be composed of large biofilm panels over which the wastewater flows. These panels can either be placed horizontally, at an angle such as the Algal Turf Scrubber (Craggs et al. 1996), or vertically in rows such as the Twin Layer system (Shi et al. 2007). Such microalgal biofilms may be used at different stages of the wastewater treatment. A first scenario is using microalgal biofilms as a post-treatment system. In light of the EU Water Framework Directive objective to obtain good chemical and ecological status for all surface waters by 2015, this can be an interesting concept. The high affinity of microalgae for N and P and the lack of requirement of an organic carbon source are advantages over currently available post-treatment systems. A microalgal biofilm can also be used to remove N and P after a highly loaded activated sludge system. The microalgal biofilm then serves as an alternative for nitrification and denitrification and chemical or biological P removal. This scenario holds the advantages of a higher net heterotrophic biomass yield, and a lower energy input for aeration compared to a conventional wastewater treatment system.

A third option is applying an algal-bacterial biofilm to treat the wastewater directly. This scenario makes use of a symbiotic relationship that may develop when using microalgae and heterotrophs together. During this symbiosis the microalgae produce

oxygen (O_2) that is needed by aerobic heterotrophs, and the carbon dioxide (CO_2) that is released by these heterotrophs is in turn used by the microalgae. In this manner no external O_2 supply is needed, which saves the energy otherwise required for aeration of the activated sludge system.

Previous studies have shown that microalgal biofilms systems can achieve good removal of N and P from wastewater. Removal capacities over 90% were measured for ammonium (NH_4^+), nitrate (NO_3^-) and over 80% for phosphate (PO_4^{3-}) (de Godos et al. 2009; González et al. 2008; Shi et al. 2007), and up to 75% of the Chemical Oxygen Demand (COD) was removed from diluted swine manure in an algal-bacterial biofilm (González et al. 2008). However, the feasibility of the application of microalgal biofilms in wastewater treatment will be determined by more factors than the removal capacity. These factors include the achieved effluent concentrations, biomass production and the area requirement. Especially the latter is a point of concern, as algal systems are known for their relatively large area requirement. Unfortunately, little is known about these aspects of microalgal biofilms and how the three different scenarios mentioned above compare.

This study aims to get insight in the feasibility of using microalgal biofilms for municipal wastewater treatment. A scenario analysis will be performed for the three different concepts of using microalgal biofilms in municipal wastewater treatment. This analysis compares the area requirement, achieved effluent concentrations and biomass production under the conditions of municipal wastewater treatment in the Netherlands. In addition, this study seeks to determine what knowledge is still lacking in order to be able to make a final conclusion on the feasibility of microalgal biofilms in wastewater treatment.

MATERIAL AND METHODS

Scenarios

Three different scenarios were defined in which microalgae are integrated in a municipal wastewater treatment plant (WWTP), as shown in Figure 2.1. In Scenario 1 the microalgal biofilm system is used as a post-treatment system for effluent from an activated sludge process. In Scenario 2 the first stage of wastewater treatment removes the bulk of the COD. Nitrification is prevented in this stage by operating at a short sludge retention time (SRT; 2.5 days). The second stage consists of a microalgal biofilm system removing N and P. In contrast to Scenario 1, N is mainly present as NH_4^+ rather than NO_3^-. In Scenario 3 the microalgae are used in a symbiotic process of algae and bacteria.

N is removed by combined nitrification and denitrification and via assimilation by microalgae, COD is removed by heterotrophs, and P is mainly assimilated by microalgae.

In all scenarios the target effluent values were 2.2 mg/L total N and 0.15 mg/L total P. These values are the maximum tolerable risk (MTR) guidelines which are used by the Dutch water boards, as the classification of the good chemical and ecological status of surface water of the Water Framework Directive is not yet known.
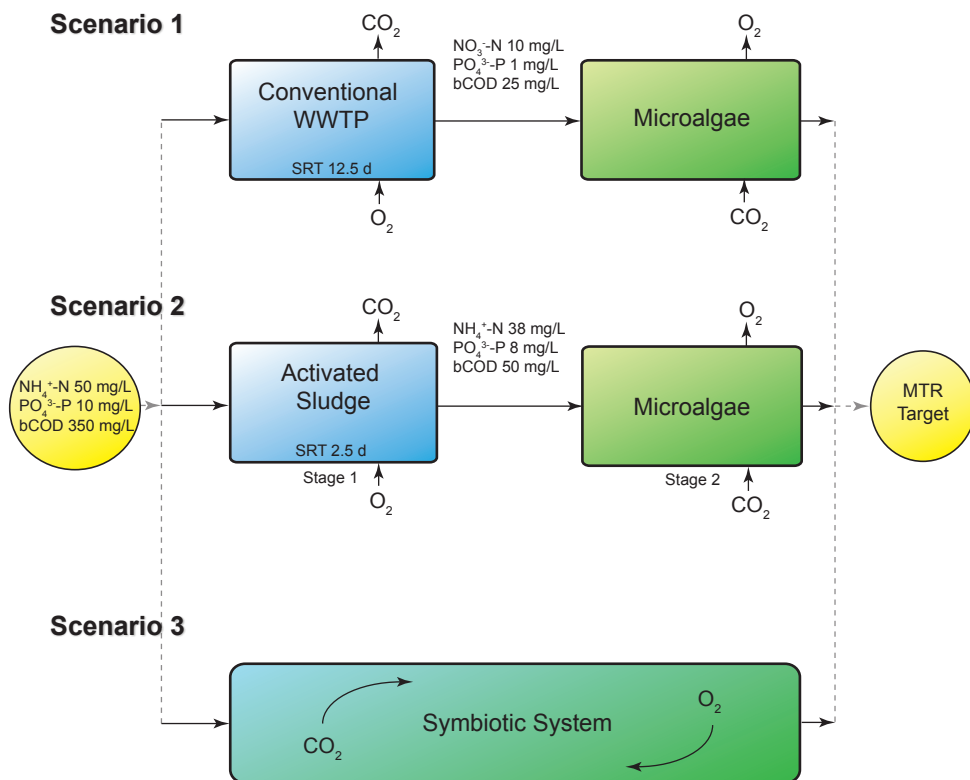
Figure 2.1 — Schematic overview of the three different scenarios of using microalgal biofilms in municipal wastewater treatment. The incoming wastewater and target effluent MTR values of 2.2 mg/L N and 0.15 mg/L P are equal for all scenarios. The sludge retention time (SRT) is shown for the activated sludge compartments of Scenarios 1 and 2.

Calculations and Parameters

Microalgae

The WWTP in this study was located in the Netherlands and receives wastewater from 100 000 inhabitants producing 130 L per person equivalent (PE) per day. In the Netherlands, microalgal systems offer the highest potential at tourist locations during the period late spring-early autumn, when an increased wastewater production is accompanied by the highest irradiation of the year. Therefore, only the period late spring-early autumn was considered in this analysis, corresponding with the tourist season. The microalgal biofilm system therefore receives irradiation summed over the months May until October. The microalgae utilize 43% of this irradiation, equivalent to the photosynthetic active radiation (PAR, 400–700 nm). The variation of irradiance during the day and over these months has not been taken into account, but will be discussed subsequently. The summed irradiation was equal to 4773 mol photons/m^2 (see Appendix A).

An important parameter of the microalgal system is the quantum requirement of the photosynthetic process. This is the efficiency with which the microalgae take up light energy and convert it to chemical energy, i.e., new biomass, while releasing O_2. Under low light intensities, approximately 10 PAR photons are required for the liberation of one molecule of O_2 (Bjorkman and Demmig 1987; Ley and Mauzerall 1982). At higher light intensities, photosaturation takes place and part of the absorbed light is lost in the form of heat. Considering this photosaturation effect, a vertical positioning of the microalgal biofilm system is proposed and a minimal quantum requirement of 20 PAR photons per O_2 is envisioned (Qiang et al. 1998). This corresponds to a maximum oxygen quantum yield (QY_{O2}) of 0.05 O_2/photon. With QY_{O2} the amount of O_2 produced per photons received per m^2 of ground area is calculated:

$$R_{o,A,algae} = QY_{O2} \cdot PFD \quad [mol/m^2/d] \tag{2.1}$$

with $R_{o,A,algae}$ the areal oxygen production by microalgae [mol/m^2/d] and PFD the photon flux density [mol photons/m^2/d].

The following stoichiometrical reactions are used for microalgae, with either nitrate (assumed in scenario 1) or ammonium (assumed in scenario 2 and 3) as nitrogen source:

$$CO_2 + 0.94H_2O + 0.12NO_3^- + 0.01H_2PO_4^- \rightarrow CH_{1.78}O_{0.36}N_{0.12}P_{0.01} + 1.42O_2 + 0.13OH^- \tag{2.2}$$

$$CO_2 + 0.70H_2O + 0.12NH_4^+ + 0.01H_2PO_4^- \rightarrow CH_{1.78}O_{0.36}N_{0.12}P_{0.01} + 1.18O_2 + 0.11H^+ \tag{2.3}$$

The areal amount of biomass produced ($P_{x,A,algae}$) is calculated with Equation 2 or 3; 1.42 mol O_2 coincides with 1 mol of biomass (on C-basis) in case of NO_3^- uptake or 1.18 mol O_2 with 1 mol of biomass in case of NH_4^+ uptake. This biomass is assumed to be present in a biofilm kept at optimal thickness through regular harvesting of the biofilm. Keeping the biofilm at this thickness will reduce respiration losses and ensure an optimal nutrient uptake capacity.

It is expected that the microalgal biofilm will be composed of a mixed culture of microalgae, due to varying conditions with respect to temperature, and N and P concentrations. An average microalgal biomass composition was assumed for this mixed culture of 7.8% N and 1.4% P (w/w, based on algal biomass of $CH_{1.78}O_{0.36}N_{0.12}P_{0.01}$) (Duboc et al. 1999; Ahlgren et al. 1992; Healey 1973). With the amount of biomass produced known and the fraction of N and P present in the biomass, the uptake of N and P from the wastewater is calculated. The following calculation shows the uptake of N, but the calculation of the P uptake is equivalent:

$$R_{N,A,algae} = P_{x,A,algae} \cdot f_{N,algae} \quad [g/m^2/d] \tag{2.4}$$

with $R_{N,A,algae}$ the areal N uptake rate by microalgae [$g/m^2/d$], $P_{x,A,algae}$ the areal microalgal biomass production rate [$g/m^2/d$] and $f_{N,algae}$ the fraction of N in the microalgal biomass [g/g].

Using the desired amount of N or P removed, the area was calculated as:

$$A = \frac{Q \cdot (N_{in} - N_{out})}{R_{N,A,algae}} \quad [m^2] \tag{2.5}$$

with A the area [m^2] and Q the flowrate [m^3/d].

Heterotrophs

It was assumed that biomass production in the activated sludge process is only accounted for by the heterotrophic biomass converting COD. The following formula is used (Metcalf & Eddy 2003):

$$P_{x,sludge} = Q \cdot Y_{sludge} \cdot \frac{(COD_{b,in} - COD_{b,out})}{1 + k_d \cdot SRT} \cdot (1 + f_d \cdot k_d \cdot SRT) \quad [g\ VSS/d] \tag{2.6}$$

with $P_{x,sludge}$ the sludge production [g volatile suspended solids (VSS)/d], Y_{sludge} the biomass yield [g VSS/g bCOD], SRT the sludge retention time [d], f_d the fraction remaining as cell debris [g VSS/g VSS] and k_d the decay coefficient [d^{-1}].

The sludge in the WWTP was assumed to have an average composition of 12% N and

2% P (w/w based on sludge biomass of $C_1H_{1.4}O_{0.4}N_{0.2}$) (Metcalf & Eddy 2003). With the amount of biomass produced known and the fraction of N and P present in the biomass, the uptake of N ($R_{N,sludge}$) and P from the wastewater is calculated. Calculation shown for N:

$$R_{N,sludge} = P_{x,sludge} \cdot f_{N,sludge} \quad [g/d] \tag{2.7}$$

Additional calculations of O_2 and CO_2 production and consumption, and a list of all parameters can be found in Appendix A.

2 RESULTS

Table 2.1 shows the area requirement of the microalgal biofilm and the corresponding effluent concentrations for the different scenarios. The area requirements are based on the calculated uptake capacities of 1.85 g N/m²/d and 0.34 g P/m²/d in Scenario 1 and 2.2 g N/m²/d and 0.41 g P/m²/d in Scenarios 2 and 3. The area requirement of the post-treatment system of Scenario 1 is the smallest with 0.32 m²/PE, followed by the symbiotic system of Scenario 3 requiring 0.76 m²/PE. The large area requirement of 2.1 m²/PE of Scenario 2 in comparison to Scenarios 1 and 3 was due to the larger amount of N that needed to be assimilated by the microalgae in this scenario.

Table 2.1 — *The required ground area and effluent concentrations of N and P of a microalgal biofilm system treating wastewater from 100 000 inhabitants in the Netherlands during May to October for the three different scenarios.*

	Area requirement (m²/PE)	Effluent total N (mg/L)	Effluent total P (mg/L)
Scenario 1	0.32	5.39	0.15
Scenario 2	2.10	2.20	1.40
Scenario 3	0.76	2.20	6.07

The limiting nutrient was found to be P for Scenario 1 and N for Scenarios 2 and 3. The calculations were therefore performed for P reaching the desired MTR value in Scenario 1 and for N reaching the desired value for Scenarios 2 and 3. Consequently, in the P limiting Scenario 1, the N concentration remained above target with 5.39 mg N/L, while in the N limiting Scenarios 2 and 3 the P concentration remained above target. The latter two also did not comply with current EU effluent discharge requirements of 1 mg P/L. Consequently, the desired effluent values for both N and P could not be reached simultaneously.

In Scenario 3, a symbiotic relationship between microalgae and heterotrophs was assumed to develop. The O_2 production by the microalgae and the O_2 consumption

by the heterotrophs were balanced, by adjusting the fraction of N that was removed by combined nitrification and denitrification and the fraction that was assimilated by microalgae. Figure 2.2 shows that the O_2 in the system was balanced when 70% of the NH_4^+ was converted by the heterotrophs (nitrification-denitrification) and the remaining 30% by the microalgae. With this balance, the microalgae supply all O_2 for the heterotrophs, and aeration is theoretically not needed. However, it can also be seen from Figure 2.2 that the CO_2 production and consumption could not be balanced at the same time. Approximately 40% additional CO_2 needs to be supplied or fixed by the microalgae from the air.
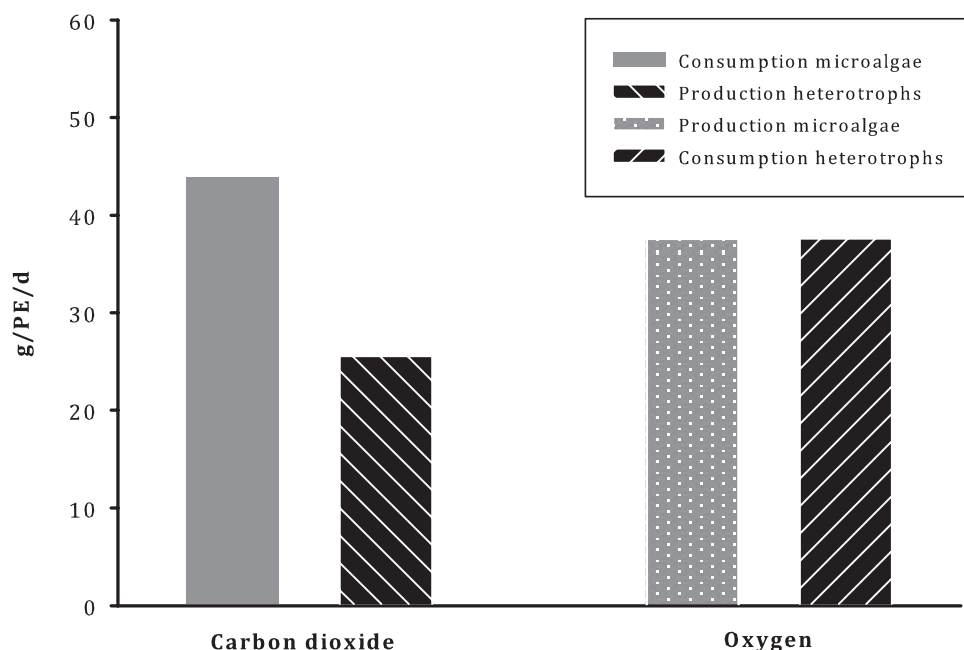
Figure 2.2 *— The consumption of CO_2 by microalgae alongside the production of CO_2 by heterotrophs, and the production of O_2 by microalgae alongside the consumption of O_2 by heterotrophs in the symbiotic system of Scenario 3. The amounts are expressed in gram per person equivalent (PE) per day.*

Figure 2.3 shows the amount of activated sludge and microalgal biomass produced in the three different scenarios. The microalgal biomass per PE was based on the calculated microalgal biomass production of 24 $g/m^2/d$ in Scenario 1 and 28 $g/m^2/d$ in Scenarios 2 and 3. In Scenario 1 similar amounts of activated sludge and microalgal biomass were produced. Scenario 2 had the largest microalgal biomass production of 59 g/PE/d, because larger amounts of nutrients needed to be assimilated in this scenario.
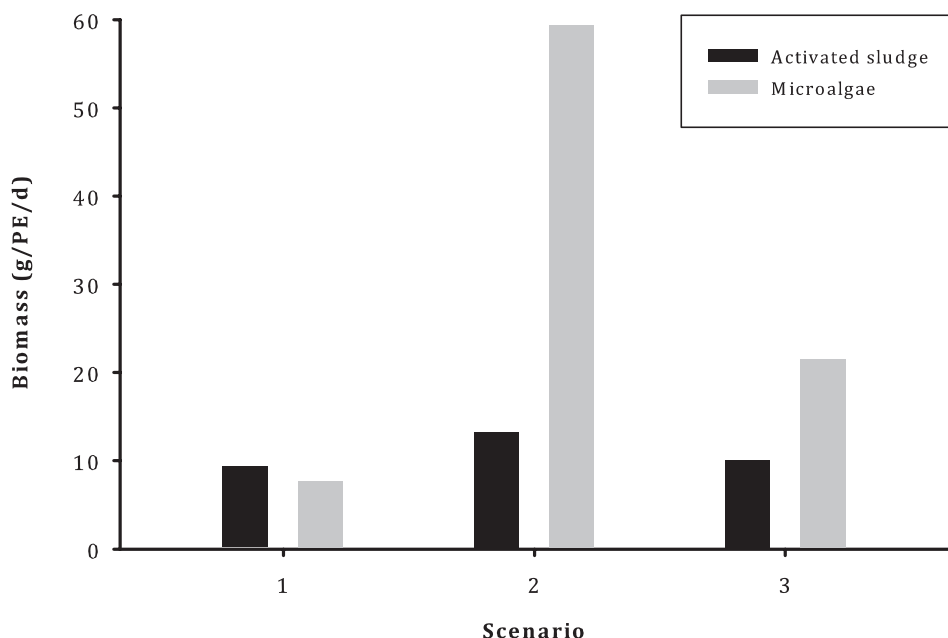
Figure 2.3 — *The microalgal biomass and activated sludge in the three scenarios for a WWTP of 100 000 inhabitants in the Netherlands from May to October. The amount of activated sludge is expressed in grams volatile suspended solids (VSS) and the amount of microalgae in grams dry weight, both per person equivalent (PE) per day.*

DISCUSSION

Effluent Concentrations

The results of this scenario analysis showed that it was not possible to simultaneously remove the N and P in the wastewater to the target values of 2.2 mg N/L and 0.15 mg P/L. In the post-treatment scenario P, while in Scenarios 2 and 3 N was limiting the microalgae growth. Indeed, given the ratio of N:P in wastewater, N will always be the limiting nutrient, if the molar ratio of C:N:P of 100:12:1 represents the real average elemental composition of microalgae grown in such systems. However, elemental composition in microalgae is known to be highly variable. Compositions with C:P ratios between 34:1 and 418:1, and N:P ratios between 3.5:1 and 38:1 are reported in literature for different species of microalgae (Ho et al. 2003; Ahlgren et al. 1992). Also the growth conditions, with respect to nutrient and/or light limitation, influence the elemental composition. Molar N:P ratios as low as 3:1 have been reported under N limiting conditions, while under conditions of P limitation a N:P ratio of 100:1 is possible (Elrifi and Turpin 1985; Goldman et al. 1979). At low growth rates, the N:P ratio of the

biomass composition can sometimes match the supply ratio. Especially luxury uptake of P with storage as polyphosphate, is known to take place in microalgae (Powell et al. 2008; Klausmeier et al. 2004). This luxury uptake might make it possible to not only achieve MTR quality with respect to N, but also with respect to P.

In the scenario analysis only N and P removal by microalgal assimilation was taken into account. Additional removal of P by precipitation with cations such as calcium and magnesium is also possible. This precipitation occurs at higher pH levels caused by microalgae changing the CO_2/HCO_3^-/CO_3^{2-} equilibrium when more CO_2 is taken up than can be supplied via absorption from the atmosphere (Roeselers et al. 2008; Powell et al. 2008). With such a pH rise expected within the biofilm, it is likely that in practice a larger P removal occurs than was calculated.

Area Requirement

This study found area requirements for the three scenarios between 0.32 and 2.1 m^2/PE. A conventional WWTP is estimated to have an area requirement around 0.2–0.4 m^2/PE. Hence, with 0.32 m^2/PE, the microalgal post-treatment requires a similar area to that of the activated sludge plant. The two-stage system of Scenario 2 requires the largest area of 2.1 m^2/PE. However, the first activated sludge stage will be considerably smaller than in a conventional WWTP, because nitrification is absent. In addition, more sludge is produced, and this sludge will have a higher energy value. This implies that more methane can be produced when digesting the sludge anaerobically.

The symbiotic system of Scenario 3 has an area requirement of 0.76 m^2/PE, which is smaller than the area of the system of Scenario 2, and similar to the conventional WWTP combined with microalgal post-treatment in Scenario 1. Moreover, this system has the advantage that the O_2 production by microalgae and O_2 consumption by heterotrophs can be balanced. This balance implies no need for an external oxygen supply, giving energy and cost savings. Although very attractive, the technology required to support a symbiotic biofilm system still needs to be developed.

The area requirements are based on the calculated uptake capacities of 1.85 g N/m^2/d and 0.34 g P/m^2/d in the post-treatment scenario and 2.2 g N/m^2/d and 0.41 g P/m^2/d in Scenarios 2 and 3. These calculated uptake capacities are higher than the 0.1–0.6 g N/m^2/d and 0.006–0.09 g P/m^2/d measured in lab-scale biofilm systems (de Godos et al. 2009; González et al. 2008), but lower than the 0.7–2.1 g P/m^2/d measured in other pilot scale microalgal biofilms systems (Christenson and Sims 2012; Craggs et al. 1996). This indicates that the calculated uptake capacities in this study can be considered a good average estimation.

The area requirement calculated for the different microalgal systems depends on the elemental composition of microalgal biomass, as well as on the irradiance and the photosynthetic efficiency. As mentioned above, the elemental composition can vary in microalgae. Clearly a higher N and P content in the microalgae will result in a lower area requirement, while a lower content will increase the required area. This again illustrates the importance of knowing the real elemental composition of the microalgae when growing on wastewater.

The effect of irradiance on the area requirement can only be changed by either moving the system to another location, or by applying artificial illumination. However, the addition of artificial light yields no substantial area reduction. If all produced biomass, both activated sludge as well as microalgal biomass, would be converted into biogas to produce electricity for artificial light, the area reduction for the three scenarios is at most 0.8% (see Appendix B). This extremely low reduction is related to the energy losses in the process of methanogenesis, in converting biogas into electricity, electricity into light and light into new biomass via photosynthesis. Clearly these large scale microalgae based processes can only be fueled by sunlight.

In this analysis the oxygen quantum efficiency was assumed to be 0.05 mol O_2/mol photons. This value is not reached in horizontal microalgal systems, but has been reached in vertical panel photobioreactors (Qiang et al. 1998). This efficiency has been determined with light as the limiting substrate. However, it is likely that CO_2 limitation will occur when the biofilm is only exposed to ambient air. Modeling of microalgal biofilms has shown that CO_2 limitation can easily occur, the level of limitation depending on the bulk pH and alkalinity (Liehr et al. 1988). Therefore, the assumed efficiency can only be reached in a vertical biofilm system, if CO_2 limitation can be prevented. Using heterotrophic microorganisms to directly supply the CO_2 to the microalgae as in Scenario 3, may therefore be a very attractive way to accomplish this.

Seasonal Variation in Temperature and Light Intensity

Both microalgal growth and uptake of N and P decrease at lower temperatures and light intensity (Goldman and Carpenter 1974). Therefore, the capacity of the microalgal system will change throughout the day and the seasons. Low uptake of nutrients by microalgae during winter may be one of the main limitations of the application of microalgal wastewater treatment systems in a country such as the Netherlands. In this scenario analysis, the system was assumed to be running only in the tourist season, from May until October. The application of the microalgal system in places where a much higher capacity is needed during summer is the most interesting application of this technology in the Netherlands. The microalgal system will provide additional capacity during

summer, whereas during winter the existing WWTP capacity will be sufficient. Such a microalgal system may be applied on the islands in the Wadden Sea of the Netherlands, being a tourist location during summer. On the island Ameland for example, wastewater production during summer can be more than three times the amount during the rest of the year. With these conditions a microalgal biofilm system is an interesting option to treat the additional wastewater in summer, instead of increasing the size of the wastewater treatment plant to be able to treat the summer wastewater load.

Daily Variation in Light Intensity

The microalgae production was based on the total irradiation received in five months, and therefore the diurnal light cycle was not taken into account. In general, uptake of N and P by microalgae changes throughout the day and is faster during daytime than in the dark (Klausmeier et al. 2004; Elrifi and Turpin 1985). N-limited microalgae, on the other hand, are known to take up either NO_3^- or NH_4^+ in the dark. Uptake of NH_4^+ can be more than 50% of the daylight value in N-limited microalgae (Vona et al. 1999). Consequently, when N is the limiting nutrient for microalgae in the treatment of municipal wastewater, considerable uptake of N during darkness might be expected. In addition, the wastewater loading rate of N and P is expected to be lower during the night, possibly compensating for the reduced nutrient uptake.

Application of Microalgal Biomass

When using microalgal biofilm systems in wastewater treatment, substantial amounts of microalgal biomass are produced. In Scenario 1 the microalgal biomass production was 24 g/m^2/d based on the consumption of NO_3^- and in Scenarios 2 and 3 the production was 28 g/m^2/d based on the consumption of NH_4^+. These biomass productions are slightly higher than biomass production of 11–18 g/m^2/d measured in pilot photobioreactors (Min et al. 2011; Hulatt and Thomas 2011) and in the range of biomass production of 24–31 g/m^2/d measured in other biofilm pilot systems (Christenson and Sims 2012; Craggs et al. 1996). With this biomass production, a WWTP for 100 000 inhabitants with the microalgal post-treatment of Scenario 1 produces 1.2 $\cdot 10^5$ kg (dry weight) microalgal biomass during the five summer months of operation. In Scenarios 2 and 3 this amount of biomass is even larger. With such a substantial amount of biomass, it is important to find an efficient way to harvest the biomass, and a proper destination.

To ensure an actively growing biofilm, and to prevent washout of valuable biomass with the effluent, the biofilm will need to be harvested regularly. This regular harvesting will reduce respiratory biomass losses or even cell death, which otherwise would lead to release of N and P from the biofilm. Two ways of harvesting can be distinguished, passive

and active. Passive harvesting entails collecting the microalgal biomass that naturally detaches from the top of the biofilm when it ages. This might involve the addition of a settler tank, resulting in extra area requirement. Active harvesting techniques currently applied to remove biofilms in other systems include pH shock (Knuckey et al. 2006), backwashing and scraping. Active harvesting appears more attractive as it gives the possibility to harvest very regularly, hereby reducing the respiratory losses as much as possible.

Nitrogen was shown to be the limiting nutrient when integrating microalgal biofilms in the wastewater treatment (Scenarios 2 and 3). In this case, it might be possible to accumulate lipids in the microalgal biomass, as microalgae start to accumulate these under conditions of N-limitation (Converti et al. 2009; Solovchenko et al. 2008). To achieve this N-starvation and induce lipid accumulation the C:N ratio should be twice as high as was assumed in the scenario analysis. Although this increased ratio would result in an area requirement twice as large, the amount of produced biomass will also be doubled and thus larger amounts of lipids may be produced. In Scenario 1 these lipids would approximately amount to 79 ton during the five summer months of operation (see Appendix C). However, further research is still needed to induce the accumulation of specific desired lipids, to obtain a stable (mixed) culture of the desired species in the system, and to set up the biorefinery needed to extracts these lipids as well as valorize the remaining biomass constituent (Hulatt and Thomas 2011; Vona et al. 1999).

Depending on the microalgal biomass composition other products might also be possible. Using the biomass as fertilizer is very attractive but is only possible when no heavy metals or other recalcitrant compounds are present in the wastewater and accumulated by microalgae. Anaerobic digestion for biogas production is another possibility, although afterwards still autotrophic N and P removal or recovery will be necessary. The CO_2 that is produced during digestion might be recycled to the microalgal biofilm system as an additional CO_2 supply (Mussgnug et al. 2010; Muñoz and Guieysse 2006).

CONCLUSIONS

This study investigated the potential of a hypothetical microalgal biofilm system as a seasonal wastewater treatment system in the Netherlands. The analysis showed that the area requirement of the microalgal biofilm system was 0.32 m^2/PE for a post-treatment system, 2.10 m^2/PE for a two stage wastewater treatment system and 0.76 m^2/PE for a one-stage symbiotic system. In addition, it was found that microalgae growing on wastewater treatment plant effluent are P limited and microalgae growing on untreated or partially treated wastewater are N limited. The microalgae will

produce a substantial amount of biomass. For the application of microalgal biofilms in countries such as the Netherlands, further research should look into the effect of the daily variation of both the wastewater flows and of the irradiation and temperature. In addition, the destination of the produced biomass is an important topic for future studies. Finally, real (pilot) tests should be performed to establish if indeed a photosynthetic efficiency of 0.05 mol O_2/mol photons can be reached and whether CO_2 limitation will occur.

ACKNOWLEDGEMENTS
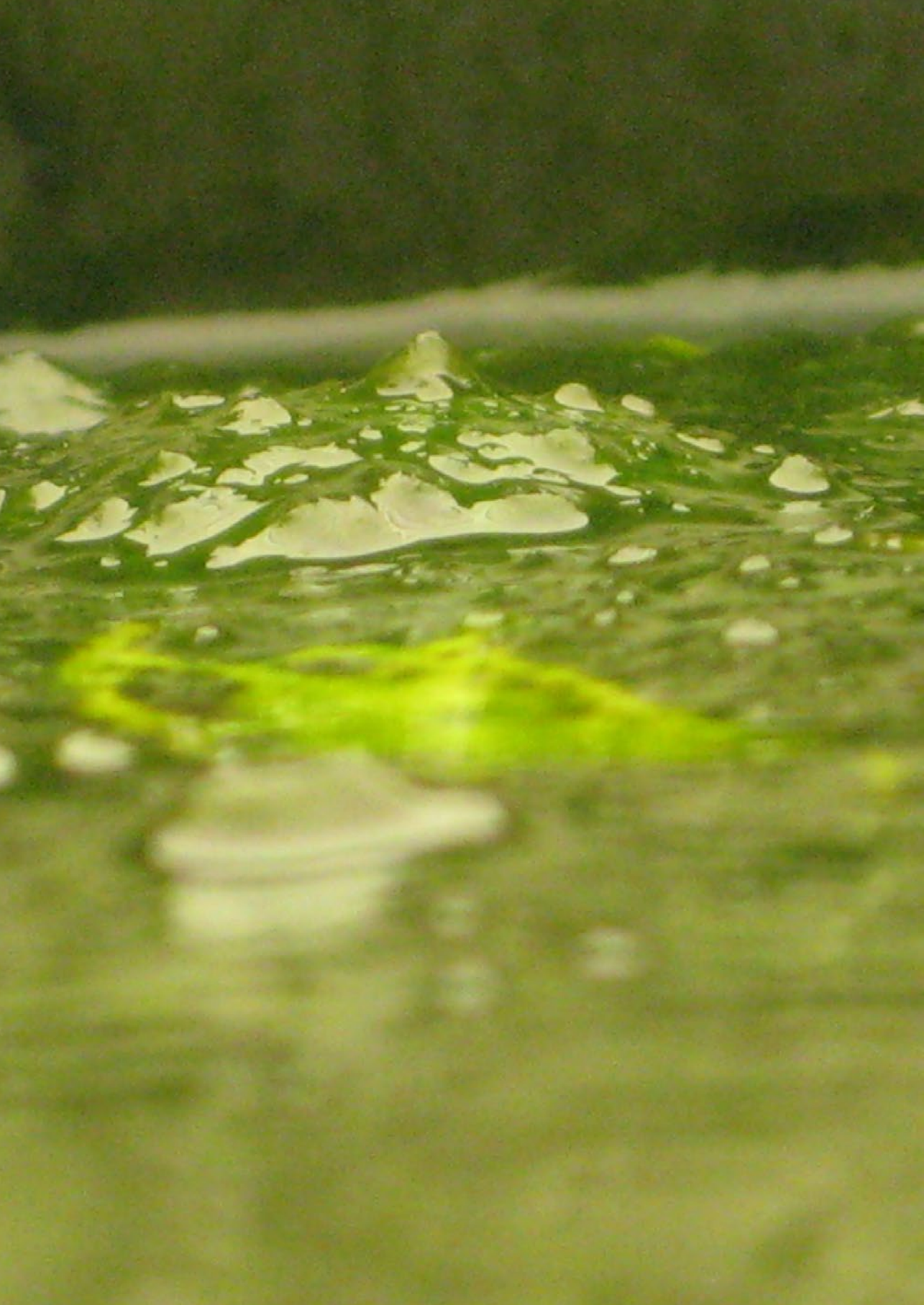
Chapter 3

Nitrogen and Phosphorus Removal from Municipal Wastewater Effluent Using Microalgal Biofilms

Nadine C. Boelee
Hardy Temmink
Marcel Janssen
Cees J.N. Buisman
René H. Wijffels

ABSTRACT

Microalgal biofilms have so far received little attention as post-treatment for municipal wastewater treatment plants, with the result that the removal capacity of microalgal biofilms in post-treatment systems is unknown. This study investigated the capacity of microalgal biofilms as a post-treatment step for the effluent of municipal wastewater treatment plants. Microalgal biofilms were grown in flow cells with different nutrient loads under continuous lighting of 230 μmol/m^2/s (PAR photons, 400-700 nm). It was found that the maximum uptake capacity of the microalgal biofilm was reached at loading rates of 1.0 g/m^2/day nitrogen and 0.13 g/m^2/day phosphorus. These maximum uptake capacities were the highest loading rates at which the target effluent values of 2.2 mg/L nitrogen and 0.15 mg/L phosphorus were still achieved. Microalgal biomass analysis revealed an increasing nitrogen and phosphorus content with increasing loading rates until the maximum uptake capacities. The internal nitrogen to phosphorus ratio decreased from 23:1 to 11:1 when increasing the loading rate. This combination of findings demonstrates that microalgal biofilms can be used for removing both nitrogen and phosphorus from municipal wastewater effluent.

3

INTRODUCTION

Microalgae have been used to treat wastewater in large ponds for many years. Interest in microalgae and wastewater treatment has been renewed by recent findings suggesting that microalgal biofuel production could be made economically viable and sustainable when using wastewater as a nutrient supply (Pittman et al. 2011; Clarens et al. 2010; Wijffels et al. 2010). The costs of harvesting microalgae from diluted suspensions has led to the investigation of alternative microalgal systems, including biofilms (Shi et al. 2007). Microalgal biofilm systems have the advantage that they are able to retain the biomass, while operating at a short hydraulic retention time. It is also expected that little or no separation of microalgae and water is required before discharging the effluent (Roeselers et al. 2008; Schumacher et al. 2003), presumably making harvesting much easier than in suspended systems. Moreover, no stirring is needed in the system, resulting in a lower energy requirement compared to suspended microalgal systems. Nevertheless, the performance of algal biofilm systems could be limited by photoinhibition and diffusion limitation of nutrients or carbon dioxide (CO_2) (Murata et al. 2007; Liehr et al. 1988).

So far, little attention has been given to the possibility of using microalgal biofilms as a post-treatment system for municipal wastewater. However, the EU Water Framework Directive's objective to obtain good chemical and ecological status for all surface waters by 2015, leads to the need for wastewater treatment plants to further reduce their nitrogen (N) and phosphorus (P) emissions. Microalgae have the ability to assimilate N and P down to very low concentrations (Collos et al. 2005; Hwang et al. 1998). With this ability and the potential to recover N and P from the algal biomass, microalgae present an interesting and more sustainable alternative to existing post-treatment systems such as denitrifying filters, which require an organic carbon source and emit CO_2.

The aim of this study was to investigate whether microalgal biofilms can be used as a post-treatment system for municipal wastewater treatment plants. The main issues addressed in this study are the uptake capacity and the final effluent concentrations obtained by the microalgal biofilms. The values 2.2 mg/L total N and 0.15 mg/L total P were used as target values for the effluent processed by the microalgal biofilms. These values are currently in use by the Dutch water boards as discharge guidelines for sensitive water bodies, and were used in this study because the classification of a good chemical and ecological status of surface water of the Water Framework Directive is yet unknown. Furthermore, the biomass growth, composition and washout, as well as the photosynthetic efficiency of the biofilm were studied in order to evaluate the potential of the microalgae biofilm process as post-treatment system.

MATERIAL AND METHODS

Experimental Setup

All experiments were performed in a system consisting of a flow cell (STT products B.V., the Netherlands) with an inflow of (synthetic) wastewater effluent, and a recycle vessel with both an outflow of effluent and a recycle flow back to the flow cell. This system is shown in Figure 3.1. In the horizontal flow cell, a water layer of 2 cm flowed over a 1 mm plastic sheet (PVC; 0.018 m^2), on which the microalgal biofilm grew. The microalgal biofilm was continuously illuminated by a bank of fluorescent lamps (CF-LE 55W/840, Sylvania, UK) at a light intensity of 230 μmol/m^2/s (PAR photons, 400-700 nm). Light intensity was measured with a 2π PAR quantum sensor (SA190, LI-COR Biosciences, USA) at the level of the biofilm surface. The transparent top of the flow cell contained an outlet covered by a septum, through which gas formed during the experiment was sampled and removed. In the 400 mL recycle vessel, the pH was measured and controlled at pH 7 by pulse-wise addition of CO_2 gas. The temperature was controlled at 22°C with the water jacket of the recycle vessel. The dissolved oxygen concentration was measured continuously (InPro 6050/120, Mettler Toledo, Switzerland) at the inlet and outlet of the flow cell. Using the oxygen measurement at the inlet of the flow cell, the dissolved oxygen concentration in the inflowing synthetic wastewater was controlled at 35% air saturation by pulse-wise addition of N_2 gas to the recycle vessel.
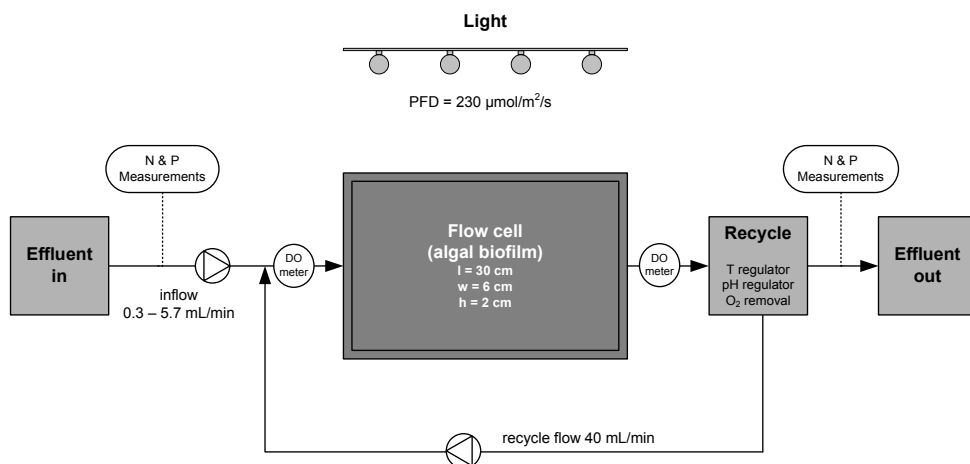
Figure 3.1 — Schematic overview of the experimental setup.

The inflow of synthetic wastewater effluent was adjusted between 0.3 mL/min and 5 mL/min, depending on the desired nitrogen and phosphorus load. The recycle flow was 40 mL/min, giving laminar flow velocities of about 0.6 mm/s and a retention time inside the flow cell of around 9 minutes. Based on the large recycle flow which was efficiently mixed with the influent before entering the flow cell, and on visual observations, it can be safely assumed that all of the biofilm was exposed to the same loading rate. The effluent flow was collected and stored for a maximum of 24 hours at 2°C, in order to measure the microalgal dry weight in the effluent. To prevent microalgal growth in the system outside the flow cell, all tubing was black, glassware was brown and all glassware and connections were covered in aluminum foil.

Table 3.1 shows the 18 experiments with their loading rates, duration, and corresponding hydraulic retention times (HRTs). The NO_3^--N and PO_4^{3-}-P concentrations were measured daily in the influent and effluent and the suspended solids were measured daily in the effluent. At the end of the experiment the biomass was harvested by scraping the biofilm from the plastic sheet. From 11 experiments this wet microalgal biomass was frozen at -80°C until analyses were performed to determine the total amount of biomass and its C, N, P content.

3

Table 3.1 — *Settings of the experiments performed in the flow cells with loading rates, duration time and hydraulic retention time (HRT).*

Experiment	Load NO_3^--N (g N/m^2/d)	Load PO_4^{3-}-P (g P/m^2/d)	Duration experiment (d)	HRT system (d)
1[a]	0.11	0.011	9	1.9
2[a]	0.17	0.018	11	1.4
3	0.18	0.022	15	1.5
4[a,b]	0.22	0.039	10	1.4
5[a]	0.31	0.033	11	0.8
6	0.34	0.033	21	2.3
7[a]	0.36	0.034	9	0.6
8[a,b]	0.45	0.078	10	0.7
9[a]	0.52	0.076	14	3.5
10	0.64	0.079	13	0.4
11[a]	0.78	0.072	15	0.7
12[a]	1.01	0.094	15	0.5
13	1.23	0.126	22	0.6
14	1.23	0.126	25	0.6
15[a]	1.49	0.152	13	0.4
16[a]	1.97	0.200	13	0.3
17[a]	3.60	0.399	12	0.2
18[a]	4.53	0.502	12	0.1

[a] Biomass collected at the end of the experiment.
[b] Experiments performed with real wastewater effluent, all other experiments were performed with synthetic wastewater effluent.

Microalgal Biofilm Cultivation

Microalgae were scraped off the surface of a settling tank of the effluent of the municipal wastewater treatment plant in Leeuwarden, the Netherlands. These microalgae were grown on four pieces of PVC sheet in 250 mL Erlenmeyer flasks containing 100 mL synthetic wastewater effluent. The Erlenmeyers were kept in a growth chamber (Innova 44, New Brunswick Scientific, USA) on an orbital shaker (100 rpm) at a temperature of 25°C. The growth chamber was continuously illuminated with 40 μmol photons/m^2/s, and a concentration of 2% CO_2 was maintained in the gas phase. Every two weeks, synthetic wastewater effluent was replaced and most of the microalgal biofilm was scraped from the plastic sheet to allow the microalgal biofilms to re-grow and keep the culture viable. The plastic sheet of the flow cell was scratched with sandpaper before the inoculation procedure prior to the experiment. Starting this procedure, the pieces of the

inoculum from the growth chamber were rubbed over the flow cell sheet. Afterwards, the flow cell sheet was left in synthetic wastewater effluent for a minimum of two hours before being put into the flow cell.

The synthetic wastewater effluent contained N and P in the typical species and concentrations of municipal wastewater effluent, being 10 mg/L NO_3^--N and 1.1 mg/L PO_4^{3-}-P. In addition, the synthetic effluent contained (micro) nutrients based on Wright's cryptophyte medium (Andersen 2005), to rule out limitations of any nutrients other than N or P. The synthetic effluent lacked an organic carbon source in order to obtain a microalgal biofilm with as little heterotrophic bacteria as possible. The synthetic wastewater effluent composition was as follows: 60.67 mg/L $NaNO_3$, 36.76 mg/L $CaCl_2.2H_2O$, 36.97 mg/L $MgSO_4.7H_2O$, 420.04 mg/L $NaHCO_3$, 28.42 mg/L $Na_2SiO_3.9H_2O$, 6.19 mg/L K_2HPO_4. Trace elements and vitamins: 3.82 mg/L $EDTA.2H_2O$, 1.90 mg/L $FeCl_3$, $1.00 \cdot 10^{-2}$ mg/L $CuSO_4.5H_2O$, $2.20 \cdot 10^{-2}$ mg/L $ZnSO_4.7H_2O$, $9.99 \cdot 10^{-3}$ mg/L $CoCl_2.6H_2O$, 0.147 mg/L $MnCl_2.2H_2O$, $6.00 \cdot 10^{-3}$ mg/L $Na_2MoO_4.2H_2O$, 1.00 mg/L H_3NO_3, 0.10 mg/L vitamin B1, $5.00 \cdot 10^{-4}$ mg/L vitamin H, $5.00 \cdot 10^{-4}$ mg/L vitamin B12. Apart from the experiments with synthetic wastewater two experiments were performed with real wastewater effluent. The effluent was collected from the wastewater treatment plant in Leeuwarden, the Netherlands, and was enriched with $NaNO_3$ and used as inflow in the experiment. The concentrations of NO_3^--N and PO_4^{3-}-P were respectively 5.57 mg N/L and 0.97 mg P/L.

Analytical Procedures

Samples were taken from the influent and effluent flow during operation. After filtering through a 0.45 μm filter (Millex-LCR, Merck Millipore, USA), samples were analyzed for NO_3^--N and PO_4^{3-}-P with ion chromatography (Compact IC 761, Metrohm, Switzerland). The Compact IC 761 was equipped with a conductivity detector with the pre-column Metrosep A Supp 4/5 Guard and with the column Metrosep A Supp 5, 150/4.0 mm (Metrohm, Switzerland). Gas samples were analyzed, to determine the amount of oxygen gas formed in addition to the dissolved oxygen, with gas chromatography (GC) (CP-4900, Varian, USA). The GC was equipped with a thermal conductivity detector using a Mol Sieve 5Å PLOT 10 m column at 80°C and a PoraPlot U 10m column at 65°C, and argon as carrier gas at 1.47 mL/min. Microalgal dry weight in the effluent was determined by filtration of the effluent through pre-weighed glass fiber filters (Whatman GF/F, UK) and oven drying at 105°C for at least 24 hours. The stored biomass from the flow cells was also oven dried at 105°C for 24 hours, ground and dried for at least another 24 hours. The C and N content of this microalgal biomass was measured in duplicate with an elemental analyzer (EA 1110, ThermoQuest CE Instruments, USA) utilizing a vertical quartz tube (combustion tube) maintained at 1000°C with a constant flow of helium at

120 mL/min, an oxidation catalyst (WO_3) zone, a copper zone followed by a Porapack PQS column maintained at 60°C and finally, followed by a TCD detector. To determine the P content, duplicates of the biomass were digested using 8 mL HNO_3 (68%) per 0.4 g microalgal biomass, first heating to 180°C at up to 1000 W for 15 minutes, followed by 15 minutes at 180°C at up to 1000 W in a microwave (ETHOS 1, Milestone, Italy). After this digestion, the total P concentration was measured with inductive coupled plasma (ICP) (Optima 5300 DV, Perkin Elmer, USA equipped with an optical emission spectrometer).

Scanning Electron Microscopy

At the end of the experiment, a small piece of plastic sheet with the microalgal biofilm was cut from the plastic sheet in the flow cell. This piece was gently washed three times in phosphate buffer solution (137 mmol/L NaCl, 2.7 mmol/L KCl, 10 mmol/L Na_2HPO_4, 2 mmol/L KH_2PO_4, pH 7.4). The biofilm was then fixed using 2.5% glutaraldehyde at room temperature for two hours. The fixed sample was dehydrated sequentially with 30%, 50%, 70%, 90%, 100% (v/v) ethanol, each step taking 20 minutes. The sample was then dried at 35°C for a minimum of 15 minutes. The samples were sputter coated with a thin 5 nm gold layer, and observed with a scanning electron microscope (SEM) (JSM-6480LV, JEOL, Japan) in high vacuum mode (acceleration voltage 10 - 15 kV, working distance 10 mm).

Calculations

The measured percentage of oxygen (%) was converted to oxygen concentration (mmol/L) using the maximum oxygen solubility in the air-saturated synthetic wastewater. This solubility was determined by sequentially adding 20 mL of sodium sulfite to 8 mL of air-saturated synthetic wastewater. Each step displayed a 15% oxygen decrease, resulting in an oxygen solubility of 0.24 mmol/L or 7.61 mg/L. As a measure of photosynthetic efficiency, the quantum yield of oxygen evolution (QY_{O2}) was calculated:

$$QY_{O2} = \frac{\sum (O_2(g) \cdot V_g) + O_2(l) \cdot Q_l \cdot t}{PFD \cdot A \cdot t} \quad [\text{mol } O_2/\text{mol photons}] \tag{3.1}$$

with $O_2(g)$ the oxygen concentration in the gas phase (mol/L), V_g the volume of the gas formed inside the flow cell (L), O_2 (l) the oxygen concentration in the liquid (mol/L), Q_l the flow rate of the liquid (L/d), t the time (d), PFD the PAR photon flux density (mol photons/m^2/d) and A the area (m^2).

The final effluent concentrations of NO_3^--N and PO_4^{3-}-P of each experiment were calculated as the average concentration of the effluent samples taken during the quasi-steady state at the end of the experiment.

RESULTS

Biofilm Growth

During the experiments, the microalgal biofilm covered the plastic sheet with a thin layer after about four days, although the plastic could still be seen in some places. After this coverage, filamentous green microalgae started to grow from the biofilm into the overlaying water layer, forming streamers. After about 12 days, these streamers started to detach. This pattern of growth was similar at all loading rates. However, higher loading rates resulted in a visually greener and more loosely attached biofilm.

SEM pictures revealed that the top layer of the biofilm grown on synthetic wastewater effluent consisted mainly of pennate diatoms (*Nitzschia* sp.) and that the green filaments were lying on top of this biofilm, as presented in Figure 3.2A. It can be seen from Figure 3.2B that the experiments with real effluent showed a larger diversity of microalgae, although these experiments were started with the same inoculum originating from a municipal wastewater treatment plant. Presumably, the wastewater effluent further inoculated the biofilm with new species.
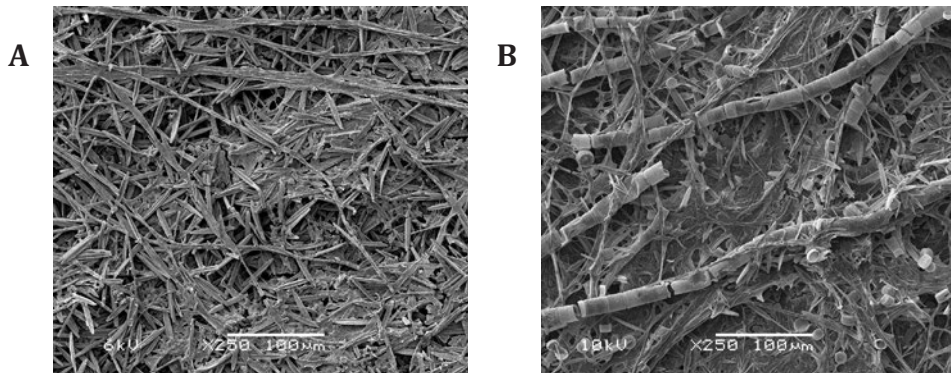
Figure 3.2 — *SEM pictures of the microalgal biofilm of experiments with synthetic wastewater effluent (A) and real wastewater effluent (B).*

Removal of Nitrate and Phosphate from Synthetic and Real Wastewater Effluent

Figure 3.3A and B show the removal of nitrate (NO_3^-) and phosphate (PO_4^{3-}) by the microalgal biofilm at representative low, intermediate and high nutrient loads, using synthetic and real wastewater effluent. Figures 3.3 shows that a similar removal pattern was observed during the experiments. The first two to four days of the experiment were considered a start-up phase. During this phase the biomass began to populate the carrier material and little uptake of NO_3^--N and PO_4^{3-}-P was observed. As the algae grew, the NO_3^--N and PO_4^{3-}-P concentrations decreased further, and finally remained stable during four to eight days. This phase was described as quasi-steady state, were the uptake of NO_3^--N and PO_4^{3-}-P was stable. The effluent concentrations reached during this quasi-steady state phase were dependent on the applied loading rate, where the higher loading rates gave higher final effluent concentrations. Moreover, at the higher loading rates an increase of both NO_3^--N and PO_4^{3-}-P concentrations was observed at the end of the experiment. Finally, Figure 3.3 shows that the removal pattern of the real wastewater effluent was similar to the removal pattern of the synthetic wastewater effluent.

Figure 3.3 — *Effluent concentrations of NO_3^--N (A) and PO_4^{3-}-P (B) during four flow cell experiments using synthetic wastewater effluent at loading rates of 0.18, 1.01 and 1.49 g NO_3^--N/m²/d and 0.022, 0.094 and 0.152 g PO_4^{3-}-P/m²/d, and using real wastewater effluent at a loading rate of 0.45 g NO_3^--N/m²/d and 0.078 g PO_4^{3-}-P/m²/d.*
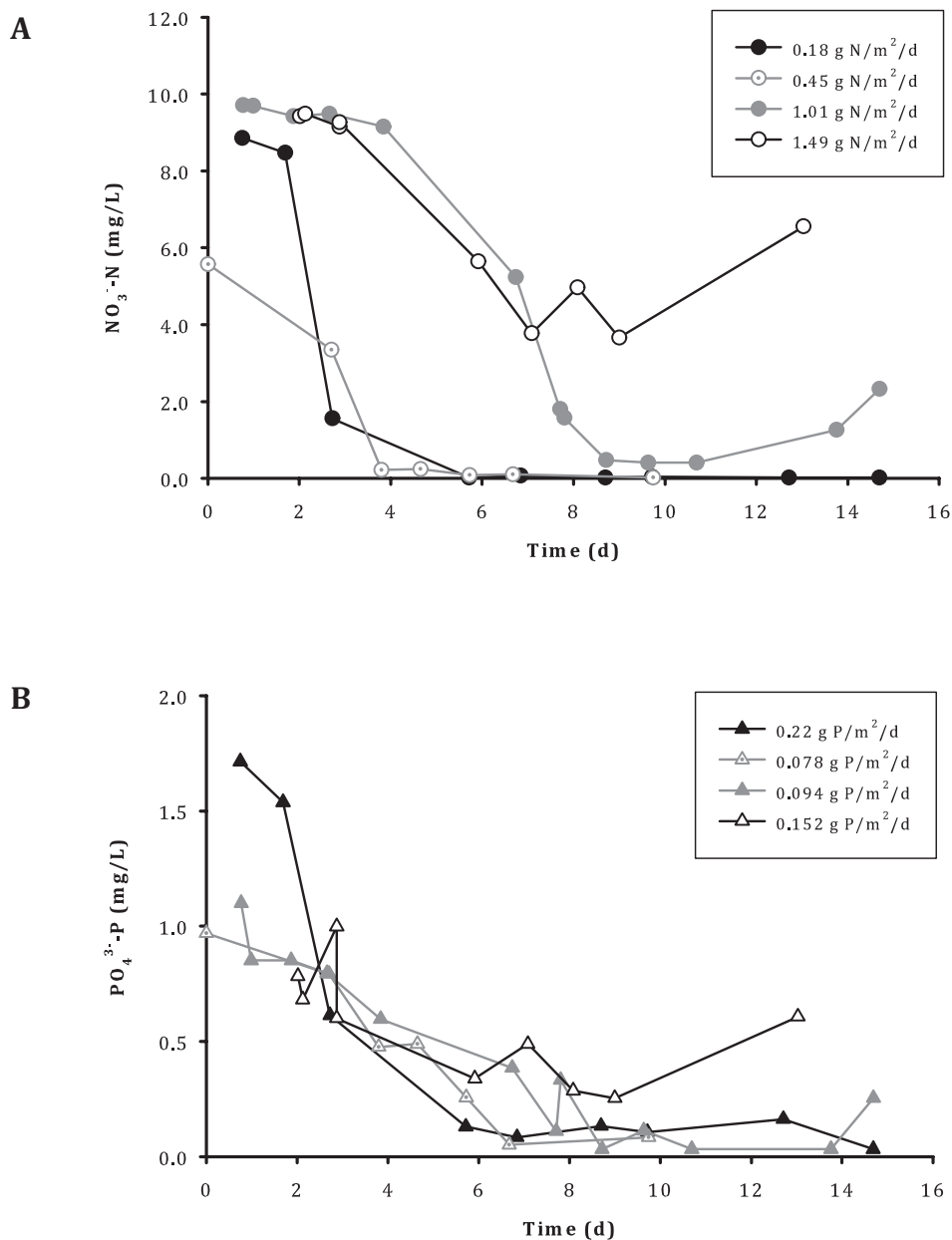
Uptake Capacity and Microalgae Washout

Figure 3.4A presents the uptake rate of NO_3^--N during the quasi-steady state at the end of the experiments performed at different loading rates. All rates are expressed relative to the biofilm surface in m^2. In addition, Figure 3.4A shows the removal of NO_3^--N during the two experiments with real effluent. As was expected, the uptake first increased approximately linearly with increasing loading rates. The uptake was no longer linear above a loading rate of 1.0 g NO_3^--N/m^2/d. The uptake of PO_4^{3-}-P showed a similar behavior, as can be seen in Figure 3.4B. Figure 3.4 also shows that at low loading rates, the measured uptake rates of the experiments applying the real effluent were comparable to the uptake rates of the experiments applying the synthetic effluent.

It can be seen from Figure 3.5A that the final NO_3^--N concentrations in the effluent increased with increasing loading rates, from 0.03 mg NO_3^--N/L at a low loading rate of 0.18 g NO_3^--N/m^2/d to 7.3 mg NO_3^--N/L at the highest load of 4.5 g NO_3^--N/m^2/d. Up to a loading rate of 1.0 g NO_3^--N/m^2/d the NO_3^--N effluent concentrations remained below the target of 2.2 mg N/L. Therefore, 1.0 g NO_3^--N/m^2/d was referred to as the maximum uptake capacity of NO_3^--N, being the highest load at which the target effluent value was still achieved. Figure 3.5B shows the effluent concentrations of PO_4^{3-}-P. With one exception, the final effluent concentrations of PO_4^{3-}-P also remained below the target value of 0.15 mg P/L up to a loading rate of 0.13 g PO_4^{3-}-P/m^2/d. Thus, the maximum uptake capacity of PO_4^{3-}-P was found to be 0.13 g PO_4^{3-}-P/m^2/d.

Some washout of microalgae occurred during the experiments. The amount of suspended solids that washed out remained stable until about 12 days when the quasi-steady state period ended and chunks of biofilm were released. Figure 3.5 shows the average microalgae washout, as associated N and P concentration, until the end of the quasi-steady state period. This N and P concentration was calculated with an internal N and P content of the microalgae of 0.039 g N/g biomass and 0.0055 g P/g biomass, the average values of the measurements described in the following paragraph. Interestingly, the average washout of microalgae from the different experiments was always around 3.2 mg/L suspended solids. This corresponds to an average washout of 0.13 mg N/L and 0.018 mg P/L.

A

B

Figure 3.4 — Uptake of nitrogen (A) and uptake of phosphorus (B) by the microalgal biofilms at different nitrogen loads using synthetic and real wastewater effluent. The straight dotted line indicates a hypothetical linear relationship.
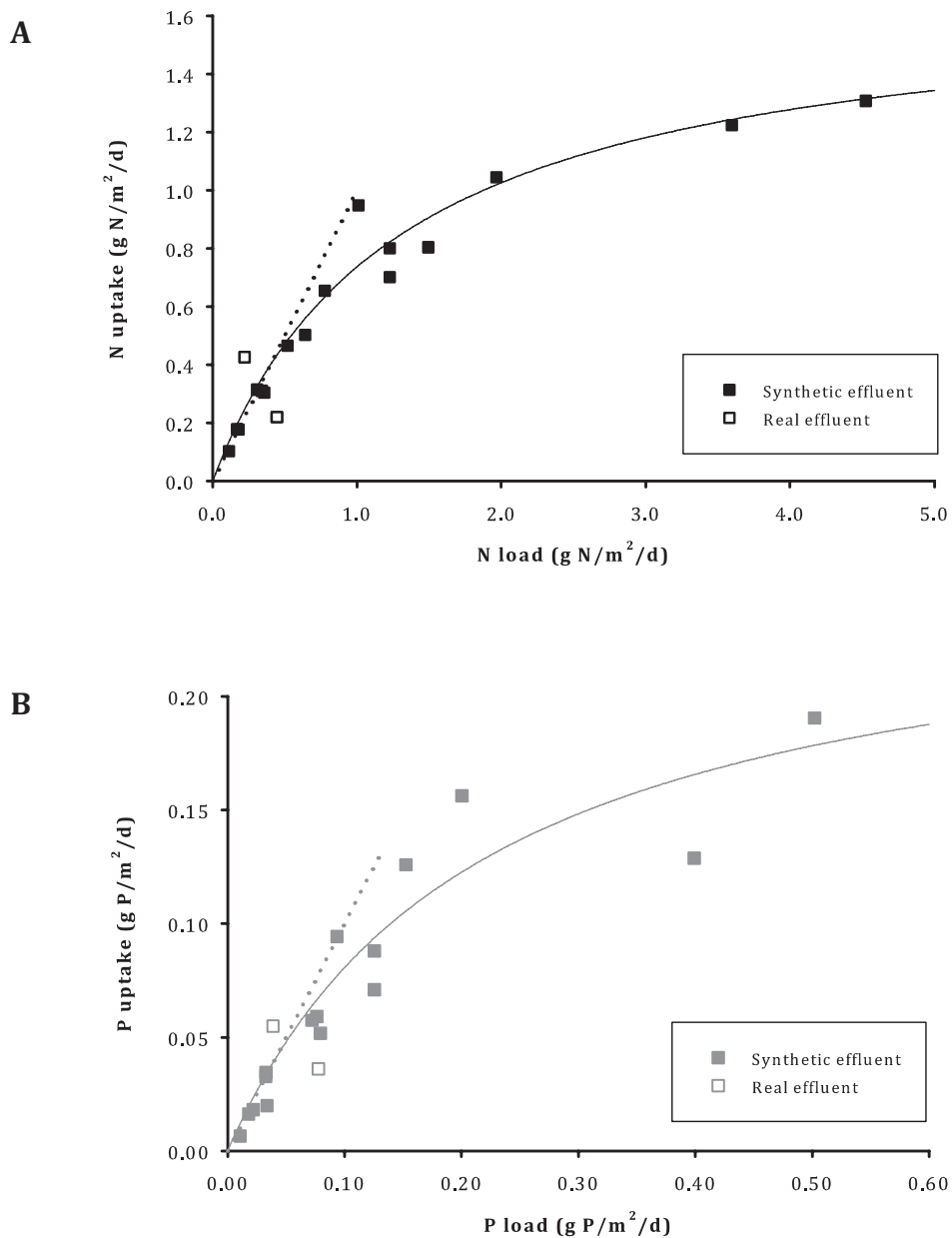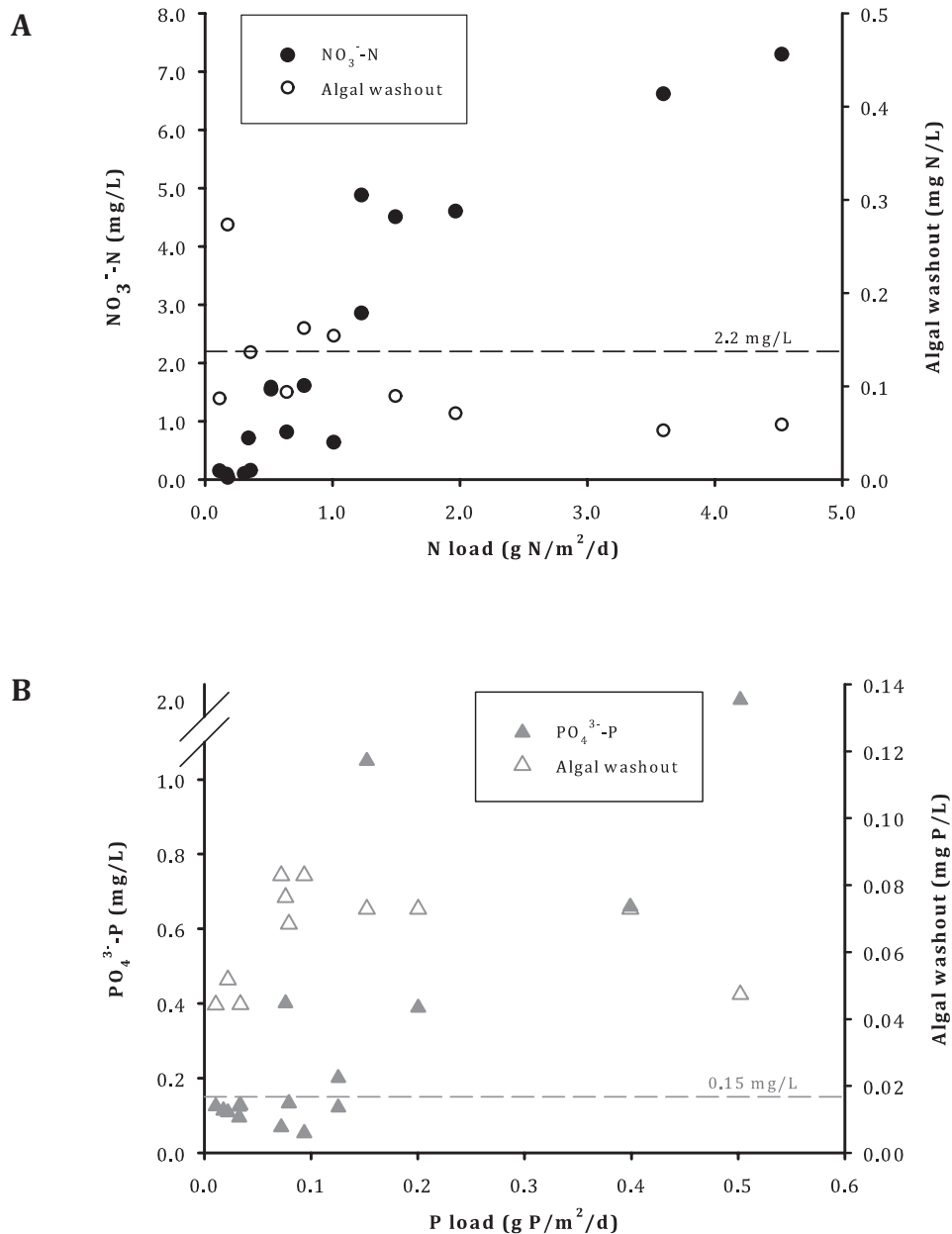
Figure 3.5 — *Effluent concentrations of NO_3^--N (A) and PO_4^{3-}-P (B) and the calculated average washout of microalgal biomass (assuming 0.039 g N/g biomass and 0.0055 g P/ g biomass) at different nitrogen and phosphorus loads. The dotted lines indicate the target values for the final effluent of 2.2 mg N/L and 0.15 mg/L P.*

Microalgal Biomass

The carbon (C), N and P content of the microalgal biomass were determined. The carbon content remained nearly constant during the experiments and was on average 0.45 g C/g biomass. Figure 3.6 shows the internal N and P content of the microalgal biomass at different loading rates of NO_3^--N and PO_4^{3-}-P. Both the internal N and P content increased with increasing loading rates until the maximum loading rates of 1.0 g NO_3^--N/m^2/d and 0.13 g PO_4^{3-}-P/m^2/d. At higher loading rates, the N content was stable with 0.048 g N/g biomass and the P content only increased marginally from 0.0072 until 0.0099 g P/g biomass. Figure 3.6B also shows the molar N:P ratio of the different experiments with increasing loading rates. The N:P ratio decreased from approximately 23:1 at low loading rates to approximately 14:1 at the maximum uptake capacity. At higher loading rates the ratio only decreased slightly as a result of the marginally increasing P content while the N content remained stable. The N:P ratio had decreased to 11:1 at the highest loading rate of 4.5 g NO_3^--N/m^2/d.

A

B
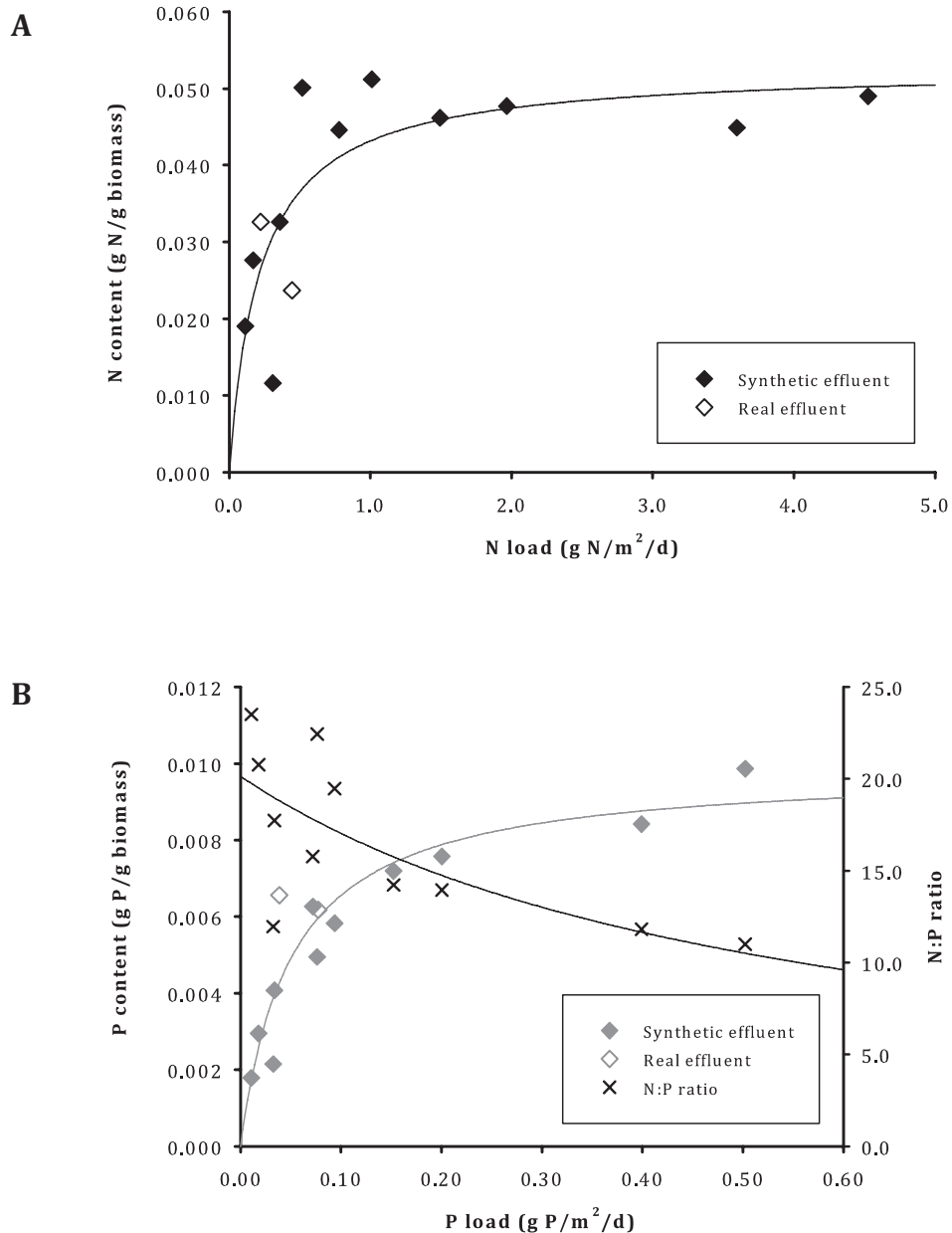
Figure 3.6 — Measured nitrogen content (A) and phosphorus content (B) and the corresponding molar N:P ratio (B) of the microalgal biomass grown under different nitrogen and phosphorus loads using synthetic and real wastewater effluent. The synthetic wastewater effluent contained nitrogen and phosphorus at a molar N:P ratio of 20:1.

Figure 3.7 presents the average biomass production, calculated from all biomass produced during the entire experiment. Although this average biomass production showed variations, the production appeared to increase with the increasing nutrient load. The highest biomass production of 7.7 g/ m^2/d was found at a loading rate of 1.97 g NO_3^--N/ m^2/d, and the lowest production was 2.1 g/m^2/d and was found at a loading rate of 0.11 g NO_3^--N/m^2/d.
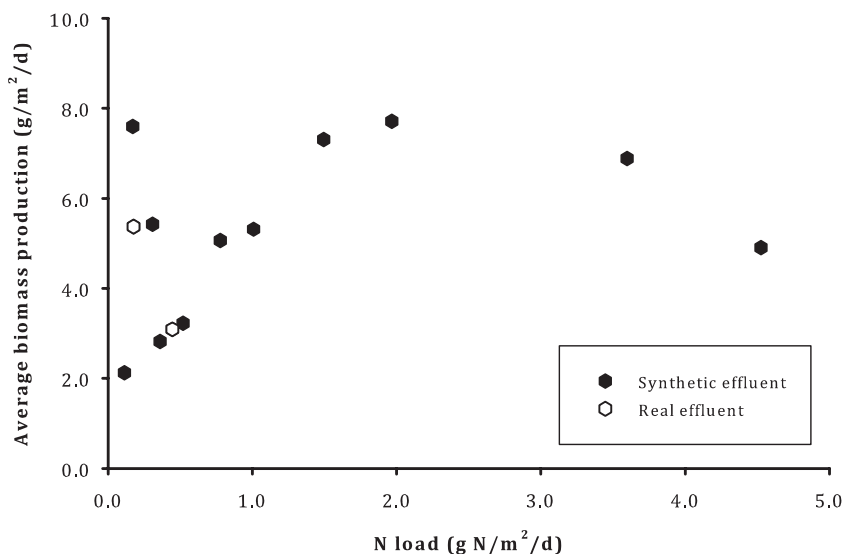
Figure 3.7 — *The average microalgal biomass production rate (dry weight) during the experiments at different nitrogen loads for both the experiments with synthetic wastewater effluent and the experiments with real wastewater effluent.*

Photosynthetic Efficiency

Figure 3.8 shows the calculated quantum yield of oxygen production during the quasi-steady state period of the 16 experiments. It is apparent from the figure that this yield varied with the experiments, similar to the average biomass production, and no direct relationship was observed between the yield and the loading rate. The highest quantum yield of 0.043 mol O_2/mol photons was found at a loading rate of 2.0 mg NO_3^--N/m^2/d, while the lowest yield of 0.012 mol O_2/mol photons was found at the loading rate 0.34 g NO_3^--N/m^2/d.
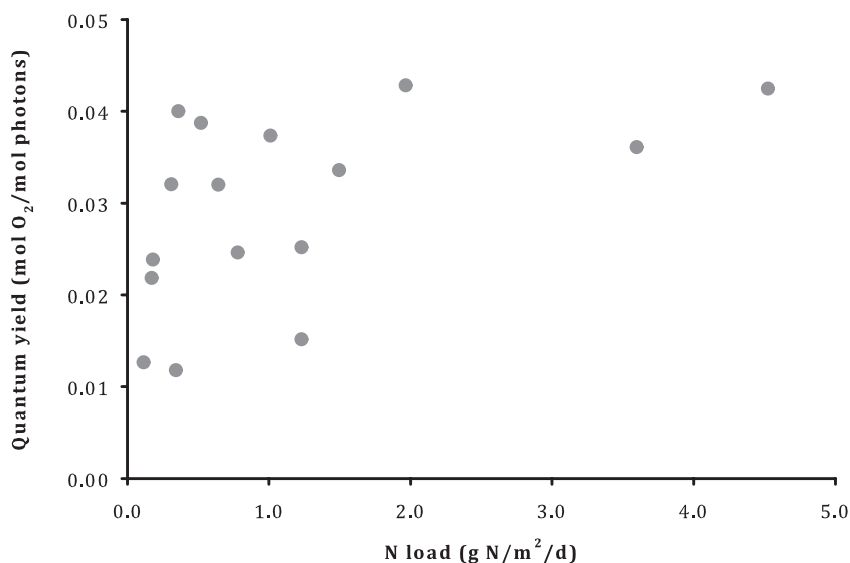
Figure 3.8 — *Calculated quantum yield of oxygen production at different nitrogen loading rates for the experiments with synthetic wastewater effluent.*

DISCUSSION

The results of this study show that it is possible to simultaneously decrease NO_3^--N and PO_4^{3-}-P concentrations in wastewater effluent to the target values 2.2 mg N/L and 0.15 mg P/L using a microalgal biofilm. These results are in contrast to initial expectations that N and P could not be removed simultaneously from the effluent, due to the supply ratio of around 20 N:1P in municipal wastewater effluent. This N:P ratio is not optimal for freshwater microalgae, which have an average N:P ratio of 12:1 (Duboc et al. 1999; Ahlgren et al. 1992; Healey 1973). However, varying internal compositions are reported in literature for different algal species (Ho et al. 2003; Ahlgren et al. 1992) and under different growth conditions, the latter especially through luxury uptake of P (Powell et al. 2008; Klausmeier et al. 2004).

The possibility of varying internal ratios was confirmed during this study, where the internal N:P ratio was found to decrease with increasing loading rates. Despite the variable data at low loading rates, the results suggest that the internal N:P ratio decreased only until the maximum uptake capacities of 1.0 g NO_3^--N/m²/d and 0.13 g PO_4^{3-}-P/m²/d. At higher loading rates the decrease in N:P ratio was only marginal. At the highest loading rates a N:P ratio of about 11:1 was found, equal to the average N:P ratio in freshwater microalgae. In addition, nutrients remained in the effluent at the loading rates above the

maximum uptake capacity, which indeed shows that there were enough nutrients and the microalgae assimilated the nutrients in preferred ratios.

At the low loading rates the N:P ratio of the microalgal biomass was close to the 20:1 ratio of the supplied synthetic wastewater effluent. It can thus be suggested that at, or below, the maximum uptake capacity it will be possible to simultaneously obtain the desired low effluent values for both NO_3^--N and PO_4^{3-}-P. Due to the varying internal N:P ratio in the microalgae, this will also be possible when the ratio in the supplied wastewater is suboptimal for microalgae and varying.

The final effluent concentrations that can be achieved using microalgal biofilms in practice are determined by the uptake capacity of NO_3^--N and PO_4^{3-}-P as measured in this study, but also by the molecular form of the nutrients and by the biomass washout. The N and P in wastewater effluent will not only consist of NO_3^--N and PO_4^{3-}-P, as was the case in our synthetic wastewater effluent. It is probable that only the inorganic forms of the nutrients will be taken up by the microalgae, and that organic and particulate forms of N and P will either remain in the effluent or be entrapped into the biofilm and mineralized. Although the N in the wastewater effluent typically comprises of less than 10% dissolved organic N, this dissolved organic N can become dominant, up to 85% of the total N, when the total N concentration reaches very low levels (Pagilla et al. 2006; Pehlivanoglu and Sedlak 2004). A bioavailability assay of phosphorus in municipal wastewater effluent (Ekholm and Krogerus 1998) showed that 36% of the total phosphorus was available to algae. Therefore, in practice, the final total N and P concentrations could be higher than the concentrations measured during this study.

In this study, the washout of algae was measured as suspended solids and calculated with the measured content of N and P in the microalgal biomass of the biofilm. As the washout consisted of detached microalgae from the biofilm, it was assumed that the internal nutrient content was the same. Contrary to expectations, the washout of microalgae remained stable throughout each experiment with 3.2 mg/L suspended solids, giving an average washout of 0.13 mg N/L and 0.07 mg P/L. Taking these concentrations into account, the N effluent concentrations were still below target up to the loading rate of 1.0 g NO_3^--N/m^2/d, while the P concentrations were often slightly above target up to this loading rate. It is expected that the washout would increase during longer experiments, when the biofilm is no longer in a quasi-steady state (Horn et al. 2003). This biomass loss and also unwanted mobilization of fixed nutrients are the result of biofilms becoming too thick. Too thick biofilms also lead to a decreased uptake rate and increasing effluent concentrations, as was seen at the end of the flow cell experiments (Figure 3.3). However, this will not be pertinent for the application in practice where the biofilm will be harvested while at steady state, in order to maintain low effluent concentrations.

With the maximum uptake capacity obtained in this study, a first rough estimation can be made of the size of a full scale post-treatment system. The required area of microalgal biofilms for 100 000 inhabitants would be around 10 ha (100 000 inhabitants · 130L wastewater/inhabitant/day · (10 - 2.2 mg N/L) ÷ 1.0 g NO_3^--N/m^2/d). However, this calculated area is dependent on the uptake capacity, which in turn depends on various factors including the actual supply of sunlight in an outdoor system and the efficiency at which the algae convert this light into biomass.

This study found maximum uptake capacities of 1.0 g NO_3^--N/m^2/d and 0.13 g PO_4^{3-}-P/m^2/d. These values are higher than the removal rates of 0.1-0.6 g N/m^2/d and 0.006-0.09 g P/m^2/d measured in tubular biofilm photo-reactors treating swine slurry (de Godos et al. 2009; González et al. 2008). However, 0.13 g PO_4^{3-}-P/m^2/d is lower than 0.73 g P/m^2/d measured in an Algal Turf Scrubber treating wastewater (Craggs et al. 1996). The continuous illumination of 230 μmol/m^2/s used in this study could be considered modestly low for summer and very high for winter. This irradiation corresponds to a daily irradiation of 20 mol/m^2/d, while an average summer day in the Netherlands gives about 34 mol/m^2/d and a winter day gives 5 mol/m^2/d (Huld and Suri 2007). An irradiation of 34 mol/m^2/d would decrease the area requirement to about 6 ha. In the Netherlands the irradiation is 20 mol/m^2/d or higher from April until September. As this half year period corresponds to the time when eutrophication of surface waters can take place, it is possible to use the algal biofilm as post-treatment of municipal wastewater effluent removing the residual N and P to prevent eutrophication.

Regarding the efficiency at which algae convert light into biomass, the oxygen quantum yield was assessed. Under low light intensities minimally 10 photons (PAR) are required for the liberation of one molecule of O_2 (Bjorkman and Demmig 1987; Ley and Mauzerall 1982) corresponding to an oxygen quantum yield of 0.1. This study found a large range of oxygen quantum yields of 0.012 to 0.043 mol O_2/mol photons. The reason for this large range is unknown, although it is likely that the yield increases with loading rate. A higher efficiency leads to a higher biomass production and thus a higher removal capacity. The previously mentioned 10 ha could decrease to 6 ha when the yield is improved from 0.03 mol/mol to 0.05 mol/mol (100 000 inhabitants · 130L wastewater/inhabitant/day · (10 - 2.2 mg N/L) ÷ (0.05 ÷ 0.03 · 1.0 g N/m^2/d)).

In addition to area requirement, there are three other aspects to consider when applying microalgal biofilms as post-treatment systems. Firstly, CO_2 availability to the algae in the biofilm will need to be considered. Although a modeling study (Liehr et al. 1988) has shown that it is probable that CO_2 will become a limiting factor when the biofilm is exposed to ambient air, wastewater effluent can contain sufficient inorganic carbon to sustain algal growth (Van Vooren et al. 1999). Therefore, further investigations can

determine if limitation imposed by CO_2 will be an important restraint to the biofilm system.

Secondly, the effect of the diurnal light cycle on the uptake of nutrients needs to be considered. Most researchers have studied microalgae and microalgal nutrient uptake under continuous illumination, as was also done in this study. However, for application in practice it will need to be known if there is any uptake at night, as this is one of the factors determining the system design. There are indications that uptake may continue at night at a reduced rate, for instance uptake of NH_4^+ was found to be more than 50% of the daylight value in N-limited microalgae (Vona et al. 1999). This reduced uptake rate may be compensated by the expected lower loading rate of N and P at night.

A final consideration for the future application of microalgal biofilm systems is the harvesting of the microalgal biomass. The microalgal biomass production measured during this study indicates a significant biomass production in a microalgal biofilm system operating on municipal wastewater effluent. The production for the post-treatment system for 100 000 inhabitants would be around $2 \cdot 10^3$ kg/d (1.0 g N/m^2/d ÷ 0.0512 g N/g biomass · 10 ha). The harvesting of this biomass can either take place passively or actively, the former being the collection of the biomass that naturally detaches from the biofilm, and the latter involving techniques like backwashing, pH shock or scraping.

CONCLUSIONS

The present study has shown that microalgal biofilms can be used to treat municipal wastewater effluent and remove residual NO_3^--N and PO_4^{3-}-P to the lower discharge demands of 2.2 mg N/L and 0.15 mg P/L. A maximum uptake capacity was found at a load of 1.0 g NO_3^--N/m^2/d and 0.13 g PO_4^{3-}-P/m^2/d under a light intensity of 230 μmol/m^2/s. Up to this maximum uptake capacity the internal N and P content of the microalgae was dependent on the loading rate. This implies that microalgae can assimilate both nitrogen and phosphorus at N:P ratios present in wastewater effluent. Furthermore, it was estimated that a full scale microalgal biofilms post-treatment system for 100 000 inhabitants would be around 10 ha, producing $2 \cdot 10^3$ kg of biomass per day.

ACKNOWLEDGEMENTS

3

3

Chapter 4

The Effect of Harvesting on Biomass Production and Nutrient Removal in Phototrophic Biofilm Reactors for Effluent Polishing

Nadine C. Boelee
Marcel Janssen
Hardy Temmink
Lina Taparavičiūtė
Rungnapha Khiewwijit
Ágnes Jánoska
Cees J.N. Buisman
René H. Wijffels

ABSTRACT

An increasing number of wastewater treatment plants require post-treatment to remove residual nitrogen and phosphorus. This study investigated various harvesting regimes that would achieve consistent low effluent concentrations of nitrogen and phosphorus in a phototrophic biofilm reactor. Experiments were performed in a vertical biofilm reactor and in horizontal flow lanes with biofilms of variable thickness. Contrary to the expectations, the biomass production doubled when the biofilm thickness was increased from 130 µm to 2 mm. This increased production was explained by the lower density and looser structure of the 2 mm biofilm. It was also possible to maintain low nitrogen and phosphorus concentrations in the effluent of the vertical biofilm reactor by regularly harvesting half of the biofilm. The average areal biomass production rate achieved a 7 g dry weight/m^2/d for all different harvesting frequencies tested (every two, four, or seven days), corresponding to the different biofilm thicknesses. Apparently, the biomass productivity is similar for a wide range of biofilm thicknesses. The biofilm could not be maintained for more than two weeks as, after this period, it spontaneously detached from the carrier material. It was concluded that, concerning biomass production and labor requirement, the optimum harvesting frequency is once per week.

4

INTRODUCTION

Microalgal biofilms can be applied for wastewater treatment and post-treatment of wastewater effluents to remove nitrogen (N) and phosphorus (P) (Boelee et al. 2012 / Chapter 2). As in all phototrophic systems, microalgal biofilms exhibit the potential to recover the N and P incorporated in the produced microalgal biomass. Biofilm systems also possess several advantages over suspended systems. First, biofilm systems are able to perform during shorter hydraulic retention times and, secondly, it is easier to harvest the biomass from biofilm systems than from suspended systems. Finally, while suspended microalgal systems experience a high energy input (Norsker et al. 2011), biofilm systems are expected to demand less energy due to the easier harvesting and the absence of mixing.

Microalgal biofilm systems can be applied as post-treatment of municipal wastewater when the discharge of N and P must be reduced as a consequence of stricter regulations such as the EU Water Framework Directive. In concordance with this directive, the N and P concentrations must be reduced from the current European discharge requirements of 10 mg N/L and 1 mg P/L to concentrations appropriate for discharge to 'sensitive' water bodies. Current Dutch guidelines for these sensitive water bodies are 2.2 mg/L total N and 0.15 mg/L total P. Laboratory studies have demonstrated that microalgal biofilms are able to remove N and P from wastewater effluent at removal rates of 0.1–1.3 g N/m^2/d and 0.006–0.19 g P/m^2/d (Boelee et al. 2011 / Chapter 3; Godos et al. 2009; González et al. 2008) and can attain effluent concentrations below the target values mentioned above (Boelee et al. 2011 / Chapter 3).

Generally, the growth of phototrophic biofilms follows a pattern of two phases. The first phase is the growth phase which begins with the colonization of the carrier material often by diatoms and green algae (Johnson et al. 1997; Biggs 1996). The biomass initially grows exponentially and, later, linearly, and the community evolves toward filamentous green algae and cyanobacteria (Sekar et al. 2002; Johnson et al. 1997; Biggs 1996). Biofilm growth, subsequently, decreases and, at a certain biofilm thickness, the growth becomes equal to the losses experienced through respiration, cell death, parasitism, disease, and grazing. This initiates the beginning of the second phase, the loss phase, where losses exceed growth (Biggs 1996).

When applying microalgal biofilms for wastewater treatment, the biofilm should be continuously maintained in the exponential or linear growth phase. This ensures a high biomass production and, thereby, a high nutrient removal rate. Regular harvesting of the biofilm can maintain the biofilm in the growth phase by preventing the biofilm from reaching the thickness at which the loss phase begins. When harvesting the biofilm, a

4

fraction of the biomass should remain on the carrier material to allow continuous growth and removal of nutrients. This can, for instance, be achieved by employing scraping as a harvesting technique (Ellwood et al. 2011; Johnson and Wen 2009). However, only minimal attention has been paid to harvesting microalgal biofilms, and therefore, it is uncertain what amount of the biofilm should be harvested and at what frequency this harvesting should occur.

The aim of this study was to assess the fraction of a phototrophic biofilm that should be harvested and the frequency of harvesting required to maintain effluent concentrations below 2.2 mg N/L and 0.15 mg P/L. A comparison was conducted between harvesting the entire biofilm surface and harvesting only half of the biofilm back to the carrier material. In addition, the effect of three different harvesting frequencies was determined on the biomass production rate and on the N and P effluent concentrations in a vertical phototrophic biofilm reactor. Finally, the hypothesis that biomass productivity decreases with increasing biofilm thickness was investigated in horizontal flow lanes with biofilms of 130 µm, 250 µm, 500 µm, 1 mm and 2 mm.

4

MATERIAL AND METHODS

Vertical Phototrophic Biofilm Reactor

Figure 4.1 and Figure 4.3 depict the vertical phototrophic biofilm reactor employed in this study. The biofilm was grown on a 0.125 m^2 layer of Polyfelt Geolon PE180 (TenCate Geosynthetics, the Netherlands), a polyethylene-based woven geotextile. This layer was situated on top of a layer of Polyfelt P120, a polypropylene-based nonwoven geotextile (TenCate Geosynthetics, the Netherlands), and both layers were fixed to a polypropylene support plate. To obtain a homogeneous liquid distribution, a flexible tube (Masterflex Norprene L/S 16, Core-Parmer, USA) was positioned above the polypropylene plate 5 mm above the biofilm. This tube was cut along its length such that the liquid dripped from the tube onto the biofilm, resulting in a completely wet biofilm. A gutter placed below the biofilm collected the liquid which was then pumped to a 400 mL recycle vessel. In this vessel, the pH was measured and controlled at pH 7 by a pulse-wise addition of CO_2 gas. The liquid, with an average temperature of 21°C, was recycled at 170 mL/min and mixed with the inflow of 7 mL/min synthetic wastewater. The overflow of the recycle vessel resulted in the effluent of the biofilm reactor. This effluent was amassed and stored in the dark at 2°C for a maximum of 24 hours to determine the dry weight concentration of the suspended biomass. To prevent microalgal growth outside of the Polyfelt layer, the gutter featured a polypropylene cover, all tubing was black, glassware was brown, and all glassware and connections were covered in aluminum foil.

The phototrophic biofilm was continuously illuminated by a bank of four compact fluo-rescent lamps (MASTER PL-L Polar 36W/840/4P, Phillips, the Netherlands) at an aver-age light intensity of 180 µmol/m^2/s. The light intensity was measured with a 2π PAR quantum sensor (SA190, LI-COR Biosciences, USA) arranged at the level of the biofilm surface. Nutrient loading rates of 0.8 g N/m^2/d and 0.9 g P/m^2/d were selected (Table 4.1) which were comparable to previous work where maximum uptake capacities of 1.0 g N/m^2/d and 0.13 g P/m^2/d were determined at 220 µmol/m^2/s (Boelee et al. 2011 / Chapter 3).
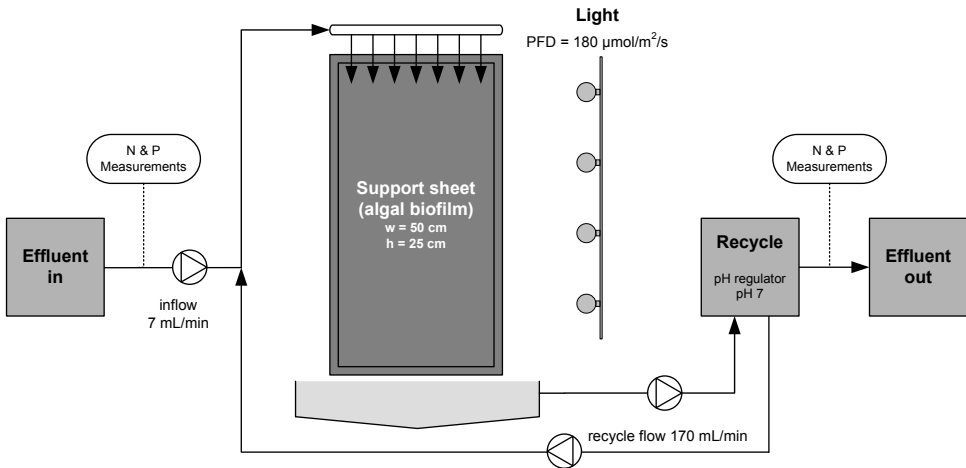
Figure 4.1 — Schematic overview of the vertical phototrophic biofilm reactor.

Horizontal Flow Lanes

The flow lane biofilm reactor (Ontwikkelwerkplaats WUR, the Netherlands) is schemat-ically demonstrated in Figure 4.2. This flow lane reactor was comprised of five parallel flow lanes of 80 cm long and 3.5 cm wide. The five flow lanes displayed edges of 3.5 mm on both sides and depths of 130 µm, 250 µm, 500 µm, 1 mm and 2 mm. The flow lanes were separated by vertical side walls with a height of 1.5 cm.

Synthetic wastewater entered a rotatable container positioned above the flow lanes with a flow rate of 4.4 mL/min. While the container was filling, the center point of grav-ity changed, and the container rotated when filled causing a wave to roll over the flow lanes. The flow lane setup was positioned at a slight angle to enable the liquid to flow over the lanes. The liquid, with an average temperature of 24°C, was collected at the end of the lanes and pumped to a 400 mL recycle vessel. In this vessel, the pH was measured and controlled at pH 7 by a pulse-wise addition of CO_2 gas. From the recycle vessel a recycle flow of 200 mL/min was combined with the influent and returned to the rotat-

able container. The overflow of the recycle vessel resulted in the effluent of the system. The phototrophic biofilms in the flow lanes were continuously illuminated by LED light (FYTO Panel – Model B cool white LEDs, 280 pc, PSI, Czech Republic). Employing a light controller (Light Controller LC 150, PSI, Czech Republic), the light intensity was specified at 200 μmol/m^2/s. The light intensity was measured with a 2π PAR quantum sensor (SA190, LI-COR Biosciences, USA) situated at the level of the biofilm surface. Plates covered with aluminium foil were positioned at the sides of the flow lanes to produce a more uniform light distribution among the biofilms.
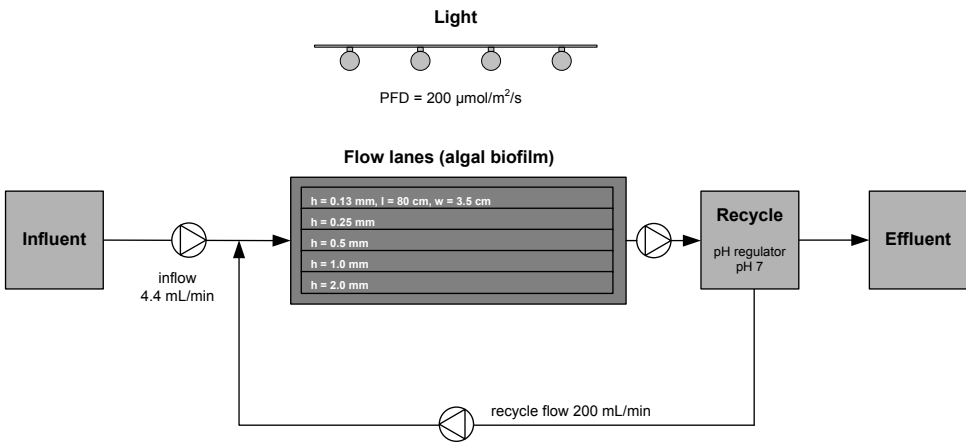
Figure 4.2 — *Schematic overview of the horizontal flow lane setup.*

Microalgal Biofilm Cultivation

Microalgal biofilm material was scraped from the surface of a settling tank of the effluent of the municipal wastewater treatment plant in Leeuwarden, the Netherlands and were further cultivated on small PVC sheets as described in Boelee et al. (2011 / Chapter 3). During the experiments with the vertical biofilm reactor, the Polyfelt sheet was inoculated by rubbing it with the PVC sheets containing biofilm. The flow lanes were also inoculated by rubbing them with the PVC sheets containing biofilm and also by rubbing fresh biofilm material from the wastewater treatment plant in Leeuwarden over the bottom of the lanes.
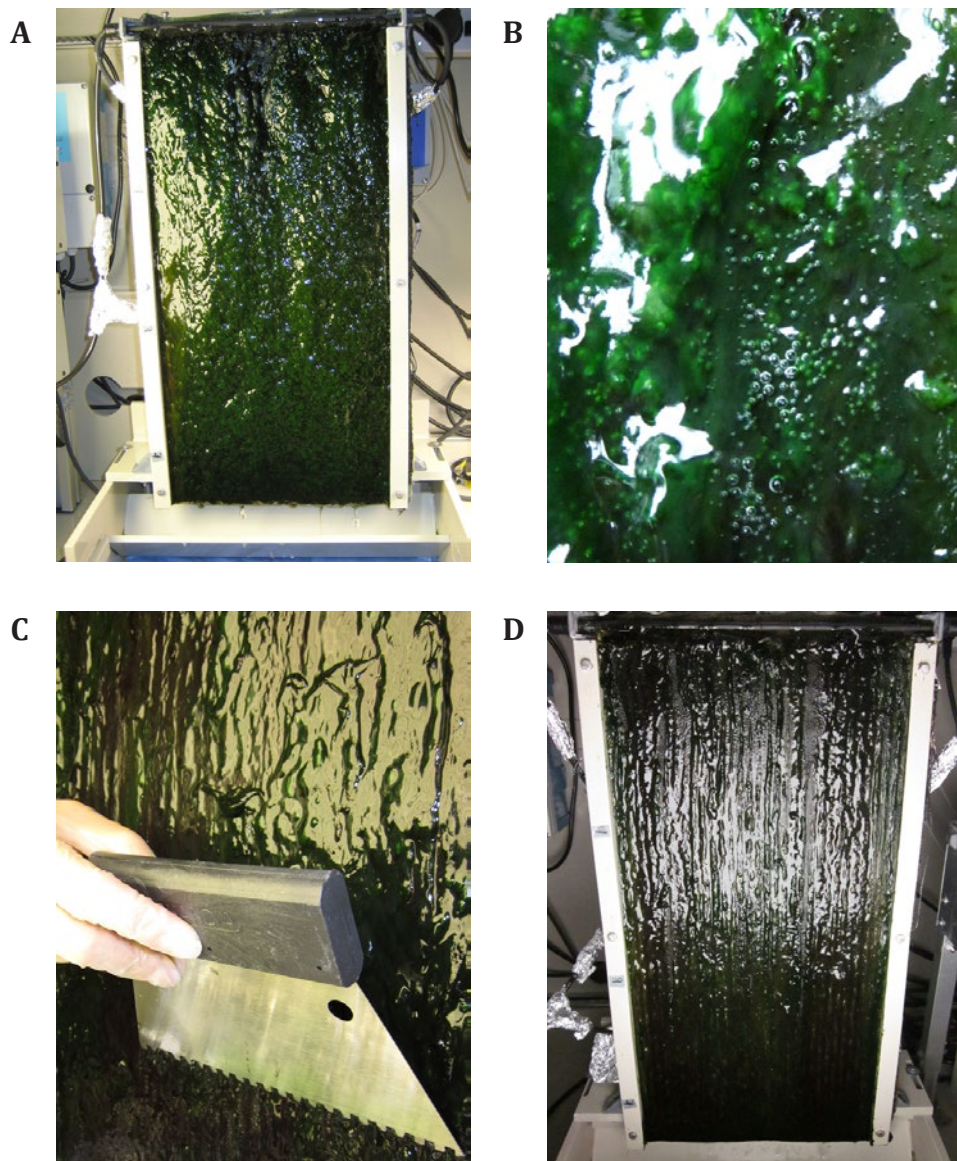
Figure 4.3 — The vertical phototrophic biofilm reactor (A), a close-up of the biofilm before harvesting (B), harvesting part of the biofilm with the adhesive comb (C) and the biofilm setup after harvesting (D).

The synthetic wastewater effluent supplied to the vertical biofilm reactor was designed to resemble the effluent from a typical municipal wastewater treatment plant and contained 10 mg/L NO_3^--N and 1.1 mg/L PO_4^{3-}-P. In addition, the synthetic wastewater contained (micro) nutrients based on Wright's cryptophyte medium (Andersen 2005) to rule out limitations of nutrients other than N or P. The synthetic wastewater lacked an organic carbon source in order to avoid heterotrophic growth. The synthetic wastewater composition of the vertical biofilm reactor was as follows: 60.67 mg/L $NaNO_3$, 36.76 mg/L $CaCl_2.2H_2O$, 36.97 mg/L $MgSO_4.7H_2O$, 28.42 mg/L $Na_2SiO_3.9H_2O$, 6.19 mg/L K_2HPO_4. Trace elements and vitamins: 3.82 mg/L $EDTA.2H_2O$, 1.90 mg/L $FeCl_3$, $1.00 \cdot 10^{-2}$ mg/L $CuSO_4.5H_2O$, $2.20 \cdot 10^{-2}$ mg/L $ZnSO_4.7H_2O$, $9.99 \cdot 10^{-3}$ mg/L $CoCl_2.6H_2O$, 0.147 mg/L $MnCl_2.2H_2O$, $6.00 \cdot 10^{-3}$ mg/L $Na_2MoO_4.2H_2O$, 1.00 mg/L H_3NO_3, 0.10 mg/L vitamin B1, $5.00 \cdot 10^{-4}$ mg/L vitamin H, $5.00 \cdot 10^{-4}$ mg/L vitamin B12.

The biofilms contained within the horizontal flow lanes were grown under light limitation by applying elevated nutrient concentrations at a high loading rate of 3.5 g N/m^2/d and 0.38 g P/m^2/d, as indicated in Table 4.1. In this manner, a dark zone may develop in the biofilm which will be accompanied by losses through respiration and cell death. The synthetic wastewater effluent of the horizontal flow lanes was as follows: 442 mg/L $NaNO_3$, 268 mg/L $CaCl_2.2H_2O$, 269 mg/L $MgSO_4.7H_2O$, 207 mg/L $Na_2SiO_3.9H_2O$, 45.1 mg/L K_2HPO_4. Trace elements and vitamins: 2.78 mg/L $EDTA.2H_2O$, 1.38 mg/L $FeCl_3$, $7.29 \cdot 10^{-3}$ mg/L $CuSO_4.5H_2O$, $1.60 \cdot 10^{-2}$ mg/L $ZnSO_4.7H_2O$, $7.27 \cdot 10^{-3}$ mg/L $CoCl_2.6H_2O$, 0.107 mg/L $MnCl_2.2H_2O$, $4.37 \cdot 10^{-3}$ mg/L $Na_2MoO_4.2H_2O$, 0.729 mg/L H_3NO_3, 0.0728 mg/L vitamin B1, $3.64 \cdot 10^{-4}$ mg/L vitamin H, $3.64 \cdot 10^{-4}$ mg/L vitamin B12.

Harvesting Experiments

Three different experiments were performed: Experiments 1 and 2 in the vertical biofilm reactor and Experiment 3 in the horizontal flow lanes. Table 4.1 demonstrates the harvesting procedures that were followed during the three experiments. In Experiment 1, the entire biofilm was scraped from the 0.125 m^2 surface using a spatula, after which phototrophs could only have remained between the fibers of the Polyfelt material. In Experiment 2, a scraper was employed which was constructed from an adhesive comb. This scraper was designed to harvest half of the biofilm back to the Polyfelt material and was scraped over the biofilm from top to bottom, as illustrated in Figure 4.3C. Harvesting occurred every two, four, or seven days (Experiments 2A, 2B and 2C). The biofilms in the flow lanes of Experiment 3 were harvested by running a blade over the edges of the flow lanes every day from Monday through Friday. In this manner, only the top layer of the biofilm was harvested, and the remaining biofilm was of the thickness determined by the depth of the flow lanes (130 μm, 250 μm, 500 μm, 1 mm or 2 mm).

Table 4.1 — *The NO_3^--N and PO_4^{3-}-P loading rate, harvesting method and frequency of the three experiments.*

Experi-ment	Experimental setup	NO_3^--N loading rate ($g/m^2/d$)	PO_4^{3-}-P loading rate ($g/m^2/d$)	Harvesting method	Harvesting frequency
1	Vertical reactor	0.8	0.08	Scraping entire biofilm	Every approx. 20 days
2A	Vertical reactor	0.8	0.08	Scraping half of the biofilm	Every 2 days
2B	Vertical reactor	0.8	0.08	Scraping half of the biofilm	Every 4 days
2C	Vertical reactor	0.8	0.08	Scraping half of the biofilm	Every 7 days
3	Flow lanes	3.5	0.38	Scraping entire top of the biofilm	5 days per week

Analytical Procedures

Samples were extracted from the influent and effluent of the vertical biofilm reactor and filtered through a 0.45 µm filter (Millex-LCR, Merck Millipore, USA). These samples were analyzed for NO_3^--N and PO_4^{3-}-P with ion chromatography (Compact IC 761, Metrohm, Switzerland). The Compact IC 761 was equipped with a conductivity detector with the pre-column Metrosep A Supp 4/5 Guard and with the column Metrosep A Supp 5, 150/4.0 mm (Metrohm, Switzerland). The collected outflow was filtered through pre-weighed glass fiber filters (GF/F, Whatman, UK) to determine the suspended dry weight in the outflow. These filters were dried at 105°C for at least 24 hours.

To determine the dry weight of the harvested biomass, it was dried at 105°C for at least 24 hours. The biomass density of the wet biofilms was estimated from the volume of the wet biofilm and its dry weight content. In Experiment 2, the volume of the harvested biomass was measured in a graduated cylinder for each harvest. In Experiment 3, the volume of all five flow lanes was known and, therefore, following the final harvest at the end of the experiment, all remaining biomass was removed from inside the flow lanes, and its dry weight was determined.

The C, N and H content of dried and ground biomass was measured in duplicate with an elemental analyzer (EA 1110, ThermoQuest CE Instruments, USA) utilizing a vertical quartz tube (combustion tube) maintained at 1000°C with a constant flow of helium at 120 mL/min, an oxidation catalyst (WO_3) zone, a copper zone followed by a Porapack PQS column maintained at 60°C and finally, followed by a TCD detector. To determine

the Ca, Fe, K, Mg, Na, P, S, and Si content, duplicates of the biomass were digested using 10 mL HNO_3 (68%) per 0.5 g dry biomass. During digestion, the temperature was increased over a 15 minute duration until 180°C was achieved in a microwave (ETHOS 1, Milestone, Italy) at 1000 W, and maintained an additional 15 minutes. Following digestion, the concentrations of the elements were measured with inductive coupled plasma (ICP) (Optima 5300 DV equipped with an optical emission spectrometer, Perkin Elmer, USA). The ash content was determined by burning the dried ground biomass at 550°C for 2 hours and dividing the ash weight by the dry weight.

Microscopy

Digital images of the biofilm were taken using a camera (Canon IXUS 105) and a Leica DM750 microscope (400x).

Calculation of the Elemental Composition

The molar elemental composition of the biofilm, including oxygen, was calculated according to Duboc et al. (1999) using the measured weight of C, H, N, S, P and ash.

RESULTS

Biofilm Growth in the Vertical Biofilm Reactor

During Experiments 2A-C, the biofilm was excessively green before harvesting while the underlying layer uncovered after harvesting was brown. The biofilm thickness varied and gas bubbles of varying sizes were observed within the biofilm as depicted in Figure 4.3B. Microscopic observations such as those demonstrated in Figure 4.4, indicated that the top layer of the biofilm consisted almost exclusively of the filamentous cyanobacterium *Phormidium*. This was in contrast to Experiment 1 where this cyanobacterium was not observed before or after harvesting the biofilm. *Phormidium* is a well-known filamentous cyanobacterium that was also dominant in other studies (Ellwood et al. 2011; Guzzon et al. 2008; Johnson et al. 1997). In the bottom layer of the biofilms in Experiments 2A-C, different cyanobacteria and microalgae were also discovered including the cyanobacteria *Pseudanabaena*, the diatom *Nitzschia,* and the green microalgae *Scenedesmus*. This pattern was consistently observed throughout Experiments 2A-C and is comparable with findings in other studies (Guzzon et al. 2008; Johnson et al. 1997).
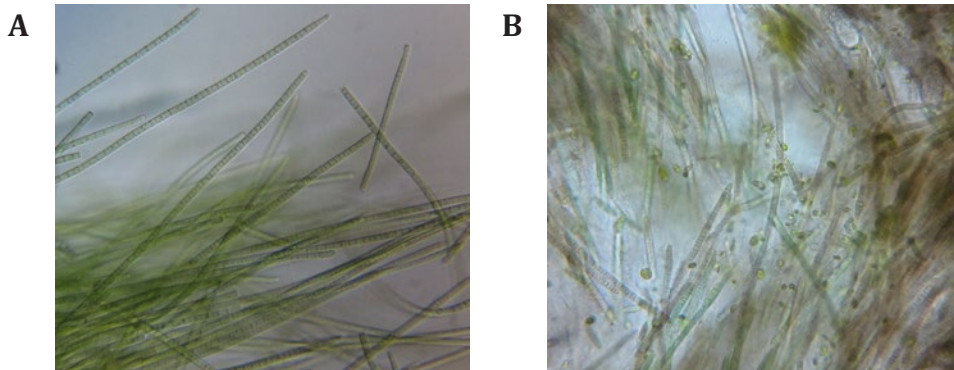
Figure 4.4 — Phormidium *in the green top of the biofilm (A) and* Phormidium *together with other phototrophs in the browner bottom of the biofilm (B).*

Removal of NO_3^--N and PO_4^{3-}-P in the Vertical Biofilm Reactor

Figure 4.5 depicts the concentrations of NO_3^--N and PO_4^{3-}-P in the effluent of the vertical biofilm system during Experiment 1. Until day 23, the NO_3^--N and PO_4^{3-}-P concentrations had only slightly decreased to 7.3 mg NO_3^--N/L and 0.36 mg PO_4^{3-}-P/L.
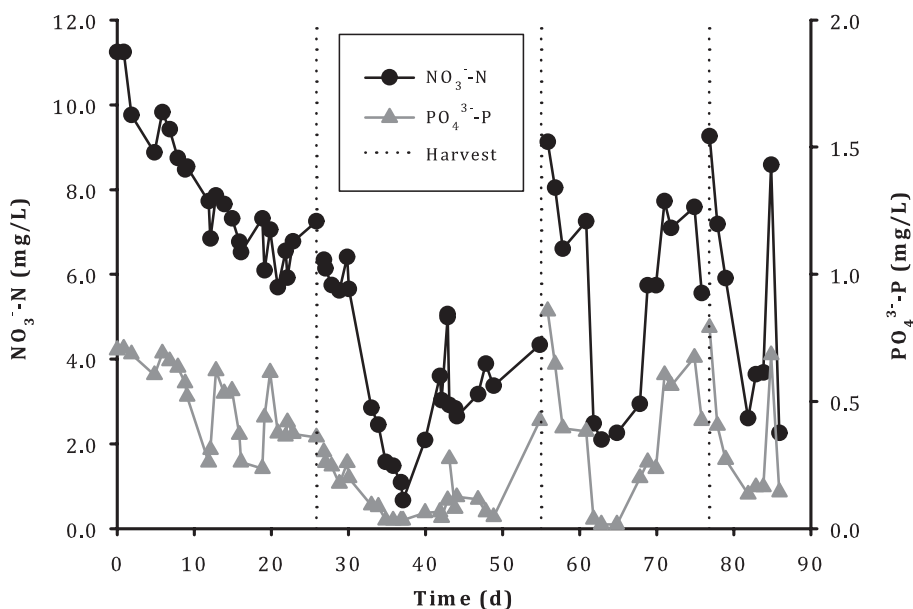
Figure 4.5 — Effluent concentrations of NO_3^--N and PO_4^{3-}-P during Experiment 1 with an influent of 10 mg NO_3^--N/L and 1.0 mg PO_4^{3-}-P/L. The dotted lines indicate the time of harvest when the entire biofilm was scraped from the carrier material.

After the entire biofilm was harvested on day 26, the NO_3^--N and PO_4^{3-}-P concentrations decreased more rapidly. On day 37, the lowest concentrations were achieved of 0.66 mg NO_3^--N/L and 0.03 mg PO_4^{3-}-P/L, after which the nutrient concentration began to increase. A similar pattern was observed following the subsequent two harvests, but the time required to achieve the lowest effluent concentrations shortened after each harvest: 14 days after the first harvest, eight days after the second and only six days after the third. However, the NO_3^--N and PO_4^{3-}-P concentrations remained low for only a brief period of time.

Figure 4.6 presents the effluent concentrations of NO_3^--N and PO_4^{3-}-P during Experiments 2A-C when approximately half of the biofilm was harvested. The effluent concentrations remained low throughout the experiments and were, generally, below the target values of 2.2 mg N/L and 0.15 mg P/L. An increase in the NO_3^--N and PO_4^{3-}-P concentrations can be ascertained immediately after most harvests in Experiment 2A, and this increase became more evident at the lower harvesting frequencies in Experiments 2B and C.

Experiment 2C did not exhibit an increase in the effluent concentrations of NO_3^--N and PO_4^{3-}-P above the target values of 2.2 mg N/L and 0.15 mg P/L following the first two harvests. Therefore, it was decided to postpone the third harvest until the effluent concentrations increased above the target concentrations. Figure 4.6C indicates that, surprisingly, such an increase was not evidenced. After nine days, the biofilm fell from the carrier material, and the same occurred after a consecutive growth period of 11 days.
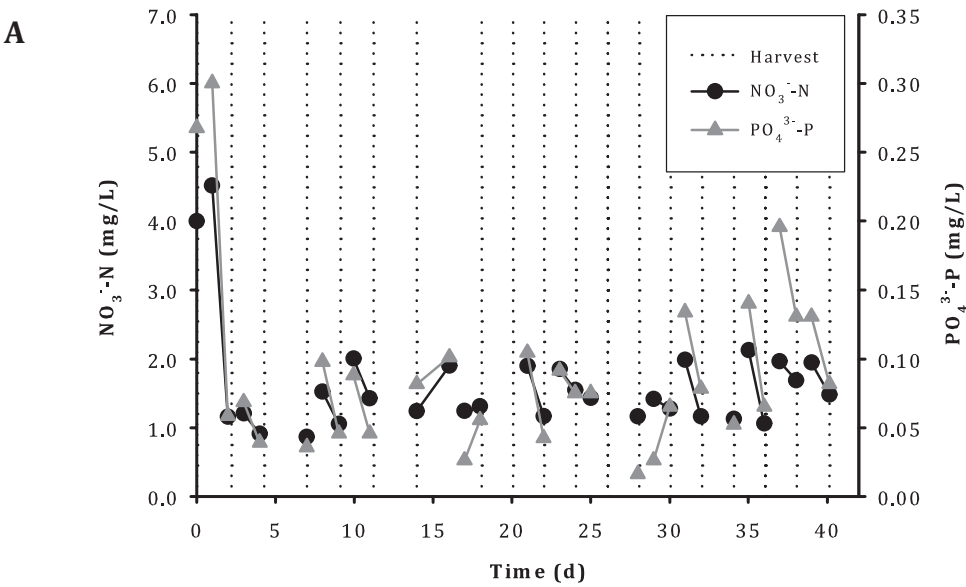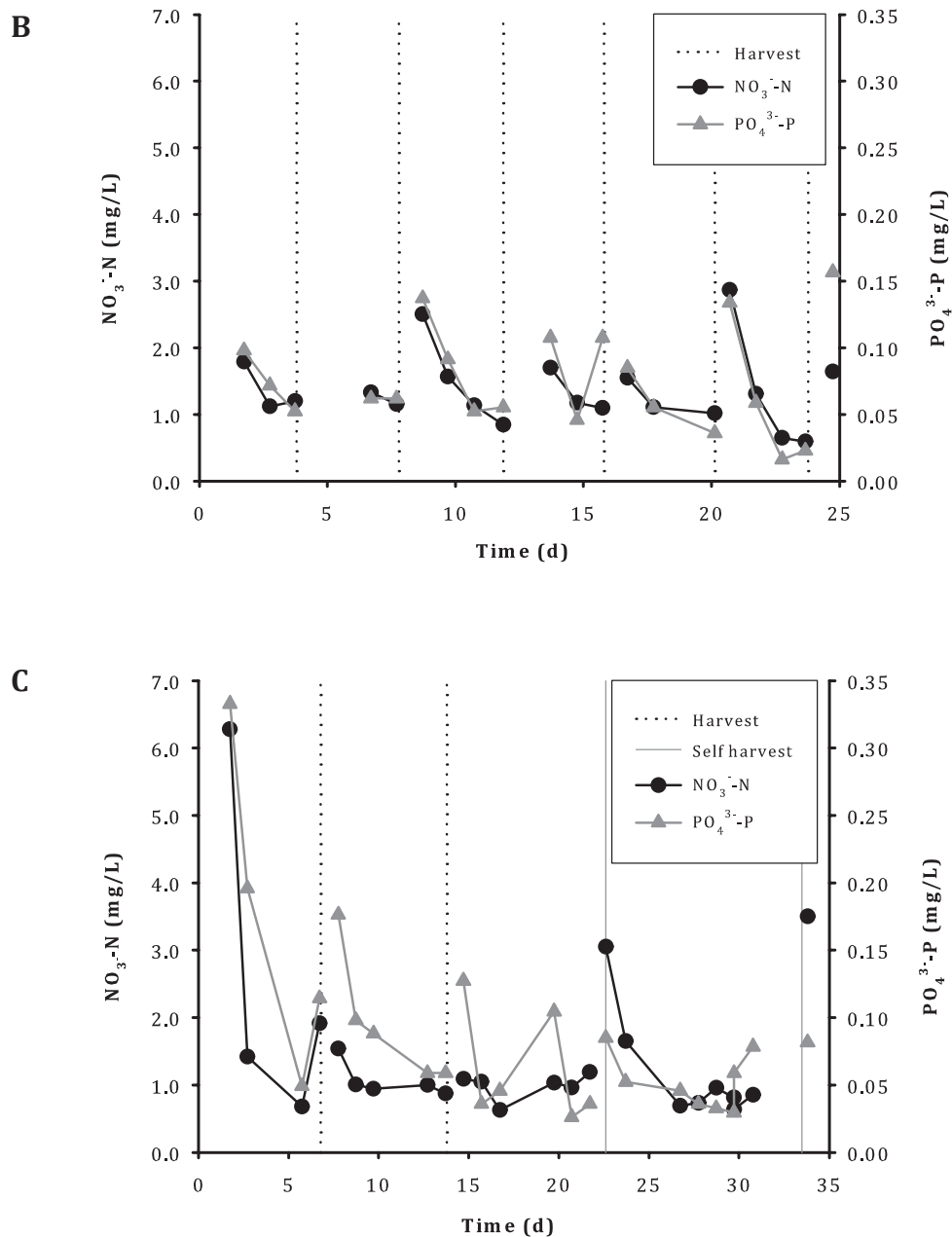
Figure 4.6 — *Effluent concentrations of NO_3^--N and PO_4^{3-}-P during Experiment 2A (A), Experiment 2B (B) and Experiment 2C (C) with an influent of 10 mg NO_3^--N/L and 1.0 mg and PO_4^{3-}-P/L. The dotted lines (A-C) indicate the time of harvest when about half of the biofilm was scraped from the carrier material, the grey line (C) indicates the time when the biofilm fell from the carrier material.*

Biomass Production in the Vertical Biofilm Reactor

Figure 4.7 illustrates that the areal biomass production rate was excessively variable during the experiments and that no clear differences were observed between the different harvesting frequencies of Experiments 2A-C. However, the areal biomass production rate in Experiment 1 whereby, the entire biofilm was harvested, was considerably lower than the production rates in Experiments 2A-C. For all harvesting regimes, the biomass production of the first one or two harvests was lower than the production of the later harvests.
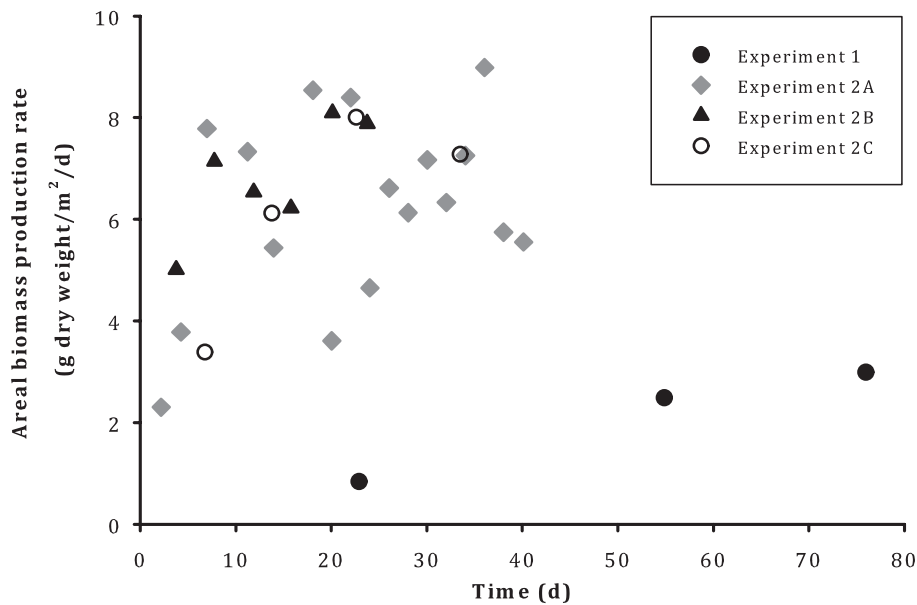
Figure 4.7 — *The areal biomass production rates during Experiment 1 (harvesting the entire biofilm), Experiment 2A (harvesting every two days), 2B (harvesting every four days) and Experiment 2C (harvesting every seven days).*

The average areal biomass production rates of Experiments 1 and 2 are compared in Table 4.2. The average biomass production rate of Experiment 1 was 2.7 g dry weight/m^2/d while the average biomass production rate of Experiments 2A-C was 7 g dry weight/m^2/d (the first harvests were not taken into consideration). This biomass production, combined with the applied light intensity of 180 μmol/m^2/s results in a biomass yield on light energy of 0.18 g dry weight/mol photons for Experiment 1 and of 0.43 and 0.46 g dry weight/mol photons for Experiments 2A and 2B-C.

Table 4.2 also demonstrates the water content of the biofilms which was determined at 90% in Experiment 1 and 94% in Experiments 2A-C. The ash content of the biomass

ranged between 39 and 88 mg/g dry weight. The biofilm density was estimated from the measured volume and dry weight of the harvested biomass during Experiments 2A-C. The biofilm thickness was estimated based on the biofilm surface area, the measured volume of the harvested biomass, and the assumption that half of the biofilm was harvested. The biofilm density diminished with decreasing harvesting frequency or increasing biofilm thickness from 59 g dry weight/L at 500 μm to 31 g dry weight/L at 4.2 mm.

Table 4.2 — *The average areal biomass production rate, biomass yield on light energy and the water content (measured as difference between wet and dry biomass) for Experiments 1 and 2. The measured ash content and the estimated biofilm density and biofilm thickness for Experiment 2. In brackets the standard deviation and the number of samples n.*

Experiment	Areal biomass production rate (g dry weight/m^2/d)	Yield (g dry weight/mol photons)	Water content (%)	Biomass ash content (mg/g dry weight)	Est. density (g dry weight/L)	Est. biofilm thickness (μm)
1	2.7 (n =2)	0.18	90 (n=2)			
2A	6.7 (±1.9 n=17)	0.43	94 (±0.8 n=17)	62 (±20 n=4)	59	500
2B	7.2 (±0.82 n=5)	0.46	94 (±0.01 n=5)	88 (±22 n=3)	47	1300
2C	7.1 (±0.95 n=3)	0.46	94 (±1.6 n=3)	39 (±9 n=3)	31	4200

Mass Balances N and P of the Vertical Biofilm Reactor

Figure 4.8 provides the N and P mass balances for Experiments 1 and 2A-C. The average suspended dry weight concentrations were 7.5 mg/L during Experiment 1; 1.4 mg/L during Experiment 2A; and 0.9 mg/L during Experiments 2B and 2C. It was assumed that the N and P content of these suspended solids was identical to the N and P content of the biomass in the biofilm. Figure 4.8 illustrates that only 1% N and P departed from the system as suspended solids in the effluent in Experiments 2A-C. In Experiment 1, this was more extensive with 6% N and 9% P leaving the systems as suspended solids. The distribution of N and P was very similar in Experiments 2A-C where 63% of N and 85% of P was harvested with the biomass, and only 12% of N and 9% P departed from the reactor in a dissolved form with the effluent. In Experiment 1, only 26% of N and 39% of P was harvested with the biomass, and a major fraction of the nutrients left the reactor in dissolved form with the effluent (45% N and 26% P). The mass balances were not completely closed as between 22-25% for N and between 2-26% for P was unaccounted for.

A
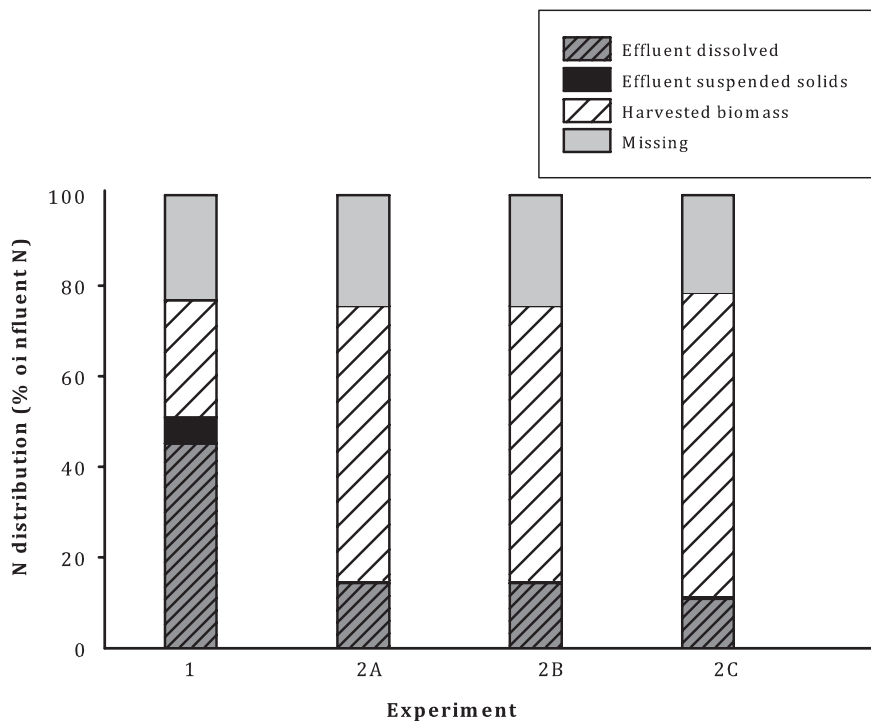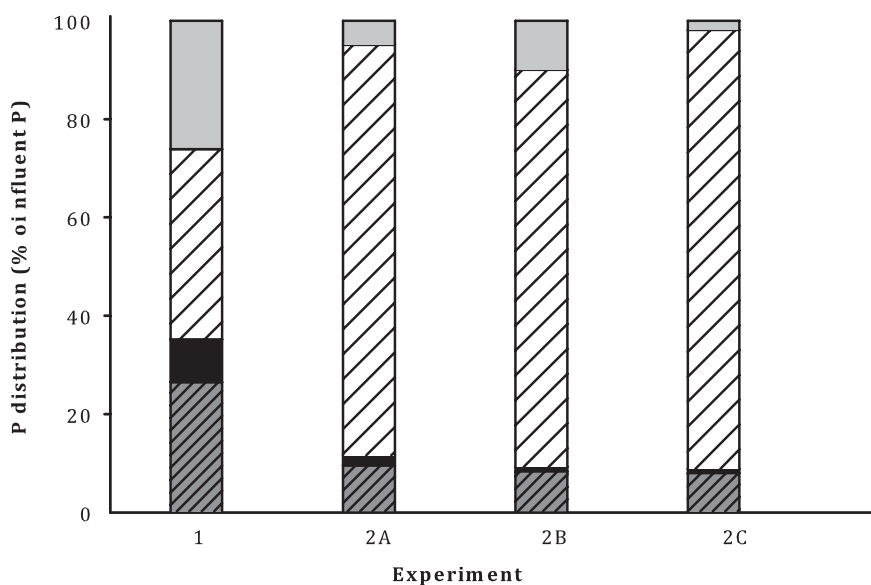
Figure 4.8 — The mass balance for N (A) and for P (B). The mass balance shows the dissolved N or P in the effluent, the N or P in suspended solids in the effluent, the N or P in the harvested biomass and the missing fraction as the percentage of the influent values for Experiments 1 and 2A-C.

Biofilm Growth in the Flow Lanes

To investigate the effect of biofilm thickness on biomass production in more detail, in Experiment 3, biofilms were grown in flow lanes with varying thicknesses of 130 μm, 250 μm, 500 μm, 1 mm and 2 mm. The biofilms were harvested back to the default thickness five days a week. It proved difficult to harvest exactly to the default biofilm thickness as the biomass in the biofilms clung together resulting in often large patches of biofilm being harvested. This harvesting allowed sections of the flow lanes to be uncovered by the biofilms, as demonstrated in Figure 4.9. Moreover, the structure of the thickest 2 mm biofilm in lane 5 was especially different from the other biofilms. This biofilm had a looser structure and contained more filamentous phototrophs and more gas bubbles.

Biomass Production Rates in the Flow Lanes

All five biofilms in the horizontal flow lanes of Experiment 3 were comprised of an area of 0.0266 m^2 available for phototrophic growth. Figure 4.10 presents the cumulative biomass produced in each flow lane. During the first three weeks (day 0-20), PO_4^{3-} precipitated in the influent supply vessel. Therefore, K_2HPO_4 was dissolved in a separate vessel and directly added to the system beginning on day 22. After day 22, the biomass production rate increased. The daily biomass production varied due to the uncontrolled harvesting described previously. Nevertheless, the cumulative biomass production exhibited the greatest biomass production of 398 g dry weight/m^2 in the 2 mm biofilm and the lowest biomass production of 234 g dry weight/m^2 in the 130 μm biofilm.

Table 4.3 demonstrates the average areal biomass production rates between days 22 and 50. The biomass production rates of the two thinnest biofilms were 4.5 g dry weight/m^2/d. The other biofilms exhibited an increasing biomass production rate with thicker biofilms. The highest average areal biomass production rate of 9.9 g dry weight/m^2/d was attained with the 2 mm biofilm. From these production rates, the biomass yields on light energy were calculated between 0.26 and 0.57 g dry weight/mol photons. The biomass density of the five biofilms was determined at the end of the experiment when all biofilms were completely harvested. Table 4.3 indicates that this density decreased from 215 g dry weight/L at 250 μm to 37 g dry weight/L at 2 mm. The thinnest biofilm of 130 μm had a density of 104 g dry weight/L.
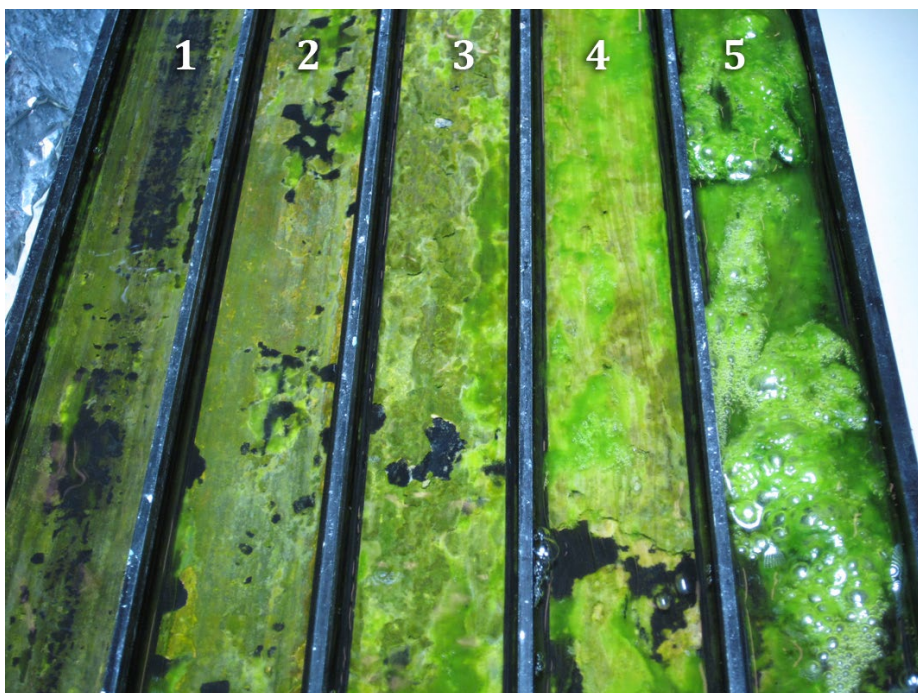
Figure 4.9 — *The biofilms in the flow lanes 1 (130 µm), 2 (250 µm), 3 (500 µm), 4 (1 mm) and 5 (2 mm).*
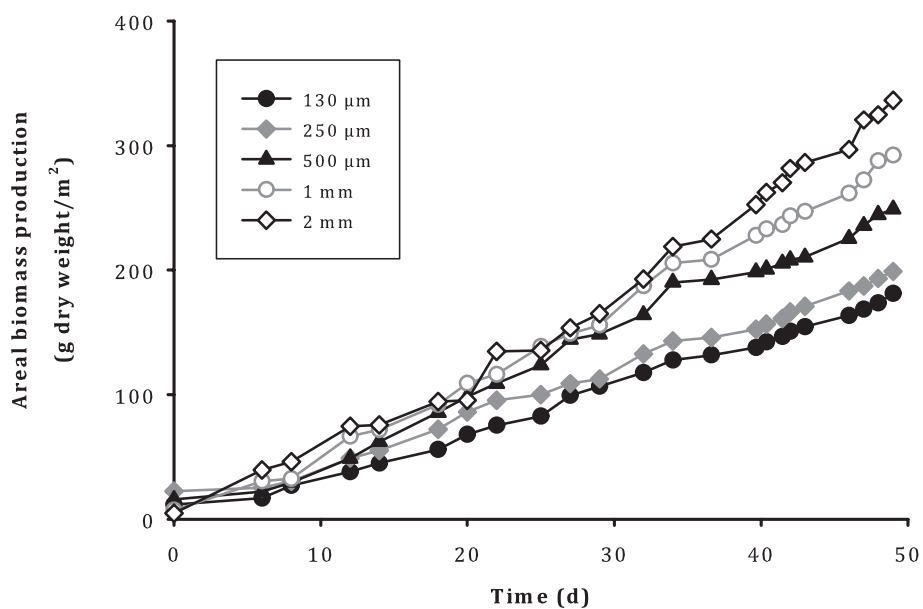
Figure 4.10 — *The cumulative biomass production of the biofilms 130 µm, 250 µm, 500 µm, 1 mm and 2 mm (day 0-20 precipitation of PO_4^{3-} in the influent).*

Table 4.3 — *The average areal biomass production rate from week 4-8, the average biomass yield on light energy and the corresponding biofilm density for the biofilms of 130 µm, 250 µm, 500 µm, 1 mm and 2 mm.*

Biofilm thickness (µm)	Average areal biomass production rate (g dry weight/m²/d)	Yield (g dry weight/ mol photons)	Density (g dry weight/L)
130	4.5	0.26	104
250	4.5	0.26	215
500	5.5	0.32	188
1000	6.8	0.40	97
2000	9.9	0.57	37

Elemental Composition Biomass

The elemental composition of the biomass was determined in order to construct the N and P mass balances depicted in Figure 4.8. In Table 4.4, the composition of the biofilms harvested during Experiments 1 - 3 are compared with an average elemental composition of microalgae (Healey 1973). While the elemental composition of the biofilms of Experiments 1 and 2A-C was comparable to the composition in accordance to Healey (1973), Experiment 3 exhibited an increased content of P, magnesium (Mg) and calcium (Ca). These extensive amounts of P, Mg and Ca indicate that precipitation of calcium and magnesium phosphates occurred in the biofilm. This also corresponds with the low amount of carbon (C) in the biofilm material, indicating that less C was fixed than expected if the biofilm was constructed entirely of phototrophic biomass. The low Si content in all of the experiments implies that the number of diatoms in the biofilms was minimal.

Based on the elemental composition measurements and the ash measurement, the average molar elemental composition of the biomass in Experiment 2 was $C_1H_{1.77}O_{0.59}N_{0.15}P_{0.008}S_{0.0032}$, corresponding to a molar C:N:P ratio of 133:19:1. Whereas the H, N, and S content is comparable to other studies, the O content is high compared to the range of 0.40-0.47 reported by others (Kliphuis et al. 2010; Duboc et al. 1999; Hecky and Kilham 1988). The N:P ratio is close to the ratio of 20:1 that was supplied, and was also found previously by Boelee et al. (2011 / Chapter 3) employing identical wastewater effluent.

4

Table 4.4 — *The average elemental composition of the harvested biofilm for Experiment 1 and Experiment 2A-C and the elemental composition of the biomass from the final harvest of Experiment 3 as mg element per g total dry weight. In brackets the standard deviation, the average microalgae composition from (Healey 1973), n.d. = not determined, n= number of samples.*

Experiment	C (mg/g)	N (mg/g)	H (mg/g)	P (mg/g)	K (mg/g)	S (mg/g)	Mg (mg/g)	Fe (mg/g)	Ca (mg/g)	Na (mg/g)	Si (mg/g)	n
1	443	77.9	65.8	10.4	6.76	5.62	3.36	3.58	5.05	0.620	0.410	2
2A-C	450 (±8.7)	76.7 (±3.8)	66.8 (±2.0)	8.78 (±0.63)	8.84 (±0.81)	3.88 (±0.21)	2.85 (±0.20)	2.72 (± 0.59)	1.99 (±0.20)	0.47 (±0.047)	0.222 (±0.074)[a]	10
3	304 (± 24)	49.9 (±4.8)	44.9 (±1.7)	35.6 (±2.3)	5.35 (±1.1)	5.52 (±0.37)	31.5 (±14)	0.16 (±0.083)	81.0 (±7.3)	5.30 (1.4)	3.02 (±1.5)	5
Micro-algae average	430	55	65	11	17.3	5.9	5.6	5.9	8.7	6.1	54	

[a] The average only of the samples above the detection limit of 0.0662 mg/g (n=4)

DISCUSSION

When applying phototrophic biofilms as wastewater treatment, a thick biofilm is preferable as it requires less harvesting and results in more biomass per harvest. This study has demonstrated that the biomass production rates are comparable for biofilms harvested every two, four or seven days in a vertical biofilm reactor. Consequently, with similar biomass productions at different harvesting frequencies, the nutrient uptake rates and effluent concentrations obtained in a reactor with thick biofilms are comparable to a thin biofilm, while less labor is required and each harvest yields more biomass. Therefore, it will be most optimal to maintain as extended time intervals as possible. With intervals exceeding seven days, there is a risk of biofilm detachment which was emphasized in Experiment 2C. It is, therefore, concluded that the optimum harvesting frequency is once a week for a phototrophic biofilm reactor in which a section of the biofilm is harvested (as in this study). Within this period, the biofilm will remain stable and effluent concentrations will remain low.

This study investigated the hypothesis that biomass productivity decreases with increasing biofilm thickness. A low biomass production is undesirable as this will result in lower nutrient removal rates and higher nutrient effluent concentrations. The results of the vertical phototrophic biofilm reactor exhibited that the desired low effluent concentrations of 2.2 mg N/L and 0.15 mg P/L can only be obtained when harvesting half of the biomass but not when harvesting the entire biofilm. However, the results did not support the hypothesis of thicker biofilms being less productive as no differences were discovered between the areal biomass production rate with different harvesting frequencies (Experiment 2). In addition, the effluent N and P concentrations consistently remained below the target concentrations, though more frequent harvesting resulted in more stable effluent concentrations.

The hypothesis that an increasing biofilm thickness results in lower biomass production rates was also tested in more detail by growing biofilms of specific thicknesses under light limiting conditions (Experiment 3). The results demonstrated that the biomass production rate even increased with increasing biofilm thickness, whereas, the biomass density decreased with thicker biofilms. Furthermore, the thickest biofilm of 2 mm was found to have a more loose structure with more filamentous phototrophs compared to the thinner and denser biofilms. It is presumed that the light regimes experienced by the phototrophs were comparable for the thin and thick biofilms because the biofilm density approximately halved when the biofilm thickness doubled. This provides a similar number of phototrophs in the thin and thick biofilm and, therefore, a similar amount of light available for each phototroph. Therefore, the light regime was not responsible for the difference in biomass production between the different biofilm thicknesses.

4

The results suggest that the thickness of the biofilm affects its structure and, subsequently, its biomass production and nutrient uptake. In studies regarding bacterial biofilms, it was discovered that biofilms thicker than 400 µm had a lower density than thinner biofilms (Bishop et al. 1995; Hoehn and Ray 1973). A biofilm with a lower density will presumably result in an increased flux of nutrients into the biofilm as a decrease in the biomass volume fraction results in a higher effective diffusive permeability (Stewart 1997). Furthermore, the higher water content of a low density biofilm may enable more convection inside the biofilm, resulting in less diffusion limitations. In addition to the low density, the irregular surface of the thick biofilms in this study is also expected to provide lower mass transfer resistances and a higher diffusion rate of nutrients at the interface of the biofilm and the bulk liquid (Wäsche et al. 2002; De Beer et al. 1994). Additional measurements of the O_2 profiles of the different biofilms determined that only the thick 2 mm biofilm had a profile which was constant at all depths with O_2 concentration of more than 100% dissolved oxygen. This implies the presence of active phototrophs throughout the entire biofilm thickness, which corresponds with the assumed deep penetration of the nutrients. Cumulatively, the higher nutrient flux and deeper penetration of nutrients into thick biofilms with a low density appear to have led to increased biomass productions.

The biomass yield on light energy was almost equal at the different biofilm thicknesses of the vertical biofilm reactor in Experiment 2, ranging between 0.43-0.46 g dry weight/mol photons. The biomass yield on light energy ranged between 0.26 to 0.57 g dry weight/mol photons in the flow lanes of Experiment 3. In suspended microalgal cultures in photobioreactors, higher yields have been measured of 0.8 g dry weight/mol photons (Kliphuis et al. 2010; Morita et al. 2000). A similar yield of 0.8 g dry weight/mol photons has also been considered possible for a vertical biofilm reactor (Boelee et al. 2012 / Chapter 2) but was not achieved in this study. This lower biomass yield on light energy may have been caused by the PO_4^{3-} limitation in the biofilm. Nevertheless, the measured yields are higher than biomass yields on light energy measured in other biofilms setups of 0.15-0.27 g dry weight/mol photons at lower light intensities with monocultures of phototrophs (Ozkana et al. 2012; Johnson and Wen 2009).

Employing well-known models (e.g. described in Pérez et al. (2005)), estimations were made of the penetration of light, CO_2, NO_3^- and PO_4^{3-} into the biofilms of Experiment 2 (see appendix D). Table 4.5 indicates that PO_4^{3-} had the smallest penetration depth of 150 µm, therefore, constituting the limiting nutrient. Light can also limit microalgal growth in the biofilm when the light intensity is lower than the compensation point, i.e., the light intensity at which the rate of photosynthesis is equal to the rate of respiration. This compensation point is reported to be between 8-40 µmol/m^2/s (Clegg et al. 2012; Hill 1996). At the penetration depth of the limiting nutrient (of PO_4), the light intensity

was calculated to range between 40-75 $\mu mol/m^2/s$ (see appendix D) which is higher than the compensation point. It is, therefore, expected that PO_4^{3-} was indeed the limiting compound during Experiment 2. In this study, the synthetic wastewater was enriched with CO_2 for pH control, and the phototrophs were, therefore, not CO_2 limited. However, in the situation when CO_2 can only diffuse from the ambient air, CO_2 will constitute the limiting compound with a penetration depth of 25 μm. Therefore, CO_2 addition to the liquid will be required to maintain a high biomass production unless the wastewater contains sufficient inorganic carbon to sustain microalgal growth (Van Vooren et al. 1999).

Table 4.5 — *The calculated penetration depths of NO_3^-, PO_4^{3-} and HCO_3^- into the biofilm during Experiment 2 and of HCO_3^- when HCO_3^- in the water is in equilibrium with the air. In addition, the light intensity at each penetration depth for low light adapted to high light adapted phototrophs.*

Compound	Penetration depth (μm)	Light intensity at the penetration depth ($\mu mol/m^2/s$)
NO_3^-	355	10-35
PO_4^{3-}	150	40-75
HCO_3^- (experiment)	250	20-50
HCO_3^- (air equilibrium)	25	125-150

The estimated biofilm thicknesses in the vertical biofilm reactor (500 μm, 1.3 mm and 4.2 mm) are greater than the estimated penetration depths of light, CO_2, and nutrients. However, the actual biofilm thickness was even larger due to the gas bubbles which were entrapped in the biofilm and were discharged from the biofilm only during harvesting (and, thus, not included in the measurements). It was presumed that, at a certain biofilm thickness, the net phototrophic growth would decrease due to increased rates of endogenous respiration and cell death. Presumably, the time-scale of the experiments in this study had not been long enough to observe these losses.

Finally, for phototrophic biofilms in wastewater treatment, the method employed to supply the wastewater onto the biofilm is of great significance. The elemental composition of the biomass indicated the presence of precipitates in the biofilms of the flow lanes in Experiment 3, which is in contrast to the biofilms of the vertical reactor in Experiment 2. The precipitation in the flow lanes was most likely the result of the different manner of supplying liquid onto the biofilm between the two experiments. Whereas wastewater flowed continuously over the biofilm in the vertical reactor of Experiment 2, waves rolled over the biofilm in the horizontal flow lanes of Experiment 3 which may have resulted in a longer retention time of the liquid inside the biofilm. This longer retention time could have allowed the phototrophs to take up additional CO_2 and NO_3^- accompanied by a larger pH increase inside the biofilm. As precipitation of calcium

4

or magnesium phosphates occurs at elevated pH, this may explain the precipitation that was detected in the biofilms within the flow lanes.

CONCLUSIONS

The present study has demonstrated that it was possible to continuously achieve effluent values below 2.2 mg N/L and 0.15 mg P/L employing a phototrophic biofilm reactor. To attain these low effluent values, it is necessary to frequently harvest a section of the biofilm but not the entire biofilm. The biomass productivity is optimal for a wide range of biofilm thicknesses as was indicated by the similar biomass production rate of 7 g dry weight/m^2/d when harvesting every two, four, or seven days. Additional measurements in flow lanes demonstrated that, contrary to expectations, the areal biomass production rate increased with increasing biofilm thicknesses from 130 μm until 2 mm. Nevertheless, it is expected that increasing the biofilm thickness further will eventually result in lower biomass production due to losses exceeding the biomass growth. The optimal harvesting frequency was determined to be once a week as the biofilm remains stable during this period (no self-detachment), and the system maintains low nutrient effluent concentrations.

ACKNOWLEDGEMENTS

4

Chapter 5

Nutrient Removal and Biomass Production in an Outdoor Pilot-Scale Phototrophic Biofilm Reactor for Effluent Polishing

Nadine C. Boelee
Marcel Janssen
Hardy Temmink
Rabin Shrestha
Cees J.N. Buisman
René H. Wijffels

ABSTRACT

An innovative pilot-scale phototrophic biofilm reactor was evaluated over a five month period to determine its capacity to remove nitrogen and phosphorus from Dutch municipal wastewater effluents. The areal biomass production rate ranged between 2.7 and 4.5 g dry weight/m^2/day. The areal nitrogen and phosphorus removal rates averaged 0.13 g N/m^2/day and 0.023 g P/m^2/day, which are low compared to removal rates achieved in laboratory biofilm reactors. Nutrient removal increased during the day, decreased with decreasing light intensity and no removal occurred during the night. Additional carbon dioxide supply was not requisite as the wastewater was comprised of enough inorganic carbon to sustain microalgal growth. The study was not conclusive for the limiting factor that caused the low nutrient removal rate, possibly the process was limited by light and temperature, in combination with pH increases above pH 9 during the daytime. This pilot-scale study demonstrated that the proposed phototrophic biofilm reactor is not a viable post-treatment of municipal wastewater effluents under Dutch climate conditions. However, the reactor performance may be improved when controlling the pH and the temperature in the morning. With these adaptations, the use of a phototrophic biofilm reactor could be feasible at lower latitudes with higher irradiance levels.

5

INTRODUCTION

Many municipal wastewater treatment plants in the Netherlands and other EU member states are required to further reduce their nitrogen (N) and phosphorus (P) emissions due to the EU Water Framework Directive regulations. In concordance with this directive, effluent N and P concentrations must to be reduced from the current EU discharge requirements of 10 mg N/L and 1 mg P/L to concentrations appropriate for discharge to 'sensitive' water bodies. In the Netherlands current guidelines for discharging effluents to sensitive water bodies are 2.2 mg N/L and 0.15 mg P/L.

Available technologies for the post-treatment of municipal wastewater include denitrifying filters and iron dosing. However, these technologies are not sustainable as they require chemicals, are accompanied by carbon dioxide (CO_2) emissions and remove, rather than recover, N and P. Microalgal biofilm systems may constitute a more sustainable alternative. Phototrophs employ light energy and CO_2 and, therefore, do not require an organic carbon source. A microalgal biofilm system can operate at short hydraulic retention times and, in contrast to suspended microalgal systems, little or no separation of microalgae and water is required before the effluent can be discharged (Roeselers et al. 2008; Schumacher et al. 2003).

Recent studies have demonstrated that microalgal biofilm systems can achieve high removal efficiencies of more than 90% nitrate (NO_3^-), the main N source in Dutch municipal wastewater effluents, and more than 80% phosphate (PO_4^{3-}) (Godos et al. 2009; González et al. 2008; Shi et al. 2007). During laboratory experiments it was revealed that the high affinity of phototrophs for NO_3^--N and PO_4^{3-}-P (Collos et al. 2005; Hwang et al. 1998; Halterman and Toetz 1984; Eppley et al. 1969) enables phototrophic biofilms to achieve effluent concentrations well below the target concentrations of 2.2 mg N/L and 0.15 mg P/L (Boelee et al. 2011 / Chapter 3). With the promising results of microalgal biofilm systems in the laboratory, it is important to scale up these systems to a pilot-scale study and test the systems under variable and realistic outdoor conditions over a prolonged period of time.

The first aspect that should be investigated in a pilot-scale study is the reactor performance during the day/night cycle because laboratory studies are predominantly performed under continuous light conditions. During the day, microalgae are in their growth phase, and carbon (C) and energy are fixed during photosynthesis. At night, phototrophs utilize the carbohydrates that they have accumulated during the day, and protein synthesis and cell division occur (Lacour et al. 2012; Needoba and Harrison 2004). The assimilation of N and P, therefore, exhibits oscillations with increased assimilations during the day compared to those during the night (Lacour et al. 2012;

Needoba and Harrison 2004; Ahn et al. 2002; Vincent 1992; Jansson 1988). Uptake of N in the dark is known to occur in vertically migrating phytoplankton in the seas and oceans where N is limited and, therefore, must be absorbed whenever encountered (Needoba and Harrison 2004). A lower N assimilation in the dark has been documented in various studies, especially under N limiting conditions (Clark et al. 2002; Vona et al. 1999). This assimilation was determined to deviate among different phototrophs as diatoms exhibit increased N assimilation rates in the dark over flagellates (Clark et al. 2002). However, N uptake at night has not been observed in all studies (Lacour et al. 2012). It has, therefore, not been ascertained whether microalgal biofilms treating wastewater will continue assimilating N and P during the night, while this is essential in the application of a biofilm reactor as wastewater must be treated both day and night.

The second aspect that requires further investigation is the performance of a microalgal biofilm reactor experiencing continuously changing, outdoor climatic conditions. Deviation from the optimum light intensity and temperature will reduce phototrophic growth rates, and subsequently nutrient removal rates. At low light intensities, microalgal growth increases linearly with increasing light intensity until the light becomes saturating, generally around 200-400 $\mu mol/m^2/s$ (Hill 1996). At light intensities above this saturating intensity, the specific microalgal growth rate will stabilize at its maximum level. The exposure of phototrophs to excessive light during a part of the day could be a significant impediment when scaling up phototrophic biofilm reactors. Excess light that is absorbed by phototrophs is initially dissipated as heat, but under sustained excess light conditions, photoinhibition can occur (Muñoz et al. 2009).

The effect of temperature is often described by Arrhenius Law where microalgal growth increases with increasing temperature up to an optimum growth temperature. Each microalgal species has its own optimum growth temperature but, generally, maximum growth rates of mesophilic microalgae occur between 20 and 25°C (Ras et al. 2013). The optimum growth temperature can, however, vary under environmental conditions including nutrient availability. Microalgal growth rapidly decreases above the optimum growth temperature until lethal temperatures are reached (Ras et al. 2013). Light intensity and temperature vary throughout the day, the season and in different locations, therefore, their effects are important aspects for the performance of phototrophic biofilms.

The nutrients required for the growth of microalgae must diffuse from the bulk water into the biofilm. Consequently, microalgal biofilm reactors may function under diffusion limited conditions. Models of microalgal biofilms predict that phototrophs located in the inner layers of thick biofilms become inactive due to diffusion limitation of CO_2 (Wolf et al. 2007; Liehr et al. 1990). Limitations with respect to the diffusion of other nutrients may also occur with wastewater effluents because they have relatively low nutrient concentrations.

This study aims to acquire knowledge on the performance of a phototrophic biofilm reactor treating municipal wastewater treatment effluent under realistic outdoor conditions, in particular with respect to the above mentioned aspects: the day/night cycle, changing climatic conditions, diffusion limitation and temporal conditions of excess light. A pilot-scale phototrophic biofilm reactor was operated from June until the end of October 2012 in Leeuwarden, the Netherlands, to treat effluent from the local municipal wastewater treatment plant. The reactor was placed vertically as this was expected to enhance productivity compared to horizontal positioning. The daily and seasonal removal of NO_3^--N and PO_4^{3-}-P was monitored as well as the pH, temperature, and light intensity. Moreover, the biomass production and composition were measured in order to establish possible reuse options for the microalgal biomass.

MATERIAL AND METHODS

Experimental Setup

The phototrophic biofilm pilot-scale reactor was located at the wastewater treatment plant of Leeuwarden, the Netherlands (53.196°N, 5.827°E), facing south, and is depicted in Figure 5.1 and Figure 5.2. The reactor consisted of a 10 m^2 (5.0 m x 2.0 m) carrier material, of which 8.08 m^2 was made available for phototrophic growth. This carrier material was a polyethylene-based woven geotextile (Polyfelt Geolon PE180, TenCate Geosynthetics, the Netherlands) with a nominal pore size of 170 μm. This Polyfelt was situated on top of a layer of Polyfelt P120 (a polypropylene-based non-woven geotextile, TenCate Geosynthetics, the Netherlands) and another layer of Polyfelt Geolon PE180. All three layers were mounted in an aluminum frame which was arranged vertically. A 5 m long gutter was positioned against the top part of the Polyfelt, and the overflow of this gutter was distributed over the biofilm and collected into another gutter located below the frame. From this gutter, the water flowed into a 59 L vessel. To protect the pump and prevent clogging, the liquid was filtered (filter diameter 0.8 mm) and pumped (submersible pressure pump) via the nitrate sensor into a 636 L recycle vessel. From the latter vessel, the liquid was filtered (filter diameter 0.5 mm) and pumped at 24 L/min (submersible pressure pump) back to the carrier layer.

A buffer tank was continuously replenished with filtered effluent (filter diameter 0.8 mm) from the wastewater treatment plant. The liquid from the buffer tank was filtered again (filter diameter 0.5 mm) and pumped into the large recycle vessel at 0.9 L/min after adding additional N and P from a concentrated solution. The overflow from the large recycle vessel became the effluent for the system.

Figure 5.1 — *Schematic overview of the pilot-scale phototrophic biofilm reactor. Influent samples were taken at sample point 1 (P1) and effluent samples at sample point 2 (P2). The pH, dissolved oxygen concentration and the flow rate were also measured at these sample points.*

In the influent and effluent, the following parameters were measured every 3 minutes: the pH, the dissolved oxygen concentration (Oxymax COS61D, Endress-Hauser, Switzerland), the NO_3^--N concentration (Viomax CAS51D, Endress-Hauser, Switzerland) and the flow rate (MIK 0.16-3.2 and 1.6-32 L/min, Kobold, Germany). The influent and effluent NO_3^--N concentration was alternately measured for 15 minutes using a single NO_3^--N sensor. From September 20 until October 25, the pH of the effluent was controlled at 8.1 by the pulse-wise addition of CO_2 gas into the large recycle vessel. The light intensity on the vertical plane was measured at 1.5 m on the right-hand side of the aluminum frame employing a 2π PAR quantum sensor (SA190, LI-COR Biosciences, USA). During specific sunny days samples were collected each hour from the influent or effluent employing an autosampler (ASP Station 2000, Endress-Hauser, Switzerland).

Influent Characteristics

The characteristics of the influent of the biofilm reactor are depicted in Table 5.1. The concentrations of N and P in the wastewater treatment plant effluent were extremely low, and it was therefore, decided to increase the NO_3^- and PO_4^{3-} concentrations. Media of 29.0 g/L $NaNO_3$ and 2.49 g/L K_2HPO_4 or 5.61 g/L K_2HPO_4 was supplied at 1 mL/min in order to achieve an average of 5 mg N/L and 0.5 mg P/L from May 25 until June 25, and 5 mg N/L and 1 mg P/L from June 26 until October 25.

Figure 5.2 — *The pilot-scale phototrophic biofilm reactor at the wastewater treatment plant in Leeuwarden.*

Table 5.1 — *The average temperature, dissolved oxygen concentration and pH of the influent of the biofilm reactor during the five months of operation.*

Month	Temperature (°C)	Dissolved oxygen (mg/L)	pH (-)
June	17.9	0.6	7.1
July	20.3	1.0	7.1
August	21.1	1.4	7.2
September	18.1	0.7	7.0
October	14.7	0.5	6.9

Harvesting

A portion of the biofilm was harvested once a week which was the optimal harvesting frequency determined in a lab-scale vertical biofilm reactor (Boelee et al. 2013). The biofilm was harvested utilizing a scraper constructed from a large, adhesive comb. This scraper was designed to harvest either half or one third of the biofilm from the carrier material and was scraped over the biofilm from top to bottom. During harvest events 1-3, the scraper consisted of 7 mm teeth with a 7 mm gap (approximately half of the biomass harvested) while the scraper possessed 7 mm teeth with a 14 mm gap (about one third of the biomass harvested) during the remaining harvests.

Analytical Procedures

Grab samples from the inflow and outflow of the pilot-scale reactor were analyzed for total N and total P using colorimetric cuvette tests (LCK 138 and LCK 249, Hach Lange, Germany). To determine the NO_3^--N and PO_4^{3-}-P concentrations, the samples were filtered through a 0.45 µm filter (Millex-LCR, Merck Millipore, USA) and analyzed for NO_3^--N and PO_4^{3-}-P with ion chromatography (Compact IC 761, Metrohm, Switzerland). The Compact IC 761 was equipped with a conductivity detector with the pre-column Metrosep A Supp 4/5 Guard and with the column Metrosep A Supp 5, 150/4.0 mm (Metrohm, Switzerland). Filtered samples were also analyzed for inorganic carbon employing a TOC organic carbon analyzer (TOC-V_{CPH}, Shimadzu, Japan).

Following each harvest, the total wet weight was measured after which representative samples of the harvested wet biomass of a known volume were dried at 105°C for at least 24 hours. With the resulting dry weight the density and the total dry weight harvest were calculated. To determine the elemental composition of the biomass, it was ground and dried for another 24 hours. The C, N and H content was measured in duplicate with an elemental analyzer (EA 1110, ThermoQuest CE Instruments, USA) utilizing a vertical quartz tube (combustion tube) maintained at 1000°C with a constant flow of helium at 120 mL/min, an oxidation catalyst (WO_3) zone, a copper zone followed by a Porapack PQS column maintained at 60°C and, finally, followed by a TCD detector.

To determine the Ca, P, K, Na, S, Mg, Fe, Al, Mn, Si, Cu and Zn content, duplicates of the biomass were digested using 10 mL HNO_3 (68%) per 0.5 g biomass. During digestion, the temperature was increased in a microwave (ETHOS 1, Milestone, Italy) over a 15 minute time period until reaching 180°C at 1000 W, and maintained at 180°C for an additional 15 minutes. Following digestion, the concentrations of the elements were measured with inductive coupled plasma (ICP) (Optima 5300 DV equipped with an optical emission spectrometer, Perkin Elmer, USA).

Finally, the ash content was determined by burning the dried ground biomass at 550°C for 2 hours. The ash content was calculated by dividing the ash weight by the dry weight. The caloric value of the biomass was determined for the harvested biomass on July 24, October 25 and a mixed sample of harvests from July 3, 10, 17, 24, 31; August 7, 14; September 13, 20, 27; October 4, 11, 18 and 25. The caloric value of the biomass was determined by burning the biomass under high oxygen pressure in an isoperibol oxygen bomb calorimeter (Model 6300, Parr Instrument Company, USA). The gross calorific value was calculated from the corrected temperature increase and the effective heat capacity of the calorimeter.

Calculation of the Elemental Composition

The molar elemental composition of the biofilm, including oxygen, was calculated according to (Duboc et al. 1999) employing the measured weight of C, H, N, S, P and ash.

RESULTS

Biofilm Growth

The phototrophic biofilm was spread over the entire 8.08 m^2 carrier layer. Using the scraper for harvesting resulted in a subsequent striped pattern in the biofilm, as illustrated in Figure 5.3. As the biofilm grew the days after each harvest, this pattern slowly disappeared.

Microscopic observations indicated that phototrophs were the principle organisms in the biofilm with the cyanobacterium *Phormidium autumnale* as the dominant species. Table 5.2 depicts that this species was dominant in July and October but less so in September when other cyanobacteria and a diatom, specifically, *Pseudanabaena* sp., *Chroococcus* sp. and *Nitzschia palea*, were also well represented. In mid-July, numerous mosquito larvae were observed in the biofilm as well as various phototrophic species, which are also shown in Table 5.2 for July, September, and October. The taxonomic variability in the biofilm was lower when compared to other studies regarding phototrophic biofilms at wastewater treatment plants. However, these studies also reported seasonal shifts in the presence of species and their dominance (Congestri et al. 2006; Davis et al. 1990).

Influent and Effluent Characteristics and Light Intensity

The average inorganic C concentration of the influent was 69 mg/L. The average effluent inorganic C concentration was 54 mg/L during the day and 67 mg/L during the night, indicating autotrophic uptake of inorganic C during the day. After September 19, the average inorganic C concentration in the effluent increased to 77 mg/L due to the additional CO_2 that was supplied to control the pH at 8.1. The average dissolved O_2 concentration in the influent was 0.9 mg/L but demonstrated a daily cycle between 0.2 mg/L at night and 6.0 mg/L during the day. The average dissolved O_2 concentration in the effluent was 9 mg/L.

Figure 5.3 — *Close-up of the biofilm on September 6 (three days after harvesting).*

Figure 5.4A and B depict the monthly averages of the daily variation of light and effluent temperature between June and October. The greatest light intensities on the vertical plane of the biofilm reactor of 660 and 670 μmol/m^2/s were measured between 12:00 and 13:00 hours in August and between 13:00 and 14:00 hours during September. The light distribution over the biofilm surface was not homogenous due to shadows of the reactor construction. On a sunny day, for instance, light intensities between 270 and 1400 μmol/m^2/s were measured at different locations on the biofilm. The light intensity in Figure 5.4A measured by the fixed sensor is, therefore, not the average light intensity received by the biofilm surface. However, this light intensity does give an indication of the variation in light intensity during the day and the months.

The highest effluent temperature of 23.3°C was measured between 14:00-15:00 hours in August. In general, the temperature increase and decrease follows one or two hours after the light increase and decrease. Figure 5.4C demonstrates the effect of the daily variations of light and temperature on the phototrophic process. The effluent pH increased between 8:00-16:00 hours as a consequence of the uptake of NO_3^- and CO_2 by the phototrophs during the day and decreased afterwards as a result of the decrease and later cessation of photosynthesis during the night. The most significant pH increases to 9.5 and 9.6 were detected in July between 15:00 and 18:00 hours and, in August, between 14:00 and 17:00 hours. The maximum pH detected on a specific day was 10.1

in June and July and 10.8 and 10.9 in August and September, respectively. The maximum and minimum temperatures were 31°C and 7.5°C in July and October, respectively, and the maximum light intensities were 1800 and 1870 μmol/m^2/s in September and October, respectively.

Table 5.2 — *Taxonomical analysis of the species present in the biofilm in July, September and October.*

Species	24 July	13 September	25 October
Dominant species			
Cyanobacteria	*Phormidium autumnale (80%)*	*Phormidium autumnale (30%)*	*Phormidium autumnale (70%)*
Rare species (5-10%)			
Cyanobacteria		*Pseudanabaena sp. Chroococcus sp.*	
Diatoms		*Nitzschia palea*	
Rare species (1-5%)			
Coccal green algae	*Scenedesmus brasiliensis*	*Scenedesmus brasiliensis Scenedesmus quadricauda* *Chlorella sp.*	*Scenedesmus brasiliensis* *Scenedesmus acutus*
Cyanobacteria	*Pseudanabaena galeata unidentified coccal cyanobacteria*		*Pseudanabaena galeata*
Diatoms	*Cymbella minuta Melosira varians Gomphonema parvulum Nitzschia palea* *Synedra ulna*	*Cymbella minuta Melosira varians* *Nitzschia frustulum* *Eunotia sp.*	*Cymbella minuta Melosira varians Gomphonema parvulum Nitzschia palea Nitzschia frustulum Nitzschia capitellata Synedra ulna* *Navicula gregaria*
Filamentous green algae			*Ulothrix sp.*

5
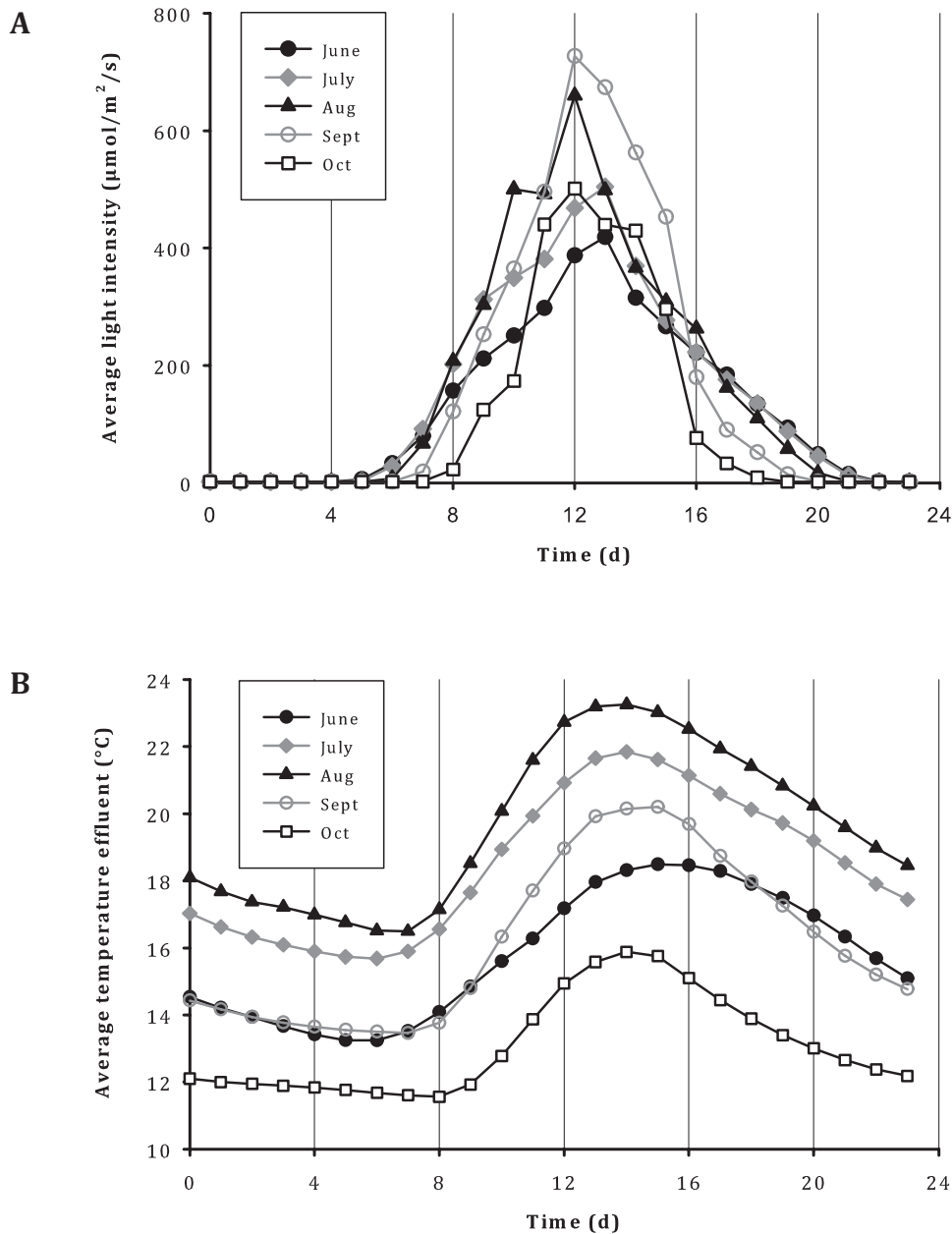
Figure 5.4 — Monthly averages of the light intensity received by the vertical plane of the pilot-scale biofilm reactor for each hour of the day (A), and of the temperature (B) and the pH (C) in the effluent for each hour of the day. The pH was controlled at 8.1 from September 20 until the end of October.

C
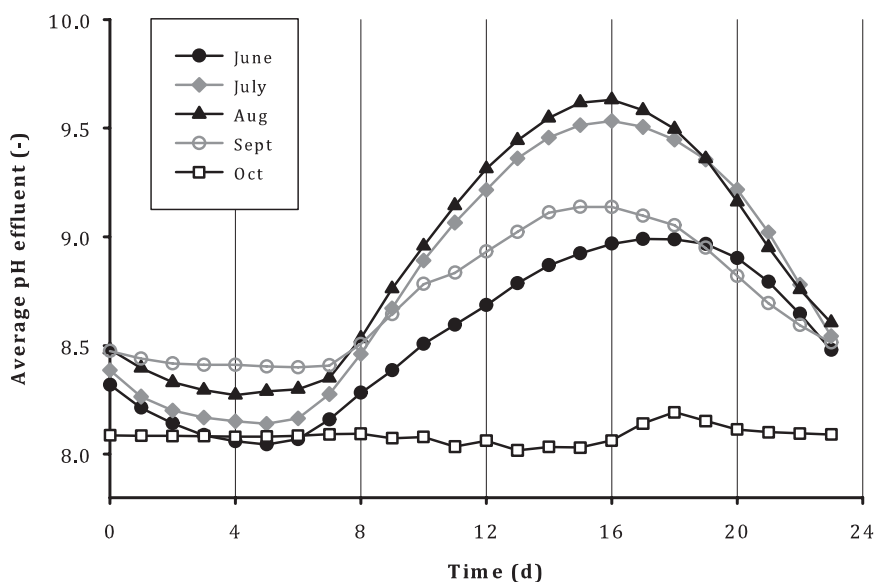
Nutrient Removal

NO_3^--N and PO_4^{3-}-P removal were monitored over 24 hour time periods on selected sunny days; Figure 5.5 and Figure 5.6 provide two examples. On July 2 and 3, the effluent concentrations of NO_3^--N and PO_4^{3-}-P decreased during the day and achieved the lowest concentrations of 1.5 mg NO_3^--N/L and 0.50 mg PO_4^{3-}-P/L at 16:00 hours. Hereafter, the effluent concentrations gradually increased to attain maximum concentrations of 3.1 mg NO_3^--N/L and 1.2 mg PO_4^{3-}-P/L at 6:00 hours. At this point in time, the PO_4^{3-}-P effluent concentration was similar to the influent concentration, whereas the NO_3^--N effluent concentration remained lower than the influent concentration. On July 5, the skies became cloudy between 14:00 and 18:00 hours, and this sudden decrease in light and temperature immediately provided a lower uptake of NO_3^--N and PO_4^{3-}-P. At night, the absence of photosynthesis and the dilution of the reactor with the influent resulted in nutrient effluent concentrations.

5

A

B

5
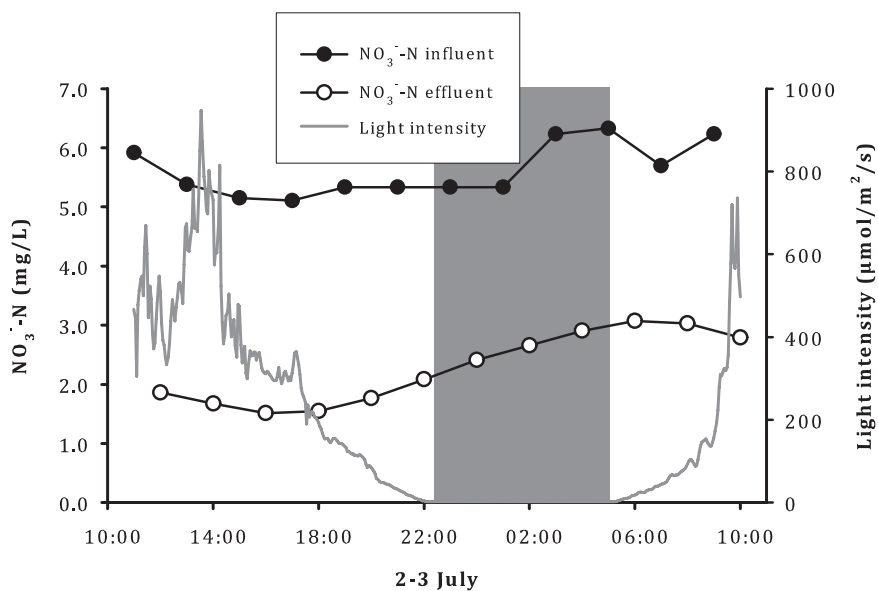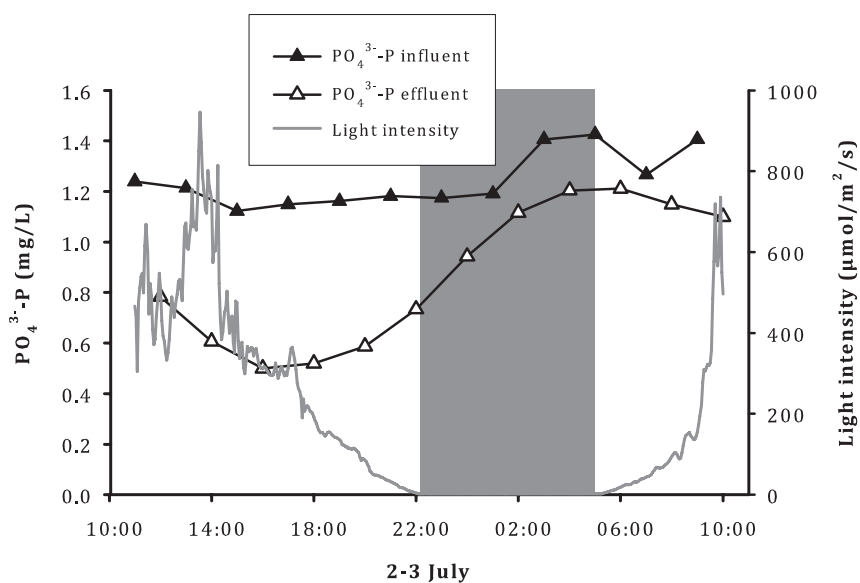
Figure 5.5 — NO_3^--N (A) and PO_4^{3-}-P (B) concentrations in influent and effluent, and the light intensity (A and B) on July 2 and 3. The grey area indicates the night.

A

B

Figure 5.6 — NO$_3^-$-N (A) and PO$_4^{3-}$-P (B) concentrations in influent and effluent, and the light intensity (A and B) on July 5 and 6. The grey area indicates the night.
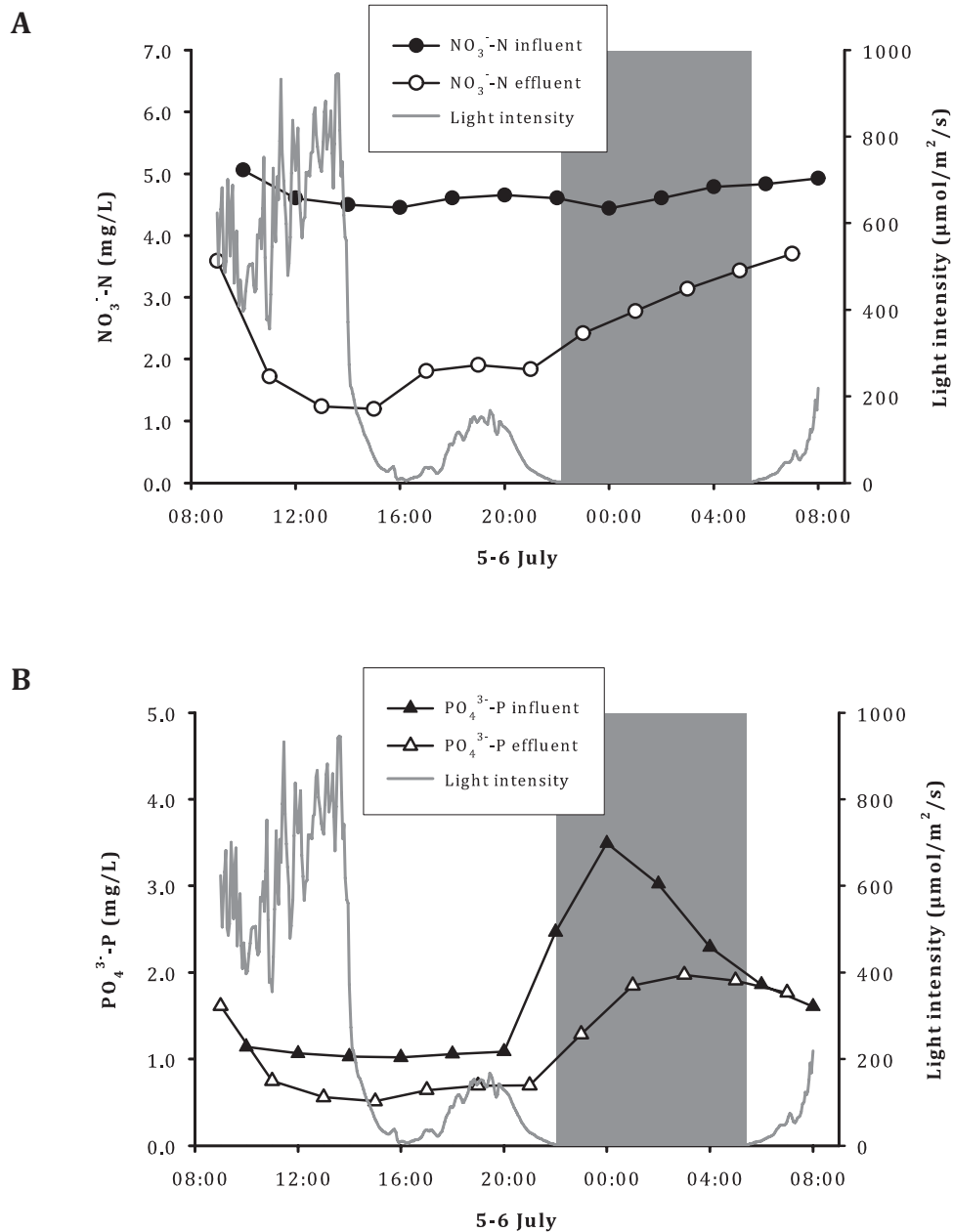
The average influent and effluent concentrations of NO_3^--N in Table 5.3 demonstrate that the monthly average removal of NO_3^--N was only 6-28% corresponding to a removal rate of 0.03-0.18 g $N/m^2/d$. The average PO_4^{3-}-P removal efficiency from June until the end of October was only 14% corresponding to a removal rate of 0.023 g $P/m^2/d$. In order to reduce the nutrient load, the flow rate, therefore, was reduced to 0.5 L/min between August 21 - September 6 and to 0.7 L/min between September 6 - 13. However, the decreased flow rate did not result in lower effluent concentrations. From the end of September and throughout October, CO_2 was supplied to the effluent an additional measure to stimulate the removal rates. This also did not result in increased removal rates compared to the previous months, although, in October the daily light intensity was lower, implying that other factors such as light or temperature may also have influenced the low nutrient uptake during this time. Throughout June-October an average of 80% of the total N in the influent consisted of NO_3^- and 65% of the total P consisted of PO_4^-. The effluent contained similar fractions of NO_3^- and PO_4^{3-} with an average of 76% NO_3^- and 66% PO_4^{3-}.

Table 5.3 — *The average NO_3^--N concentrations measured online in the inflow, outflow, the corresponding average NO_3^--N removal, the average light intensity received by the vertical plane of the reactor and the average temperature of the effluent. The values in parentheses are standard deviations.*

Month	Average NO_3^--N in (mg/L)	Average NO_3^--N out (mg/L)	Average removal efficiency (%)	Average removal rate (g/m²/d)	Average light intensity (mol/m²/d)	Average temperature effluent (°C)
June	5.11 (±0.67)	4.82 (±2.67)	6	0.030	11	15.8
July	3.82 (±1.86)	3.35 (±1.29)	12	0.082	13	18.5
August	4.84 (±2.09)	3.49 (±1.70)	28	0.18	14	19.6
September	4.11 (±1.76)	3.40 (±1.31)	17	0.11	14	16.2
October	6.06 (±1.32)	5.15 (±1.58)	15	0.18	9	13.1

Biomass Production

The biofilm of the reactor was harvested every week and achieved an average density of 91 g dry weight/L. Figure 5.7 illustrates the areal biomass production rate for all harvests. The areal biomass production varied between 2.7 and 4.5 g dry weight/m²/d. The lower biomass production on June 26 (harvest 3) was a consequence of a variation in the harvesting procedure, whereby one third of the biofilm was harvested instead of half of the biofilm, as was harvested during the first two harvests. The cause of the sudden lower biomass production on August 7 (harvest 9) is unknown.
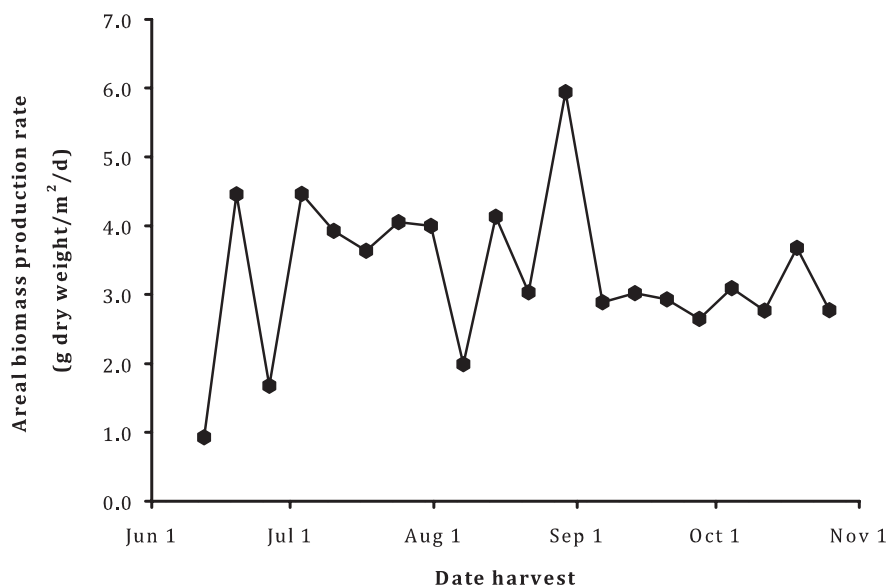
Figure 5.7 — *Areal biomass production rate for each harvest event.*

In Table 5.4 the elemental composition of the biofilm is presented and compared to an average composition of microalgae as reported by Healey (1973). This comparison demonstrates that the fractions of the most important elements in the biofilm of the pilot-scale reactor were slightly lower than what was expected, with the exception of calcium (Ca) and manganese (Mn) of which mass fractions were 10 and 20 times higher than the average microalgae fractions. In addition, the ash content of 367 mg/g was very high compared to an average ash content of microalgae of 60.9 mg/g biomass (Duboc et al. 1999). The high Ca and ash content indicate the presence of precipitates in the biofilm, for instance, of calcium carbonate ($CaCO_3$). Based on the measured Ca mass fraction, the $CaCO_3$ was estimated to constitute 50% of the ashes. The precipitates may have included Mn as this element is known to co-precipitate with $CaCO_3$ (Temman et al. 2000; Lorens 1981). The Si content was lower than an average microalgae composition but with an average effluent concentration of 9 mg Si/L, this was probably not related to a lack of Si in the wastewater. Si is essential for diatom growth (Healey 1973) and, therefore, the low Si content in the biomass can be explained by the relatively low amount of diatoms in the biofilm. Based on the measured elemental composition, the average molar elemental composition of the biomass was calculated to be $C_1H_{1.61}O_{0.49}N_{0.16}P_{0.012}S_{0.0055}$ which corresponds to a molar C:N:P ratio of 86:14:1. The average caloric value of the biomass was 13 MJ/kg dry weight.

Table 5.4 — The elemental composition and ash content as mg element per g total dry weight, and the caloric value as MJ/kg dry weight of the harvested biofilm. The average microalgae composition was obtained from (Healey 1973), and the average microalgae ash content and caloric value were obtained from (Duboc et al. 1999).

Date harvest	C (mg/g)	N (mg/g)	H (mg/g)	P (mg/g)	K (mg/g)	Na (mg/g)	S (mg/g)	Mg (mg/g)	Fe (mg/g)	Al (mg/g)	Mn (mg/g)	Si (mg/g)	Cu (mg/g)	Zn (mg/g)	Ash (mg/g)	Caloric value (MJ/kg)
12/06	144	20.7	17.5	3.16	2.52	2.57	2.12	2.52	1.53	1.25	1.08	0.42	0.039	$<3.3 \cdot 10^{-5}$	767	
19/06	264	44.1	35.9	4.95	6.13	3.54	3.47	3.09	0.66	0.41	0.38	0.15	0.039	$<3.3 \cdot 10^{-5}$	479	
10/07	331	67.9	46.1	9.33	7.40	2.06	5.11	2.99	1.22	0.41	0.89	0.25	0.039	$<3.3 \cdot 10^{-5}$	360	
24/07	326	62.2	43.9	8.19	6.66	2.79	4.38	2.84	0.89	0.28	0.76	1.07	0.035	$<3.3 \cdot 10^{-5}$	388	13
14/08	335	61.4	44.6	9.87	7.10	2.40	4.64	5.51	4.64	0.43	0.81	1.76	0.039	0.175	363	
13/09	331	57.6	43.9	11.24	6.19	2.66	4.46	5.80	4.46	0.35	0.56	1.06	0.041	0.163	334	
27/09	356	68.5	49.8	10.06	7.84	2.06	5.32	3.66	5.32	0.41	0.94	2.05	0.055	0.190	305	
11/10	320	54.5	42.6	10.25	7.80	3.67	4.95	3.42	4.95	0.60	1.25	3.19	0.070	0.245	381	
25/10	279	46.2	37.8	9.28	6.97	3.12	4.74	2.88	4.74	1.00	2.39	1.80	0.079	0.376	434	12
Average [a]	325.43	59.76	44.10	9.75	7.14	2.68	4.80	3.87	3.75	0.50	1.09	1.60	0.051	0.23 [b]	367	13 [c]
Microalgae average	430	55	65	11.0	17.3	6.1	5.9	5.6	5.9	-	0.06	54.0	0.1	0.28	60.9	22.7

[a] The average excludes the harvests of 12/6 and 19/6
[b] The average only of the samples in which Zn was measured
[c] The average caloric value was determined for a mixed sample of 14 harvests

Relationship Between Biomass Production, Nutrient Removal, Temperature and Light

It was expected that nutrient removal and biomass production would be correlated with the light intensity and with the temperature that the biofilm was exposed to but, surprisingly, no such correlations were discovered. Figure 5.8 depicts an insignificant positive relationship between the amount of light received by the biofilm and the NO_3^--N removal and also between temperature during the daytime and NO_3^--N removal. No correlation was detected between the amount of light received by the biofilm and the biomass production rate or between the temperature during the daytime and the biomass production rate.

DISCUSSION

The NO_3^- and PO_4^{3-} removal from the wastewater with the pilot-scale phototrophic reactor increased during the day and decreased with decreasing light intensity until no removal occurred during the night. The lowest effluent NO_3^- and PO_4^{3-} concentrations were observed at the end of the afternoon around 16:00; the highest concentrations were in the early morning around 6:00. This removal pattern is comparable to a previous study in a high rate algal pond in which the microalgal productivity and nutrient removal was greatest during the afternoon between 13:00-15:00 hours and lowest at the end of the night (Picot et al. 1993). The NO_3^- and PO_4^{3-} removal pattern also corresponded with the pH. The pH increased during the day from around 8:00 until 16:00 and then decreased afterwards, indicating phototrophic activity during the day. Although N uptake was observed in a number of studies in the absence of light (Needoba and Harrison 2004; Clark et al. 2002; Vona et al. 1999), this could not be confirmed in this study. The measured increase in NO_3^- and PO_4^{3-} effluent concentrations during the night corresponds to the calculated increase in the absence of photosynthesis. While the system dimensions such as the hydraulic retention time (0.6 d) will have an effect on the rate of increase of the nutrient effluent concentrations during the night, the target nutrient concentrations of 2.2 mg N/L and 0.15 mg P/L presumably will not be achieved. Therefore, it will be necessary to buffer the effluent at night.

A
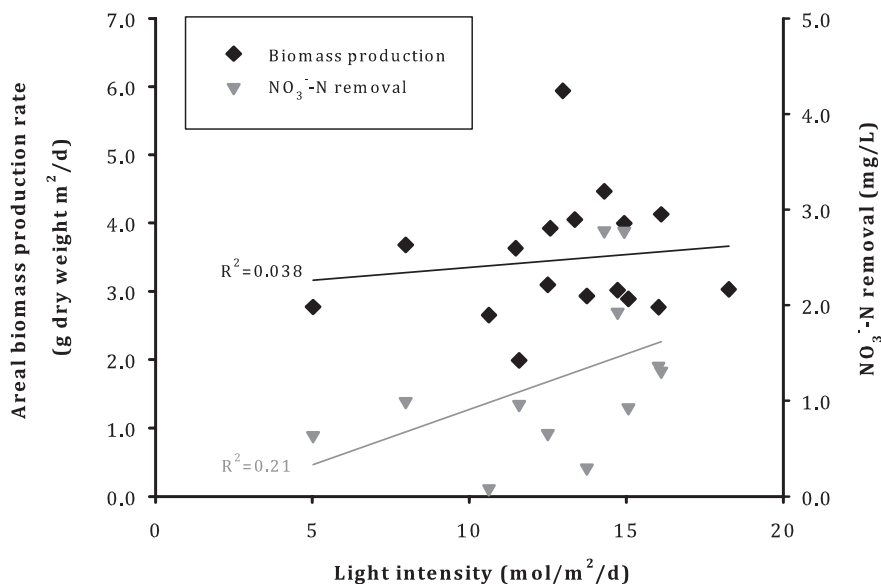
B
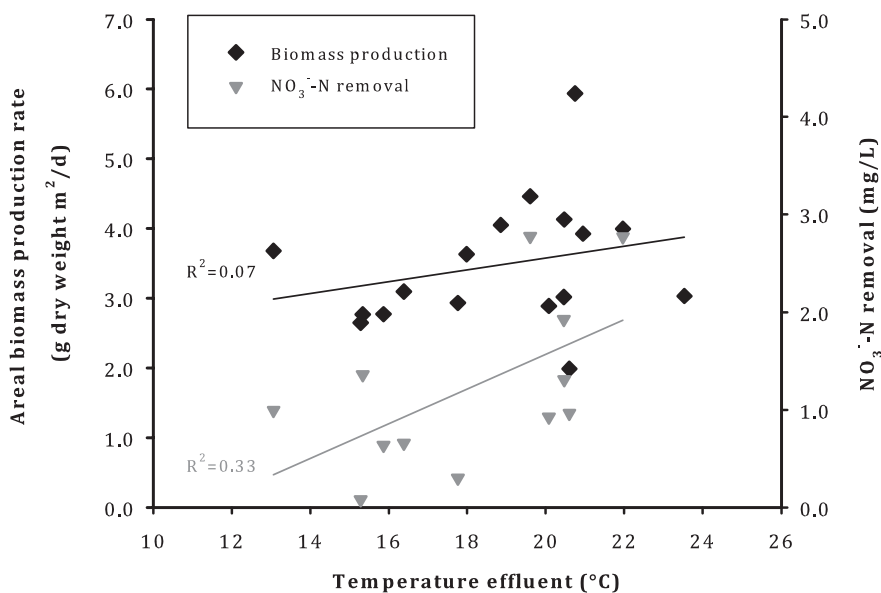
Figure 5.8 — *Relationship between the average light intensity received by the vertical plane of the pilot-scale biofilm reactor and the areal biomass production rate and average NO_3^--N removal (A). The relationship between the average effluent temperature and the areal biomass production rate and average NO_3^--N removal (B) for each harvest.*

Although substantial N and P removal was observed on specific sunny days (Figure 5.5 and Figure 5.6), the average nutrient removal from June until the end of October was minimal. The N removal rates ranged between 0.03 and 0.2 g $N/m^2/d$. This removal constitutes the lower range of the 0.1 to 0.6 g $N/m^2/d$ measured in continuously illuminated tubular biofilm reactors treating swine slurry (Godos et al. 2009; González et al. 2008) but is much lower than the 0.7 g $N/m^2/d$ achieved in a laboratory-scale vertical biofilm reactor (Chapter 4). Moreover, in contrast to the latter laboratory-scale study, effluent concentrations below the target concentrations of 2.2 mg N/L and 0.15 mg P/L were not achieved.

It is possible to obtain high biomass productivities in outdoor microalgal reactor systems. In pond systems, biomass productions between 8-15 $g/m^2/d$ have been measured (Arbib et al. 2013; Craggs et al. 2012; Olguín et al. 2003) while biomass productivities as high as 11-35 $g/m^2/d$ have been accomplished in photobioreactors (Arbib et al. 2013; Hulatt and Thomas 2011; Min et al. 2011). However, the biomass productivity in these studies employed much higher nutrient concentrations (26-1500 mg N/L and 2-26 mg P/L) compared to the pilot-scale reactor in this study, and certain reactors were either situated at lower latitudes with more favorable light and temperature conditions or were continuously illuminated.

The density of the harvested biomass of 91 g dry weight/L demonstrates one of the benefits of the biofilm reactor. This density is 10-1000 times higher than the 0.1-4 g/L that can be achieved in suspended systems (Arbib et al. 2013; Chisti 2007) and is comparable to densities obtained after centrifugation of suspended microalgae (Brennan and Owende 2010). As centrifugation contributes 8-13% to the costs of microalgae cultivation in ponds (Norsker et al. 2011), the omission of centrifugation is a significant advantage of a biofilm system.

The average caloric value of the biomass of 13 MJ/kg was low compared to a value of 22.7 MJ/kg that was reported to be an average caloric value for microalgal biomass by Duboc et al. (1999) and also compared to the 19-23 MJ/kg of activated sludge generated by municipal wastewater treatment (Metcalf & Eddy 2003). However, the ash-free caloric value of the biomass of the pilot reactor of 20.5 MJ/kg is similar to these literature values.

Table 5.5 — *The average and maximum measured metal content of the harvested biomass of the biofilm reactor and the maximum allowable concentrations in biomass which is to be used as soil improver in the EU (directive 2006/799/EC). n.d. = not determined.*

	Cd (mg/g)	Cr (mg/g)	Cu (mg/g)	Hg (mg/g)	Ni (mg/g)	Pb (mg/g)	Zn (mg/g)
Average pilot	$<3.3 \cdot 10^{-5}$	$<3.3 \cdot 10^{-5}$	0.051	n.d.	$<3.3 \cdot 10^{-5}$	n.d.	0.23[a]
Maximum pilot	$<3.3 \cdot 10^{-5}$	$<3.3 \cdot 10^{-5}$	0.079	n.d.	$<3.3 \cdot 10^{-5}$	n.d.	0.38
Maximal allowed soil im-prover	0.001	0.1	0.1	0.001	0.05	0.1	0.3

[a] The average only of the samples in which Zn was measured

Fertilizer is often mentioned as one of the applications for microalgal biomass originating from wastewater (Roeselers et al. 2008). Using phototrophic biomass for fertilizer is only feasible if heavy metals, micropollutants, and pathogens are present in acceptably low concentrations. Table 5.5 compares the average metal content of the biomass produced in this study and the maximum allowable concentrations in biomass to be employed as a soil improver in the EU. The metal content of the biomass grown from wastewater effluent in Leeuwarden was well below the maximum concentrations allowed in fertilizer, which indicates that fertilizer is a viable destination for the phototrophic biomass.

For a phototrophic system, the presence of light is essential, which was illustrated by the nutrient removal only during the day time. Even when sufficient light is available, microalgal growth and nutrient uptake rates can be low due to diffusion limitation of nutrients or CO_2 or by a deviation from the optimum growth temperature or pH. Employing well known models (e.g., described in Pérez et al. (2005), see appendix D for the calculation) the penetration depths of CO_2, NO_3^- and PO_4^{3-} into the biofilm of the pilot-scale reactor were estimated. The penetration depths, exhibited in Table 5.6, were thinner than the biofilm thickness, which was estimated to be 700 μm based on the measured volume and dry weight of the harvested biomass. As the biofilm contained gas bubbles that were released during harvesting and not included in the measurements, the real biofilm thickness presumably was even greater than 700 μm. This indicates that microalgae at the bottom of the biofilm presumably experienced diffusion limitation of nutrients.

Table 5.6 — *Calculated penetration depths of NO_3^-, PO_4^{3-} and HCO_3^- into the biofilm during pilot operation. The estimated biofilm thickness based on the area, the measured volume of the biomass and the assumption that one third of the biofilm was harvested. The light intensity ensuring microalgal growth throughout the penetration depth.*

Compound	Penetration depth (µm)	Light intensity required for microalgal growth throughout the penetration depth[1] (µmol/m²/s)
NO_3^-	400	1430
PO_4^{3-}	260	570
HCO_3^-	520	2900
Estimated biofilm thickness	770	

[1] To ensure microalgal growth throughout the penetration depth, the light intensity at the end of the biofilm should be higher than the compensation point, the light intensity at which the rate of photosynthesis is equal to the rate of respiration. The compensation point is reported between 8-40 µmol/m²/s (Clegg et al. 2012; Hill 1996) and 40 µmol/m²/s was used for this calculation

For each penetration depth, the light intensity was also calculated to ensure microalgal growth throughout the penetration depth (see appendix D). Light was calculated to be the limiting component when the light intensity was lower than 580, 1470 or 3210 µmol/m²/s for PO_4^{3-}, NO_3^- and CO_2, respectively (Table 5.6). From June until the end of October, the light intensity was higher than 580 µmol/m²/s during only 15% of the day (24 hours). It can, therefore, be concluded that the phototrophs were subjected to limited light throughout most of the day. When light was not limiting, diffusion limitation of PO_4^{3-} was presumed to affect phototrophic growth more than diffusion limitation of NO_3^- or CO_2. Indeed, while CO_2 is often determined to be the compound limiting microalgal growth in pilot scale studies in microalgal ponds (Heubeck et al. 2007; Azov et al. 1982), in this study, no effect was ascertained on biomass production or nutrient removal when additional CO_2 was supplied. This also corresponds with the minimal variances in inorganic carbon concentrations in the effluent without and with CO_2 addition.

The increasing effluent pH during the day indicated microalgal activity. The effluent pH increased to a maximum of 10.9 and the pH inside the biofilm must have been even higher, presumably also explaining the high ash content of the biomass. On the one hand, these high pH values indicate phototrophic activity, however, on the other hand, it is expected that microalgal growth may have been inhibited at such high pH values. In general, freshwater microalgae prefer environments of pH 5-7, and cyanobacteria prefer environments of pH 7-9 (Andersen 2005). The biofilm consisted mainly of the cyanobacterium *Phormidium autumnale*, for which it can be presumed that pH values above 9 were reducing its growth rate.

During most of the day, it was not possible to distinguish between the effects of light and temperature as elevated light intensities always corresponded with a high effluent temperature, and vice versa. The interdepence of the microalgal growth rate, light and temperature has also been previously demonstrated (Dauta et al. 1990). However, the increase and decrease in temperatures in the effluent followed one to two hours after the increase and decrease of the light intensity. Therefore, in the early morning when sufficient light was conducive for microalgal growth, the temperature could have limited growth and nutrient uptake. Both NO_3^- and PO_4^{3-} uptake respond to temperature changes with a lower nutrient uptake at temperatures below and above the optimum growth temperature (Powell et al. 2008; Reay et al. 1999). With the average night and morning temperatures in June, September, and October below 15°C, a negative effect of temperature seems probable as most microalgae are mesophilic and grow between temperatures of 15-40°C (Martínez et al. 1999). The diminished temperatures in October might also explain why no increase was observed in the nutrient removal in October even though the pH was controlled.

It seems that low light intensity, temperature and also the pH increase were responsible for the low biomass productivity and nutrient uptake of the pilot-scale biofilm reactor. In addition, the inhomogeneous light distribution over the biofilm surface may have caused decreased microalgal growth due to both light limitation and oversaturation. The amount of sunlight and the temperature in Leeuwarden (the Netherlands) from May-October in 2012 was comparable to the average over the past 56 years (KNMI 2013). Consequently, results obtained with the pilot biofilm reactor can be considered representative of the effects of irradiance and temperature under Dutch conditions. It can, therefore, be concluded that the current vertical phototrophic biofilm reactor is not a suitable post-treatment process under Dutch climate conditions.

The biofilm reactor may still be applicable when controlling the pH and the temperatures in the morning. In the current reactor design, all sunlight which falls on the biofilm and is not employed for microalgal growth (>95%) is absorbed and transferred to heat before it is lost to the environment. These heat losses lead to large temperature fluctuations in comparison to submerged biofilm systems, where the surrounding water buffers these fluctuations. However, submerged biofilm systems can only be utilized if the water is not turbid and the effect of the turbidity of wastewater is unclear. Alternatively, for the biofilm reactor the temperature losses to the environment may be reduced, hereby diminishing the influence of the low temperatures on microalgal growth. Currently, the heat loss to the environment is substantial due to the significant recycling rate of the reactor. This recycling rate can be decreased by altering the water supply to the biofilm and by reducing the pipe lengths in the reactor. Alternatively, the biofilm reactor may also be situated in a greenhouse, although this increases the costs

of the system. The pH can be controlled by the addition of flue gasses containing high amounts of CO_2. In locations at lower latitudes with higher irradiance and temperature, the biofilm reactor should be viable as a post-treatment of municipal wastewater when including a pH control and possibly a temperature control in the early morning.

CONCLUSIONS

This pilot-scale study investigated the nutrient removal and biomass production in a phototrophic biofilm reactor as post-treatment of municipal wastewater under Dutch climate conditions. The areal biomass production rate ranged between 2.7 and 4.5 g dry weight/m^2/d, and the average nitrogen and phosphorus removal were 0.13 g N/m^2/d and 0.023 g P/m^2/d. No nutrient removal occurred during the night. The wastewater contained sufficient inorganic carbon to sustain phototrophic growth, and CO_2 addition did not lead to an increased biomass production or nutrient removal. While a direct relationship was observed between light intensity and nutrient removal on sunny days, this relationship was not apparent from long term monitoring data. The target effluent concentrations of 2.2 mg N/L and 0.15 mg P/L could not be achieved. It is expected that the low light intensity, temperature, and the high pH during the day were limiting microalgal growth in the biofilm reactor.

5

ACKNOWLEDGEMENTS

Chapter 6

Symbiotic Microalgal-Bacterial Biofilms Remove Nitrogen, Phosphorus and Organic Pollutants from Municipal Wastewater

Nadine C. Boelee
Hardy Temmink
Marcel Janssen
Cees J.N. Buisman
René H. Wijffels

ABSTRACT

Symbiotic microalgal-bacterial biofilms can be very attractive for municipal wastewater treatment. Microalgae remove nitrogen and phosphorus and simultaneously produce the oxygen that is required for the aerobic, heterotrophic degradation of organic pollutants. In this study symbiotic microalgal-bacterial biofilms were grown in flow cells with ammonium and phosphate, and with acetate as biodegradable organic pollutant. The symbiotic biofilms removed acetate without an external oxygen or carbon dioxide supply, but ammonium and phosphate could not be completely removed. The biofilm was shown to obtain considerable heterotrophic denitrification capacity, indicating the possibility of further nitrogen removal by nitrification and denitrification. The symbiotic relationship between microalgae and aerobic heterotrophs was proven by subsequently removing light and acetate. In both cases this resulted in the cessation of the symbiosis and in increasing effluent concentrations of both acetate and the nutrients ammonium and phosphate.

6

INTRODUCTION

In aerobic wastewater treatment the organic pollutants are degraded by heterotrophic microorganisms, a process which requires extensive aeration. If oxygen (O_2) can be produced in situ by microalgae, this can result in considerable savings on energy, compressors and maintenance. The application of microalgae in wastewater treatment has been studied extensively in microalgal ponds, where microalgae and bacteria live together in a symbiotic relationship (Babu et al. 2011; Craggs et al. 2000; Buhr and S.B. 1983). In this symbiotic relationship the microalgae release O_2 which is consumed as electron acceptor by the heterotrophic bacteria. In turn, the bacteria release carbon dioxide (CO_2) which is taken up by the microalgae for cell growth. Combined microalgal and bacterial growth can have further advantages. The bacteria can stimulate microalgal growth through the release of growth factors (Ukeles and Bishop 1975), or by reducing the photosynthetic O_2 tension hereby preventing the inhibition of photosynthesis which occurs at high concentrations of O_2 (Mouget et al. 1995). In microalgal ponds nitrogen (N) and phosphorus (P) are taken up via microalgal and bacterial growth and nitrogen is also removed via nitrification and denitrification (Babu et al. 2011; Craggs et al. 2000; McLean et al. 2000).

One of the difficulties in the application of symbiotic microalgal-bacterial systems is an efficient separation of the microalgal-bacterial biomass from the treated wastewater. Efforts have been made to grow microalgae and bacteria together in flocs (Van Den Hende et al. 2010; Su et al. 2012), but microalgal-bacterial cultures can also be grown in biofilms on flat plates. A biofilm forms a natural separation between the biomass and the treated wastewater. The potential of symbiotic microalgal-bacterial biofilms for wastewater treatment was evaluated and found to be attractive due to the inherent oxygen production capacity of the microalgae (Boelee et al. 2012 / Chapter 2). An application of microalgal-bacterial biofilms was already tested in a tubular biofilm reactor for the treatment of swine slurry, where N, P and Chemical Oxygen Demand (COD) removal efficiencies up to 100%, 90% and 75% were measured without an external O_2 supply (de Godos et al. 2009; González et al. 2008).

To be applicable for wastewater treatment, symbiotic biofilms will need to remove both the organic pollutants and the nutrients ammonium (NH_4^+) and phosphate (PO_4^{3-}). Typically, municipal wastewater contains 350 mg biodegradable COD/L, 50 mg NH_4^+-N/L and 10 mg PO_4^{3-}-P/L. Using stoichiometrical equations for microalgal growth and aerobic degradation of organic pollutants, it can be calculated that a microalgal-bacterial biofilm can grow on this wastewater and degrade all organic compounds without an external O_2 or CO_2 supply.

6
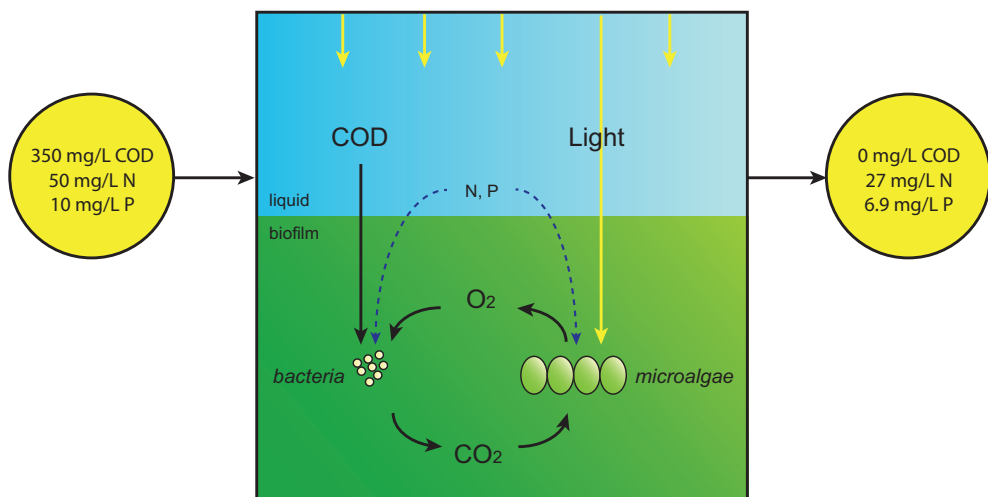
Figure 6.1 — *Schematic overview of the symbiotic cycling of O_2 and CO_2 in the biofilm which leads to the degradation of organic compounds by heterotrophic bacteria and to the assimilation of N and P by microalgae.*

Figure 6.1 shows a schematic overview of the symbiotic biofilm. The growth equation of the microalgae on CO_2, NH_4^+ and PO_4^{3-} can be written as follows, assuming a microalgal biomass composition of $CH_{1.78}O_{0.36}N_{0.12}P_{0.01}$ (Duboc et al. 1999; Ahlgren et al. 1992; Healey 1973):

$$CO_2 + 0.12NH_4^+ + 0.01H_2PO_4^- + 0.69H_2O \rightarrow 1.19O_2 + 0.11H^+ + CH_{1.78}O_{0.36}N_{0.12}P_{0.01} \qquad (6.1)$$
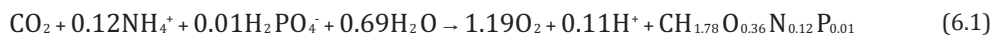
The organic pollutants in wastewater can be represented by acetate, resulting in the following stoichiometrical equation for aerobic degradation, assuming a biomass yield of 0.4 g volatile suspended solids (VSS)/g COD and a bacterial biomass composition of $CH_{1.4}O_{0.4}N_{0.2}P_{0.017}$ (Metcalf & Eddy 2003):

$$CH_3COO^- + 0.96O_2 + 0.21NH_4^+ + 0.01H_2PO_4^- + 0.8H^+ \rightarrow \\ 0.97CO_2 + 1.6H_2O + 1.03CH_{1.4}O_{0.4}N_{0.2}P_{0.017} \qquad (6.2)$$
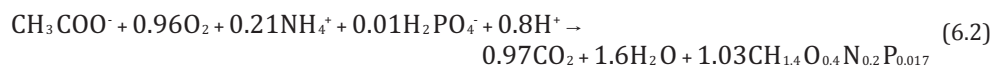
From the stoichiometry in equation 2 it follows that 155 mg O_2/L (4.8 mmol/L) is required by bacteria to convert all the acetate, and the corresponding CO_2 production is 218 mg/L (5.0 mol/L). When the microalgae produce 155 mg O_2/L, they will need 179 mg CO_2/L (4.1 mmol/L). As this is less than the 218 mg CO_2/L produced by the bacteria, it is expected that it is possible to degrade all the acetate using a microalgal-bacterial biofilm without an external supply of either O_2 or CO_2. The calculated residual nutrient concentrations are 27 mg NH_4^+-N/L and 5.7 mg PO_4^{3-}-P/L. This implies that additional

N and P removal would be needed when using a microalgal-bacterial biofilm growing according to this closed O_2 balance. If more light is applied, the calculated residual produced CO_2 may also sustain additional microalgal growth, resulting in further N and P removal.

The aim of this study was to obtain a symbiotic biofilm of microalgae and bacteria which takes up the calculated amounts of acetate, N and P and which does not require additional O_2 for the heterotrophic degradation of organic pollutants. Firstly, it was determined if it was possible to grow such a biofilm by monitoring the effluent concentrations of acetate, N and P. Secondly, acetate and light were subsequently removed to prove the symbiotic relationship between microalgae and bacteria. Finally, it was investigated if nitrification and denitrification could provide additional N removal in the biofilm.

MATERIAL AND METHODS

Experimental Setup

All experiments were performed in a flow cell system, as shown schematically in Figure 6.2. In the flow cell (STT products B.V., the Netherlands) a liquid layer of 2 cm flowed over a 1 mm plastic sheet (PVC; $0.018m^2$), on which the symbiotic biofilm grew. Sensors were positioned at the inlet and outlet of the flow cell to measure the pH and the dissolved O_2 concentration (InPro 6050/120, Mettler Toledo, Switzerland). The pH of the inflow was controlled at 7.2 by supplying either acetate or a mixture of acetate and acetic acid (described below). The temperature was controlled at 23°C with a water jacketed glass tube through which the synthetic wastewater was recycled.

6
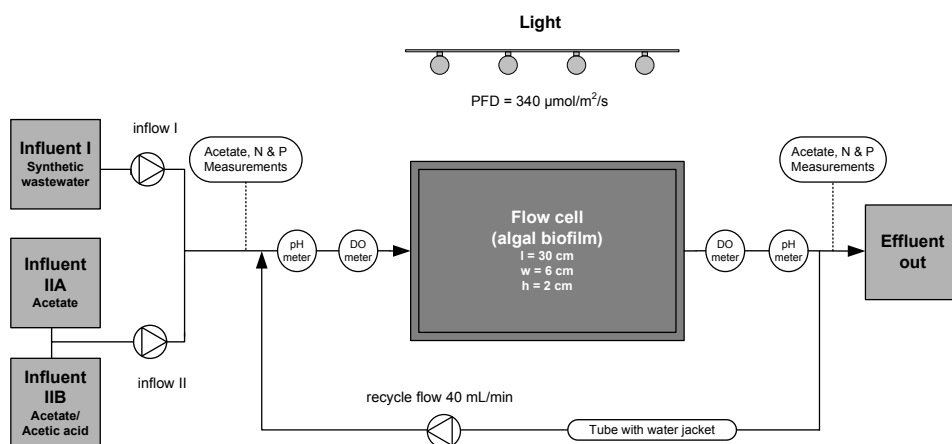
Figure 6.2 — Schematic overview of the experimental setup.

The inflow of the flow cell consisted of synthetic wastewater containing NH_4^+ and PO_4^{3-} (influent I), acetate (influent II) and a recycle flow of 40 mL/min. Table 6.1 shows the settings of the inflow of the four experiments and the corresponding N loading rate and hydraulic retention time (HRT). The wastewater inflow of 3.4 mL/min during Experiment 1 was based on the desired HRT of 2.6 hours and the volume of the system of 0.54 L. The pump rates were decreased in Experiments 2-4 to obtain a lower acetate and nutrient load at the same influent concentrations. The total inflow gave laminar flow velocities of about 0.6 mm/s and a retention time inside the flow cell of approximately 9 minutes. To prevent microalgal growth outside the flow cell, all tubing was black, glassware was brown and all glassware and connections were covered in aluminum foil. The flow cell system was cleaned approximately once a week to prevent the growth of suspended biomass. The flow cell was opened and all suspended biomass was removed. The effluent in the system was filtered (GF/F, Whatman, UK) and returned to the system.

Table 6.1 — The pump settings of the synthetic wastewater (influent I) and acetate (influent II), the corresponding NH_4^+-N concentration, NH_4^+-N loading rate and hydraulic retention time (HRT), the addition of HCO_3^- and the light intensity of the four experiments.

Expe- riment	Influent I (mL/ min)	Influent II (mL/ min)	N in synthetic waste- water (mg/L)	N loading rate (g/m²/d)	HRT (h)	Extra HCO_3^-	Light intensity (µmol/ m²/s)
1	2.7	0.7	50	14	2.6	-	615
2	1.6	0.4	50	8	4.5	-	323
3	1.6	0.4	50	8	4.5	yes	340
4	1.6	0.4	50	8	4.5	yes	340

The biofilm was continuously illuminated by a bank of fluorescent lamps (MASTER PL-L Polar 36W/840/4P, Phillips, the Netherlands). The light intensities presented in Table 6.1 were chosen based on the light required to grow enough microalgae to obtain the desired O_2 production. This light requirement was calculated by assuming a quantum yield of 0.03 mol O_2/mol PAR-photons (400-700 nm) (Boelee et al. 2011 / Chapter 3) and by using the area of 0.018 m² and the influent flow rate. The light requirement for Experiment 1 was 550 µmol/m²/s (inflow 3.4 mL/min) and the requirement for Experiments 2, 3 and 4 was 323 µmol/m²/s (inflow 2 mL/min). The light intensity was measured with a 2π PAR quantum sensor (SA190, LI-COR Biosciences, USA) at the level of the biofilm surface.

Different short-term tests were performed during the four experiments in the time period where the acetate, N, and P effluent concentrations remained stable. Table 6.2 shows an overview of these tests. In Test A the light supply was turned off. During Experiment 4 this test was also performed while bubbling air (Test B) to prevent O_2 limitation for the bacteria. For Test B the water jacketed tube of the setup was replaced by a water jacketed vessel which was aerated. The light was turned off a third time to investigate denitrification in Experiment 4 (Test C) after switching from NH_4^+ to NO_3^- as the N source. In Test D the acetate flow (influent II) was turned off. This test was performed during all experiments and in Experiments 2-4 the acetate flow was replaced by an equivalent flow of demineralized water.

Table 6.2 — Settings of the four tests for symbiosis in the biofilm.

Test	Light	Acetate	Air	N-source	Experiment
A	off	on	-	NH_4^+	1,2,3,4
B	off	on	on	NH_4^+	4
C	off	on	-	NO_3^-	4
D	on	off	-	NH_4^+	1,2,3,4

Microalgal Biofilm Cultivation

Microalgae were scraped off the surface of a settling tank of the effluent of the municipal wastewater treatment plant in Leeuwarden, the Netherlands. These microalgae were cultivated in the laboratory as described in (Boelee et al. 2011 / Chapter 3). One day before the start of the experiment, the plastic sheet of the flow cell was scratched with sandpaper, rubbed with the cultivated microalgal biofilms and left in synthetic wastewater for a minimum of 12 hours. Two hours before the experiment around 20 mL of settled bacterial sludge was poured on top of the plastic sheet. In Experiment 1 and 2 this sludge originated from an aerobic membrane bioreactor running at the Wetsus laboratory (Leeuwarden, the Netherlands). On day 22 of Experiment 2 the flow cell was cleaned and the biofilm was harvested by scraping the plastic sheet, after which only a very thin biofilm remained. This biofilm was used again in Experiment 3. In Experiment 4 the bacterial sludge was taken from the aeration tank (where nitrification takes place) at the wastewater treatment plant in Leeuwarden, the Netherlands.

The synthetic wastewater (influent I) contained N and P in the typical species and concentrations of Dutch municipal wastewater being 50 mg NH_4^+-N/L and 10 mg PO_4^{3-}-P/L. Besides N and P also (micro) nutrients were added based on Wright's cryptophyte medium (Andersen 2005). The synthetic wastewater composition was as follows: 239 mg/L NH_4Cl, 45.9 mg/L $CaCl_2.2H_2O$, 46.2 mg/L $MgSO_4.7H_2O$, 26.5 mg/L $Na_2SiO_3.5H_2O$,

70.3 mg/L K_2HPO_4. Trace elements and vitamins: 4.78 mg/L $EDTA.2H_2O$, 2.38 mg/L $FeCl_3$, 1.25 $\cdot 10^{-2}$ mg/L $CuSO_4.5H_2O$, 2.75 $\cdot 10^{-2}$ mg/L $ZnSO_4.7H_2O$, 12.5 $\cdot 10^{-3}$ mg/L $CoCl_2.6H_2O$, 0.184 mg/L $MnCl_2.2H_2O$, 7.50 $\cdot 10^{-3}$ mg/L $Na_2MoO_4.2H_2O$, 1.25 mg/L H_3NO_3, 0.125 mg/L vitamin B1, 6.25 $\cdot 10^{-4}$ mg/L vitamin H, 6.25 $\cdot 10^{-4}$ mg/L vitamin B12. In Experiments 3 and 4 also 1.05 g/L $NaHCO_3$ (10 mmol/L) was added. Furthermore, NH_4Cl was replaced with $NaNO_3$ (379 mg/L) on day 18 of Experiment 4.

Acetate was used to represent the biodegradable organic pollutants at a typical Dutch wastewater concentration of 350 mg COD/L (323 mg acetate/L). To prevent bacterial growth in the influent vessel, the acetate was kept separate from all other nutrients. Two vessels of only acetate solution were made: influent IIA with 3.72 g/L $CH_3COONa.3H_2O$ (27.4 mmol/L) and influent IIB with 27.4 mmol/L of CH_3COOH and $CH_3COONa.3H_2O$ at ratios between 0.8:1 and 4:1. The pH of the inflow of the flow cell was regulated by the automatic addition of either influent IIA or IIB, to counteract the pH increase as a result of microbial growth. When the N source was changed from NH_4^+ to NO_3^- on day 18 of Experiment 4, also additional acetate was added to the influent to be certain that there was enough acetate to support denitrification.

Analytical Procedures

Samples were taken from the influent and effluent flow during operation and filtered through a 0.45 μm filter (Millex-LCR, Merck Millipore, USA). NH_4^+-N was analyzed using a colorimetric cuvette test (LCK303, Hach Lange, Germany). Acetate, NO_3^--N and PO_4^{3-}-P were analyzed with ion chromatography (Compact IC 761 equipped with a conductivity detector, Metrohm, Switzerland). For the acetate measurement the ion chromatograph was equipped with the pre-column Metrosep Organic Acids Guard (Metrohm, Switzerland) and a column Synergi 4u hydro-RP 80A (Phenomenex , USA). For the NO_3^--N and PO_4^{3-}-P measurements the ion chromatograph was equipped with the pre-column Metrosep A Supp 4/5 Guard and the column Metrosep A Supp 5, 150/4.0 mm (Metrohm, Switzerland).

Photosynthesis Inhibition Test

The quantum yield of PSII photochemistry was determined by chlorophyll fluorescence to test whether acetate inhibited microalgal photosynthesis. Biomass from the biofilm of Experiment 3 was incubated with acetate to obtain five microalgae suspensions with 0, 23, 123, 223 and 323 mg/L acetate (as $CH_3COONa.3H_2O$) at an optical density of 0.2 at 680nm. These solutions were left in the dark for 15 minutes and subsequently the quantum yield was measured using the LC1 program of the Aquapen-C AP100 (PSI, Czech Republic).

Biomass Separation

To separate microalgae and bacteria by weight, the biomass of Experiment 3 was first centrifuged at low centrifugal force at 1000 rcf (Allegra X-12R, Beckman Coulter, USA) to separate the microalgae from the suspension and afterwards the supernatant was centrifuged at 3273 rcf to separate the bacteria from the liquid. However, both microalgae and clumps of bacteria settled after the first centrifugation step. Therefore, a solution of 9 mmol EGTA/g dry weight was prepared, which should dissolve the extracellular polymeric substances holding the bacteria and microalgae together in clumps. The pH was controlled at 10.2 by the addition of sodium hydroxide and the solution was centrifuged as stated above.

RESULTS

Biofilm Growth

During all four experiments a green biofilm developed with distinct round lumps on its surface, as shown in Figure 6.3.
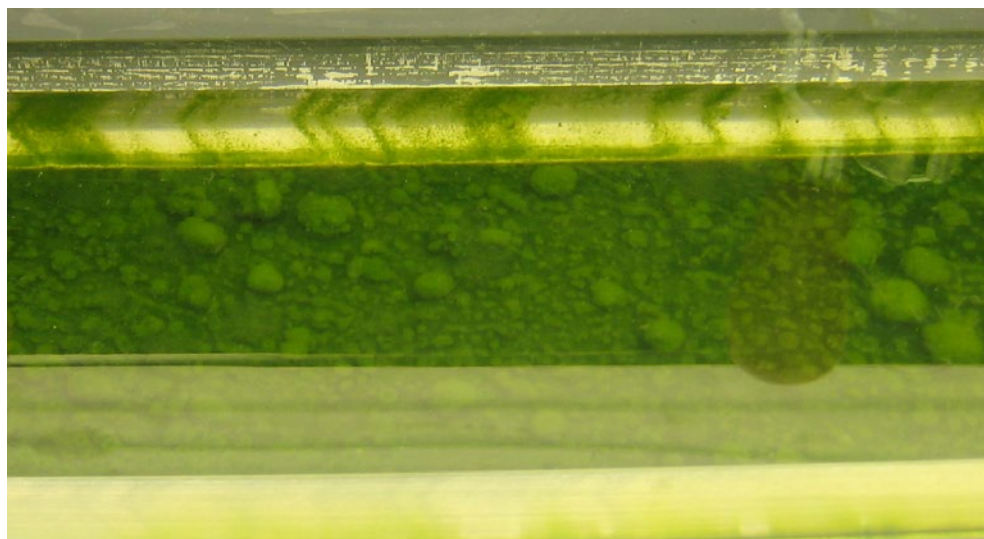
Figure 6.3 — *The symbiotic microalgal-bacterial biofilm on day 16 of Experiment 1 showing the round bacterial lumps covered by microalgae.*

The biofilm structure was rather loose and the flow cell was cleaned every week to prevent suspended growth. When harvesting the biofilm, visual observation showed that the round white lumps of the biofilm stuck together even after harvesting. Microscopic observations showed that these clumps mainly consisted of bacteria, presumably held together by extracellular polymeric substances (EPS). The microalgae in the biofilm were predominantly the green microalgae *Monoraphidium* sp. (about 60%) and *Scenedesmus acutus* (about 40%).

Single bacterial and microalgal cells can be separated by centrifugation due to their difference in weight. The first centrifugation step should yield microalgal biomass, the second step bacterial biomass. However, this was not possible with the microalgal and bacterial clumps in the biofilms of these experiments, as the pellet obtained after the first centrifugation step consisted of both algae and bacteria. Biomass of Experiment 3 was therefore treated with EGTA. EGTA removes calcium which is an essential constituent of EPS (Grotenhuis et al. 1991). The treatment visually gave a better separation, and the pellet obtained after the second centrifugation step increased in size. This supports the hypothesis that the bacteria in the clumps were held together by EPS. Nevertheless, visual observation showed that the separation was still insufficient, and therefore the actual bacterial fraction must have been higher than the measured 11%.

Removal of Acetate, NH_4^+ and PO_4^{3-}

During Experiment 1 a biofilm was obtained with microalgae and bacteria. However, the effluent concentrations of acetate, NH_4^+-N and PO_4^{3-}-P were higher than the expected concentrations as presented in Table 3. Therefore, in Experiment 2 the loading rates were lowered from 88 g acetate/m^2/d, 14 g N/m^2/d and 2.7 g P/m^2/d, to 52 g acetate/m^2/d, 8 g N/m^2/d and 1.6 g P/m^2/d respectively. To match these lower loads, the light intensity was lowered to 323 µmol/m^2/s, which is comparable to the 24-hours average light intensity from late spring to early autumn in the Netherlands (Huld and Suri 2007). However, as indicated in Table 3, while the NH_4^+-N effluent concentration decreased to 30 mg/L, this did not result in lower effluent concentrations of acetate and PO_4^{3-}-P. Apparently, the high loading rates of Experiment 1 were not the cause of the low acetate and nutrient removal.

In Experiment 3 a test was performed to assess the tolerance of the microalgal biomass to acetate (0, 23, 123, 223 and 323 mg acetate/L). Inhibition by acetate would decrease the microalgal O_2 production, possibly explaining the high acetate effluent concentrations observed in Experiments 1 and 2. The quantum yield of (PSII) photosynthesis of the microalgal biomass was measured by fluorescence after dark adaptation, and during exposure to increasing light intensities. The maximum dark-adapted quantum yield

that can be obtained lies around 0.8 at low light intensities (Flameling and Kromkamp 2006; Baker 2008; Parkhill et al. 2001). Under illumination with increasing light intensities the quantum yield decreases as a result of photosaturation, during which part of the absorbed light is lost in the form of heat. Figure 6.4 presents the measured quantum yield. The dark-adapted PSII quantum yield was 0.74 at all acetate concentrations, which indicates a non-inhibited microalgae population (Parkhill et al. 2001; Flameling and Kromkamp 2006). As expected, the quantum yield decreased with increasing light intensities, but was similar for all acetate concentrations. Hence, these results show that acetate did not inhibit photosynthesis at the tested concentrations.
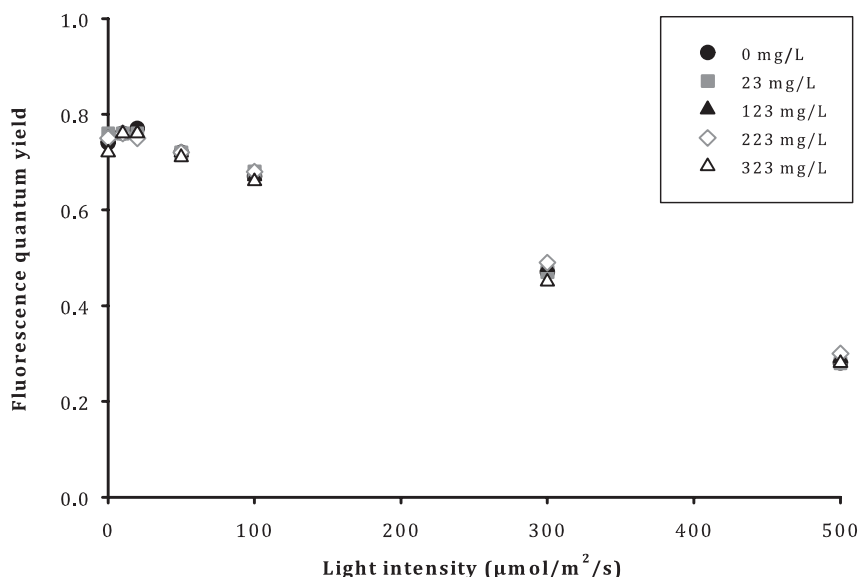
Figure 6.4 — The quantum yield of PSII photosynthesis of biofilm biomass in suspensions of different acetate concentrations at increasing light intensities.

It was suspected that, at the start of the experiments, CO_2 limitation delayed or even prevented the commencement of the symbiosis between microalgae and bacteria. Therefore, bicarbonate (HCO_3^-) was added to the influent during Experiment 3 at a concentration of 10 mmol/L. This concentration was an excess compared to the 4.4 mmol/L of inorganic carbon that was calculated to be needed by the microalgae. After the addition of HCO_3^-, the concentrations of acetate and NH_4^+-N rapidly decreased. Subsequently, the concentration of HCO_3^- was decreased stepwise from day 16 until day 29 to 0 mmol HCO_3^-/L. Even when no more HCO_3^- was added to the influent, the average concentrations in the effluent remained low at 39 mg acetate/L, 30 mg NH_4^+-N/L, and 5.7 mg PO_4^{3-}-P/L. These concentrations were similar to the calculated concentrations (Table 6.3).

Table 6.3 — *The influent concentrations, the calculated effluent concentrations and the average measured effluent concentrations of NH_4^+-N, PO_4^{3-}-P and acetate.*

	NH_4^+-N (mg/L)	PO_4^{3-}-P (mg/L)	Acetate (mg/L)
Influent	50	10	323
Effluent calculated	27	5.7	0
Effluent Experiment 1	43	7.4	179
Effluent Experiment 2	30	7.9	166
Effluent Experiment 3	30	5.7	39

Additional N removal of the residual N in the effluent is necessary for symbiotic biofilms treating municipal wastewater. This additional N removal can be obtained by nitrification and denitrification or by applying more light and CO_2 to induce more microalgal growth. Both cases would no longer be based on a closed O_2 balance between the heterotrophs and the microalgae. In the case of nitrification and denitrification, additional O_2 is required for nitrification. In the case of additional light and CO_2, the algae will produce more O_2 than is needed by the aerobic heterotrophs. In Experiment 4 it was tested if additional N removal could be obtained via nitrification and denitrification. Accordingly, the biofilm was inoculated with sludge from a nitrifying wastewater treatment plant. Again 10 mmol/L HCO_3^- was added at the start of the experiment, but this addition was stopped in one step on day 6 of the experiment. Figure 6.5 shows that the effluent concentrations of Experiment 4 decreased during the first 18 days to an average of 75 mg acetate/L, 30 mg NH_4^+-N/L and 7.5 mg PO_4^{3-}-P/L. Similar to Experiment 3, the acetate and nutrient effluent concentrations were not affected when the HCO_3^- addition was stopped on day 6. This confirms that the additional HCO_3^- only is required to start up the symbiosis. Despite the inoculation with nitrifying sludge, the concentration of NH_4^+-N remained around 30 mg NH_4^+-N/L and the concentration of NO_3^- remained below the detection limit of 0.15 mg NO_3^--N/L until day 18, indicating that no nitrification took place.

On day 18 of Experiment 4 the N source was switched from NH_4^+ to NO_3^- to test the denitrification capacity of the biofilm. Figure 6.5 shows that already after one day of adding 50 mg NO_3^--N/L, the N concentration had decreased to 14 mg NO_3^--N/L and the acetate concentration to 24 mg/L. Although wastewater generally contains enough COD to support denitrification, an additional 184 mg acetate/L was added on day 19 to further support denitrification and demonstrate the full denitrification capacity of the biofilm. This additional acetate was calculated based on a COD requirement of 6.6 g COD/g NO_3^--N (Metcalf & Eddy 2003) and on the 30 mg NH_4^+-N/L left in the effluent before day 18. With the new influent concentration of acetate of 507 mg/L, the average effluent concentrations of acetate and NO_3^--N were 45 mg acetate/L and 2 mg NO_3^--N/L

6

respectively. Most likely, part of the acetate and the NO_3^--N was removed by heterotrophic denitrification, while the other part of the acetate was removed by aerobic heterotrophs and the other part of the NO_3^--N was removed by microalgae. The uptake of the additional acetate presumably led to more CO_2 production and thus to more microalgal growth. Indeed, the biofilm increased in thickness and became more green, and large gas bubbles were produced in the flow cell. The PO_4^{3-}-P concentrations decreased from 7.5 to 4.1 mg PO_4^{3-}-P/L, which can also be attributed to enhanced microalgal growth.
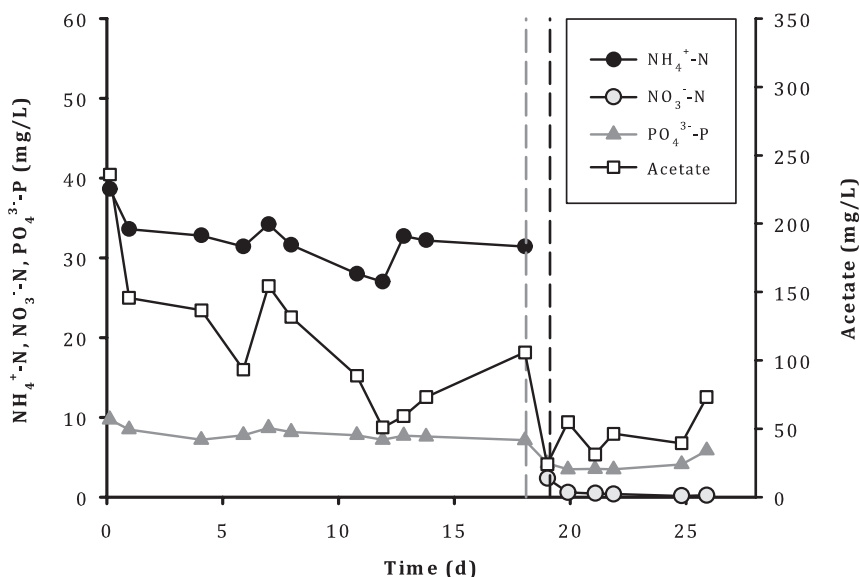
Figure 6.5 — *The effluent concentrations of NH_4^+-N, NO_3^--N, PO_4^{3-}-P and acetate during Experiment 4. The influent concentrations were 50 mg NH_4^+-N/L, 10 mg PO_4^{3-}-P/L and 323 mg/L acetate from day 0 until day 18. From day 18 until the end of the experiment NH_4^+-N in the influent was replaced by NO_3^--N and from day 19 the acetate influent concentration was increased to 507 mg/L. The gray dashed line indicates the switch from NH_4^+ to NO_3^- in the influent, the black dashed line indicates the increase in acetate in the influent.*

Symbiosis

In all the experiments tests were performed to prove that the microalgae and bacteria in the biofilm were growing in symbiosis. In Tests A, B and C the light was turned off, while in Test D the addition of acetate was stopped.

Darkness and Symbiosis

Figure 6.6 presents the acetate and nutrient concentrations and the pH after the light was turned off in Test A during Experiment 4. These results are similar to the results of identical tests performed during Experiments 1, 2 and 3. All effluent concentrations increased after the light was turned off, which was expected due to the anticipated cessation of symbiotic microalgal and bacterial growth. The theoretical increase in concentrations in the absence of microbial activity is also presented in Figure 6.6. Figure 6.6A illustrates that the increase of the NH_4^+-N concentration was as expected, while the increase of the PO_4^{3-}-P concentration was higher than expected. The latter is presumably due to a measurement error (possibly a deviation in pumping rates) as the effluent concentrations are slightly above the influent concentration of 10 mg PO_4^{3-}-P/L. The increase of the acetate concentrations in Figure 6.6B was similar to the calculated concentrations until three hours. After three hours the acetate concentration was lower than expected in the absence of microbial activity, the cause of which is unknown.

The measured dissolved O_2 concentration was 0% in the effluent throughout the test, as was expected due to the inactivity of the microalgae. The effluent pH rapidly decreased from 7.6 to 7.0 during the first half hour of the test, as shown in Figure 6.6B. After this initial decrease the pH continued to decrease more gradually to 6.5. The rapid initial pH decrease may have been caused by the release of CO_2 by the microalgae respiring in the dark. This respiration slows down when most of the O_2 in the biofilm has been consumed.

In Experiment 4 a second test was performed (Test B) in which the light was turned off but also air was bubbled into the system. The bubbling of air should keep the aerobic bacteria active, while the darkness should prevent photosynthesis. The influent pH was still controlled at 7.2 by the addition of acetate or a mixture of acetate and acetic acid. Figure 6.7 illustrates that the acetate concentration only slightly increased from 59 to 75 mg acetate/L, which is much less than in the situation without microbial activity. The dissolved O_2 concentration was around 100% in the inflow and 0% in the effluent of the flow cell. This indicates that the bacteria consumed all the O_2 that was supplied. It is therefore possible that the slight increase in acetate concentration was due to O_2 limitation. The NH_4^+-N and PO_4^{3-}-P concentrations did increase and especially the PO_4^{3-}-P concentrations were similar to the calculated concentrations in absence of microbial activity. This shows that there was almost no nutrient uptake by bacteria during Test B and suggests that the majority of the nutrients is taken up by microalgal growth.
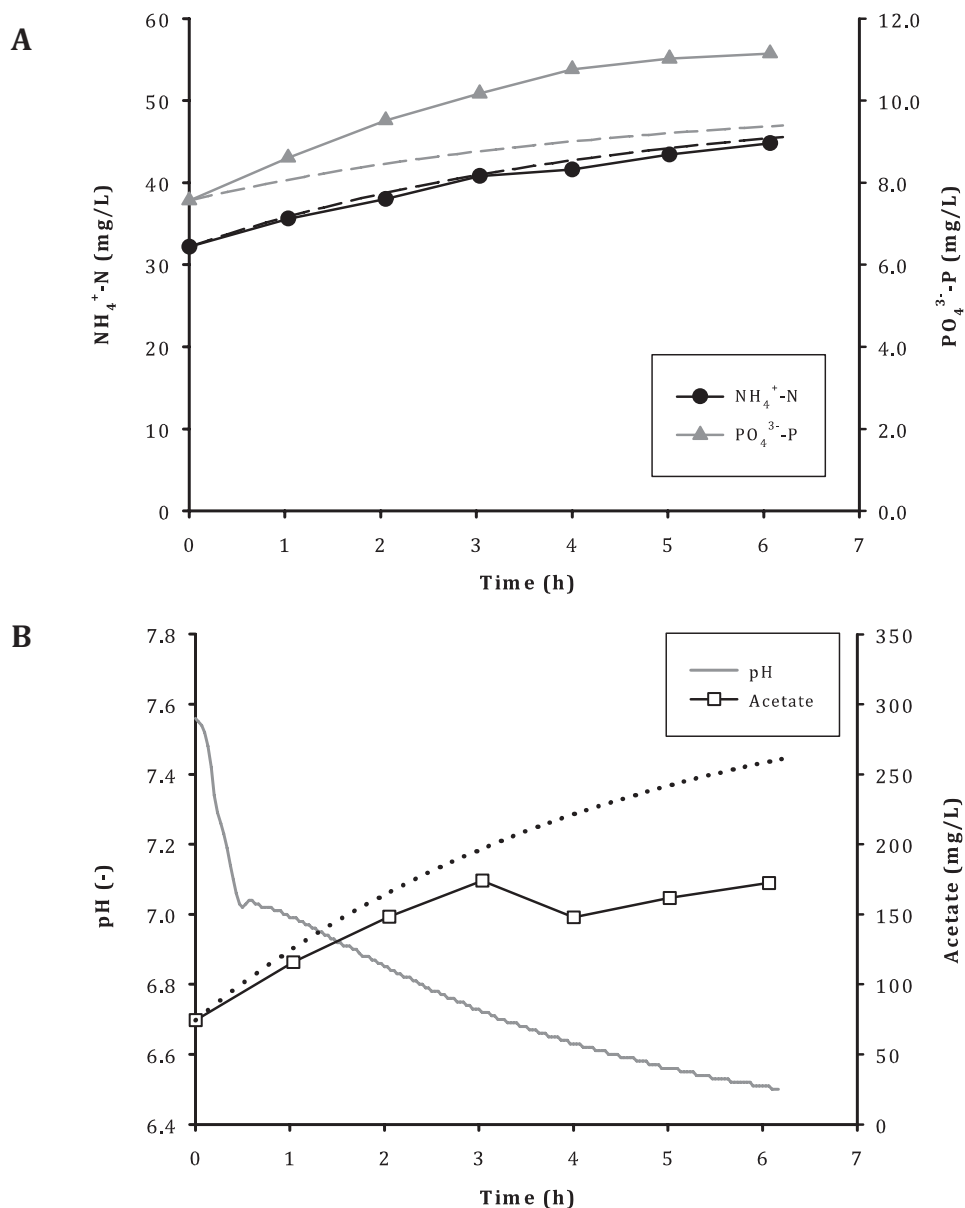
Figure 6.6 *— The effluent concentrations of NH$_4^+$-N and PO$_4^{3-}$-P (A) and of acetate and the pH (B) after the light had been turned off during Experiment 4 (Test A). The influent concentrations were 50 mg NH$_4^+$-N/L, 10 mg PO$_4^{3-}$-P/L and 323 mg/L acetate. The black and gray dashed lines (A) and the black dotted line (B) show the theoretical increase in concentrations of NH$_4^+$-N, PO$_4^{3-}$-P and acetate as a result of the dilution by the inflow only. This increase was calculated using C$_t$= exp(-Q/V·t) ·(C$_0$-C$_{in}$)+C$_{in}$ (with C$_t$ the concentration of the compound at time t, t the time, Q the flow rate, V the volume and C$_0$ and C$_{in}$ the concentration of the compound at time 0 and in the influent).*
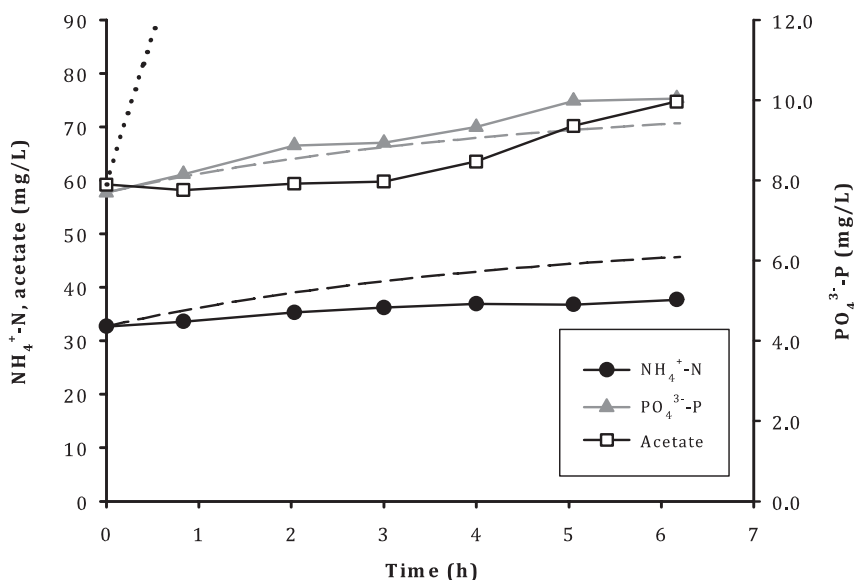
Figure 6.7 — *The effluent concentrations of NH_4^+-N, acetate and PO_4^{3-}-P after the light had been turned off and the system was bubbled with air during Experiment 4 (Test B). The influent concentrations were 50 mg NH_4^+-N/L, 10 mg PO_4^{3-}-P/L and 323 mg/L acetate. The black and gray dashed lines and the black dotted line show the theoretical increase in concentrations of NH_4^+-N, PO_4^{3-}-P and acetate as a result of the dilution by the inflow only (see caption Figure 6.6 for details).*

A third test (Test C) was performed at the end of Experiment 4 after NH_4^+ has been replaced by NO_3^-. In this test the light was turned off to determine the extent of heterotrophic denitrification. Throughout Test C the pH remained between 7.1 and 7.3. Figure 6.8 presents the acetate and nutrient effluent concentrations after the light was turned off. Both the acetate and PO_4^{3-}-P concentrations increased, while the NO_3^--N concentration rapidly decreased to 0.35 mg NO_3^--N/L. The increase in the PO_4^{3-}-P concentration can be attributed to the ceasing microalgal growth. The aerobic acetate degradation by bacteria also ceased, as the microalgae no longer produced O_2. However, the acetate concentrations did not increase to the theoretical concentrations, suggesting that acetate continued to be consumed by denitrification. The ratio between acetate and NO_3^--N removal was 5.9 g COD/g NO_3^--N, which indeed is in the range that can be expected for heterotrophic denitrification.
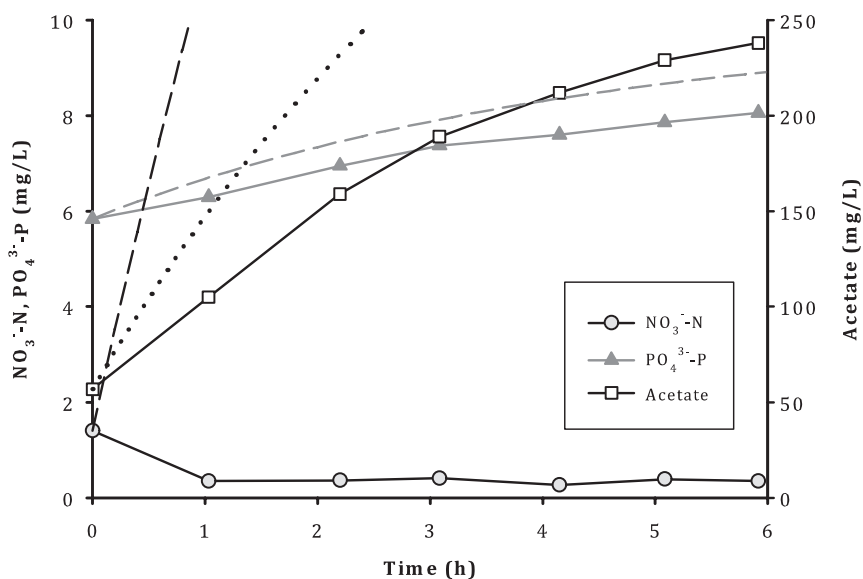
Figure 6.8 — *The effluent concentrations of NO_3^--N, PO_4^{3-}-P and acetate after the light had been turned off during Experiment 4 (Test C). The influent concentrations were 50 mg/L NO_3^--N, 10 mg PO_4^{3-}-P/L and 507 mg/L acetate. The black and gray dashed lines and the black dotted line show the theoretical increase in concentrations of NO_3^--N, PO_4^{3-}-P and acetate as a result of the dilution by the inflow only (see caption Figure 6.6 for details).*

Acetate Depletion and Symbiosis

In Test D the addition of acetate was stopped. Figure 6.9 shows the results of Test D of Experiment 4, which are similar to the results of identical tests performed during Experiments 1, 2 and 3. Within three hours the acetate concentration decreased to 0 mg/L. Figure 6.9B shows that the pH increased during these first three hours. The active microalgae still produced O_2, but this O_2 was no longer taken up for aerobic acetate degradation. The O_2 thus started to accumulate in the flow cell and effluent. It was expected that the microalgal growth now would become limited by either a deficiency in CO_2 or by high O_2 concentrations. However, the results suggest that the microalgal activity did not decrease, as the NH_4^+-N and PO_4^{3-}-P effluent concentrations increased only slightly and the dissolved O_2 concentration increased until the end of the test. Possibly, an excess of CO_2 was produced during Experiment 4, as may also be expected based on the stoichiometrical calculations in the introduction. This excess of CO_2 would enable part of the microalgal growth even after the acetate addition was turned off. Perhaps the microalgae also continued to grow and assimilate NH_4^+-N and PO_4^{3-}-P based on the CO_2 released during endogenous respiration by heterotrophs or by the microalgae themselves.
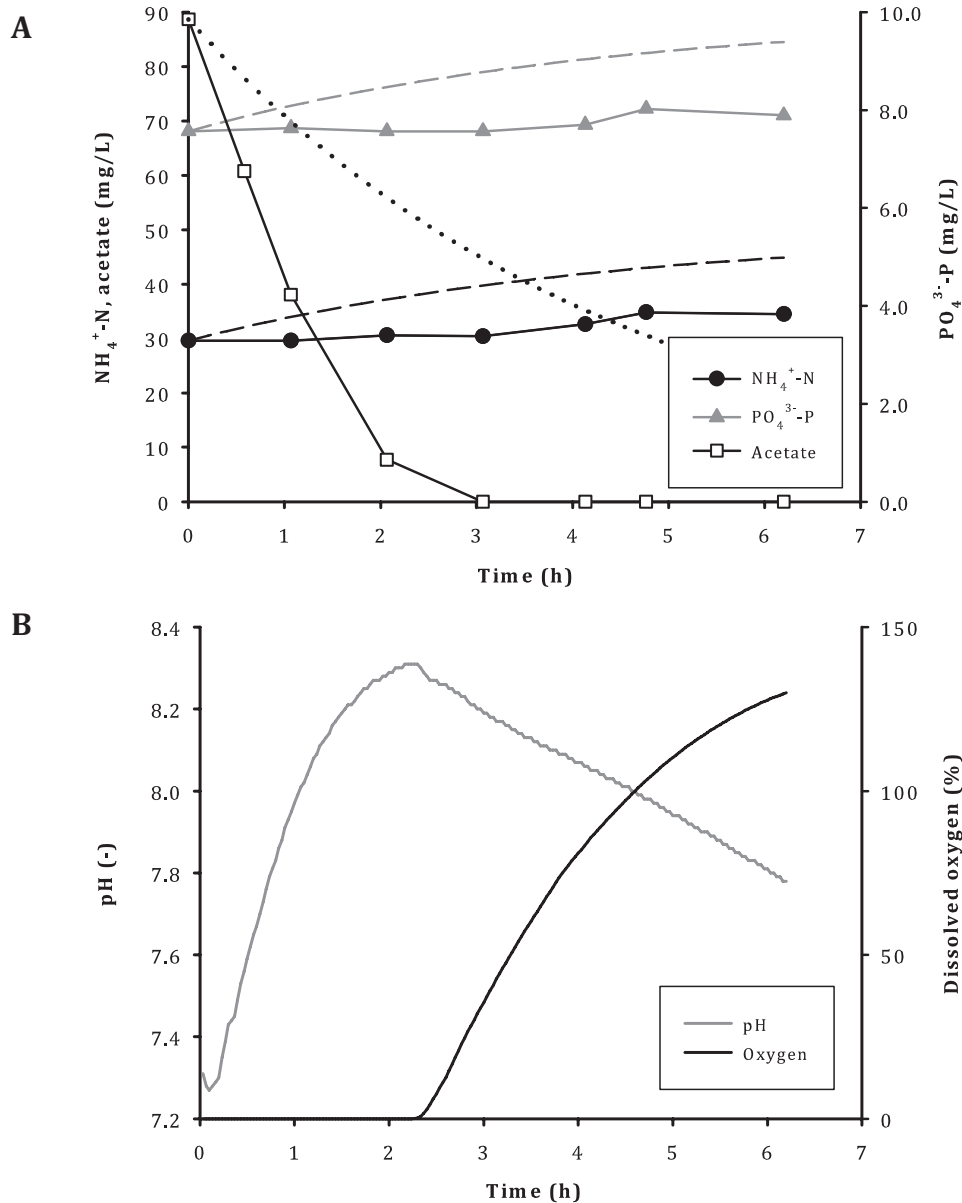
Figure 6.9 — *The effluent concentrations of NH_4^+-N, acetate and PO_4^{3-}-P (A) and the pH and dissolved oxygen (B) after the addition of acetate had been turned off during Experiment 4 (Test D). The influent concentrations were 50 mg NH_4^+-N/L, 10 mg PO_4^{3-}-P/L and 323 mg/L acetate. The black and gray dashed lines and the black dotted line (A) show the theoretical increase in concentrations of NH_4^+-N, PO_4^{3-}-P and acetate as a result of the dilution by the inflow only (see caption Figure 6.6 for details).*

DISCUSSION

The results of this study demonstrated that it is possible to grow a symbiotic microalgal-bacterial biofilm without an external O_2 and CO_2 supply. The symbiotic relationship could only fully develop when HCO_3^- was added during the startup of the biofilm. Furthermore, chlorophyll fluorescence measurements showed that acetate did not inhibit microalgal growth up to concentrations of at least 323 mg acetate/L. This acetate concentration is slightly higher than the concentration of 295 mg acetate/L, but lower than the concentrations above 400 mg acetate/L which were reported to inhibit microalgal photosynthesis by Bouaraba et al. (2004) and Chen and Johns (1994), respectively.

The symbiotic biofilm expressed removal rates of 3.2 g NH_4^+-N/m^2/d, 0.41 g PO_4^{3-}-P/m^2/d and 43 g COD/m^2/d which were higher than the removal rates of 1.0 g NO_3^--N/m^2/d and 0.13 g PO_4^{3-}-P/m^2/d obtained with a microalgal biofilm in a previous study in flow cells (Boelee et al. 2011 / Chaper 3). These removal rates, however, may not be directly comparable as the latter study focused on obtaining low effluent concentrations of 2.2 mg NO_3^--N and 0.15 mg PO_4^{3-}-P, while low effluent nutrient concentrations were not reached in the current study. Acetate was effectively removed, but the symbiotic microalgal-bacterial biofilm could not remove all NH_4^+ and PO_4^{3-}, as there was not enough light and CO_2 for microalgae to take up these residual nutrients. Consequently, additional N and P removal is required if symbiotic biofilms are to be applied for municipal wastewater treatment. This additional nutrient removal can be achieved by the addition of light and CO_2 to achieve more microalgal growth. The light intensity of the experiments was comparable to the average light intensity of 30 mol/m^2/d in the Netherlands from late spring to early autumn (Huld and Suri 2007). Therefore, the additional light requirement points to tropical climates as more suitable locations for a symbiotic biofilm system.

Additional N removal can also be achieved via nitrification and denitrification. Previous studies have already indicated the potential of nitrification and denitrification in biofilms grown in ponds systems (Babu et al. 2011) and of nitrification in a photobioreactor (Karya et al. 2013). While municipal wastewater generally contains enough organic pollutants for denitrification, the symbiotic system cannot provide the additional O_2 needed for nitrification. Supplying additional O_2 would lead to additional costs and energy consumption. Additional P removal can be obtained by precipitation of calcium- or magnesium phosphate or of struvite in the biofilm as a result of the pH increase inside the biofilm (Roeselers et al. 2008).

Although the biofilm of Experiment 4 was inoculated with nitrifying sludge, no nitrification was measured in this experiment. Possibly, the O_2 concentration in the biofilm was

too low, as dissolved O_2 concentrations in the effluent were 0%. Nitrification depends on the O_2 concentrations in the bulk, where low O_2 concentrations lead to low nitrification rates, as was shown for instance in biofilms in microalgal ponds (Babu et al. 2010; Craggs et al. 2000). Another possible explanation is that the inoculation procedure and growth period of 19 days did not result in sufficient nitrifiers in the biofilm. In a previous study an inoculation procedure of three weeks was used to obtain a mixed culture of microalgae and nitrifiers (Karya et al. 2013), instead of a one day procedure as used in this study. Nevertheless, nitrifying populations are often observed in microalgal-bacterial biofilms submerged in microalgal ponds (Craggs et al. 2000; McLean et al. 2000) and therefore it is expected that it should be possible to obtain nitrification in a symbiotic biofilm.

In Experiment 4 the N source was switched from NH_4^+ to NO_3^- to test the denitrification capacity of the biofilm. After this switch almost all the NO_3^- was removed from the wastewater. This higher removal of NO_3^--N as compared to NH_4^+-N can be the result of either enhanced microalgal assimilation or of heterotrophic denitrification. Microalgal assimilation is not a likely cause as NH_4^+ is considered the preferable N source compared to NO_3^- (Vincent 1992). Consequently, the rapid NO_3^- removal suggests that denitrifiers where already present in the biofilm in niches with low O_2 concentrations. These denitrifiers then switched from O_2 to NO_3^- as electron acceptor when NO_3^- was applied (Schramm et al. 1999; Lloyd et al. 1987). The COD consumption of 5.9 g COD/g NO_3^--N when the light was switched off is similar to what can be expected for heterotrophic denitrification (Metcalf & Eddy 2003). However, it is noted that the conditions in this short-term test are different from conditions during normal operation when O_2 is produced in the presence of light, creating less favorable conditions for heterotrophic denitrification.

If symbiotic biofilms are to be applied for municipal wastewater treatment, several issues need to be considered. Firstly, (biodegradable) particles in the wastewater may be entrapped in the biofilm, where they can be hydrolyzed and removed. However, if this is not the case a pre- or post-treatment step will be necessary. The additional particle removal by a pre-treatment would result in a lower COD supply thus a lower CO_2 production by the heterotrophs. Additional CO_2 would then need to be supplied to sustain microalgal growth. Secondly, microalgae are not active at night, and therefore symbiotic biofilms may only be applied in combination with conventional wastewater treatment. Thirdly, while microalgal biomass is often mentioned for its promising purposes, it was not possible to separate the microalgae and bacteria in this study. This implies that a destination needs to be found for the mixed microalgal and bacterial biomass grown on wastewater. The biomass may be reused as fertilizer if no heavy metals or recalcitrant compounds are present in the biomass. Alternatively, the biomass could make feedstock for biogas production via anaerobic digestion, although afterwards still autotrophic N and P removal would be necessary.

CONCLUSIONS

This study has shown that it is possible to grow a symbiotic microalgal-bacterial biofilm that removes acetate, ammonium and phosphate from wastewater at removal rates of 3.2 g NH_4^+-N/m^2/d, 0.41 g PO_4^{3-}-P/m^2/d and 43 g COD/m^2/d. After shortly supplying additional HCO_3^- at the start of the experiment, the symbiotic relationship established and an additional supply of O_2 or CO_2 was no longer required. Temporarily removing light or acetate proved the symbiotic relationship of the bacteria and the microalgae in the biofilm. The absence of either light or acetate led to the cessation of microalgal and bacterial growth. The symbiotic biofilm was not able to remove all nitrogen and phosphorus from the wastewater. Additional nitrogen removal should be possible via the supply of additional light and CO_2 and/or via nitrification and denitrification, as this study has shown that denitrifying bacteria quickly established in the symbiotic biofilm.

ACKNOWLEDGEMENTS

6

Chapter 7

Microalgal Biofilms for Wastewater Treatment: General Discussion

7

WASTEWATER TREATMENT

Microalgal biofilms can be employed to remove nitrogen (N) and phosphorus (P) from municipal wastewater. The promising results of the scenario analysis of Chapter 2 were the basis for further research towards the application of microalgal biofilms for post-treatment of municipal wastewater effluents and for symbiotic microalgal-bacterial biofilms for full wastewater treatment. The aim of this chapter is to discuss the results from laboratory and pilot-scale research with phototrophic biofilm reactors and evaluate the practical application of such reactors.

Post-Treatment of Municipal Wastewater Effluent

Microalgal biofilm systems may be applied as post-treatment of municipal wastewater effluents when the discharge of N and P must be further reduced as a consequence of stricter regulations, such as formulated in the EU Water Framework Directive. Microalgal biofilm systems may present an interesting and more sustainable alternative to existing post-treatment systems for N or P removal such as denitrifying filters or iron dosing, as they do not require chemicals, do not emit carbon dioxide (CO_2), and have the potential to recover N and P. Advantages of biofilm systems compared to suspended systems are the ability to operate at shorter hydraulic retention times and the lower energy demand because it is easier to harvest the biomass and because no mixing is required to keep microalgae in suspension.

Nutrient Removal

Table 7.1 presents the influent and effluent concentrations of N and P of the biofilm reactors that were investigated in this thesis and in other microalgal wastewater treatment systems. According to the scenario analysis of Chapter 2 it appeared not possible to simultaneously remove all N and P, and only P was removed to the target effluent concentration of 0.15 mg P/L. However, the biofilms grown in horizontal flow cells (Chapter 3) demonstrated removal of both nitrate (NO_3^-) and phosphate (PO_4^{3-}) to the target concentrations of 2.2 mg N/L and 0.15 mg P/L at loading rates up to 1.0 g NO_3^--N/m^2/d and 0.13 g PO_4^{3-}-P/m^2/d. The effluent concentrations were different from the scenario analysis due to the different biomass N:P ratio. This ratio matched the N:P supply at low loading rates, hereby enabling removal of both N and P below the target concentrations. Based on these results, a vertical phototrophic biofilm reactor was designed (Chapter 4). This reactor could also achieve the target effluent concentrations, albeit at slightly lower loading rates of 0.8 g NO_3^--N/m^2/d and 0.08 g PO_4^{3-}-P/m^2/d, as a result of the lower light intensity of 180 μmol/m^2/s compared to the 220 μmol/m^2/s in Chapter 3.

Table 7.1 — *Wastewater influent and effluent concentrations of N and P in the scenario analysis, the laboratory-scale and pilot-scale phototrophic biofilm reactor, pilot-scale high rate algal ponds and in a pilot-scale tubular photobioreactor.*

System	N influent (mg/L)	P influent (mg/L)	N effluent (mg/L)	P effluent (mg/L)	Reference
Scenario analysis	10	1.0	5.39	0.15	This thesis (Chapter 2)
Laboratory-scale photo-trophic biofilm reactor	10	1.1	2.2	0.15	This thesis (Chapter 4)
Pilot-scale phototrophic biofilm reactor	5	1	4.3	0.91	This thesis (Chapter 5)
Pilot-scale high rate algal pond (the Netherlands)	12	1.2	6	0.1	Horjus et al. (2011)
Hectare-scale high rate algal pond (New Zealand)	24	1.9	8	1.5	Craggs et al. (2012)
Pilot-scale high rate algal pond (Spain)	25	2	7	0.9	Arbib et al. (2013)
Pilot-scale tubular photo-bioreactor (Spain)	25	2	2.6	0.2	Arbib et al. (2013)

Table 7.2 shows that the nutrient removal rates of 0.7 g N/m^2/d and 0.07 g P/m^2/d (Chapter 4) attained in the laboratory-scale biofilm reactor were lower than the rates which were assumed in the scenario analysis (Chapter 2). The lower removal rates corresponded with a lower areal biomass production of 7 g/m^2/d versus 23.7 g/m^2/d in the scenario analysis. This lower rate may have been partially caused by the lower illumination (photosynthetic active radiation, PAR; 400-700 nm) of 16 mol PAR photons/m^2/d compared to 31 mol PAR photons/m^2/d in the scenario analysis, but most likely also diffusion limitation of nutrients resulted in a lower production rate (Chapter 4). The P content of the biomass was 8.8 mg P/g dry weight versus 14 mg P/g biomass in the scenario analysis, and resulted in a simultaneous removal of N and P to the target values.

Table 7.2 — *The areal nitrogen and phosphorus removal rates in the scenario analysis, the laboratory-scale and the pilot-scale phototrophic biofilm reactor.*

System	Areal N removal rate (g N/m^2/d)	Areal P removal rate (g P/m^2/d)	Reference
Scenario analysis	1.85	0.34	This thesis (Chapter 2)
Laboratory-scale photo-trophic biofilm reactor	0.69	0.073	This thesis (Chapter 4)
Pilot-scale phototrophic biofilm reactor	0.13	0.023	This thesis (Chapter 5)

Whereas the phototrophic biofilm reactor performed well under laboratory conditions, an outdoor pilot-scale reactor performed unsatisfactory (Chapter 5). Table 7.2 demonstrates that the N and P removal rates were limited to 0.13 g N/m^2/d and 0.023 g P/m^2/d and that the target effluent concentrations could not be achieved (Table 7.1). This poor performance probably was related to the Dutch climate and the absence of pH control. It was concluded that phototrophic biofilm reactors may be applied for post-treatment of wastewater effluent at lower latitudes with higher irradiance and temperature, but that the current reactor design is not feasible under Dutch climate conditions. An exception may be for an improved reactor design (see design improvements in the paragraph 'Design and operational aspects of the phototrophic biofilm reactor' below) on touristic locations such as the Wadden islands in the Netherlands. On this location additional wastewater treatment is only required during the touristic summer months, which coincides with the highest light intensity and temperature of the year.

Biomass Production and Area Requirement

One of the main concerns for microalgal treatment systems is the required ground area. In the scenario analysis of Chapter 2 an area requirement of 0.32 m^2/person equivalent (PE) was calculated based on an estimated biomass yield on light of 0.76 g dry weight/mol photons, the average irradiance on the biofilm and an estimated N and P content of the biomass. While yields of 0.8 g dry weight/mol photons have been reported for suspended microalgae systems (Kliphuis et al. 2010; Morita et al. 2000), Table 7.3 shows that a lower yield of 0.45 g dry weight/mol photons was achieved in the laboratory-scale biofilm reactor. The yield of the reactor was slightly lower than the yield of a pilot-scale tubular photobioreactor of 0.53 g dry weight/mol photons (Arbib et al. 2013). Microalgal growth in the experiments was most likely reduced by diffusion limitation of PO$_4^{3-}$ (Chapter 4).

The lower yield in the experiments compared to the scenario analysis translates to a higher area requirement of 0.95 m^2/PE compared to the 0.32 m^2/PE in the scenario analysis. As a conventional wastewater treatment plant has an estimated area requirement of 0.2-0.4 m^2/PE, the post-treatment biofilm reactor would at least double the total area requirement. Particularly in highly populated areas such as the Netherlands, this may prevent the application of phototrophic biofilm reactors for post-treatment of municipal wastewater effluent.

7

Table 7.3 — *The biomass yield on light in the scenario analysis, the laboratory-scale and pilot-scale phototrophic biofilm reactor, in pilot-scale high rate algal ponds and a pilot-scale tubular photobioreactor. The N and P content in the biomass in the scenario analysis and the laboratory-scale and pilot-scale phototrophic biofilm reactors, and the corresponding area requirement per person equivalent (PE) for a wastewater treatment plant treating wastewater effluent of 100 000 inhabitants[1].*

System	Yield (g biomass/ mol photons)	N content biomass (mg/g)	P content biomass (mg/g)	Area requirement (m^2/PE)	Reference
Scenario analysis	0.76	78	14	0.32	This thesis (Chapter 2)
Laboratory-scale phototrophic biofilm reactor	0.45	77	8.8	0.95	This thesis (Chapter 4)
Pilot-scale high rate algal pond (the Netherlands)	0.34[a]				Horjus et al. (2011)
Pilot-scale high rate algal pond (Spain)	0.27[b]				Arbib et al. (2013)
Pilot-scale tubular photobioreactor (Spain)	0.53[c]				Arbib et al. (2013)

[1] Assuming a wastewater production of 130 L per inhabitant, influent concentrations of 10 mg N/L and 1 mg P/L, effluent concentrations of 2.2 mg N/L and 0.15 mg P/L and a light intensity of 31 mol photons/m^2/d

[a] Calculated from 5.57 mg/Wh photosynthetic active radiation (PAR, 43% of the solar irradiation)

[b] Calculated from 1.9 mg/Wh

[c] Calculated from 3.8 mg/Wh

Design and Operational Aspects of the Phototrophic Biofilm Reactor

The design of the phototrophic biofilm reactor needs to be (re)considered. pH control is required to prevent high pH levels during the daytime when high microalgal growth occurs. This pH control can be accomplished by on-demand supply of CO_2-rich gas from small or large-scale combustion engines, power plants or biogas systems. In addition, harvesting of the biofilm should be automated. This thesis has demonstrated that scraping was an easy and effective way to harvest the biofilm and can be achieved by running a scraper along the biofilm once a week.

A biofilm reactor will not only remove nutrients, but also take up energy from the sunlight which could be recovered as heat. The results of the pilot-scale study indicated that the relatively low morning temperatures may have reduced microalgal growth and nutrient uptake. Therefore, the temperature should be increased in the morning, preferably by using the heat energy taken up by the biofilm from the sunlight. All sunlight

falling on the biofilm which is not employed for microalgal growth (>95%) is absorbed and transferred to heat before it is lost to the environment through conduction, convection, radiation and evaporation. A biofilm reactor treating wastewater effluent at a wastewater treatment plant of 100 000 inhabitants will convert around 1% of the solar irradiation into biomass (43% of the solar irradiation is photosynthetic radiation (PAR) and absorbed by the microalgae at an efficiency of 2% (Chapter 4)). On an average day in May until September with 15.8 MJ/m^2/d of solar irradiation (Huld and Suri 2007), the heat energy taken up by the water is 44-150 GJ per day (assuming 0.32-0.95 m^2/PE). This energy is equivalent to a 8-27°C temperature increase[1] of the 13 000 m^3 wastewater treated in the reactor (0.1-0.4 m^3 wastewater/m^2 biofilm reactor). Although care should be taken not to increase the temperature of the effluent above discharge limits, the temperature of the wastewater can be increased to achieve a higher biomass production and nutrient removal.

At the pilot-scale reactor a lot of the heat absorbed by the biofilm was directly exchanged with the environment when recirculating the wastewater effluent. However, by changing the reactor design this heat loss can be reduced and the heat can be retained in the wastewater. The heat loss can be reduced by decreasing the effluent recirculation and the length of the pipes in the system. Another possibility is to place the reactor in a greenhouse which further prevents losses to the environment, although this would increase the costs. The biofilm should not be fully covered as evaporation during the daytime also cools the biofilm, preventing the temperature in the biofilm from becoming too high (Murphy and Berberoğlu 2011). With the substantial daily heat production it is crucial to develop the technology required to prevent the heat loss and support the heat recovery in order to increase the temperatures of the wastewater in the morning.

While no nutrient uptake was measured at the pilot-scale reactor at night, previous studies have reported reduced nutrient uptake at night (Clark et al. 2002; Vona et al. 1999), and also a recent study has revealed substantial nutrient uptake at night by microalgae growing on urea (Tuantet et al., to be published). The energy for night nutrient uptake is supplied by carbohydrates stored by microalgae during the day. With the low microalgal growth rates in the pilot-scale reactor, it is possible that not enough carbohydrates were stored to sustain night uptake of nutrients. Reduced nutrient uptake at night cannot yet be excluded for the phototrophic biofilm reactor, but the results of the pilot-scale reactor suggest that no night uptake takes place from effluents with low nutrient concentrations. In the situation when there is no nutrient uptake during a 12 hour night, half of the wastewater flow would need to be buffered. This is equivalent to

---

[1] Assuming 130 L/PE and the heat capacity of water at 20°C of 75.27 J/mol/K (as the biofilm consists for 90% of water).

a buffer capacity of 6 500 m^3 for phototrophic biofilm reactor at a wastewater treatment plant of 100 000 inhabitants.

A fifth aspect to consider is the position of the reactor. The pilot-scale biofilm reactor was placed vertically to achieve light dilution and in this manner prevent photoinhibition. A vertical placement can enhance the microalgal productivity per ground area in high irradiance areas (Cuaresma et al. 2011). However, it was found that although the light was diluted, the light distribution was not homogeneous, resulting in light intensities of both limitation and oversaturation. The vertical placement of the pilot-scale reactor also causes the wastewater to fall along the biofilm at high speed. To avoid a short hydraulic retention time, the effluent should be recycled many times. In addition, a large recycle rate was required to provide enough pressure for a good water distribution over the biofilm. The 2 m high biofilm reactor was calculated to possess a substantial energy demand of 0.68 MJ/d,[1] based on the pressure drop and excluding pump inefficiency. With this energy demand, a biofilm reactor treating the effluent of a wastewater treatment plant of 100 000 inhabitants would require 8 GJ/d which accounts for 13% of the total energy usage of 59 GJ/d at an average 100 000 inhabitant wastewater treatment plant in the Netherlands (CBS and STATLINE 2011b). This is the reason to change the reactor design of the pilot-scale biofilm reactor in order to lower the energy demand (improvements discussed below).

The biomass production of the pilot-scale reactor was 3.3 g dry weight/m^2/d. Assuming the energy demand of the reactor consisted of only the energy required for recirculation, 25 MJ was needed to produce 1 kg of biomass. In Table 7.4 this energy demand is compared to that of the laboratory-scale reactor and other microalgal biofilm and suspended systems. Only the energy demand of tubular photobioreactors is larger than the pilot-scale reactor and, therefore, the claimed potential benefit of a lower energy demand of biofilm systems in comparison to suspended systems is not valid. However, the energy demand of other biofilm systems and the laboratory-scale biofilm reactor lies between 1-5 MJ/kg biomass which indeed is lower than all suspended microalgal systems. The large difference between the lab-scale and pilot-scale reactor can be explained by longer hydraulic retention time (1 hour versus 15 hours in the pilot-scale reactor) and thus more recycling of the pilot-scale reactor as a result of the poor reactor performance.

---

[1] The hydraulic power P$_h$ is calculated as P$_h$ = Q · ρ · g · Δh; with Q the recycle flow of 24 L/min, ρ the density of water of 1000 kg/m^3, g the gravity of 9.81 m/s^2 and Δh the differential height of 2 m.

Table 7.4 — *The energy requirement to produce 1 kg of microalgal biomass in different biofilm systems and in raceway ponds, flat-plate and tubular photobioreactors.*

System	Energy input for 1 kg biomass (MJ/kg)	Reference
Laboratory-scale phototrophic biofilm reactor (0.125 m^2)	1.4	This thesis (Chapter 4)
Tilted horizontal biofilm reactor (0.275 m^2)	4.7	Ozkana et al. (2012)
Pilot-scale phototrophic biofilm reactor (8.08 m^2)	25	This thesis (Chapter 5)
Vertical Twin-Layer biofilm reactor (1 m^2 per module, 8 modules possible)	3.6	Naumann et al. (2012)
Rotating Algal biofilm reactor (4.26 m^2)	3.9	Christenson and Sims (2012)
Pilot-scale Algal Turf Scrubber (30 m^2)	1.1	Mulbry et al. (2008)
Raceway ponds	9.2	Ozkana et al. (2012)
Flat-plate photobioreactor	17	Ozkana et al. (2012)
Tubular photobioreactor	386	Ozkana et al. (2012)

To reduce the energy demand of the biofilm reactor the recycling rate will need to be decreased either by changing the manner of water application onto the biofilm, or by changing the position of the biofilm. The first option may be achieved by applying a drip irrigation system such as applied in the Twin-Layer system (Naumann et al. 2012), presumably giving a similar energy demand of 3.6 MJ/kg biomass. It would be more beneficial, however, to change the vertical position of the reactor to a slightly tilted horizontal position, comparable to the Algal Turf Scrubber. This placement would provide a longer contact time of the water in the biofilm, possibly eliminating the need to recycle the wastewater. If the pilot-scale biofilm reactor was placed horizontally at a 2% slope (Mulbry et al. 2008), the water would only need to be pumped to a height of 0.05 m, which reduces the energy demand to 0.6 MJ/kg biomass produced. This energy demand is lower than all other microalgal systems. In addition, the lower recycling rate would presumably lower the heat loss to the environment. With such an energy benefit of placing the reactor horizontally, it is advantageous to look into other possibilities to achieve light dilution. Especially interesting are those which also result in a more homogenous light distribution, such as applying diffuse glass, which has been found to improve the light use efficiency and lead to higher yields of greenhouse crops (Li et al. 2012; Hemming et al. 2008). Concluding, the biofilm reactor should be placed horizontally at a slight angle to achieve a low energy demand for the wastewater treatment.

7

Treatment of Municipal Wastewater Using a Symbiotic Biofilm

Microalgae and heterotrophic bacteria can live together in a symbiotic relationship in which the microalgae release oxygen (O_2) which is utilized as electron acceptor by the heterotrophic bacteria to oxidize organic compounds, while the bacteria release CO_2 which is taken up by the microalgae for cell growth. In wastewater treatment, such a symbiotic relationship with in situ O_2 production could result in considerable savings on energy, compressors and maintenance. The symbiotic system may be applied for full wastewater treatment in tropical climates, where enough light is available and the temperature is constant throughout the year.

Experiments (Chapter 6) demonstrated that symbiotic biofilms can simultaneously remove organic pollutants, N and P from municipal wastewater. However, both calculations and experimental results revealed that it is not possible to remove all organic pollutants and N and P in a closed cycle for O_2 and CO_2. Two scenarios can be distinguished to remove residual N and P; either more microalgal growth should be facilitated by additional light and CO_2 or additional nutrient removal processes should be applied.

Additional light intensity can be obtained in two ways. The symbiotic biofilms (Chapter 6) were grown at a light intensity of 28 mol/m^2/d, which is equivalent to the average irradiation from April-October on a horizontal surface in the Netherlands. Around 50% of the wastewater ammonium (NH_4^+) and PO_4^{3-} was removed at this light intensity, and therefore a doubling of the light intensity would be required (56 mol/m^2/d) to remove all N and P. As the addition of artificial light to the symbiotic system is not economically feasible in the Netherlands (Dekker et al. 2013), a higher light intensity may only be available for symbiotic systems located in more sunny locations. For example, the average light intensity in Almeria in Spain is 38 mol/m^2/d, with 50 mol/m^2/d in the summer months, and the average light intensity in Khartoum in Sudan is 48 mol/m^2/d. Hence, even for biofilm reactors in very sunny locations there most probably is not enough light available to remove all the N and P via microalgal uptake at loading rates of 56 g chemical oxygen demand (COD)/m^2/d, 8.0 g N/m^2/d and 1.6 g P/m^2/d.

Additional light for the microalgal can also be obtained by lowering the wastewater load, hereby increasing the hydraulic retention time and the light received per volume unit of wastewater. This would, however, result in an increased area requirement (decreasing the wastewater load by half would double the area requirement). In this first scenario of the microalgal-bacterial biofilm, the wastewater load is adapted to the light intensity and heterotrophic bacteria remove the organic pollutants and the microalgae remove the N and P. This scenario requires a large area and the addition of CO_2.

The remaining N and P can also be removed utilizing other processes. Additional P removal can be achieved by precipitation of calcium- or magnesium phosphate or of struvite in the biofilm as a result of the pH increase inside the biofilm (Roeselers et al. 2008). The experiments in Chapter 6 also indicated the potential of nitrification and denitrification in the symbiotic biofilm for additional N removal. Based on calculations it is expected that there will be enough COD available to denitrify all remaining N, but that additional O_2 will need to be supplied for the nitrification (110 g O_2/L; based on nitrifying 27 mg/L and requiring 4.33 g O_2 per gram NH_4^+-N). In this second scenario of the microalgal-bacterial biofilm, the heterotrophic bacteria remove the organic pollutants, the microalgae remove part of the N and P, the remaining N is removed via nitrification and denitrification, and the remaining P is removed via precipitation. While nitrification can take place in the aerobic zones of the biofilm, denitrification should take place in anaerobic niches. This scenario requires the addition of O_2.

BIOMASS PRODUCTION

Phototrophic biofilm reactors for wastewater (post-) treatment will produce substantial amounts of biomass. The biomass production rate of 7 g dry weight/m^2/d in the laboratory-scale reactor (Chapter 4) and an area requirement of 0.95 m^2/PE (Table 7.3) yields a biomass production of 665 kg dry weight/d during post-treatment at a 100 000 inhabitants wastewater treatment plant. This production is comparable to the estimated 768 kg dry weight/d in the scenario analysis (Chapter 2) and almost doubles the biomass production at the wastewater treatment plant (sludge production 937 kg volatile suspended solids (VSS)/d, Chapter 2). Therefore, it is important to find suitable reuse options for this biomass which contains nutrients and energy.

Biomass Characteristics

Harvesting the biofilms proved to be easy at both the laboratory- and pilot-scale biofilm reactors. During harvesting half or one third of the biomass was harvested, and the remaining biomass continued to grow and enabled the reactor to continuously remove the nutrients from the wastewater. Table 7.5 presents the measured densities in the biofilm reactor and the density of biomass harvested from suspended microalgal systems. The density of the biomass harvested from a biofilm reactor is between 100 and 1800 times higher than in the suspended microalgal systems, and is comparable to microalgae harvested from suspended systems by -for instance- centrifugation (Brennan and Owende 2010). Omitting centrifugation would achieve a saving of 8-13% of the costs of suspended microalgae cultivation in ponds (Norsker et al. 2011). Hence, the high density of the harvested biomass is an advantage of a biofilm system compared to a suspended growth system.

The density of the biomass of the pilot-scale biofilm reactor was three times higher than the density of the biofilm cultured under laboratory conditions. Measurements of the elemental content of the biomass indicated precipitation of calcium carbonate and possibly other precipitates in the pilot-scale biofilm reactor. These precipitations could explain the higher density of the biomass produced in the pilot-scale reactor. The density might also have been increased by the entrapment of suspended solids, which were still present in the wastewater effluent treated by this reactor.

Table 7.5 — The biomass density in the laboratory-scale and pilot-scale phototrophic biofilm reactor, pilot-scale high rate algal ponds, and in a tubular photobioreactor.

System	Biomass density (g dry weight/L)	Application	Reference
Laboratory-scale phototrophic bio-film reactor	46	Post-treatment wastewater	This thesis (Chapter 4)
Pilot-scale phototrophic biofilm reactor	91	Post-treatment wastewater	This thesis (Chapter 5)
Pilot-scale high rate algal pond (the Netherlands)	0.05-0.4	Post-treatment wastewater	Horjus et al. (2011)
Hectare -scale high rate algal pond (New Zealand)	0.18-0.22	Wastewater treatment	Craggs et al. (2012)
Pilot-scale high rate algal pond (Spain)	0.16	Post-treatment wastewater	Arbib et al. (2013)
Pilot-scale tubular photobioreactor (Spain)	0.45	Post-treatment wastewater	Arbib et al. (2013)

The cyanobacterium *Phormidium autumnale* was the main phototroph present in the biofilm of the pilot-scale reactor, and also in the laboratory-scale reactor a *Phormidium* species was determined to be the dominant species. The dominance of certain species may be related to environmental conditions including temperature, light, pH, CO_2, nutrients and nutrient ratios (Huszar and Caraco 1998). The changing environmental conditions outdoors result in shifts in the dominant species throughout the season (Congestri et al. 2006; Jöbgen et al. 2004; Davis et al. 1990). With the influence of so many factors, the specific species composition remains unpredictable. Diatoms have for instance been discovered to be dominant under P limiting conditions, and cyanobacteria under P abundant conditions (Van Der Grinten et al. 2004a). A temperature increase from 20 to 30°C resulted in the dominance of the cyanobacteria *Synechocystis* instead of the green microalgae *Chlorococcum* (Di Pippo et al. 2011), and low light intensity resulted in more cyanobacteria (Zippel and Neu 2005). Under N limiting conditions, N_2-fixing cyanobacteria are expected to dominate, but also diatoms have been determined to be dominant under N limiting conditions (Van Der Grinten et al. 2004b). In general,

filamentous green algae and cyanobacteria become dominant in a well-established biofilm (Sekar et al. 2002; Johnson et al. 1997; Biggs 1996) and therefore, it is expected that an open phototrophic biofilm system at a wastewater treatment plant will always contain filamentous cyanobacteria.

Cyanobacteria are perhaps most well-known for the ability of various species to produce toxins. In general, these toxins are endotoxins and include neurotoxins (block neurotransmissions), hepatotoxins (inhibit protein phosphatases, change membranes and cause liver damage) and dermatotoxins (cause skin irritations, allergic reactions and gastroenteritis). Wild and domestic mammals, birds, amphibians, fish and humans can be affected by toxic cyanobacterial blooms, scums or mats. *Phormidium* is one of the members of the mat and biofilm forming toxic genera (Codd et al. 2005). Teneva et al. (2005) observed that extracts of *Phormidium autumnale* exhibited neurotoxic and hepatotoxic affects, but that different compounds were present in these extracts and in the used growth medium. When keeping the biofilm young through frequent harvesting of the biofilm, toxic compounds probably will not be released through cell lysis which is, in general, the method of endotoxin release. Therefore, if the cyanobacteria do not release toxins, the presence of cyanobacteria in the biofilm will not cause problems when discharging the treated wastewater. Nevertheless, the presence and effect of cyanobacterial toxins remains a point of attention and reason for regular monitoring of the presence of toxins in the effluent.

Recovery of Nutrients

Nutrient recovery from microalgae grown on wastewater is an interesting destination for the produced biomass, especially in view of the depleting phosphorus resources (Driver et al. 1999). Mulbry et al. (2005) have demonstrated that cucumber and corn seedlings grown on dried algal biomass (algae grown in dairy manure) revealed comparable growth to seedlings grown on commercial fertilizer. 15-20% of the applied N and 38-60% of the applied P was consumed within 20 days. This looks promising for the reuse of microalgal biomass as a fertilizer. However, there still are concerns when using microalgae grown on wastewater effluent as fertilizer. First, the heavy metal content of the biomass is a point of concern. Microalgae are known to remove heavy metals through various processes and also microalgae in biofilms have been documented to remove heavy metals (Travieso et al. 2002; Liehr et al. 1994). Nevertheless, the heavy metal content of the biomass produced in the pilot-scale biofilm reactor was very low, and even below the requirements for biomass reuse as soil improver (directive 2006/799/EC, Chapter 5). Hence, the heavy metal content may not be a major concern for biomass grown on municipal wastewater effluent in a post-treatment system. In a symbiotic biofilm system more biomass is produced than in a conventional wastewater

7

treatment plant (Chapter 2) and, therefore, lower concentrations of heavy metals may be expected in the produced biomass. However, further investigations should indicate whether the presence of heavy metals is a point of concern for biomass from a symbiotic biofilm system.

Secondly, the presence of pathogens in the biomass should be considered. Earlier work on microalgal biofilms documented a decrease in bacteria following post-treatment with algal biofilms from 1 000 000 colony forming units (CFU)/100 mL to the required value for bathing water quality of 10 000 CFU/100 mL (EU-Directive 76/160/EWG) in 4 hours (Schumacher and Sekoulov 2003). This bacteria reduction may be related to the sunlight, and to the pH increase and the high O_2 concentrations as a result of the micro-algal growth (Davies-Colley et al. 1999). Therefore, also this aspect may not be a major concern for biomass grown on municipal wastewater effluents but should be monitored.

Thirdly, the presence of cyanobacterial toxins in the fertilizer is a point of concern. While the fate of cyanobacterial toxins in the aquatic environment is well studied (for instance reviewed by Zurawell et al. (2005)), the fate of toxins in cyanobacterial biomass applied on agricultural lands in not well known. Most likely the degradation of toxins mainly occurs by microbial degradation as in aquatic environments (Chen et al. 2006). Microcystins (hepatotoxin) from cyanobacterial biomass applied on soils were also demonstrated to adsorb in the soil, the extent of adsorption depending on the clay content and metal ions present. The microcystins degradation half-times ranged between seven and 18 days (Chen et al. 2006). While this degradation time may provide enough time for the toxin to effect crop growth and soil life, soil enriched with cyano-bacterial biomass containing microcystins did not affect the survival or reproduction of the sensitive springtail *Folsomia candida* (Lána et al. 2011). This latter suggests that uti-lizing cyanobacterial biomass may not cause harmful effects to soil life and crop growth. However, it is necessary to study this in more detail. All in all, fertilizer is a promising application for the biomass from biofilm reactors grown on wastewater effluent which provides the possibility to recycle nutrients into agriculture.

Recovery of Energy

The ash-free caloric value of the biomass produced at the pilot-scale biofilm reactor was 20.5 MJ/kg dry weight. This energy could become available when drying the bio-mass (in the sun) and subsequently combusting it. Table 7.6 shows that if all municipal wastewater treatment plants in the Netherlands were to place a phototrophic biofilm reactor to polish their effluents, the electricity production would be 493 TJ/yr which is equivalent to 9% of the electricity employed in municipal wastewater treatment plants in the Netherlands.

Suspended microalgae grown on municipal wastewater have been reported to contain lipids ranging from 6% up to 25% dry weight content (Dickinson et al. 2013; Kong et al. 2010; Woertz et al. 2009; Órpez et al. 2009) and the lipid content of *Phormidium* sp., the main species observed in the pilot-scale reactor, has been reported to range between 6-11% when grown on municipal and swine wastewater (Ramachandra et al. 2013; Cañizares-Villanueva et al. 1995). However, cyanobacterial lipids are, generally, more difficult to utilize than microalgal lipids as these are membrane lipids and are not accumulated as neutral lipids in the cells. If all municipal wastewater treatment plants in the Netherlands were to place a phototrophic biofilm reactor to polish their effluents, the energy production would only be 2.6-11% of the total energy consumed yearly by municipal wastewater treatment plants, and only 0.025-0.1% of the energy utilized for transportation in the Netherlands (CBS and STATLINE 2012). With the expected difficulties in utilizing cyanobacterial lipids and considering the current oil prices, oil production from microalgal biomass generated during wastewater effluent polishing is not an interesting application of the microalgal biomass.

Anaerobic digestion of microalgae can yield 100-395 mL CH_4/g volatile solids (VS) (Ehimen et al. 2013; Prajapati et al. 2012; Alzate et al. 2012; Zamalloa et al. 2012) which is lower than a yield of 640 mL CH_4/g VS achieved with conventional wastewater treatment sludge digestion (Parkin and Owen 1986). These lower yields may be the result of the relatively low C:N ratio of some microalgae species, which results in a relatively high ammonia production inhibiting the digestive bacteria. The lower yield may also be caused by the cell wall of microalgae, which prevents the bacteria to gain excess to the more easily biodegradable intracellular substrates (Golueke et al. 1957). Different pre-treatments have been investigated including mechanical, sonication/ultrasound, enzyme treatment and thermal hydrolysis which increased the biogas production up to 60% compared to digesting untreated microalgae (Ehimen et al. 2013; Alzate et al. 2012; Chen and Oswald 1998). Although this will require additional energy, a pre-treatment of microalgae seems necessary when digesting microalgae.

7

Table 7.6 — Total theoretical microalgal yearly biomass production if all wastewater treatment plants (WWTPs) in the Netherlands were equipped with a phototrophic biofilm reactor for post-treatment of their effluent. The total yearly energy production from combustion, oil production and digestion of this biomass.

	Electricity production (TJ/yr)	Fraction of energy used in WWTPs	Reference
Municipal WWTPs the Netherlands $2.43 \cdot 10^7$ PE total treated[1] 0.95 m²/PE for post-treatment 7 g/m²/d biomass production rate $59\,000$ ton/yr biomass	5300	100%	CBS and STATLINE (2011b) CBS and STATLINE (2011c) Table 7.3 This thesis (Chapter 4) Calculated
Combustion 20.5 MJ/kg dry weight caloric value	493 [a]	9%	This thesis (Chapter 5)
Oil production 6-25 % Lipid content $0.39 - 1.6 \cdot 10^7$ m³/yr oil production[2]	138-576	2.6-11%	Dickinson et al. (2013), Kong et al. (2010), Woertz et al. (2009), Órpez et al. (2009) Calculated
Digestion 0.1-0.395 L/g VS methane yield $0.53-2.1 \cdot 10^7$ m³/yr methane production[3]	76-300 [a]	1.4-5.7%	Ehimen et al. (2013), Alzate et al. (2012), Prajapati et al. (2012), Zamalloa et al. (2012) Calculated

[a] Assuming 40% conversion efficiency to electricity

[1] In the Netherlands part of the industrial wastewater is treated at municipal wastewater treatment plants, hereby increasing the treatment capacity (person equivalents) above the number of inhabitants in the Netherlands

[2] Assuming oil density 900 kg/m³

[3] Assuming 90% of the biomass is VS and energy content of 35.8 MJ/m³ CH_4

Table 7.6 also demonstrates the theoretical methane production if all municipal wastewater treatment plants in the Netherlands would be equipped with a phototrophic biofilm reactor for the post-treatment of their effluent and the additional microalgal biomass would be digested. The electricity production of 76-300 TJ/yr is less than 6% of the total energy consumed by the wastewater treatment plants. With a waste sludge production of 3.3 ton/ yr (CBS and STATLINE 2011a), the additional microalgal biomass which can be digested is 18%. If this microalgal biomass is co-digested with the waste sludge produced in the conventional wastewater treatment plant, the heavy metal concentration of the digested biomass will be reduced, possibly enough for the biomass to be utilized as fertilizer. The digestion will result in a waste stream with the nutrients which have been previously removed by the wastewater treatment plant. The N of this

waste stream can be removed via -for instance- Anammox (Van Hulle et al. 2010). The biomass can be digested when the costs of a larger digester, the pre-treatment and Anammox are lower than the additional energy production. Anaerobic digestion can also be a good destination for the biomass produced by a symbiotic biofilm system.

SUMMARY

While phototrophic biofilm reactors can be applied for post-treatment of municipal wastewater effluent at lower latitudes with higher irradiance and temperature, the reactor design that was studied in this thesis is not feasible under Dutch climate conditions due to its low nutrient removal capacity and large area requirement. The reactor can be improved by placing the reactor horizontally at a slight angle to achieve a low energy demand, installing a pH controller, automating harvesting, and buffering at night. In addition, technology should be developed to prevent heat loss and support heat recovery in order to increase the temperatures of the wastewater in the morning. Such an improved reactor design may also be applied on touristic locations in the Netherlands such as the Wadden islands, where additional treatment is only required during the touristic summer months when light intensity and temperatures are highest of the year.

Symbiotic microalgal-bacterial biofilm systems can be applied to remove organic pollutants, N and P from wastewater. In order to remove all N and P either the wastewater loading rate should be adapted to the light intensity, or the remaining nitrogen and phosphorus should be removed by other processes. The latter could be achieved by nitrification and denitrification and by precipitation of calcium phosphate, magnesium phosphate or struvite.

An advantage of microalgal biofilms systems in comparison to suspended systems is the density of the harvested biomass; with 46 to 91 g dry weight/L the density is between 100 and 1 800 times higher compared to suspended systems. Fertilizer is a promising application for the biomass when the heavy metal, pathogen and cyanobacterial toxin content are sufficiently low. This is expected to be the case for biomass from post-treatment reactors. Whereas oil production from the microalgal biomass is not an interesting application, anaerobic digestion can also be a good destination.

7

Appendix A

Additional Scenario Analysis Calculations and Parameters

Microalgae

Table A.1 shows the solar irradiation from May-September in the Netherlands (in Wh and MJ). As discussed in Chapter 2, 43% of this irradiation is used by the microalgae, equivalent to the photosynthetic active radiation (PAR). The summed total irradiation is therefore 1038 MJ/m^2.

Table A.1 — *Solar irradiation from May-September in Leeuwarden, the Netherlands, data from Huld and Suri (2007). The fraction of PAR (400-700 nm) within sunlight (43%) calculated based on the ASTM G173-03 sunlight spectrum (RReDC 2012).*

Month	Solar irradiation (Wh/m²/day)	Solar irradiation (MJ/m²/day)	Solar irradiation PAR (43%) (MJ/m²/day)	Solar irradiation PAR (I_{sun}) (MJ/m²/month)	Solar irradiation PAR (PFD) (mol photons/ m²/month)
May	5005	18.0	7.7	240	1105
Jun	5021	18.1	7.8	233	1072
Jul	4895	17.6	7.6	235	1080
Aug	4179	15.0	6.5	201	922
Sep	2778	10.0	4.3	129	593
				(MJ/m²)	(mol photons/m²)
Total				1038	4773

To convert this amount of energy to the amount of mol photons received, first the amount of energy of a photon (e; J) is calculated using equation A.1 and a wavelength of 550 nm to represent the average energy of a sunlight photon:

$$e = h \cdot \frac{c}{\lambda} \quad [J] \tag{A.1}$$

with h Plank's constant (J·s), c the speed of light (m/s) and λ the wavelength (m).

Using Avogadro's number (N_a; mol^{-1}), the energy per mol photons (E; J/mol photons) is calculated:

$$E = e \cdot N_a \quad [J/mol\ photons] \tag{A.2}$$

with the amount of energy per mol photons known, the solar irradiation (I_{sun}; MJ/m²/d) is converted to mol photons/m²/d:

$$PFD = \frac{I_{sun}}{E} \quad [mol\ photons/m^2/d] \tag{A.3}$$

A

Carbon Dioxide Consumption

With the biomass production known, using equation A.2 or A.3 in Chapter 2, the amount of CO_2 consumed is calculated, as 1 mol of biomass always requires 1 mol of CO_2.

Heterotrophs

Oxygen Consumption

The oxygen consumption of the sludge (R_o) consists of the oxygen requirement of the heterotrophs degrading the COD present and the nitrifiers converting NH_4^+. It is hereby assumed that the amount of biomass produced by nitrifiers and denitrifiers is negligible. The R_o is calculated according to (Metcalf & Eddy 2003):

$$R_o = Q \cdot (COD_{b,in} - COD_{b,out}) - 1.42 \cdot P_x + 4.33 \cdot Q \cdot (N_{in} - N_{out}) - 2.86 \cdot (N_{in} - N_{out}) \quad [g/d] \quad (A.4)$$

Carbon Dioxide Production

Assuming acetate as COD the following stoichiometrical equation is used for oxidation by activated sludge:

$$5CH_3COO^- + 1NH_4^+ + 5O_2 \rightarrow C_5H_7O_2N + 3H_2O + 5CO_2 + 5OH^- \quad [g/d] \quad (A.5)$$
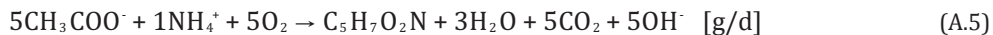
Equation A.5 shows that 1 mol of CO_2 is produced per mol of O_2 consumed during COD conversion. The CO_2 production (R_{CO2}) is therefore calculated as the total O_2 requirement minus the O_2 requirement of nitrification (in moles). The CO_2 consumption of nitrification is assumed to be negligible.

A

Table A.2 — *Symbols and parameters used in the calculations. Wastewater treatment vales from Metcalf & Eddy (2003); mass fractions N and P microalgae from Duboc et al. (1999), Ahlgren et al. (1992) and Healey (1973); and the quantum yield oxygen deducted from Qiang et al. (1998).*

Symbol	Description	Value	Unit
λ	Wavelength	$5.5 \cdot 10^{-7}$	m
A	Area of microalgal biofilm system	(Calculated)	m^2
c	Speed of light	$2.998 \cdot 10^8$	m/s
COD_b	Biologically degradable chemical oxygen demand		g/m^3
e	Energy of a photon	(Calculated)	J
E	Energy of 1 mol of photons	(Calculated)	J/mol photons
f_d	Fraction remaining as cell debris	0.15	g VSS/g VSS
$f_{N,algae}$	Mass fraction of nitrogen in biomass microalgae	7.8	% (g/g)
$f_{N,sludge}$	Mass fraction of nitrogen in biomass sludge	12.0	% (g/g)
$f_{P,algae}$	Mass fraction of phosphorus in biomass microalgae	1.4	% (g/g)
$f_{P,sludge}$	Mass fraction of phosphorus in biomass sludge	2.0	% (g/g)
h	Planck's constant	$6.626 \cdot 10^{-34}$	J·s
PFD	Photon flux density	(Calculated)	mol photons/m^2/d
I_{sun}	Sunlight irradiation	Table 1	MJ/m^2/d
k_d	Decay coefficient	0.088	d^{-1}
M_{algae}	Biomass weight microalgae	21.56 [1]	g/ C-mol biomass
M_{sludge}	Biomass weight sludge	22.6 [2]	g/ C-mol biomass
N	Nitrogen concentration		g/m^3
N_a	Avogrado's number	$6.02 \cdot 10^{23}$	mol^{-1}
$P_{x,sludge}$	Biomass production rate of sludge	(Calculated)	g VSS/d
$P_{x,A,algae}$	Areal biomass production rate of microalgae	(Calculated)	g/m^2/d
Q	Flow rate	13 000	m^3/d
$R_{N,sludge}$	Nitrogen uptake rate by sludge	(Calculated)	g/d
$R_{N,A,algae}$	Areal nitrogen uptake rate by microalgae	(Calculated)	g/m^2/d
$R_{o,sludge}$	Oxygen uptake by sludge	(Calculated)	g/d
$R_{o,A,algae}$	Areal oxygen production by microalgae	(Calculated)	mol/m^2/d
$R_{CO2,sludge}$	Carbon dioxide production by sludge	(Calculated)	g/d
SRT	Solids retention time SRT Scenario 1, 3 SRT Scenario 2	 12.5 2.5	d d d
Y_{sludge}	Biomass yield sludge	0.4	g VSS/g bCOD
QY_{O2}	Quantum yield of oxygen production	0.05	mol O_2/mol photons

[1] Biomass weight calculated based on $C_1H_{1.78}O_{0.36}N_{0.12}P_{0.01}$
[2] Biomass weight calculated based on $C_1H_{1.4}O_{0.4}N_{0.2}$

A

Appendix B

Anaerobic Digestion of Heterotrophic and Microalgal Biomass

Anaerobic digestion

The amount of energy that can be derived from anaerobic digestion of activated sludge or from both activated sludge and microalgal biomass is calculated, in order to find the possible area reduction when using this energy for artificial lighting of the microalgal biofilm system. The amount of activated sludge ($P_{x,sludge}$) and microalgal biomass produced per day have been calculated as described in Chapter 2. The activated sludge will be digested at 35°C. The biomass production is converted to amount of COD (1.42 g O_2/g VSS) and then to energy production in the form of methane (P_E), using the methane production at 35°C with heterotrophs ($Y_{h,CH4}$), the density of methane at 35°C ($\rho_{CH4,\ 35}$) and the energy content of methane (E_{CH4}):

$$P_E = 1.42 \cdot P_x \cdot Y_{h,CH4} \cdot \rho_{CH4,35} \cdot E_{CH4} \quad [kJ/d] \tag{B.1}$$

Assuming a 30% efficiency converting methane into electricity and a 30% efficiency converting energy into light, the total amount of irradiation from artificial light produced with methane (I_{CH4}) is calculated. The total percentage of area decrease (D) with this light energy can now be calculated over the desired period of five months, as follows:

$$D = \frac{I_{CH_4}}{I_{sun} \cdot A} \quad [\%] \tag{B.2}$$

The amount of energy from the anaerobic digestion of microalgal biomass is calculated in a similar manner. The methane production per microalgal biomass is taken to be 100 mL/g dry weight (Yen and Brune 2007), and with the energy content of methane, the amount of energy is calculated. The percentage of decrease is then calculated as described in equation B.2. The percentage reduction has been calculated for all three scenarios treating wastewater from 100 000 inhabitants and is shown in Table B.1.

Table B.1 — *Area requirement of a microalgal biofilm system for 100 000 inhabitants for all three scenarios (as also shown in Table 2.1 in Chapter 2). In addition the reduction of required area when the produced activated sludge or both activated sludge and microalgal biomass is anaerobically digested, and the energy from the produced methane is converted to artificial lighting.*

	Area requirement (ha)	Area reduction with biomass activated sludge (%)	Area reduction with biomass activated sludge and microalgae (%)
Scenario 1	3.2	0.69	0.79
Scenario 2	21.0	0.15	0.27
Scenario 3	7.6	0.32	0.44

A

Table B.2 — *Symbols and parameters used in the calculations. Wastewater treatment vales from Metcalf & Eddy (2003).*

Symbol	Description	Value	Unit
$\rho_{CH4, 35}$	Density methane at 35°C	634.6	g/m^3
A	Area of microalgal biofilm system	(Calculated)	m^2
D	Decrease of area requirement	(Calculated)	%
E_{CH4}	Energy content of methane	50.1	kJ/g
I_{sun}	Sunlight irradiation	Table A.1 (Appendix A)	$MJ/m^2/d$
I_{CH4}	Artificial radiant flux	(Calculated)	MJ/d
$Y_{h,CH4}$	Methane production at 35°C with heterotrophs	$4.0 \cdot 10^{-4}$	m^3/g COD
P_E	Energy production rate methane	(Calculated)	kJ/d
P_x	Production rate active sludge	(Calculated)	g VSS/d

A

Appendix C

Lipid Production from Microalgae

Lipid Production

In the scenario analysis (Chapter 2) the microalgae were assumed to be $C_1H_{1.78}O_{0.36}N_{0.12}P_{0.01}$ with a molar weight of 21.56 g/mol (M_{algae}). To calculate the required biomass composition and C:N ratio for lipid accumulation, it was assumed the microalgae will accumulate 40% lipids in the form of triacylglycerol (TAG; with C16 side chains). This lipid accumulates in addition to the original biomass. Therefore the original biomass now accounts for only 60% of the total weight. The additional weight comes from the lipid of the composition $C_1H_{1.92}O_{0.12}$ with the molar weight (M_{TAG}). Assuming 1C-mol original biomass the additional weight is calculated as follows:

$$TAG_g = \frac{40\%}{60\%} \cdot M_{algae} \quad \text{[g/mol original biomass]} \tag{C.1}$$

With M_{TAG} the additional amount of C-mol TAG per original biomass (C-mol) is now calculated:

$$TAG_{mol} = \frac{TAG_g}{M_{TAG}} \quad \text{[mol/mol original biomass]} \tag{C.2}$$

With the amounts of the original biomass and the additional TAG known, the new biomass composition is calculated with addition of the different components, example shown for O normalized to 1C.

$$O_{mol} = \frac{0.36 \cdot 1 + 0.12 \cdot TAG_{mol}}{C_{mol}} \quad \text{[mol]} \tag{C.3}$$

The new biomass composition is $C_1H_{1.85}O_{0.24}N_{0.063}P_{0.0052}$. As can be seen from this new biomass composition, the N:P ratio is still equal to 12, as it was in the original biomass, but the C:N ratio has doubled to 16 instead of 8 in the original biomass. This new biomass composition leads to new stoichiometrical reactions for microalgal growth on nitrate and ammonium. The new equations becomes:

$$CO_2 + 0.95H_2O + 0.063NO_3^- + 0.0052H_2PO_4^- \rightarrow \tag{C.4}$$
$$CH_{1.85}O_{0.24}N_{006.2}P_{0.0052} + 1.425O_2 + 0.068OH^-$$

$$CO_2 + 0.82H_2O + 0.063NH_4^+ + 0.0052H_2PO_4^- \rightarrow \tag{C.5}$$
$$CH_{1.85}O_{0.24}N_{0.063}P_{0.0052} + 1.299O_2 + 0.058H^+$$
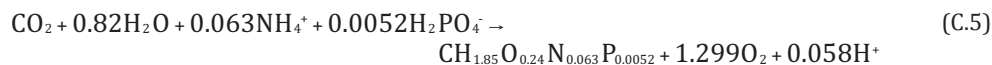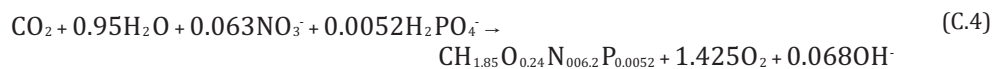
These new reaction equations give 1 mol of biomass (C-basis) per 1.43 mol O_2 consumed for nitrate and 1 mol of biomass per 1.30 mol of O_2 for ammonium uptake. As the amount of produced O_2 is known (equation 2.1 in Chapter 2), the amount of produced biomass is calculated.

The new uptake rate of N and P can be calculated with equation 2.4 in Chapter 2. The

A

fraction of N is now 4.7 % (g/g) and the fraction of P is 0.9% (g/g). With this new uptake rate the new area is calculated according to equation 2.5 from Chapter 2. The new area requirement and biomass production of the three scenarios are shown in Table C.1. In Scenario 1 the area requirement and corresponding biomass production are 1.9 times as high as the area calculated originally. In Scenarios 2 and 3, the area is 2.1 times as high. This difference is accounted for by the difference in N source; nitrate in Scenario 1 and ammonium in Scenarios 2 and 3.

Table C.1 — *Area requirement and biomass production when using original microalgal biomass (as also shown in Table 2.1 and Figure 2.3 in Chapter 2) and area requirement, biomass production, and lipid production when using biomass that has accumulated 40% lipids. Values shown for all three scenarios per person equivalent (PE) per day.*

	Area require-ment original (m^2/PE)	Area requirement (m^2/PE)	Biomass pro-duction original (g/PE/d)	Biomass production (g/PE/d)	Lipid production (g/PE/d)
Scenario 1	0.32	0.63	7.7	13	5.2
Scenario 2	2.10	4.37	59	99	40
Scenario 3	0.76	1.58	21	36	14

Table C.2 — *Symbols and parameters used in the calculations.*

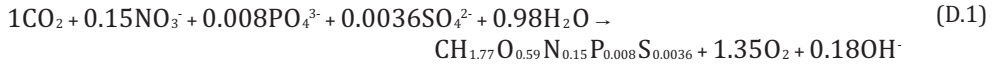| Symbol	Description	Value	Unit
C_{mol}	Carbon		mol
M_{algae}	Weight biomass microalgae	21.56 [1]	g/C-mol biomass
M_{TAG}	Weight TAG	15.83 [2]	g/mol
O_{mol}	Oxygen		mol
TAG_{mol}	Triacylglycerol	(Calculated)	mol/mol original biomass
TAG_g	Triacylglycerol	(Calculated)	g/mol original biomass

[1] Biomass weight calculated based on $C_1H_{1.78}O_{0.36}N_{0.12}P_{0.01}$
[2] TAG weight calculated based on $C_1H_{1.92}O_{0.12}$
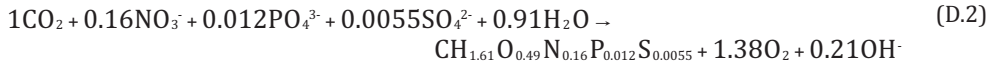
A

Appendix D

Penetration of Nutrients and Light

Penetration of NO_3^-, PO_4^{3-} and HCO_3^-

The algal growth on NO_3^-, PO_4^{3-} and CO_2 can be described by a stoichiometrical reaction equation. With the measured elemental composition of the biomass this equation is as follows for Chapter 4:

$$1CO_2 + 0.15NO_3^- + 0.008PO_4^{3-} + 0.0036SO_4^{2-} + 0.98H_2O \rightarrow \tag{D.1}$$
$$CH_{1.77}O_{0.59}N_{0.15}P_{0.008}S_{0.0036} + 1.35O_2 + 0.18OH^-$$

and as follows for Chapter 5:

$$1CO_2 + 0.16NO_3^- + 0.012PO_4^{3-} + 0.0055SO_4^{2-} + 0.91H_2O \rightarrow \tag{D.2}$$
$$CH_{1.61}O_{0.49}N_{0.16}P_{0.012}S_{0.0055} + 1.38O_2 + 0.21OH^-$$

From the stoichiometrical growth equation, the yield of the different components can be calculated. The biomass content and the yields are shown in Table D.1.

The penetration depths of NO_3^-, PO_4^{3-} and HCO_3^- are calculated according to the following formula as described for instance in Pérez et al. (2005):

$$L_{p,i} = \sqrt{\frac{2 \cdot D_i \cdot C_{i,l/b}}{\frac{\mu_{max}}{Y_i} \cdot C_x}} \quad [m] \tag{D.3}$$

with $L_{p,i}$ the penetration depth of nutrient i (m), D_i the diffusion coefficient of nutrient i (m²/s), $C_{i,\,l/b}$ the concentration of nutrient i at the liquid-biofilm interface (g/m³), μ_{max} the maximum specific growth rate (s⁻¹), Y_i the yield of biomass on nutrient i (g biomass/g nutrient i) and C_x the algae concentration (g/m³).

Table D.1 shows the parameters that were used for the calculation. For the concentrations at the biofilm surface it was assumed no mass transfer limitation occurred at the liquid-biofilm interface.

A

Table D.1 — *Parameters for calculating the penetration depth of NO_3^-, PO_4^{3-} and HCO_3^- in the biofilm and parameters for calculating the light intensity at the penetration depths.*

Parameter	Value	Reference
$\Delta\lambda$	1	Chosen
μ_{max} (s^{-1})	$1.2 \cdot 10^{-5}$	Average for *Phormidium* from Fujimoto and Sudo (1997), Blier et al. (1995), Talbot et al. (1991)
$a_\lambda{}^1$		for *Chlorella sorokiniana*
Biomass content	$C_1H_{1.77}O_{0.59}N_{0.15}P_{0.008}S_{0.0036}$ $C_1H_{1.61}O_{0.49}N_{0.16}P_{0.012}S_{0.0055}$	Measured (average Chapter 4) Measured (average Chapter 5)
$C_{HCO3\,l/b}$ (g C/m^3)	8.53	Calculated from the measured average total inorganic carbon of 10.5 mg/L at pH 7 during the experiment (Chapter 4)
	0.096	Calculated from the equilibrium value of CO_2 in water and air at pH 7 (Chapter 4)
	52.1	Calculated from the measured average total inorganic carbon during the day of 53.8 mg/L at the average pH of 8.7 (Chapter 5)
$C_{NO3\,l/b}$ (g N/m^3)	2.2 1.4	Target value (Chapter 4) Measured (average Chapter 5)
$C_{PO4\,l/b}$ (g P/m^3)	0.15 0.85	Target value (Chapter 4) Measured (average Chapter 5)
C_x (g/m^3)	$4.6 \cdot 10^4$ $9.1 \cdot 10^4$	Measured (average Chapter 4) Measured (average Chapter 5)
d	2	
D_{HCO3-} (m^2/s)	$9.38 \cdot 10^{-10}$	Average from Wolf et al. (2007), Lin et al. (2003)
$D_{PO4\,3-}$ (m^2/s)	$4.16 \cdot 10^{-10}$	Average from Liu et al. (2003), Lyons et al. (1982)
D_{NO3-} (m^2/s)	$1.29 \cdot 10^{-9}$	Average from Wolf et al. (2007), Satoh et al. (2004), Liu et al. (2003)
$E_{n,PAR,\lambda}$ (nm^{-1})^2	Phillips Master PL-L spectrum Sunlight spectrum	Measured (Chapter 4) (RReDC 2012)
PFD_{in} (µmol/m^2/s)	180	Measured during experiment
YN (g biomass/g N)	12.2 16.5	Calculated (Chapter 4) Calculated (Chapter 5)
YP (g biomass/g P)	103.5 99.3	Calculated (Chapter 4) Calculated (Chapter 4) Calculated (Chapter 5)
YC (g biomass/g P)	2.1 3.1	Calculated (Chapter 4) Calculated (Chapter 5)
z	50 steps	Calculated

[1] Data shown in Figure D.2

[2] Data shown in Figure D.1

A

Penetration of Light

The following formula was used to calculate the light intensity at depth z inside the biofilm:

$$\text{PFD}(z) = \sum_{\lambda=400}^{\lambda=700} \left(\text{PFD}_{in} \cdot E_{n,PAR,\lambda} \cdot e^{-a_\lambda \cdot C_x \cdot z \cdot d} \cdot \Delta\lambda \right) \quad [\mu mol/m^2/s] \tag{D.4}$$

with PFD_{in} the photon flux density of the incoming light ($\mu mol/m^2/s$), $E_{n,PAR,\lambda}$ the normalized spectral distribution of the PAR photons (400-700 nm; nm^{-1}), a_λ the specific absorption coefficient (m^2/g), C_x the algae concentration (g/m^3), z the biofilm depth (m), d a light-path enhancement factor[1] (-), and $\Delta\lambda$ the wavelength interval (nm).

Table D.1 shows the parameters that were used for this calculation. To obtain the $E_{n,PAR,\lambda}$ for the Phillips Master PL-L lamps in Chapter 4, the spectral photon flux density was measured using a fiber optic CCD based spectroradiometer (AvaSpec-2048 detector, Fiber FC-IR100-1-ME, Avantes, The Netherlands) at 1 nm intervals (for details on the measurement protocol see Vejrazka et al. (2011)). This measurement was normalized for the PAR range to obtain the normalized emission spectrum according to the following equation:

$$E_{n,PAR,\lambda} = \frac{\text{PFD}_\lambda}{\text{PFD}} \quad [\mu mol/m^2/s] \tag{D.5}$$

with PFD_λ the spectral photon flux density ($\mu mol/m^2/s/nm$) and PFD the photon flux density in the PAR range (400-700 nm; $\mu mol/m^2/s$).

Figure D.1 shows $E_{n,PAR,\lambda}$ of the Phillips Master PL-L lamps. The a_λ used for phototrophs adapted to high light conditions (top layer of the biofilm) was the a_λ measured for *Chlorella sorokiniana* shown in Figure D.2 (for details on the cultivation see Kliphuis et al. (2010) and for details of the measurement protocol see Vejrazka et al. (2011)). In order to simulate low light adapted phototrophs this a_λ was multiplied with a factor two.

A

---

[1] Since light will not travel perpendicular to the biofilm surface a light path enhancement factor was included. This factor was chosen to be 2 simulating the situation in which the light field is isotropic in the forward direction. Back scattering of light was neglected.

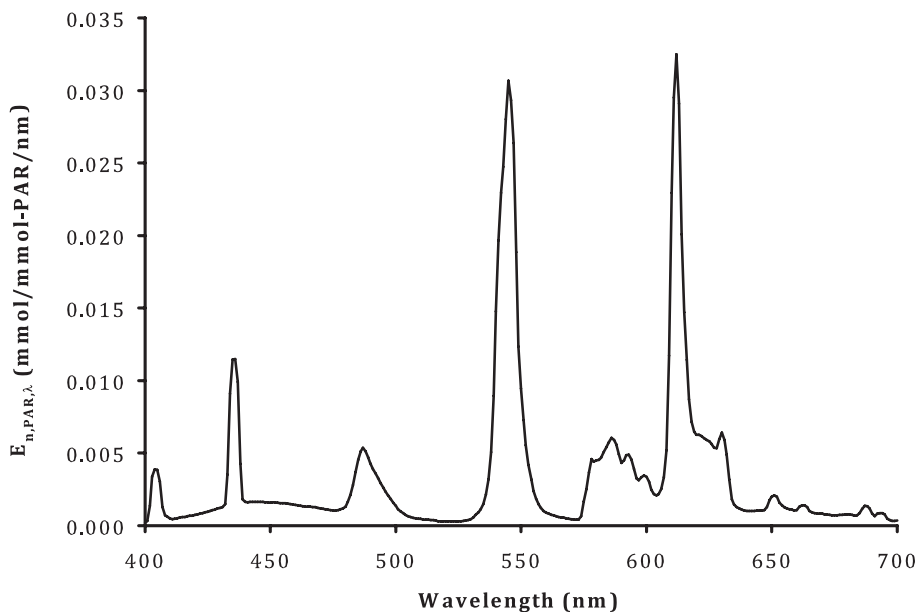**Figure D.1 —** *The normalized spectral distribution of the PAR photons ($E_{n,PAR,\lambda}$ 400-700 nm) of the Phillips Master PL-L.*
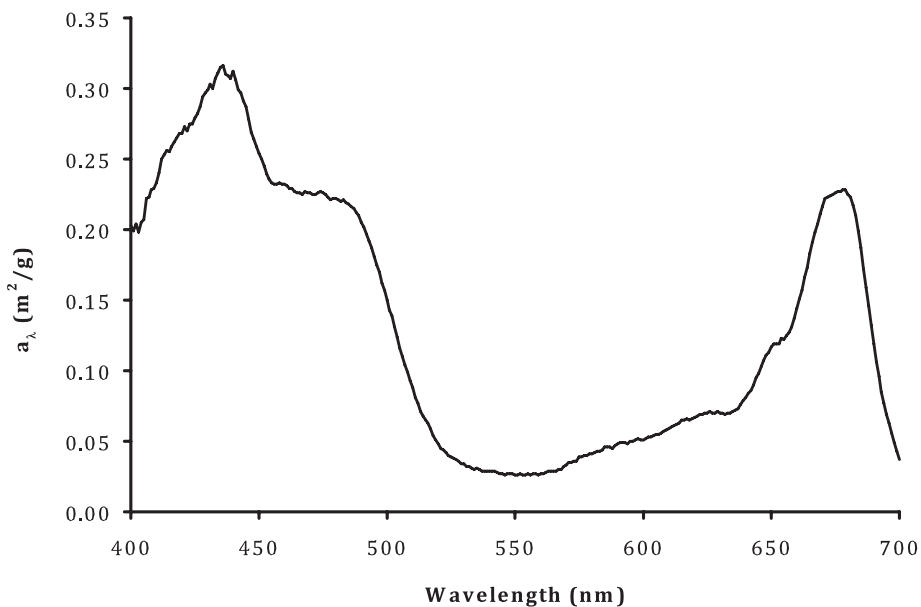

Figure D.2 — *The specific absorption coefficient (a_λ) for* Chlorella sorokiniana.

References

R

Ács É, Borsodi A, Kiss É, Kiss K, Szabó K, Vladár P, Várbíró G, Záray G (2008) Comparative Algological and Bacteriological Examinations on Biofilms Developed on Different Substrata in a Shallow Soda Lake. Aquatic Ecology 42 (4):521-531

Ahlgren G, Gustafsson IB, Boberg M (1992) Fatty-Acid Content and Chemical-Composition of Fresh-Water Microalgae. Journal of Phycology 28 (1):37-50

Ahn C-Y, Chung A-S, Oh H-M (2002) Diel Rhythm of Algal Phosphate Uptake Rates in P-Limited Cyclostats and Simulation of Its Effect on Growth and Competition. Journal of Phycology 38 (4):695-704

Alzate ME, Muñoz R, Rogalla F, Fdz-Polanco F, Pérez-Elvira SI (2012) Biochemical Methane Potential of Microalgae: Influence of Substrate to Inoculum Ratio, Biomass Concentration and Pretreatment. Bioresource Technology 123:488-494

An J-Y, Sim S-J, Lee JS, Kim BW (2003) Hydrocarbon Production from Secondarily Treated Piggery Wastewater by the Green Alga *Botryococcus Braunii*. Journal of Applied Phycology 15 (2):185-191

Andersen RA (2005) Algal Culturing Techniques. Elsevier Academic Press

Arbib Z, Ruiz J, Álvarez-Díaz P, Garrido-Pérez C, Barragan J, Perales JA (2013) Long Term Outdoor Operation of a Tubular Airlift Pilot Photobioreactor and a High Rate Algal Pond as Tertiary Treatment of Urban Wastewater. Ecological Engineering 52:143-153

Azov Y, Shelef G, Moraine R (1982) Carbon Limitation of Biomass Production in High-Rate Oxidation Ponds. Biotechnology and Bioengineering 24 (3):579-594

Babu MA, Hesb EMA, van der Steen NP, Hooijmans CM, Gijzen HJ (2010) Nitrification Rates of Algal–Bacterial Biofilms in Wastewater Stabilization Ponds under Light and Dark Conditions. Ecological Engineering 36:1741-1746

Babu MA, van der Steen NP, Hooijmans CM, Gijzen HJ (2011) Nitrogen Mass Balances for Pilot-Scale Biofilm Stabilization Ponds under Tropical Conditions. Bioresource Technology 102:3754-3760

Baker NR (2008) Chlorophyll Fluorescence: A Probe of Photosynthesis in Vivo. Annual Review of Plant Biology 59:89-113

Biggs BJF (1996) Patterns in Benthic Algae of Streams In: Stevenson RJ, Bothwell ML, Lowe RL, Algal Ecology: Freshwater Benthic Ecosystems. Academic Press Elsevier, pp 31-56

Bishop PL, Zhang TC, Fu YC (1995) Effects of Biofilm Structure, Microbial Distributions and Mass Transport on Biodegradation Processes. Water Science & Technology 31 (1):143-152

Bjorkman O, Demmig B (1987) Photon Yield of O_2 Evolution and Chlorophyll Fluorescence Characteristics at 77 K Among Vascular Plants of Diverse Origins. Planta 170:489-504

Blier R, Laliberté G, De La Noü J (1995) Tertiary Treatment of Cheese Factory Anaerobic Effluent with *Phormidium Bohneri* and *Micractinum Pusillum*. Bioresource Technology 52 (2):151-155

Boelee NC, Temmink H, Janssen M, Buisman CJN, Wijffels RH (2011) Nitrogen and Phosphorus Removal from Municipal Wastewater Effluent Using Microalgal Biofilms. Water Research 45 (18):5925-5933

R

Boelee NC, Temmink H, Janssen M, Buisman CJN, Wijffels RH (2012) Scenario Analysis of Nutrient Removal from Municipal Wastewater by Microalgal Biofilms. Water 4 (2):460-473

Bouaraba L, Dautab A, Loudikia M (2004) Heterotrophic and Mixotrophic Growth of *Micractinium Pusillum* Fresenius in the Presence of Acetate and Glucose:Effect of Light and Acetate Gradient Concentration. Water Research 38:2706-2712

Brennan L, Owende P (2010) Biofuels from Microalgae- A Review of Technologies for Production, Processing, and Extractions of Biofuels and Co-Products. Renewable and Sustainable Energy Reviews 14 (557-577)

Brock TD, Madigan MT, Martinko JM, Parker J (2000) Biology of Microorganisms. 9th edn. Prentice-Hall

Bruckner CG, Rehm C, Grossart HP, Kroth PG (2011) Growth and Release of Extracellular Organic Compounds by Benthic Diatoms Depend on Interactions with Bacteria. Environmental Microbiology 13 (4):1052-1063

Buhr HO, Miller, SB (1983) A Dynamic Model of the High-Rate Algal-Bacterial Wastewater Treatment Pond. Water Research 17:29-37

Cañizares-Villanueva RO, Domínguez AR, Cruz MS, Ríos-Leal E (1995) Chemical Composition of Cyanobacteria Grown in Diluted, Aerated Swine Wastewater. Bioresource Technology 51:111-116

CBS, STATLINE (2011a) Zuivering Van Stedelijk Afvalwater; Afzet Van Zuiveringsslib Centraal Bureau voor de Statistiek. http://statline.cbs.nl/StatWeb/publication/?DM=SLNL&PA=70155ned&D1=0-14&D2=0&D3=a,!0-10&VW=T. Accessed May 2013

CBS, STATLINE (2011b) Zuivering Van Stedelijk Afvalwater; Energieproductie En Energieverbruik. Centraal Bureau voor de Statistiek. http://statline.cbs.nl/StatWeb/publication/?DM=SLNL&PA=70155ned&D1=0-14&D2=0&D3=a,!0-10&VW=T. Accessed May 2013

CBS, STATLINE (2011c) Zuivering Van Stedelijk Afvalwater; Technische Kenmerken Installaties. Centraal Bureau voor de Statistiek. http://statline.cbs.nl/StatWeb/publication/?DM=SLNL&PA=70151ned&D1=a&D2=a&D3=43,45-56&D4=l&VW=T. Accessed May 2013

CBS, STATLINE (2012) Energiebalans; Kerncijfers. Centraal Bureau voor de Statistiek. http://statline.cbs.nl/StatWeb/publication/?DM=SLNL&PA=37281&D1=a&D2=0-1,4,7-12&D3=l&HDR=G2,G1&STB=T&CHARTTYPE=2&VW=T. Accessed May 2013

Chen F, Johns MR (1994) Substrate Inhibition of *Chlamydomonas Reinhardtii* by Acetate in Heterotrophic Culture. Process Biochemistry 29:245-252

Chen PH, Oswald WJ (1998) Thermochemical Treatment for Algal Fermentation. Environment International 24 (8):889-897

Chen W, Song L, Gan N, Li L (2006) Sorption, Degradation and Mobility of Microcystins in Chinese Agriculture Soils: Risk Assessment for Groundwater Protection. Environmental Pollution 144:752-758

Chisti Y (2007) Biodiesel from Microalgae. Biotechnology Advances 25:294-306

R

Christenson LB, Sims RC (2012) Rotating Algal Biofilm Reactor and Spool Harvester for Wastewater Treatment with Biofuels by-Products. Biotechnology and Bioengineering 109 (7):1674-1684

Clarens AF, Resurreccion EP, White MA, Colosi LM (2010) Environmental Life Cycle Comparison of Algae to Other Bioenergy Feedstocks. Environmental Science & Technology 44 (5):1813-1819

Clark DR, Flynn KJ, Owens NJP (2002) The Large Capacity for Dark Nitrate-Assimilation in Diatoms May Overcome Nitrate Limitation of Growth. New Phytologist 155 (1):101-108

Clegg M, Gaedke U, Boehrer B, Spijkerman E (2012) Complementary Ecophysiological Strategies Combine to Facilitate Survival in the Hostile Conditions of a Deep Chlorophyll Maximum. Oecologia 169 (3):609-622

Codd GA, Morrison LF, Metcalf JS (2005) Cyanobacterial Toxins: Risk Management for Health Protection. Toxicology and Applied Pharmacology 203:264-272

Collos Y, Vaquer A, Souchu P (2005) Acclimation of Nitrate Uptake by Phytoplankton to High Substrate Levels. Journal of Phycology 41 (3):466-478

Congestri R, Di Pippo F, De Philippis R, Buttino I, Paradossi G, Albertano P (2006) Seasonal Succession of Phototrophic Biofilms in an Italian Wastewater Treatment Plant: Biovolume, Spatial Structure and Exopolysaccharides. Aquatic Microbial Ecology 45:301-312

Converti A, Casazza AA, Ortiz EY, Perego P, Del Borghi M (2009) Effect of Temperature and Nitrogen Concentration on the Growth and Lipid Content of *Nannochloropsis Oculata* and *Chlorella Vulgaris* for Biodiesel Production. Chemical Engineering and Processing 48 (6):1146-1151

Craggs R, Sutherland D, Campbell H (2012) Hectare-Scale Demonstration of High Rate Algal Ponds for Enhanced Wastewater Treatment and Biofuel Production. Journal of Applied Phycology 24:329-337

Craggs RJ, Adey WH, Jenson KR, St.John MS, Green FB, Oswald WJ (1996) Phosphorous Removal from Wastewater Using an Algal Turf Scrubber. Water Science and Technology 33 (7):191-198

Craggs RJ, Tanner CC, Sukias JPS, Davies-Colley RJ (2000) Nitrification Potential of Attached Biofilms in Dairy Farm Waste Stabilisation Ponds. Water Science & Technology 42 (10-11):195-202

Cuaresma M, Janssen M, Vílchez C, Wijffels RH (2011) Horizontal or Vertical Photobioreactors? How to Improve Microalgae Photosynthetic Efficiency. Bioresource Technology 102:5129-5137

Cuhel RL, Ortner PB, Lean DRS (1984) Night Synthesis of Protein by Algae. Limnology and Oceanography 29 (4):731-744

Dauta A, Devaux J, Piquemal F, Boumnich L (1990) Growth Rate of Four Freshwater Algae in Relation to Light and Temperature. Hydrobiologia 207 (1):221-226

Davies-Colley RJ, Donnison AM, Speed DJ, Ross CM, Nagels JW (1999) Inactivation of Faecal Indicator Micro-Organisms in Waste Stabilisation Ponds: Interactions of Environmental Factors with Sunlight. Water Research 33 (5):1220-1230

R

Davis LS, Hoffmann JP, Cook PW (1990) Seasonal Succession of Algal Periphyton from a Waste-water Treatment Facility. Journal of Phycology 26 (4):611-617

De Beer D, Stoodley P, Roe F, Lewandowski Z (1994) Effects of Biofilm Structures on Oxygen Distribution and Mass Transport. Biotechnology and Bioengineering 43:1131-1138

De Godos I, González C, Becares E, García-Encina P, Muñoz R (2009) Simultaneous Nutrients and Carbon Removal During Pretreated Swine Slurry Degradation in a Tubular Biofilm Photobio-reactor. Applied Microbiology and Biotechnology 82 (1):187-194

Dekker A, Menkveld W, Franken P (2013) Symbaalzuivering. Theoretische Verkenning van de Haalbaarheid. STOWA Rapport 10.

Di Pippo F, Ellwood N, Guzzon A, Siliato L, Micheletti E, De Philippis R, Albertano P (2012) Effect of Light and Temperature on Biomass, Photosynthesis and Capsular Polysaccharides in Cultured Phototrophic Biofilms. Journal of Applied Phycology 24 (2):211-220

Dickinson KE, Whitney CG, McGinn PJ (2013) Nutrient Remediation Rates in Municipal Waste-water and Their Effect on Biochemical Composition of the Microalga *Scenedesmus* Sp. Amdd. Algal Research 2:127-134

Driver J, Lijmbach D, Steen I (1999) Why Recover Phosphorus for Recycling, and How? Environmental Technology 20 (7):651-662

Duboc P, Marison I, Stockar Uv (1999) Quantitative Calorimetry and Biochemical Engineering. In: Kemp RB, Handbook of Thermal Analysis and Calorimetry vol 4. pp 287-309

Edgar LA, Pickett-Heaps JD (1983) The Mechanism of Diatom Locomotion. I. An Ultrastructural Study of the Motility Apparatus. Proceedings of the Royal Society of London Series B, Biological Sciences 218 (1212):331-343

Ehimen EA, Holm-Nielsen J-B, Poulsen M, Boelsmand JE (2013) Influence of Different Pre-Treatment Routes on the Anaerobic Digestion of a Filamentous Algae. Renewable Energy 50:476-480

Ekholm P, Krogerus K (1998) Bioavailability of Phosphorus in Purified Municipal Wastewaters. Water Research 32 (2):343-351

Ellwood NTW, Di Pippo F, Albertano P (2011) Phosphatase Activities of Cultured Phototrophic Biofilms. Water Research 46 (2):378-386

Elrifi IR, Turpin DH (1985) Steady-State Luxury Consumption and the Concept of Optimum Nutrient Ratios: A Study with Phosphate and Nitrate Limited *Selenastrum Minutum* (Chlorophyta). Journal of Phycology 21:592-602

Eppley RW, Rogers JN, McCarthy JJ (1969) Half-Saturation Constants for Uptake of Nitrate and Ammonium by Marine Phytoplankton. Limnology and Oceanography 14 (6):912-920

Flameling IA, Kromkamp J (2006) Light Dependence of Quantum Yields for PSII Charge Separation and Oxygen Evolution in Eucaryotic Algae. Limnology & Oceanography 43 (2):284-297

Flemming H-C, Wingender J (2001) Relevance of Microbial Extracellular Polymeric Substances (Epss) – Part I: Structural and Ecological Aspects. Water Science & Technology 43:1-8

R

Fujimoto N, Sudo R (1997) Nutrient-Limited Growth of *Microcystis Aeruginosa* and *Phormidium Tenue* and Competition under Various N:P Supply Ratios and Temperatures. Limnology and Oceanography 42 (2):250-256

Goldman JC, Carpenter EJ (1974) A Kinetic Approach to the Effect of Temperature on Algal Growth. Limnology and Oceanography 19 (5):756-766

Goldman JC, McCarthy JJ, Peavey DG (1979) Growth Rate Influence on the Chemical Composition of Phytoplankton in Oceanic Waters. Nature 279:210-215

Golueke CG, Oswald WJ, Gotaas HB (1957) Anaerobic Digestion of Algae. Applied Microbiology 5 (1):47-55

González C, Marciniak J, Villaverde S, León C, García PA, Muñoz R (2008) Efficient Nutrient Removal from Swine Manure in a Tubular Biofilm Photo-Bioreactor Using Algae-Bacteria Consortia. Water Science and Technology 58 (1):95-102

Grotenhuis JTC, Van Lier JB, Plugge CM, Stams AJM, Zehnder AJB (1991) Effect of Ethylene Glycol-Bis(B-Aminoethyl Ether)-N,N-Tetraacetic Acid (Egta) on Stability and Activity of Methanogenic Granular Sludge. Appl Environ Microbiol 36:109-114

Guzzon A, Bohn A, Diociaiuti M, Albertano P (2008) Cultured Phototrophic Biofilms for Phosphorus Removal in Wastewater Treatment. Water Research 42 (16):4357-4367

Halterman SG, Toetz DW (1984) Kinetics of Nitrate Uptake by Freshwater Algae. Hydrobiologia 114 (3):209-214

Healey FP (1973) Inorganic Nutrient Uptake and Deficiency in Algae. Critical reviews in microbiology 3:69-113

Hecky RE, Kilham P (1988) Nutrient Limitation of Phytoplankton in Freshwater and Marine Environments: A Review of Recent Evidence on the Effects of Enrichment. Limnology & Oceanography 33 (4):796-822

Hemming S, Dueck T, Janse J, van Noort F (2008) The Effect of Diffuse Light on Crops. Acta Horticulturae 801 (Part 2):1293-1300

Heubeck S, Craggs RJ, Shilton A (2007) Influence of CO_2 Scrubbing from Biogas on the Treatment Performance of a High Rate Algal Pond. Water Science and Technology 55:193-200

Hill W (1996) Effects of Light. In: Stevenson RJ, Bothwell ML, Lowe RL, Algal Ecology: Freshwater Benthic Ecosystems. Academic Press Elsevier, pp 121-148

Ho TY, Quigg A, Finkel ZV, Milligan AJ, Wyman K, Falkowski PG, Morel FMM (2003) The Elemental Composition of Some Marine Phytoplankton. Journal of Phycology 39 (6):1145-1159

Hoehn RC, Ray AD (1973) Effects of Thickness on Bacterial Film. Journal Water Pollution Control Federation 45 (11):2302-2320

Hoffmann JP (1998) Wastewater Treatment with Suspended and Nonsuspended Algae. Journal of Phycology 34:757-763

Horjus F, Kersholt M, Zoutberg GR, Koot D, Goverde J (2011) Effluentpolishing met Algen. Deelstudie Pilotonderzoek op RWZI Alkmaar. STOWA Rapport 05.

Horn H, Reiff H, Morgenroth E (2003) Simulation of Growth and Detachment in Biofilm Systems under Defined Hydrodynamic Conditions. Biotechnology and Bioengineering 81 (5):607-617

R

Hulatt CJ, Thomas DN (2011) Energy Efficiency of an Outdoor Microalgal Photobioreactor Sited at Mid-Temperature Latitude. Bioresource technology 102:6687-6695

Huld T, Suri M (2007) Photovoltaic Geographical Information System. http://re.jrc.ec.europa.eu/pvgis/apps4/pvest.php. Accessed November 2010

Hultman B, Jionsson K, Plaza E (1994) Combined Nitrogen and Phosphorus Removal in a Full-Scale Continuous Up-Flow Sand Filter. Water Science & Technology 29 (10-11):127-134

Huszar VLDM, Caraco NF (1998) The Relationship between Phytoplankton Composition and Physical-Chemical Variables: A Comparison of Taxonomic and Morphological-Functional Descriptors in Six Temperature Lakes. Freshwater Biology 40:679-696

Hwang S-J, Havens KE, Steinman AD (1998) Phosphorus Kinetics of Planktonic and Benthic Assemblages in a Shallow Subtropical Lake. Freshwater Biology 40 (4):729-745

Irving TE, Allen DG (2011) Species and Material Considerations in the Formation and Development of Microalgal Biofilms. Applied Microbiology and Biotechnology 92 (2):283-294

Jansson M (1988) Phosphate Uptake and Utilization by Bacteria and Algae. Hydrobiologia 170 (1):177-189

Jiménez-Pérez MV, Sánchez-Castillo P, Romera O, Fernández-Moreno D, Pérez-Martínez C (2004) Growth and Nutrient Removal in Free and Immobilized Planktonic Green Algae Isolated from Pig Manure. Enzyme and Microbial Technology 34 (5):392-398

Jöbgen AM, Palm A, Melkonian M (2004) Phosphorus Removal from Eutrophic Lakes Using Periphyton on Submerged Artificial Substrata. Hydrobiologia 523:123-142

Johnson MB, Wen Z (2009) Development of an Attached Microalgal Growth System for Biofuel Production. Applied Microbiology and Biotechnology 85 (3):525-534

Johnson RE, Tuchman NC, Peterson CG (1997) Changes in the Vertical Microdistribution of Diatoms within a Developing Periphyton Mat. Journal of the North American Benthological Society 16 (3):503-519

Karya NGAI, van der Steen NP, Lens PNL (2013) Photo-Oxygenation to Support Nitrification in an Algal-Bacterial Consortium Treating Artificial Wastewater. Bioresource Technology 134:244-250

Khatoon H, Yusoff F, Banerjee S, Shariff M, Bujang JS (2007) Formation of Periphyton Biofilm and Subsequent Biofouling on Different Substrates in Nutrient Enriched Brackishwater Shrimp Ponds. Aquaculture 273 (4):470-477

Klausmeier CA, Litchman E, Simon AL (2004) Phytoplankton Growth and Stoichiometry under Multiple Nutrient Limitation. Limnology and Oceanography 49 (4):1463-1470

Kliphuis AMJ, de Winter L, Vejrazka C, Martens DE, Janssen M, Wijffels RH (2010) Photosynthetic Efficiency of *Chlorella Sorokiniana* in a Turbulently Mixed Short Light-Path Photobioreactor. Biotechnology Progress 26 (3):687-696

KNMI (2013) Daggegevens Van Het Weer in Nederland. http://www.knmi.nl/kd/daggegevens/download.html. Accessed February 2013

R

Knuckey RM, Brown MR, Robert R, Frampton DMF (2006) Production of Microalgal Concentrates by Flocculation and Their Assessment as Aquaculture Feeds. Aquacultural Engineering 35 (3):300-313

Kong Q, Li L, Martinez B, Chen P, Ruan R (2010) Culture of Microalgae *Chlamydomonas Reinhardtii* in Wastewater for Biomass Feedstock Production. Applied Biochemistry and Biotechnology 160:9-18

Kröpfl K, Vladár P, Szabó K, Ács É, Borsodi AK, Szikora S, Caroli S, Záray G (2006) Chemical and Biological Characterisation of Biofilms Formed on Different Substrata in Tisza River (Hungary). Environmental Pollution 144 (2):626-631

Lacour T, Sciandra A, Talec A, Mayzaud P (2012) Diel Variations of Carbohydrates and Neutral Lipids in Nitrogen-Sufficient and Nitrogen-Starved Cyclostat Cultures of *Isochrysis* Sp. Journal of Phycology 48:966-975

Laliberté G, Lessard P, De La Noüe J, Sylvestre S (1997) Effect of Phosphorus Addition on Nutrient Removal from Wastewater with the Cyanobacterium *Phormidium Bohneri*. Bioresource Technology 59:227-233

Lána J, Hofman J, Bláha L (2011) Can Cyanobacterial Biomass Applied to Soil Affect Survival and Reproduction of Springtail *Folsomia Candida*? Ecotoxicology and Environmental Safety 74 (4):840-843

Ley AC, Mauzerall DC (1982) Absolute Absorption Cross-Sections for Photosystem II and the Minimum Quantum Requirement for Photosynthesis in *Chlorella Vulgaris*. Biochimica et Biophysica Acta (BBA) - Bioenergetics 680 (1):95-106

Li T, Heuvelink E, Dueck TA, Marcelis LFM (2012) Understanding How Diffuse Light Increases Yield in Tomato. In: Proceedings of the 7th International Symposium on Light in Horticultural Systems (Book of Abstracts), Leuven

Liehr SK, Chen HJ, Lin SH (1994) Metals Removal by Algal Biofilms. Water Science and Technology 30 (11):59-68

Liehr SK, Eheart JW, Suidan MT (1988) A Modeling Study of the Effect of pH on Carbon Limited Algal Biofilms. Water Research 22 (8):1033-1041

Liehr SK, Suidan MT, Eheart JW (1990) A Modeling Study of Carbon and Light Limitation in Algal Biofilms. Biotechnology and Bioengineering 35:233-243

Lin YH, Leu JY, Lan CR, Lin PHP, Chang FL (2003) Kinetics of Inorganic Carbon Utilization by Microalgal Biofilm in a Flat Plate Photoreactor. Chemosphere 53 (7):779-787

Lind JL, Heimann K, Miller EA, van Vliet C, Hoogenraad NJ, Wetherbee R (1997) Substratum Adhesion and Gliding in a Diatom Are Mediated by Extracellular Proteoglycans. Planta 203 (2):213-221

Liu SM, Zhang J, Jiang WS (2003) Pore Water Nutrient Regeneration in Shallow Coastal Bohai Sea, China. Journal of Oceanography 59 (3):377-385

Lloyd D, Boddy L, Davies KJP (1987) Persistence of Bacterial Denitrification Capacity under Aerobic Conditions: The Rule Rather Than the Exception. FEMS Microbiology Letters 45 (3):185-190

R

Lorens RB (1981) Sr, Cd, Mn and Co Distribution Coefficients in Calcite as a Function of Calcite Precipitation Rate. Geochimica et Cosmochimica Acta 45:553-561

Lubarsky HV, Hubas C, Chocholek M, Larson F, Manz W, Paterson DM, Gerbersdorf SU (2010) The Stabilisation Potential of Individual and Mixed Assemblages of Natural Bacteria and Microalgae. PLoS ONE 5 5 (11):e13794

Lyons WB, Loder TC, Murray SM (1982) Nutrient Pore Water Chemistry, Great Bay, New Hampshire: Benthic Fluxes. Estuaries 5 (3):230-233

Martínez ME, Jiménez JM, El Yousfi F (1999) Influence of Phosphorus Concentration and Temperature on Growth and Phosphorus Uptake by the Microalga *Scenedesmus Obliquus*. Bioresource Technology 67 (3):233-240

McLean BM, Baskaran K, Connor MA (2000) The Use of Algal-Bacterial Biofilms to Enhance Nitrification Rates in Lagoons: Experience under Laboratory and Pilot-Scale Conditions. Water Science & Technology 42 (10-11):187-194

Metcalf & Eddy I (2003) Wastewater Engineering: Treatment and Reuse. 4th edn. McGraw-Hill

Min M, Wang L, Li Y, Mohr MJ, Hu B, Zhou W, Chen P, Ruan R (2011) Cultivating *Chlorella* sp. in a Pilot-Scale Photobioreactor Using Centrate Wastewater for Microalga Biomass Production and Wastewater Nutrient Removal. Applied Biochemistry and Biotechnology 165:123-137

Morita M, Watanabe Y, Saiki H (2000) High Photosynthetic Productivity of Green Microalga *Chlorella Sorokiniana*. Applied Biochemistry and Biotechnology 87:203-218

Mouget J-L, Dakhama A, Lavoie MC, De La Noüe J (1995) Algal Growth Enhancement by Bacteria: Is Consumption of Photosynthetic Oxygen Involved? FEMS Microbiology Ecology 18 (1):35-43

Mulbry W, Kebede-Westhead E, Pizarro C, Sikora L (2005) Recycling of Manure Nutrients: Use of Algal Biomass from Dairy Manure Treatment as a Slow Release Fertilizer. Bioresource Technology 96:451-458

Mulbry W, Kondrad S, Pizarro C, Kebede-Westhead E (2008) Treatment of Dairy Manure Effluent Using Freshwater Algae: Algal Productivity and Recovery of Manure Nutrients Using Pilot-Scale Algal Turf Scrubbers. Bioresource Technology 99:8137-8142

Muñoz R, Guieysse B (2006) Algal-Bacterial Processes for the Treatment of Hazardous Contaminants: A Review. Water Research 40 (15):2799-2815

Muñoz R, Köllner C, Guieysse B (2009) Biofilm Photobioreactors for the Treatment of Industrial Wastewaters. Journal of Hazardous Materials 161 (1):29-34

Murata N, Takahashi S, Nishiyama Y, Allakhverdiev SI (2007) Photoinhibition of Photosystem II under Environmental Stress. Biochimica et Biophysica Acta (BBA) - Bioenergetics 1767 (6):414-421

Murphy TE, Berberoğlu H (2012) Temperature Fluctuation and Evaporative Loss Rate in an Algae Biofilm Photobioreactor. Journal of Solar Energy Engineering 134 (1):011002.1-011002.9

Mussgnug JH, Klassen V, Schlüter A, Kruse O (2010) Microalgae as Substrates for Fermentative Biogas Production in a Combined Biorefinery Concept. Journal of Biotechnology 150:51-56

R

Naumann T, Çebi Z, Podola B, Melkonian M (2012) Growing Microalgae as Aquaculture Feeds on Twin-Layers: A Novel Solid-State Photobioreactor. Journal of Applied Phycology

Needoba JA, Harrison PJ (2004) Influence of Low Light and a Light: Dark Cycle on NO_3^- Uptake, Intracellular NO_3^-, and Nitrogen Isotope Fractionation by Marine Phytoplankton. Journal of Phycology 40 (3):505-516

Nichols DS (1983) Capacity of Natural Wetlands to Remove Nutrients from Wastewater. Water Pollution Control Federation 55 (5):495-505

Norsker N-H, Barbosa MJ, Vermuë MH, Wijffels RH (2011) Microalgal Production - a Close Look at the Economics. Biotechnology Advances 29 (1):24-27

Norton TA, Melkonian M, Andersen RA (1996) Algal Biodiversity. Phycologia 35 (4):308-326

Olguín EJ, Galicia S, Mercado G, Peréz T (2003) Annual Productivity of *Spirulina (Arthrospira)* and Nutrient Removal in a Pig Wastewater Recycling Porcess under Tropical Conditions. Journal of Applied Phycology 15:249-257

Órpez R, Martínez ME, Hodaifa G, El Yousfi F, Jbari N, Sánchez S (2009) Growth of the Microalga *Botryococcus Braunii* in Secondarily Treated Sewage. Desalination 246:625-630

Ozkana A, Kinneya K, Katza L, Berberoglub H (2012) Reduction of Water and Energy Requirement of Algae Cultivation Using an Algae Biofilm Photobioreactor. Bioresource Technology 114:542-548

Pagilla KR, Urgun-Demirtas M, Ramani R (2006) Low Effluent Nutrient Technologies for Wastewater Treatment. Water Science & Technology 53 (3):165-172

Parkhill J-P, Maillet G, Cullen JJ (2001) Fluorescence-Based Maximal Quantum Yield for PSII as a Diagnostic of Nutrient Stress. Journal of Phycology 37 (4):517-529

Parkin GF, Owen, WF (1986) Fundamentals of Anaerobic Digestion of Wastewater Sludges. Journal of Environmental Engineering 112: 867–920

Pehlivanoglu E, Sedlak DL (2004) Bioavailability of Wastewater-Derived Organic Nitrogen to the Alga *Selenastrum Capricornutum*. Water Research 38 (14-15):3189-3196

Pérez J, Picioreanu C, Van Loosdrecht M (2005) Modeling Biofilm and Floc Diffusion Processes Based on Analytical Solution of Reaction-Diffusion Equations. Water Research 39:1311-1323

Picot B, Moersidik S, Casellas C, Bontoux J (1993) Using Diurnal Variations in a High Rate Algal Pond for Management Pattern. Water Science & Technology 28 (10):169-175

Pittman JK, Dean AP, Osundeko O (2011) The Potential of Sustainable Algal Biofuel Production Using Wastewater Resources. Bioresource Technology 102 (1):17-25

Powell N, Shilton AN, Pratt S, Chisti Y (2008) Factors Influencing Luxury Uptake of Phosphorus by Microalgae in Waste Stabilization Ponds. Environmental Science & Technology 42 (16):5958-5962

Prajapati SK, Kaushik P, Malik A, Vijay VK (2012) Phycoremediation and Biogas Potential of Native Algal Isolates from Soil and Wastewater. Bioresource Technology 135:232-238

Qiang H, Faiman D, Richmond A (1998) Optimal Tilt Angles of Enclosed Reactors for Growing Photoautotrophic Microorganisms Outdoors. Journal of Fermentation and Bioengineering 85 (2):230-236

R

Ramachandra TV, Madhab MD, Shilpi S, Joshi NV (2013) Algal Biofuel from Urban Wastewater in India: Scope and Challenges. Renewable and Sustainable Energy Reviews 21:767-777

Ras M, Steyer J-P, Bernard O (2013) Temperature Effect on Microalgae: A Crucial Factor for Outdoor Production. Reviews in Environmental Science and Bio/Technology 12 (2):153-164

Reay DS, Nedwell DB, Priddle J, Ellis-Evans JC (1999) Temperature Dependence of Inorganic Nitrogen Uptake: Reduced Affinity for Nitrate at Suboptimal Temperatures in Both Algae and Bacteria. Appl Environ Microbiol 65 (6):2577-2584

Roeleveld P, Roorda J, Schaafsma M (2010) Op Weg Naar De Rwzi Van 2030. STOWA Rapport 11.

Roeselers G, Loosdrecht M, Muyzer G (2008) Phototrophic Biofilms and Their Potential Applications. Journal of Applied Phycology 20 (3):227-235

RReDC (2012) Astm G173-03 Reference Spectra Derived from Smarts V. 2.9.2. http://rredc.nrel.gov/solar/spectra/am1.5/ASTMG173/ASTMG173.html. Accessed November 2011

Schramm A, Santegoeds CM, Nielsen HK, Ploug H, Wagner M, Pribyl M, Wanner J, Amann R, de Beer D (1999) On the Occurrence of Anoxic Microniches, Denitrification, and Sulfate Reduction in Aerated Activated Sludge Appl Environ Microbiol 65 (9):4189-4196

Schumacher G, Blume T, Sekoulov I (2003) Bacteria Reduction and Nutrient Removal in Small Wastewater Treatment Plants by an Algal Biofilm. Water Science and Technology 47 (1):195-202

Sekar R, Nair KVK, Rao VNR, Venugopalan VP (2002) Nutrient Dynamics and Successional Changes in a Lentic Freshwater Biofilm. Freshwater Biology 47 (10):1893-1907

Shi J, Podola B, Melkonian M (2007) Removal of Nitrogen and Phosphorus from Wastewater Using Microalgae Immobilized on Twin Layers: An Experimental Study. Journal of Applied Phycology 19:417-423

Solovchenko A, Khozin-Goldberg I, Didi-Cohen S, Cohen Z, Merzlyak M (2008) Effects of Light Intensity and Nitrogen Starvation on Growth, Total Fatty Acids and Arachidonic Acid in the Green Microalga *Parietochloris Incisa*. Journal of Applied Phycology 20 (3):245-251

Stal LJ (2003) Microphytobenthos, Their Extracellular Polymeric Substances, and the Morphogenesis of Intertidal Sediments. Geomicrobiology Journal 20 (5):463-478

Stevenson RJ (1996) An Introduction to Algal Ecology in Freshwater Bethic Habitats. In: Stevenson RJ, Bothwell ML, Lowe RL, Algal Ecology: Freshwater Benthic Ecosystems. Academic Press Elsevier, pp 3-30

Stewart PS (1997) A Review of Experimental Measurements of Effective Diffusive Permeabilities and Effective Diffusion Coefficients in Biofilms. Biotechnology and Bioengineering 59 (3):261-272

Su Y, Mennerich A, Urban B (2012) Synergistic Cooperation between Wastewater-Born Algae and Activated Sludge for Wastewater Treatment: Influence of Algae and Sludge Inoculation Ratios. Bioresource Technology 105:67-73

Talbot P, Thébault JM, Dauta A, De La Noüe J (1991) A Comparative Study and Mathematical Modeling of Temperature, Light and Growth of Three Microalgae Potentially Useful for Wastewater Treatment. Water Research 25 (4):465-472

R

Temman M, Paquette J, Vali H (2000) Mn and Zn Incorporation into Calcite as a Function of Chloride Aqueous Concentration. Geochimica et Cosmochimica Acta 64 (14):2417-2430

Teneva I, Dzhambazov B, Koleva L, Mladenov R, Schirmer K (2005) Toxic Potential of Five Freshwater *Phormidium* Species (Cyanoprokaryota). Toxicon 45:711-725

Torzillo G, Sacchi A, Materassi R (1991) Temperature as an Important Factor Affecting Productivity and Night Biomass Loss in *Spirulina Platensis* Grown Outdoors in Tubular Photobioreactors. Bioresource Technology 38 (2-3):95-100

Travieso L, Pellón A, Benítez F, Sánchez E, Borja R, O'Farrill N, Weiland P (2002) Bioalga Reactor: Preliminary Studies for Heavy Metals Removal. Biochemical Engineering Journal 12 (2):87-91

Ukeles R, Bishop J (1975) Enhancement of Phytoplankton Growth by Marine Bacteria. Journal of Phycology 11 (2):142-149

Van Den Hende S, Vervaeren H, Saveyn H, Maes G, Boon N (2010) Microalgal Bacterial Floc Properties Are Improved by a Balanced Inorganic/Organic Carbon Ratio. Biotechnology and Bioengineering 108 (3):549-557

Van Der Grinten E, Janssen M, Simis SGH, Barranguet C, Admiraal W (2004a) Phosphate Regime Structures Species Composition in Cultured Phototrophic Biofilms. Freshwater Biology 49:369-381

Van Der Grinten E, Simis SGH, Barranguet C, Admiraal W (2004b) Dominance of Diatoms over Cyanobacterial Species in Nitrogen-Limited Biofilms. Archiv für Hydrobiologie 161 (1):99-112

Van Hulle SWH, Vandeweyer HJP, Meesschaert BD, Vanrolleghem PA, Dejans P, Dumoulin A (2010) Engineering Aspects and Practical Application of Autotrophic Nitrogen Removal from Nitrogen Rich Streams. Chemical Engineering Journal 162 (1):1-20

Van Vooren L, Lessard P, Ottoy JP, Vanrolleghem PA (1999) pH Buffer Capacity Based Monitoring of Algal Wastewater Treatment. Environmental Technology 20 (6):547 - 561

Vejrazka C, Janssen M, Streefland M, Wijffels RH (2011) Photosynthetic Efficiency of *Chlamydomonas Reinhardtii* in Flashing Light. Biotechnology and Bioengineering 108 (12):2905-2913

Vincent WF (1992) The Daily Pattern of Nitrogen Uptake by Phytoplankton in Dynamic Mixed Layer Environments. Hydrobiologia 238:37-52

Vona V, Rigano VDM, Esposito S, Carillo P, Carfagna S, Rigano C (1999) Growth, Photosynthesis, and Respiration of *Chlorella Sorokiniana* after N-Starvation. Interactions between Light, CO_2 and NH_4^+ Supply. Physiologia Plantarum 105 (2):288-293

Wang Y, Lu J, Mollet J-C, Gretz MR, Hoagland KD (1997) Extracellular Matrix Assembly in Diatoms (Bacillariophyceae): II. 2,6-Dichlorobenzonitrile Inhibition of Motility and Stalk Production in the Marine Diatom *Achnanthes Longipes*. Plant Physiology 113 (4):1071-1080

Wäsche S, Horn H, Hempela DC (2002) Influence of Growth Conditions on Biofilm Development and Mass Transfer at the Bulk/Biofilm Interface. Water Research 36:4775-4784

R

Wijffels RH, Barbosa MJ, Eppink MHM (2010) Microalgae for the Production of Bulk Chemicals and Biofuels. Biofuels, Bioproducts and Biorefining 4 (3):287-295

Woertz I, Feffer A, L, undquist T, Nelson Y (2009) Algae Grown on Dairy and Municipal Wastewater for Simultaneous Nutrient Removal and Lipid Production for Biofuel Feedstock Journal of Environmental Engineering 135 (11):1115-1122

Wolf G, Picioreanu C, van Loosdrecht MCM (2007) Kinetic Modeling of Phototrophic Biofilms: The Phobia Model. Biotechnology and Bioengineering 97 (5):1064-1079

Yen HW, Brune DE (2007) Anaerobic Co-Digestion of Algal Sludge and Waste Paper to Produce Methane. Bioresource Technology 98 (1):130-134

Zamalloa C, Boon N, Verstraete W (2012) Anaerobic Digestibility of *Scenedesmus Obliquus* and *Phaeodactylum Tricornutum* under Mesophilic and Thermophilic Conditions. Applied Energy 92:733-738

Zippel B, Neu TR (2005) Growth and Structure of Phototrophic Biofilms under Controlled Light Conditions. Water Science & Technology 52 (7):203-209

Zurawell RW, Chen H, Burke JM, Prepas EE (2005) Hepatotoxic Cyanobacteria: A Review of the Biological Importance of Microcystins in Freshwater Environments. Journal of Toxicology and Environmental Health, Part B 8 (1):1-37

R

R

SUMMARY

Microalgae are a large and diverse group of photoautotrophic organisms. Microalgae live in most soils and many different aquatic habitats, where they can live in biofilms. Microalgal biofilms are defined as attached microbial phototrophic consortia which are entrapped in a gel-like matrix of extracellular polymeric substances. This biofilm is usually visible as a slimy green layer. Microalgal biofilms can be attached to solid surfaces or only to each other and can grow on any surface or carrier material that receives sufficient moisture and light.

In municipal wastewater treatment microalgae remove inorganic nitrogen and phosphorus by assimilating these nutrients into their biomass. When microalgae are grown in biofilm systems instead of suspended systems, no separation of microalgal biomass and water is required which presumably makes harvesting of the biomass much easier. Furthermore, biofilm systems can operate at short hydraulic retention times and are expected to exhibit a diminished energy demand in comparison to suspended systems.

Microalgal biofilms appear especially interesting for the post-treatment of municipal wastewater effluents as microalgae present a more sustainable alternative to existing post-treatment systems. Many municipal wastewater treatment plants in the Netherlands and other EU member states are required to further reduce their nitrogen and phosphorus emissions due to the EU Water Framework Directive. In concordance with this directive, the nitrogen and phosphorus concentrations must be reduced from the current European discharge requirements of 10 mg/L nitrogen and 1 mg/L phosphorus to concentrations appropriate for discharge to 'sensitive' water bodies by 2015. Current Dutch guidelines for these sensitive water bodies are 2.2 mg/L nitrogen and 0.15 mg/L phosphorus.

The conventional treatment of municipal wastewater consists of activated sludge processes with a combination of nitrification and denitrification and biological or chemical phosphorus removal. Biofilms composed of microalgae and bacteria may be applied as single-step alternative to this sequence of biological processes. In such a symbiotic biofilm microalgae remove nitrogen and phosphorus, and simultaneously produce the oxygen that is required for the aerobic, heterotrophic degradation of organic pollutants. This in situ oxygen production can result in considerable savings on energy, compressors and maintenance as extensive aeration is no longer required.

The potential of a hypothetical microalgal biofilm system was investigated in Chapter 2. Three scenarios were defined for seasonal wastewater treatment in the Netherlands. In Scenario 1 the microalgal biofilm system is employed as post-treatment of municipal

wastewater effluent. In Scenario 2 the microalgal biofilm system removes nitrogen and phosphorus following a highly loaded activated sludge system. The microalgal biofilm hereby serves as an alternative for nitrification and denitrification and chemical or biological phosphorus removal. In Scenario 3 an microalgal-bacterial biofilm is applied to treat the wastewater directly. This scenario makes use of the symbiotic relationship described above that may develop when using microalgae and heterotrophs together. According to the analysis the area requirements of these biofilm systems were 0.32, 2.1, and 0.76 m^2 per person equivalent for Scenarios 1, 2, and 3, respectively. A substantial amount of biomass was produced of 8 to 59 gram per person equivalent per day. It was determined that it was not possible to simultaneously remove all nitrogen and phosphorus from the wastewater due to the difference between the nitrogen to phosphorus ratio in the wastewater and in the microalgal biomass. Scenarios 1 and 3 were selected for further research based on the area requirement, achieved effluent concentrations, and biomass production.

In Chapters 3, 4 and 5 microalgal biofilms were studied as a post-treatment step for the effluent of municipal wastewater treatment plants (Scenario 1). In Chapter 3 microalgal biofilms were grown in horizontal flow cells with different nutrient loading rates. These biofilms removed residual nitrate and phosphate in wastewater effluent to the target values of 2.2 mg/L nitrogen and 0.15 mg/L phosphorus. The maximum uptake capacity was determined at 1.0 g/m^2/day nitrogen and 0.13 g/m^2/day phosphorus. Up to this maximum capacity the internal nitrogen and phosphorus content of the microalgae was dependent on the loading rate, and the internal nitrogen to phosphorus ratio decreased from 23:1 to 11:1 at the maximum uptake capacity. At nutrient loading rates above the maximum uptake capacity the effluent concentrations increased with increasing loading rates. Based on the maximum uptake capacity and the internal nutrient content of the microalgal biomass it was estimated that the area requirement of a full scale microalgal biofilms post-treatment system for 100 000 inhabitants would be around 10 hectare. The results demonstrated that microalgal biofilms can be applied to remove both nitrogen and phosphorus despite the not optimal ratios present in municipal wastewater effluent.

When applying microalgal biofilms for wastewater treatment, the biofilm should be continuously maintained in the growth phase. This ensures a high biomass production and, thereby, a high nutrient removal rate. Regular harvesting of the biofilm can maintain the biofilm in the growth phase and, therefore, various harvesting regimes were investigated with the vertical phototrophic biofilm reactor designed in Chapter 4. It was discovered necessary to frequently harvest a section of the biofilm but not the entire biofilm, to achieve consistent low effluent concentrations of nitrogen and phosphorus. The microalgal biomass productivity is optimal for a wide range of biofilm thicknesses

as was indicated by the similar biomass production rate of 7 gram dry weight per m^2 per day when harvesting every two, four, or seven days. Additional measurements in horizontal flow lanes investigated the hypothesis that biomass productivity decreases with increasing biofilm thickness. It was demonstrated that, contrary to expectations, the areal biomass production rate doubled when the biofilm thicknesses was increased from 130 μm to 2 mm. This increased production was explained by the lower density and looser structure of the 2 mm biofilm. It is expected that increasing the biofilm thickness further will eventually result in a lower biomass production when biomass growth is exceeded by losses through respiration, cell death, parasitism, disease and grazing. It was concluded that, concerning biomass production and labor requirement, the optimum harvesting frequency is once per week.

A pilot-scale vertical phototrophic biofilm reactor was built at the municipal waste-water treatment plant in Leeuwarden, the Netherlands, based on the reactor design of Chapter 4. This reactor was operated from June 2012 until the end of October 2012. The pilot-scale reactor was evaluated in Chapter 5 to determine its capacity to remove nitrogen and phosphorus from Dutch municipal wastewater effluent. The areal biomass production rate ranged between 2.7 and 4.5 gram dry weight per m^2 per day. The areal nitrogen and phosphorus removal rates averaged 0.13 g/m^2/day nitrogen and 0.023 g/m^2/day phosphorus, which are five and three times lower than the removal rates achieved in the laboratory described in Chapter 4. The wastewater was comprised of enough inorganic carbon to sustain microalgal growth, and additional carbon dioxide supply was not requisite. A direct relationship between light intensity and nutrient removal was only observed on sunny days when the nutrient removal increased during the day and decreased with decreasing light intensity until no removal occurred during the night. However, this relationship was not apparent from long term monitoring data. The target effluent concentrations of 2.2 mg/L nitrogen and 0.15 mg/L phosphorus could not be achieved. The study was not conclusive for the limiting factor that resulted in the low nutrient removal rate, although it is possibly correlated with light and tem-perature limitation in combination with pH increases above pH 9 during the daytime. The pilot-scale study demonstrated that the current vertical phototrophic biofilm reactor is not viable as post-treatment of municipal wastewater under Dutch climate conditions. A microalgal biofilm reactor may be feasible at lower latitudes with higher irradiance levels when controlling the pH and when increasing the effluent temperature in the morning.

In Chapter 6 symbiotic microalgal-bacterial biofilms were investigated for full municipal wastewater treatment (Scenario 3). Symbiotic biofilms were grown in horizontal flow cells with ammonium, phosphate, and with acetate as biodegradable organic pollutant. The biofilms removed acetate, ammonium and phosphate from wastewater at removal

rates of 40 g/m^2/day acetate, 3.2 g/m^2/day nitrogen, and 0.41 g/m^2/day phosphorus. After briefly supplying additional bicarbonate at the beginning of the experiment, the symbiotic relationship established and an additional supply of oxygen or carbon dioxide was not required. The symbiotic relationship between microalgae and aerobic heterotrophs was proven by subsequently removing light and acetate. In both cases this resulted in the cessation of the symbiosis and in increasing effluent concentrations of acetate, ammonium, and phosphate. The symbiotic biofilm could not completely remove ammonium and phosphate, but was demonstrated to achieve considerable heterotrophic denitrification capacity, indicating the possibility of further nitrogen removal by nitrification and denitrification.

The results from the laboratory and pilot-scale research with phototrophic biofilm reactors were discussed in Chapter 7 and the practical application of the biofilm reactor was evaluated. The nutrient removal capacity of the phototrophic biofilm reactor was smaller and the area requirement was larger than assumed in the scenario analysis of Chapter 2. The current reactor design is, therefore, not feasible for the post-treatment of municipal wastewater effluent under Dutch climate conditions. The reactor can be improved by placing the reactor horizontally at a slight angle to achieve a low energy demand, installing a pH control, automating harvesting, and buffering the wastewater at night. In addition, technology should be developed to prevent heat loss from the biofilm and hereby allow heating of the biofilm and wastewater by means of sunlight. Such an improved reactor design may also be applied on touristic locations in the Netherlands such as the Wadden islands, where additional treatment is only required during the touristic summer months when light intensity and temperatures are highest of the year.

Symbiotic microalgal-bacterial biofilm systems can be applied to remove organic pollutants, nitrogen and phosphorus from wastewater. Chapter 6 demonstrated that not all nitrogen and phosphorus could be removed. Therefore, either the wastewater loading rate should be adapted to the light intensity, or the remaining nitrogen and phosphorus should be removed by other processes. The latter could be achieved by nitrification and denitrification and by precipitation of calcium phosphate, magnesium phosphate or struvite. The phototrophic biofilm reactor produces substantial amounts of biomass of a density which is 100 to 1800 times higher than in suspended systems. This microalgal biomass may be reused as fertilizer or anaerobically digested for the production of energy.

SAMENVATTING

Microalgen behoren tot de grote en diverse groep van fotoautotrofe micro-organismen en komen voor in de meeste bodems en in diverse aquatische milieus. Hier leven ze onder andere in biofilms. Een microalgenbiofilm wordt gedefinieerd als een verzameling van microbiële fototrofe populaties, omsloten door een gelachtige matrix van extracellulaire polymerische substanties. Deze biofilm ziet er meestal uit als een slijmerige groene laag. De microalgen in een biofilm zijn aan elkaar vastgehecht en kunnen daarnaast aan elk oppervlakte of dragermateriaal hechten waar voldoende vocht en licht komt.

Microalgen worden in de huishoudelijke afvalwaterzuivering toegepast om anorganische stikstof en fosfor te verwijderen door deze nutriënten op te nemen in hun biomassa. Het voordeel van microalgen in een biofilmsysteem in plaats van in een gesuspendeerde systeem, is dat er geen scheiding nodig is van microalgenbiomassa en water, wat het oogsten van de biomassa veelal makkelijker maakt. Bovendien kan een biofilmsysteem bij korte hydraulische verblijftijden werken en is er minder energie nodig dan bij een gesuspendeerd systeem.

De invoering van de EU Kaderrichtlijn Water heeft geleidt tot het zoeken naar alternatieve nazuiveringssytemen. In dit proefschrift zijn microalgenbiofilms onderzocht voor de nazuivering van huishoudelijk afvalwatereffluent. Microalgensystemen zijn duurzamer dan reeds bestaande nazuiveringssystemen en kunnen zeer lage effluent concentraties halen. Veel huishoudelijke rioolwaterzuiveringsinstallaties in Nederland en andere EU lidstaten moeten hun stikstof- en fosforemissies verminderen als gevolg van de Kaderrichtlijn Water. In overeenstemming met deze richtlijn moeten de stikstof- en fosforconcentraties voor 2015 verminderd worden van de huidige Europese lozingseisen (10 mg/L stikstof en 1 mg/L fosfor) naar concentraties geschikt voor lozing op kwetsbare wateren. De huidige Nederlandse richtlijnen voor kwetsbare wateren zijn 2,2 mg/L stikstof en 0,15 mg/L fosfor, welke zijn gehanteerd als uitgangspunt van dit proefschrift.

Naast nazuivering kunnen microalgen ook worden ingezet om het afvalwater direct te behandelen. De gangbare zuivering van huishoudelijk afvalwater bestaat uit actief-slib-processen met een combinatie van nitrificatie en denitrificatie, en met biologische of chemische fosforverwijdering. Biofilms bestaande uit microalgen en bacteriën zouden in een enkel proces toegepast kunnen worden als alternatief voor deze serie biologische processen. In een dergelijke symbiotische biofilm verwijderen microalgen stikstof en fosfor en produceren ze tegelijkertijd de zuurstof die nodig is voor de aerobe, heterotrofe omzetting van organische verontreinigingen. Deze in situ zuurstofproductie kan leiden tot aanzienlijke besparingen op kosten voor energie, compressoren en onderhoud omdat omvangrijke beluchting niet meer nodig.

Een derde optie is de toepassing van een microalgenbiofilmsysteem na een hoogbelast actief slibsysteem. Het microalgenbiofilmsysteem verwijdert de stikstof en fosfor en dient hiermee als een alternatief voor nitrificatie en denitrificatie, en voor chemische of biologische fosforverwijdering. Echter, uit een scenario analyse (hoofdstuk 2) bleek deze laatste optie niet interessant voor verder onderzoek. Volgens de analyse was het benodigde oppervlakten van dit microalgenbiofilmsysteem 2,1 m^2 per inwonerequivalent voor seizoensafvalwaterzuivering in Nederland, ten op zichte van 0,32 en 0,76 m^2 per inwonerequivalent voor respectievelijk het nazuiverings- en het symbiosesysteem. Uit de analyse bleek tevens dat het niet mogelijk was om tegelijkertijd alle stikstof en fosfor uit het afvalwater te verwijderen vanwege het verschil tussen de stikstof fosfor ratio in het afvalwater en in de microalgen biomassa.

Om te onderzoeken of het daadwerkelijk niet mogelijk is om tegelijkertijd alle stikstof en fosfor uit het afvalwater te verwijderen, werden microalgenbiofilms in het laboratorium onderzocht voor het nazuiveringsscenario. Microalgenbiofilms werden in horizontale doorstroomcellen gecultiveerd onder verschillende nutriëntenbelastingen (hoofdstuk 3). Deze biofilms verwijderden het overgebleven stikstof en fosfor uit afvalwatereffluent tot de beoogde concentraties van 2,2 mg/L stikstof en 0,15 mg/L fosfor. Tot de maximale opnamecapaciteit verwijderden de biofilms wel degelijk voldoende stikstof en fosfor om de beoogde concentraties te behalen. De maximale opnamecapaciteit werd gevonden bij een nutriëntenbelasting van 1,0 g/m^2/dag stikstof en 0,13 g/m^2/dag fosfor. Bij nutriëntenbelastingen boven de maximale opnamecapaciteit namen de effluentconcentraties toe. De microalgen konden zowel stikstof als fosfor verwijderen vanwege de afnemende interne stikstof fosfor ratio van 23:1 tot 11:1 bij de maximale opnamecapaciteit. Op basis van de maximale opnamecapaciteit en het intern stikstofgehalte van de microalgenbiomassa, werd het benodigde microalgenbiofilmoppervlakte voor een full-scale nazuiveringssysteem voor 100.000 inwoners rond de 10 hectare geschat. De resultaten toonden aan dat microalgenbiofilms gebruikt kunnen worden om zowel stikstof als fosfor te verwijderen ondanks dat de ratio hiervan in huishoudelijk afvalwatereffluent niet optimaal is.

Nu de beoogde effluentconcentraties met microalgaenbiofilms waren behaald, werd een verticale fototrofebiofilmreactor ontworpen. Met deze reactor werd het oogsten van microalgenbiofilms onderzocht (hoofdstuk 4). Wanneer microalgenbiofilms worden toegepast voor afvalwaterzuivering zal de biofilm continue in de groeifase moeten worden gehouden, bijvoorbeeld door regelmatig te oogsten. Deze groeifase zorgt voor een hoge biomassaproductie en hierdoor voor een hoge nutriëntverwijdering. Het werd aangetoond dat het noodzakelijk was om regelmatig een deel van de biofilm, maar niet de gehele biofilm, te oogsten om consistent lage effluentconcentraties van stikstof en fosfor te bereiken. Vervolgens werden verschillende oogstregimes onderzocht met

de hypothese dat de biomassaproductie afneemt met toenemende biofilmdikte. De biomassaproductiesnelheid was echter 7 gram drooggewicht per m^2 per dag, ongeacht of een oogstinterval van twee, vier of zeven dagen werd gehanteerd. De microalgenbio-massaproductiviteit bleek hiermee optimaal bij een grote range van biofilmdikten. Met aanvullende metingen in horizontale kanalen werd de hypothese verder onderzocht. Het werd aangetoond dat, in tegenstelling tot de verwachting, de biomassaproductie-snelheid per oppervlakte eenheid verdubbelde bij een toename in biofilmdikte van 130 µm naar 2 mm. Deze toegenomen productie werd verklaard door de lagere dichtheid en lossere structuur van de 2 mm biofilm. De verwachting is dat het verder verhogen van de biofilmdikte uiteindelijk zal leiden tot een lagere biomassaproductie wanneer de biomassagroei wordt overtroffen door verliezen door respiratie, celdood, parasitisme, ziekte en begrazing. Op basis van de biomassaproductie en de benodigde arbeid werd geconcludeerd dat de optimale oogstfrequentie één keer per week is.

Met de veelbelovende resultaten van microalgenbiofilms als nazuiveringssyteem in het laboratorium, is het belangrijk om dit systeem ook gedurende een langere periode te onderzoeken onder variabele en realistische condities. Daarom werd een verticale foto-trofebiofilmreactor op pilot-schaal op de rioolwaterzuiveringsinstallatie in Leeuwarden gebouwd, gebaseerd op het reactorontwerp van hoofdstuk 4. Deze reactor draaide van juni 2012 tot eind oktober 2012. In hoofdstuk 5 werd de verwijderingscapaciteit van de reactor voor stikstof en fosfor uit Nederlands huishoudelijk afvalwatereffluent beoordeeld. De biomassaproductie lag tussen de 2,7 en 4,5 gram drooggewicht per m^2 per dag. De stikstof- en fosforverwijderingssnelheden waren gemiddeld 0,13 g/m^2/dag stikstof en 0,023 g/m^2/dag fosfor, wat respectievelijk vijf en drie keer lager is dan de verwijderingssnelheden behaald in het laboratorium (zoals beschreven in hoofdstuk 4). Het afvalwater bevatte voldoende anorganisch koolstof voor de groei van microal-gen, waardoor het toevoegen van koolstofdioxide niet nodig was. Een direct verband tussen de lichtintensiteit en nutriëntenverwijdering werd alleen waargenomen op zonnige dagen, waarbij de nutriëntverwijdering toenam gedurende de dag en afnam bij afnemende lichtintensiteit totdat er geen verwijdering plaatsvond gedurende de nacht. Echter, dit verband bleek niet uit de metingen verzameld gedurende de gehele looptijd van het pilot-experiment. De beoogde effluentconcentraties van 2,2 mg/L stikstof en 0,15 mg/L fosfor konden niet worden behaald. De studie gaf geen uitsluitsel over de factor die resulteerde in de lage nutriëntverwijdering. Mogelijk werd dit veroorzaakt door licht- en temperatuurlimitatie in combinatie met de toename van de pH tot boven pH 9 gedurende de dag. De studie op pilot-schaal toonde aan dat de huidige verticale fototrofereactor niet geschikt is als nazuivering van huishoudelijk afvalwater onder Nederlandse klimaatcondities. Een microalgenbiofilmreactor is mogelijk toepasbaar onder lagere breedtegraden met hogere zonnestraling als de pH wordt gestuurd en als de temperatuur van het effluent in de ochtend wordt verhoogd.

Naast de microalgenbiofilm als nazuivering van huishoudelijk afvalwatereffluent, werd ook de symbiotische microalgen-bacteriënbiofilm onderzocht voor de volledige zuivering van huishoudelijk afvalwater. Symbiotische biofilms werden in horizontale doorstroomcellen gecultiveerd met ammonium en fosfaat, en met acetaat als biologisch afbreekbare organische verontreinigingen. De biofilms verwijderden acetaat, ammonium en fosfaat uit het afvalwater met verwijderingssnelheden van 40 g/m^2/dag acetaat, 3,2 g/m^2/dag stikstof en 0,41 g/m^2/dag fosfor. Na een korte toevoeging van bicarbonaat aan het begin van het experiment, ontstond de symbiotische relatie en verdere toevoeging van zuurstof of koolstofdioxide was niet nodig. De symbiotische relatie tussen de microalgen en aerobe heterotrofen werd bewezen door achtereenvolgens de toevoer van licht en acetaat te onderbreken. In beide gevallen resulteerde dit in het tijdelijk beëindigen van de symbiose en daardoor in toenemende concentraties van acetaat, ammonium en fosfaat in het effluent. De symbiotische biofilm kon niet alle ammonium en fosfaat verwijderen. Daarom zal de toevoersnelheid van het afvalwater aangepast moeten worden aan de lichtintensiteit, of het niet verwijderde stikstof en fosfor zal moeten worden verwijderd met andere processen. Dit laatste kan naar verwachting met behulp van nitrificatie en denitrificatie en door neerslaan van calciumfosfaat, magnesiumfosfaat, of struviet. De waargenomen ontwikkeling van een aanzienlijke heterotrofe denitrificatiecapaciteit in de symbiotische biofilm duidt de mogelijkheid van verdere stikstofverwijdering door nitrificatie en denitrifactie aan.

De resultaten van het onderzoek op laboratorium- en pilot-schaal met fototrofebiofilmreactoren worden besproken in hoofdstuk 7, en de toepasbaarheid van de biofilmreactor wordt beoordeeld. De fototrofebiofilmreactor produceerde substantiële hoeveelheden biomassa met een dichtheid die 100 tot 1800 keer zo hoog is als in gesuspendeerde systemen. Hiermee is het oogsten van de biomassa van een biofilmsysteem niet alleen makkelijker, maar levert het ook een energiebesparing op. De microalgenbiomassa zou als meststof gebruikt kunnen worden of anaeroob worden vergist voor de productie van energie.

De nutriëntverwijderingscapaciteit van de fototrofebiofilmreactor was lager en het benodigde oppervlakte was groter dan werd aangenomen in de scenarioanalyse in hoofdstuk 2. Het huidige ontwerp is daarom niet toepasbaar als nazuiveringssysteem van huishoudelijkafvalwatereffluent onder Nederlandse klimaatcondities. Het reactorontwerp kan worden verbeterd door de reactor horizontaal onder een kleine hoek te plaatsen om een laag energieverbruik te bewerkstelligen. Verder kan het systeem verbeterd worden door een pH regelaar te installeren, automatisch te oogsten en het afvalwater 's nachts te bufferen. Daarnaast zou een technologische aanpassing ervoor moeten zorgen dat de warmteverliezen van de biofilm beperkt worden, zodat de biofilm en het afvalwater met behulp van zonlicht opwarmen. Een dergelijk verbeterd reac-

torontwerp zou ook kunnen worden toegepast op toeristische locaties in Nederland zoals de Waddeneilanden, waar aanvullende waterzuivering nodig is gedurende de toeristische zomermaanden wanneer de lichtintensiteit en de temperatuur maximaal zijn.

ACKNOWLEDGEMENTS

Many people helped to bring this thesis into existence, many thanks to you all. I would further like to acknowledge my supervisors Hardy and Marcel. Thank you for all your time, input and the nice meetings and Skype sessions we had. You have greatly helped make this multidisciplinary research a success. I would also like to thank René for being my promotor and giving me the opportunity to work in your highly esteemed (algae) group. Cees, unfortunately you could not be part of my thesis committee, but thank you for your supervision nonetheless, for your interest in my project and your challenging and critical questions.

I've had a great four years at Wetsus, and I would like to thank everyone there for making Wetsus such a nice place to work. I would especially like to mention my office mates Paula, Luewton, Phillip, Claudia, Camiel, and later also Zlatica and Christina for the nice times and talks and for making our office such a nice one. And although very short, also Natalia, Fei, Lieven and Ran, you were very great in my second office. I would like to thank the technical staff for all their help and effort into my setups. Not only did I have different experimental setups that somehow kept expanding, we also went to pilot-scale and build the biofilm reactor at the demo-site in Leeuwarden. Thank you Jan, for all your work on both my lab-scale and pilot-scale reactors, Wim for all your help with choosing the right equipment and thinking of a good solution to yet another problem, Harry for all the electronics and Harm, Ernst and Foppe for many other things. Thanks Mieke, Marianne, Jelmer, Janneke, Pieter and Ton; the analytical team who were a great help measuring many samples. I also want to thank the secretarial team for all their help; Helena, Linda, Trienke, Roely and Geke. And Doede for the chair massages. Furthermore, I want to acknowledge everyone in my theme Advanced Waste Water Treatment and the steering committee of STOWA for the interesting meetings, and Yvette and Justina for being my fellow women in the team and all our nice coffee break conversations. And thanks Cláudia, Ana and Zlatica for being my fellow Wetsus algae girls.

I had the opportunity to supervise many students during my time at Wetsus; Oane, Don, Maxime, Pom, Sudarat, Julie, Lina, Rabin, Agi and Richard, my results would not have been so great without you guys. It was great working with you all, thanks for all your help, input and enthusiasm for working with the algal biofilms.

Furthermore, I would like to acknowledge all my colleagues at Bioprocess Engineering for all the help on my algae related questions and the nice times during the PhD trips. Miranda, thanks for all the help and Ellen, Kiira, and Kim for making my trips to Wageningen even more enjoyable with our nice talks.

While algal research can be both time and mind consuming, I've also met some great people while living in Groningen to keep my mind away from work. Thanks to all the members of Harmonie'67, who made Monday evenings always a pleasure, and especially to Doutsen, Rixt and Elvira for all the nice sectierepetities. I also acknowledge everyone from the concertcommissie for the nice times and dinners. Yfynke, thank you for teaching me so much more about the clarinet, and Hanneke for introducing me to yoga and your inspiring classes.

Matthijs, thanks for making this book look as great as it does, for all your enthusiasm even though things took a bit longer than you expected. And thank you Tineke for the nice picture.

Finally, I would like to thank my family and in-laws for your support and interest throughout this entire PhD-period. And of course, most important people last; Erik, thank you for all your support, the way you always put everything into perspective and for your love.

Nadine Boelee
August 2013

PUBLICATIONS

Nutrient Removal and Biomass Production in an Outdoor Pilot-Scale Phototrophic Biofilm Reactor for Effluent Polishing.
N.C. Boelee, M. Janssen, H. Temmink, R. Shrestha, C.J.N. Buisman, R.H. Wijffels, 2013, submitted for publication.

Symbiotic Microalgal-Bacterial Biofilms Remove Nitrogen, Phosphorus and Organic Pollutants from Municipal Wastewater.
N.C. Boelee, H. Temmink , M. Janssen, C.J.N. Buisman, R.H. Wijffels, 2013, submitted for publication.

The Effect of Harvesting on Biomass Production and Nutrient Removal in Phototrophic Biofilm Reactors for Effluent Polishing.
N.C. Boelee, M. Janssen, H. Temmink, L. Taparavičiūtė, R. Khiewwijit, Á. Jánoska, C.J.N. Buisman, R.H. Wijffels, 2013, submitted for publication.

A physiologically based kinetic model for bacterial sulfide oxidation.
J.B.M. Klok, M. de Graaff, P.L.F. van den Bosch, N.C. Boelee, K.J. Keesman, A.J.H. Janssen, Water Research 2013, 47 (2), 483-492.

Scenario Analysis of Nutrient Removal from Municipal Wastewater by Microalgal Biofilms.
N.C. Boelee, H. Temmink, M. Janssen, C.J.N. Buisman, R.H. Wijffels, Water 2012, 4, 460-473.

Nitrogen and Phosphorus Removal from Municipal Wastewater Effluent Using Microalgal Biofilms.
N.C. Boelee, H. Temmink, M. Janssen, C.J.N. Buisman, R.H. Wijffels, Water Research 2011, 45 (18), 5925-5933.

ABOUT THE AUTHOR

Nadina Catharina (Nadine) Boelee was born on March 25, 1984 in Geldrop, the Netherlands. From 1993-1997 she lived in Irvington, USA where she attended the Irvington Elementary and Middle School. After returning to the Netherlands she obtained her gymnasium diploma from the Hondsrug College in Emmen in 2002. Nadine started studying Environmental Sciences at Wageningen University in September of the same year.

During her BSc thesis Nadine designed wastewater treatment plants with UASB (upflow anaerobic sludge blanket) reactors which led to a thesis entitled 'Anaerobic treatment of agro-industrial wastewater in the Western Balkans'. Her Msc thesis entitled 'Full-scale dynamics of biological sulfide oxidation at halo-alkaline conditions' focused on the oxidation of hydrogen sulfide by sulfur oxidizing bacteria in air-lift reactors and the simulation of this process using Matlab. This work was carried out at the Sub-department of Environmental Technology of Wageningen University. Her internship was performed at Bioclear, the Netherlands, where she investigated the methane production during anaerobic digestion under thermophile conditions and the microbial populations in time. In August 2008 she obtained her MSc Environmental Sciences degree with a major in Environmental Technology and a minor in Process Engineering.

In December 2008 Nadine started as a PhD student at the Bioprocess Engineering group of Wageningen University, performing her research at Wetsus, Centre of Excellence for Sustainable Water Technology in Leeuwarden. Her research focussed on the application of microalgal biofilms for municipal wastewater treatment, the results of which are presented in this thesis. Nadine will continue working on developments for wastewater treatment at Nijhuis Water Technology, the Netherlands.

OVERVIEW OF COMPLETED TRAINING ACTIVITIES

Discipline specific activities

Freshwater Algae Course	2009
Advanced Biofilm Course	2009
Matlab introduction Course	2011
Seminar Trends in Environmental Biotechnology: Nitrogen removal and recovery from water and wastewater	2009
Internal Wetsus congress	2009 / 2010
Theme meetings Wetsus	2009 – 2012
Wetsus congress	2009 – 2012
Towards high productivities of microalgae in photobioreactors - minisymposium	2010
Netherlands Process Technology Symposium	2010
Algen, het groene goud? Waternetwerk Symposium	2010
Seminar Trends in Environmental Biotechnology: Phosphorus: from excess to shortage. Can technology solve the problem?	2010
Benelux Young Water Professionals congress	2011
Young Algaeneers Symposium	2012

General courses

Teaching and supervising thesis students	2009
VLAG PhD week	2009
Writing in English for Academic purposes. A publishing course for PhD students	2010
Basic Statistics	2011
PhD manage your own career	2011

Optionals

Preparation project proposal	2008
Brainstorm/PhD day BPE	2009 / 2010 / 2012
Bioprocess Engineering PhD study tour to the USA	2010
Bioprocess Engineering PhD study tour to Spain	2012